EFFECTS OF ROLLING PROCESS PARAMETERS ON THE MECHANICAL AND MICROSTRUCTURAL PROPERTIES OF HOT –ROLLED ST60Mn STEEL

BY

NWACHUKWU, PETER UGWU

B.Eng. (NAU), M. Eng. Mechanical Engineering (UNN)

(Matriculation Number: 183253)

A Thesis in the Department of Mechanical Engineering

Submitted to the Faculty of Technology

in partial fulfilment of the requirements for Degree of

DOCTOR OF PHILOSOPHY

of the

UNIVERSITY OF IBADAN

DEPARTMENT OF MECHANICAL ENGINEERING

UNIVERSITY OF IBADAN, IBADAN,

MAY 2019

ABSTRACT

Hot-rolled St60Mn steel is commonly used in the construction of bridges and houses. Reduced quality characterising hot-rolled steel has become a major research concern. Previous studies focused on the effects of chemical composition on the mechanical and microstructural properties of hot-rolled St60Mn steel. However, there is still the limitation of lower yield strength and coarsegrain size. Literature is scarce on the effects of rolling process parameters on the mechanical and microstructural properties of St60Mn steel. This study was designed to investigate the effects of Percentage Total Deformation (PTD), Rolling Strain Rate (RSR) and Finish Rolling Temperature (FRT) on the mechanical and microstructural properties of hot-rolled St60Mn steel.

Three hundred and twenty-four St60Mn steel billets of dimension 120 x 120 x 12000 mm were used for the experiment. These were charged into a reheating furnace at 1230ºC and hot-rolled to standard rebar sizes at PTD of 96.0, 96.5, 97.0, 97.5, 98.0, 98.5, 99.0 and 99.5; RSR of 4000, 4500, 5000, 5500, 6000, 6500,7000 ,7500 s^{-1} and FRT of 915, 917, 919, 921, 923, 925, 927 and 929ºC. Samples were prepared according to BS 4449. Mechanical tests were performed on the rolled samples at 27ºC to obtain the Tensile Strength (TS), Yield Strength (YS) and toughness, which were compared to those in literature. The samples were sectioned using machine fitted with abrasives and the resulting samples were mounted with bakelite and acrylic. Thereafter , these were ground with silicon carbides and aluminium oxide, polished and etched with 2.0% nittal for metallographic examination using optical microscopy. Their microstructural grain sizes were obtained and further analysed via the edge detection method. Optimum parameters were determined using response surface methodology. Data were analysed using ANOVA at $\alpha_{0.05}$.

The TS (MPa), YS (MPa) and toughness (J/mm^2) at PTD ranged from 611.2 (96.0%) to 620 (99.5%), 432 (96.0%) to 432.2 (99.5%) and 0.48 (96.0%) to 0.41 (99.5%), respectively. For RSR, the samples ranged from 611.3 (4000 s^{-1}) to 697.2 (7500 s^{-1}), 432.1 (4000 s^{-1}) to 455.8 (7500 s^{-1}) and 0.48 (4000 s^{-1}) to 0.42 (7500 s^{-1}), respectively. At

FRT, the samples also ranged from 611 (915^{o}C) to 605 (929^{o}C), 432 (915^{o}C) to 428 (929^{o}C) and 0.48 (915^{o}C) to 0.59 (929^{o}C), respectively; while that existing in literature were 500, 420 and 0.40,respectively. The microstructural grain sizes (μm) ranged from 48 (96.0%) to 41 (99.5% PTD), 48 (4000 s^{-1}) to 40 (7500 s^{-1} RSR), and from 47 (915^{o}C) to 55 (929^{o}C FRT), while that in literature was 56. Higher TS and YS were observed as PTD and RSR increased, but decreased with increasing FRT. However, increasing PTD, RSR and FRT improved the toughness and grain sizes of the hot-rolled products. Optimum RSR, FRT and PTD were obtained as 7000s^{-1},920.30°C and 99%, respectively. The effects of PTD, RSR and FRT on mechanical and microstructural properties were significant when compared with literature values.

Mechanical and microstructural properties of hot-rolled St60Mn steel were improved using higher Percentage Total Deformation and Rolling Strain Rate, with lower Finish Rolling Temperature.

Keywords: St60Mn steel, Steel grain size, Percentage total deformation, Rolling strain rate

Word count: 497

ACKNOWLEDGEMENTS

My profound gratitude goes to God Almighty who is the foundation of all knowledge and divine grace. I am thankful to God for the gift of a dedicated supervisor, Prof. Oluleke Oluwole, who painstakingly saw me through this research work. I am grateful to Dr. C. O. Anyaeche, for his advice. I thank the entire staff and students of the Mechanical Engineering department for their co-operation throughout the period of the research.

Secondly I am grateful to Mr. Aiyedun of the Production line, Dangote Intergrated Steel Company PLC, Osogbo, and Engr. J. T. Obamuyi of the Furnace Pulpit, all of Dangote Intergrated Steel Company PLC, Osogbo for their assistance. I am also grateful to Engr. I. O. Fakolujo of the Mechanical and Operations Department, and the entire staff of the Quality Control ,Research and Development Laboratory, of the same company for their assistance in the experimental works.

The experiments of the research work were carried out at the Quality Control Laboratory of the Dangote Intergrated Steel Company PLC, Osogbo and the Materials Testing Laboratory of Materials Engineering Department Obafemi Awolowo University Ile-Ife.

Finally, I would like to thank the members of my family, especially my wife and children for their tolerance throughout the years of my research.

CERTIFICATION

I certify that this work was carried out by Mr. P. U. Nwachukwu in the Department of Mechanical Engineering, University of Ibadan.

.....

Supervisor

Professor O. O. Oluwole

B.Sc. (Ife), M.Sc. (Lagos), Ph.D. (OAU)

Department of Mechanical Engineering,

University of Ibadan, Nigeria.

DEDICATION

This thesis is dedicated to God of Abraham, Isaac and Jacob, the Father of our Lord Jesus Christ, my God and Creator of the whole universe for His protection throughout the course of study.

TABLE OF CONTENTS

CHAPTER FOUR:RESULTS AND DISCUSSION

LIST OF TABLES

Table **Title** **Page**

LIST OF PLATES

LIST OF FIGURES

LIST OF SYMBOLS

Acronyms

BS	British Standard
FRT	Finish Rolling Temperature
F_{ys}	Flow Yield Strength
HMI	Human Machine Interface
HTMT	High Temperature Thermomechanical Treatment
LTMT	Low Temperature Thermomechanical Treatment
MFS	Mean Flow Stress
NIS	Nigerian Industrial Standard
PTD	Percentage Total Deformation
RSR	Rolling Strain Rate
RSM	Response Surface Methodology
St60Mn steel	Medium carbon Manganese steel
TTT	Time Temperature Transformation

GREEK SYMBOLS

α	Angle of bite
$б_T$	Tensile strength
$б_Y$	Yield strength

ENGLISH SYMBOLS

A_i	Initial cross sectional area
b	Width of work piece
E	Young's Modulus of Elasticity
E_{Imp}	Impact toughness
ΔH	Draft
H_i	Initial height
H_f	Final height
L_p	Projected length
n	Speed of the rolls
p	Roll pressure
P	Rolling load

PE	Percentage Enlongation
PRA	Percentage Reduction in Area
P_r	Radial force
R	Average roll radius
V_r	Velocity ratio
V_i	Initial velocity
V_f	Final velocity

CHAPTER ONE
INTRODUCTION

1.1. Background to the Research

Rolling is a process of plastically deforming a metal by passing it between rolls. There are two categories of rolling process such as sheet and rod rolling. The maximum thickness in sheet rolling is below 3 mm, or minimum thickness of 3 mm in plate. In rod rolling, the end profile is a round rod. The deformation of billets is done by hot-rolling. Hot-rolling is a plastic deformation of the billets by allowing it to pass through rolls. Rolling is the commonest way of deforming steel that offers close monitoring of the steel than other metal working processes.

Rolling is further categorized with respect to the temperature of metal stock being rolled. If the temperature of the metal stock is higher than the temperature of formation of austenites, it is called hot rolling. For hot rolling, the billet is fully deformed at high elongation. Rolling is the passage of the billet through two rolls that move at similar velocity. There is a gap between the two rolls through, which the billets must pass. These rolls can be smooth or contoured with profiles so as for the rolls to hold the billet and pull it, while reducing it in area and increasing its length. The first rolling process for billets is done at the roughing stand (Balogun *et al,,*2011).

The billets are thermally agitated to 1230°C,(Dutta, 1986). Steel is compressed by the rolls till the end product is obtained. A machine called a roller table, directs the billets to the rolls, and another roller table collects the billet that is emerging out of the rolls. The table in front of the rolls pushes the steel billets against the rolls, which grip and pull the steel between the billets through the rolls while another roller table collects it. The sizes of the billets are in this way reduced until the final size is achieved. One of the requirements of the hot rolling process is thermal application to the billets from 25^{o}C to 1230^{o}C. Heat is applied to the billet to a rollable temperature which is higher than the phase change temperature. This high thermal application is because steel billet contains other alloying elements like cobalt, manganese and nickel, in addition to varying percentages of carbon and iron. During hot rolling, deformation takes place all through

the drafting stages. The final draft is at a temperature higher than the temperature for the formation of austenites.

When a billet is hot-rolled through two rolls, it undergoes pressure as a result of force from the rolls and the reaction by the billet. The rolls offer pressure to the billet and the billet offers the same amount of pressure to the rolls. As a result, there is a deformation of the billet and a reduction in its area. This deformation affects the tensile strength of the billet and the size of the billet decreases as it increases in length (Dutta, 1986; Ashrafi *et al*., 2015). There is another parameter that controls hot-rolling known as draft. This is defined as the lowering in size of the billet due to the difference between the initial and final heights of the billets as it passes through the rolls.

This draft also affect the mechanical properties and microstructure of hot-rolled products (Aoda *et al*., 2012; Song *et al*., 2004). There is also another parameter that controls hot-rolling, which is called enlongation and it occurs together with a reduction in area at constant volume; and this enlongation decreases as the deformation increases (Hutchinson *et al.*, 2015). There is yet another phenomenon that controls hot-rolling known as spread. This is defined as the movement of the billet stock in the direction of least resistance (Dutta, 1986). Rolling is a process that ends up in two processes. The rolls offer a reducing pressure and this gives an increase in length and spread. The ratio of the exit width to entry width is called coefficient of spread and this coefficient increases as the coefficient of friction and resistance to the lengthwise flow increases. Spread is affected by finishing temperature and rolling strain rate.

Rolling temperature of the rolled stock affects spread significantly; the lower the rolling temperature of rolled steel billet input, the greater is the spread, as well as the strength of the hot-rolled steel. Similarly, higher FRT results in lowering of the spread, as well as the strength of the hot-rolled steel billet. Also higher RSR provokes greater spread and strength of the steel and lowering of enlongation of the hot-rolled steel. The lower the RSR, the smaller is the spread and vice versa (Sierakowski,1997; Fahker *et* al.,2014; Mihalikova *et al.*,2007; Song *et al.*,2004). Lower speed of hot-rolling results in greater spread and vice-versa.

1.2. Statement of the Problem

Most rolling mills commonly found in the developing economy and especially hot-rolling processes all over the world are characterized by coarse grain size, decrease in yield and Tensile Strength of hot-rolled St60Mn steel products and lack of optimization of rolling process parameters for improved mechanical and microstructural properties of hot-rolled St60Mn steel.These characteristics can lead to collapse or failure of structures built with products from such hot-rolled St60Mn steels. All these failures are due to the conventional rolling operated in these mills that is devoid of control and optimization of hot-rolling process parameters, mechanical and microstructural properties (Kumar *et al.,* 2012; Saroj*et al*., 2000). So there are lots of reports and complaints about the decrease in quality of mechanical and microstructural properties of hot-rolled steel rebars.These have resulted in the production of rebars with low yiel strength and coarse grain sizes These problems might not only be as a result of equipment malfunction, but lack of control or optimization of process parameters as contributors to some of these failures (Kumar *et al.,*2012; Nguyen *et al., 2019*; Fahker *et* al., 2014; Simm*et al.*, 2017).

1.3. Research Aims and Objectives

1.3.1.The study is aimed to produce St60Mn steel that is consistent and conform to standard using conventional rolling mill for structural application.

1.3.2.The objectives of this work are:

1) To study the influence of the FRT, PTD and RSR on the mechanical properties of hot-rolled St60Mn steel.
2) To study the influence of FRT, PTD and RSR on the microstructural grain sizes of St60Mn steel.
3) To optimize hot-rolling process parameters for improved properties of the steel grade.

1.4. Significance of the Study

There is high rate of collapse or failure of building structures and bridges built with hot-rolled St60Mn steel. There is need for hot-rolled steel products with high YS and fine grain sizes to be used in engineering constructions.

1.5. Scope and Limitations of the Research

The study is limited to the

(i) Effectsof PTD, RSR and FRT on TS, YS, Impact Energy, hardness, E, PRA, PE and ductility of the hot-rolled steel grade.

(ii) Effects of hot-rolling process parameters on the microstructural properties of St60Mn steel.

(iii) Optimization of the hot-rolling process parameters for improved properties of the steel grade.

1.6. Layout of the Thesis

The thesis comprises of a total of five chapters. Chapter one introduces the background statement to the research, the statement of the problems to be solved, the aims and objective, the significance of the research and the scope and limitations of the research. Chapter two contains the literature review related to this research. Chapter three explains the materials used in the study and the methodology of the research. Chapter Four presents results and discussions of the study. Chapter five presents the conclusions of the study and recommendations for the applications of its findings in the industries and suggestions for future work.

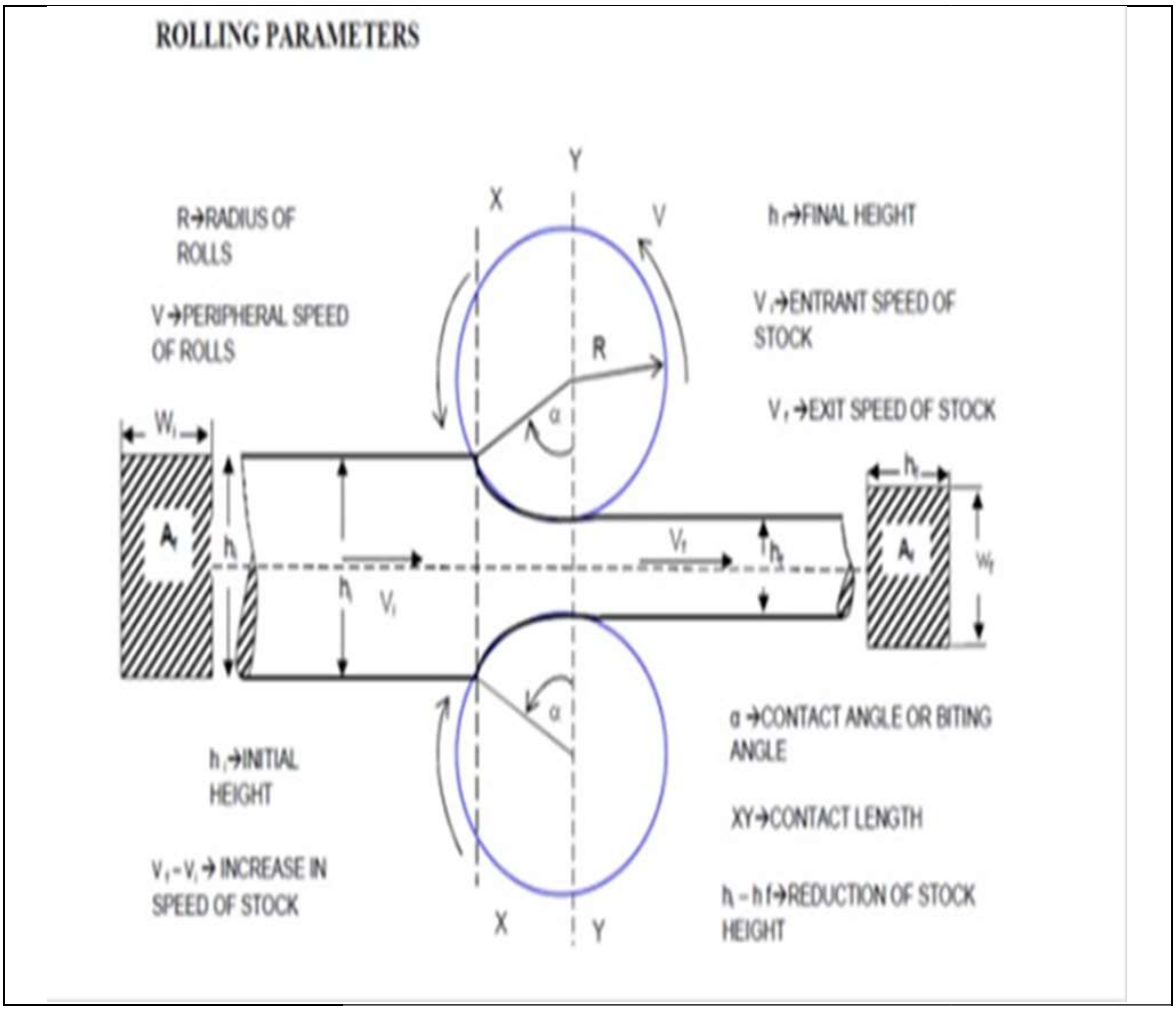

Figure 1.1. Schematic diagram showing some rolling parameters during the passage of hot- rolled stock through the rolls (source: Dutta, 1986)

CHAPTER TWO
LITERATURE REVIEW

2.1. Hot-Rolling of Metal Billets

When plastic deformation begins, the first width of the steel comes into the stands with a very high speed. It then leaves the entire rolling equipment with a reduced width and increase in linear enlongation. The forces on the steel from the hot-rolling equipment gives rise to linear enlongation as a proof that nothing from the billet was lost during the process.

If $h_i > h_f$, then $v_i < v_f$. The speed of the billet stock kept on increasing at the time it enters the rolling mill till it leaves it so that the volume of the billet is the same.

Given that $b_i = b_f$, therefore

$$\frac{h_i L_i}{t} = \frac{h_f L_f}{t} \qquad (2.1)$$

Again,

$h_i v_i = h_f v_f$, $\frac{v_i}{v_f} = \frac{h_f}{h_i}$ (Dutta, 1986)

As the billets come into the rolls while still in the front of rolling mill,there is a predominant and substantial draft that takes place on it (Figure 2.1) as it contacted (Figure 2.2) the roll gaps, which aids the subsequent deformation processes.Before the commencement of hot-rolling, billets are heated to optimum temperature in the reheating furnace for hot deformation in the rolling stands(Lenard,2007;Dieter,2007).

Minani (1990) stated that during hot-rolling, steel offers opposition to average compressive force of deformation.It is possible to find this average compressive force of each rolling pass (Macagno *et al.,1994).*Borrato *et al.,*(1988*),*looked into this average compressive force, which is obtained at hot-rolling.Devadas *et al.,* (1991), made an observation of the Misaka's proposed compressive force and Shida(1974), discovereda compressive force algorithmn that can control compressive force, which occurs at hot-rolling. McQueen *et al., (1985),*stated that during hot-rolling deformation, steel recovers and recrystallizes. Cahn (1997) stated that this recrystallization begins on application of

critical strain at any increase in amount ofdeformation and that it is followed by grain growth.. Sellars (1978) had earlier observed that the amount of grains that recrystallizes depends on energy and nucleation sites available.

The relationship between carbon level and strain rate during hot-rolling was studied by Misaka *et al., (1967).*

Gimburg (1993) studied the theories used to hot-roll with high quality and proffered solutions to the difficulties of harmonising the discrepancies in structural factors like thickness,width, cross sectional profile and flatness.

Bhanu *et al.,* (2016) researched extensively on sheet metal rolling using two roller powered machines and discovered that the effect of rolling parameters like sheet thickness,sheet width and enlongation in thickness can be used to change properties.

Reitz (1995) held a review of flat processing of steel and showed indepth processing methods for steel.

Wang *et al., (*2013) examined how a space between rolling stands could be used to combine many factors in the speedy roll stand with elevated values during unsteady lubrication and discovered the effect of the notable production factors on the speed and magnitude .

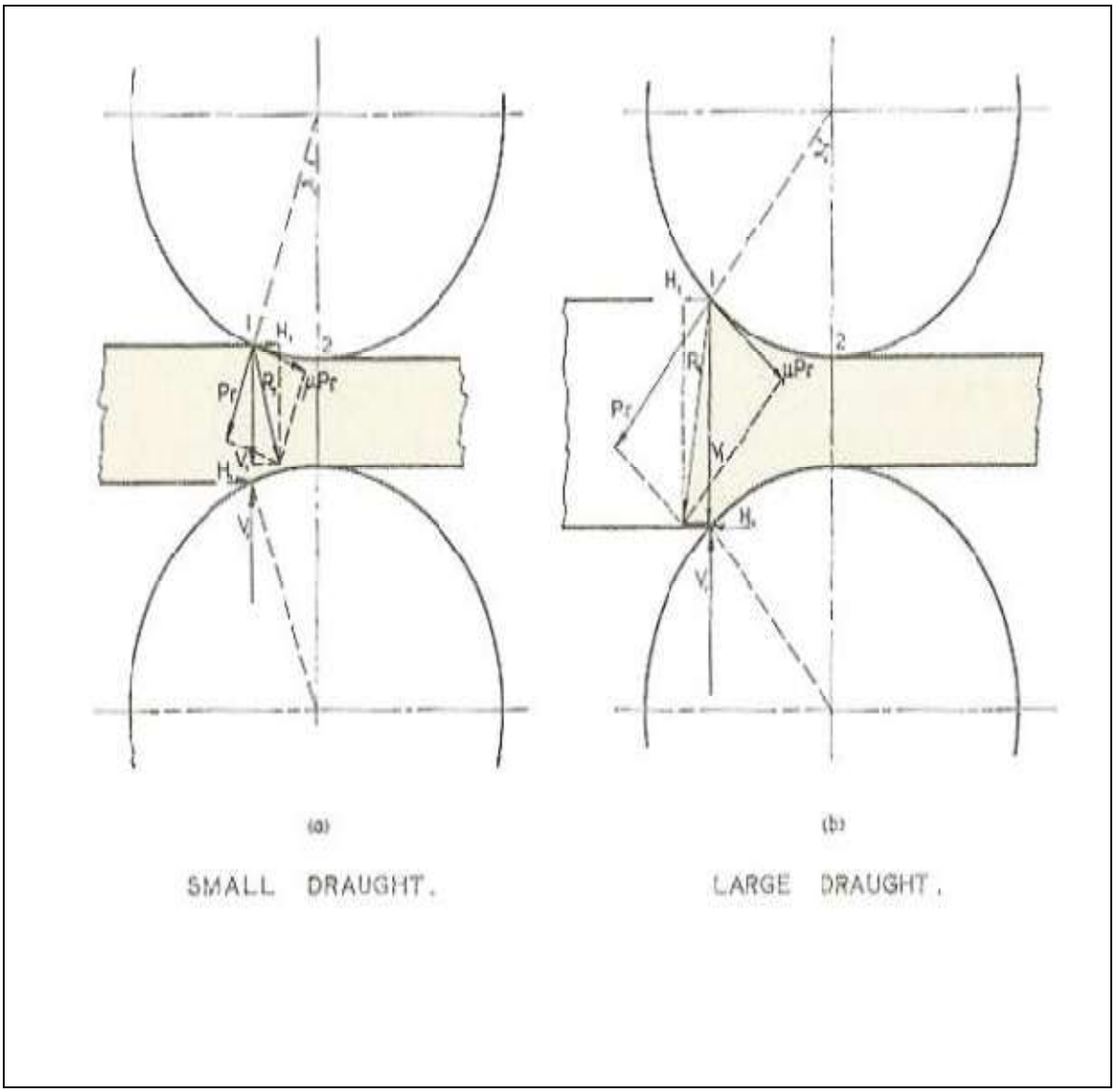

Fig.2.1:Maximum Bite Angle (Source : Mallesham *et al.,2016)*

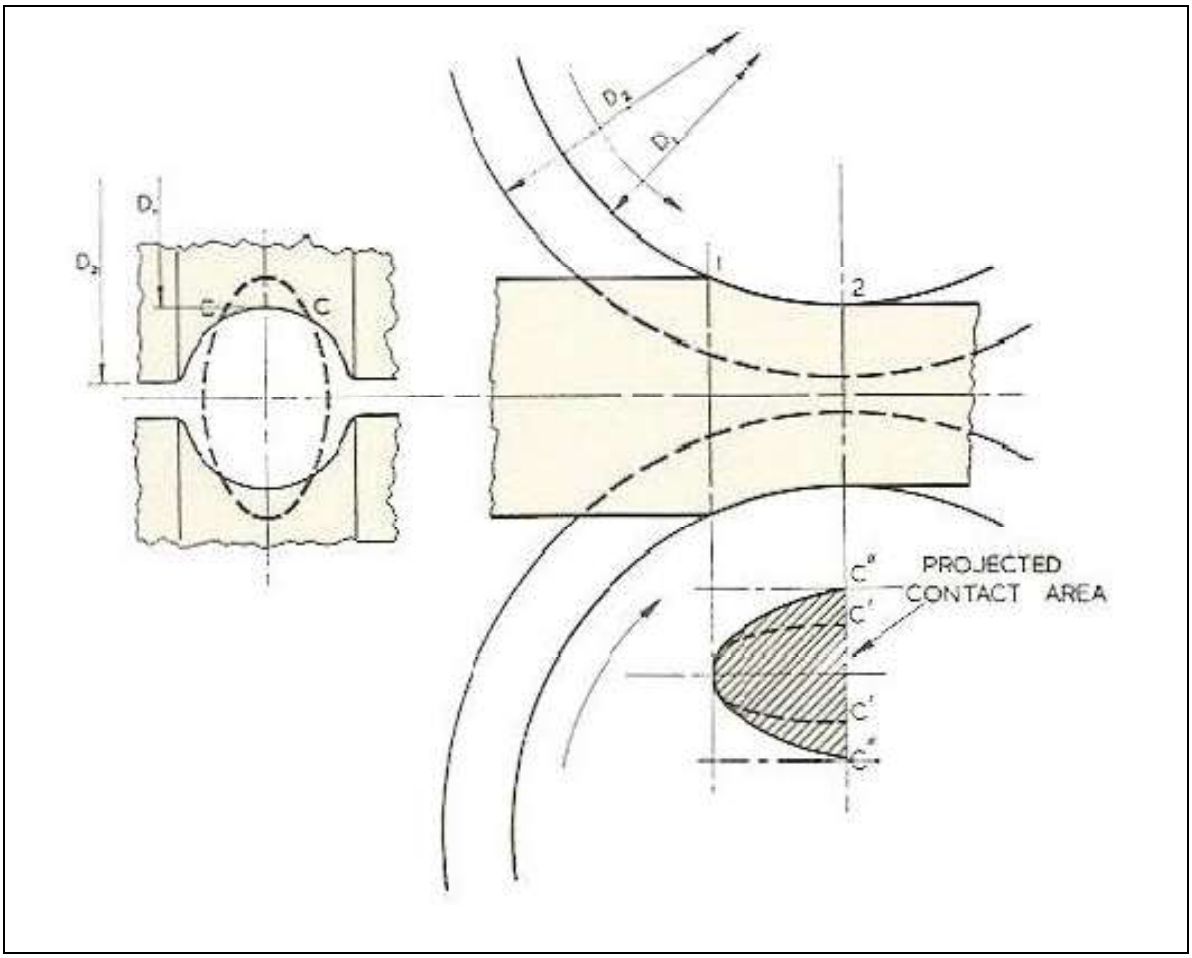

Fig.2.2:Contact Area (Source: Mallesham *et al*., 2016)

2.1.1 Forces that Act on the Billets during Hot-Rolling

Byon *et al.,* (2012) studied the use of equations of compressive force in range of average strain rates and high temperature to foretell forces of rolls in four pass continuous rod rolling and concluded that the Misaka algorithmn could be used to predict how the billets resists the deformation temperature rises and strain rates moderately.

The metal billet experiences the effect or compression of two opposing forces, which are known as the push that acts at a certain radius and the one that acts at a tangent. There is a region where the rolling speed equals the speed of the rolling stock, which is called region of neutrality or region where there is no deviation of the stock or the rolling equipment.The speed of the rolling stock is reduced when it travels halfway from the place where it enters the rolling mill to the region of neutrality; while the speed of the stock increased as it leaves the rolling mill (Figure 2.3). The direction of the frictional force is then reversed and opposes the delivery of the metal from the rolls. The location of the neutral point N is where the direction of the friction forces changes. $P_r$is the radial force, with a vertical component P (P is the rolling load - the load with which the rolls press against the billet/metal). The specific roll pressure, p, is the rolling load divided by the contact area.

$$p = \frac{P}{bL_P} \quad (2.2)$$

Where,b is the width of the billet

$L_P$is the extended arm of the locus where the billet touches the rolls. (Dutta, 1986)

$$L_P = [R (h_0 - h_f) - (\{((h_o - h_f)^2\})/4]^{1/2} \quad (2.3)$$

$$L_P = [R (h_0 - h_f)]^{1/2} \quad (2.4)$$

$$L_P = R\Delta h \quad (2.5)$$

Also as the billets passes through the roll gap,it experiences another kind of force called toque (Figure 2.4).

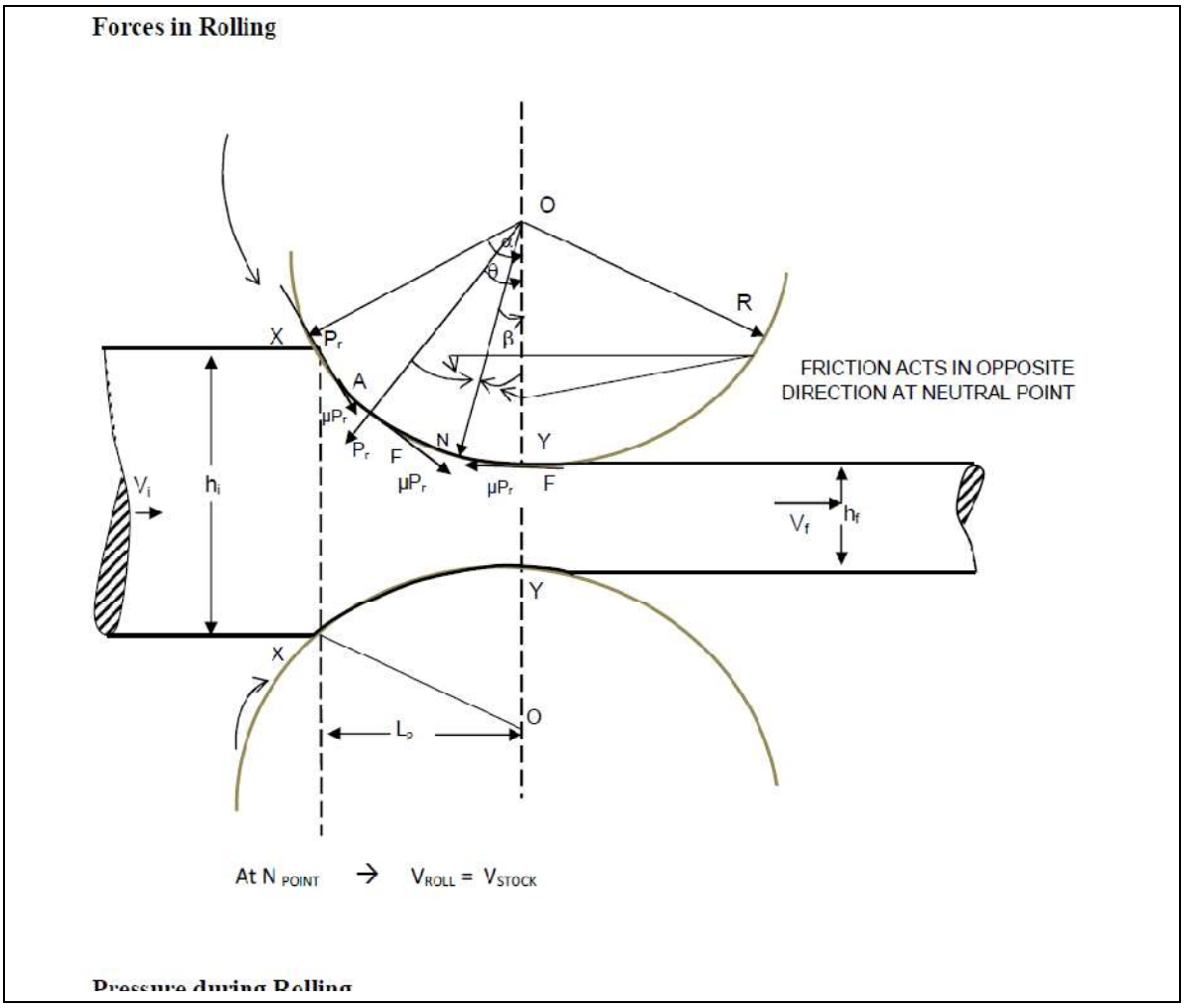

Fig.2.3: Rolling Forces During Hot-Rolling (Source: Dutta.,1986)

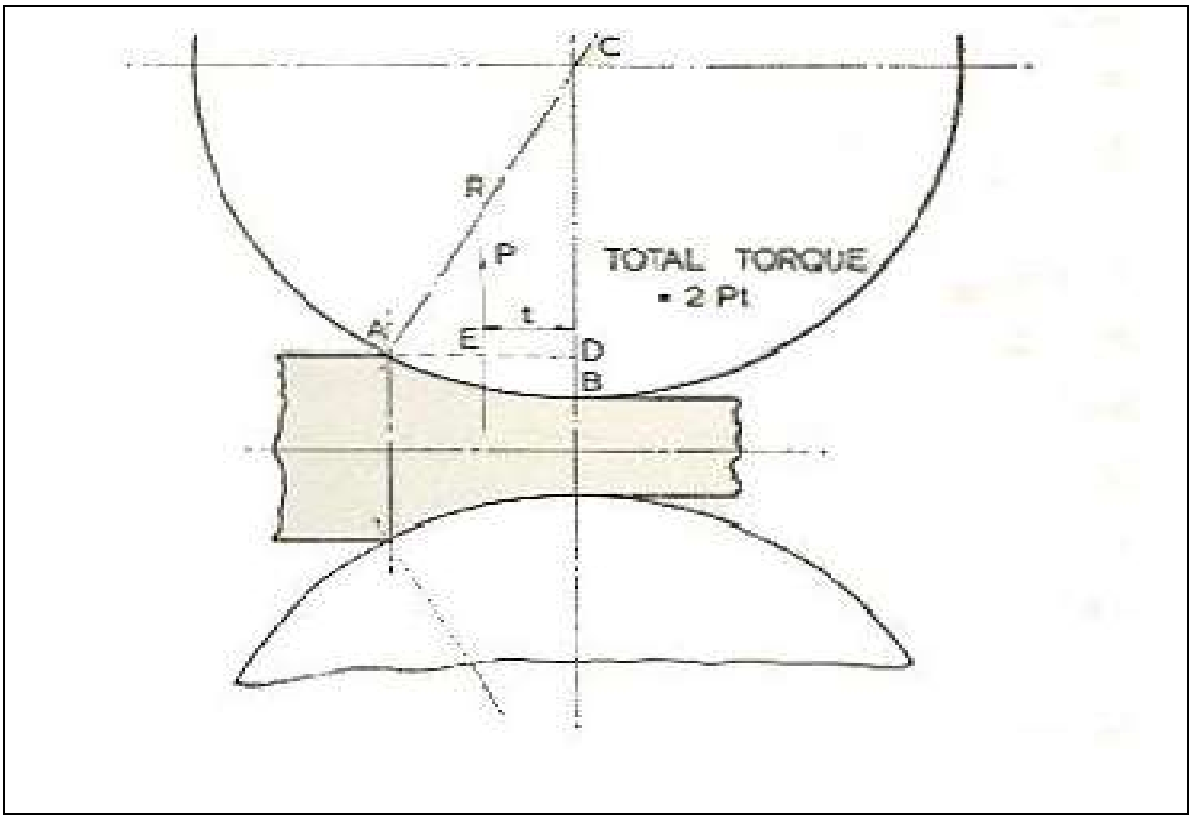

Fig.2.4:Touque(Source:Mallesham *et al*.,2016)

In hot-rolling, the Misaka equation is used to find the values of the pressures, which could always be used to foretell how a billet deforms Sang-min *et al*., (2012). During hot rolling, formation of crystals takes place and lowers the grain sizes while during cold rolling a coarse grain is produced. What happens is that as the hot-rolling process disintegrates the grains, they reform again while protecting the metal from work-hardening (Dutta, 1986).

In hot-rolling, there is no need for annealing as the high temperature hinders internal pressure in the steel, which confer good properties. There is recrystallization as the billet is deformed and this influences the formation of grain sizes and conferment of good tensile properties (Dutta, 1986). Temperature helps to soften the billet during hot-rolling to stop sudden breaking of the billets (Perelomaet *al.,*2001).

Shelke *et al.,*(2014) investigated on the procedures used to find the value of rolling load and forces that act on a special type of gear using the theory of hot-rolling and focused on how to find the value of the rolling load and forces that act on the gears of steel rolling machines.

2.1.2 Hot-rolling as a thermo-mechanical treatment.

Hot- rolling is all about allowing an alloy to go through heat and also become deformed at the same time, so as to refine its grain size (Total Materials Database, 2003). In this way hot-rolling of steels, which is widely used in the industries is used to treat steels thermally. The usual way includes moulding of various billets to temperatures above the recrystallization temperature and hot-rolling them to rebars. This is after a deformation of the moulded billet by continuous formation of crystals of austenite and also removal of impurities in the billets. Also other unpreventable impurities disintegrate uniformly in the body of the steel (Total Materials Database, 2003).

Before the commencement of every hot-rolling, the billet or bloom or ingot is heated to the ideal temperature at which any hot-rolling can take place. At that elevated pyrometer readings, the steel is changed into a single austenite state from the double states of pearlite and cementite or ferrite and pearlite (Dutta,1986).Phase or state change temperature is AC_1 temperature (Figure 2.5).

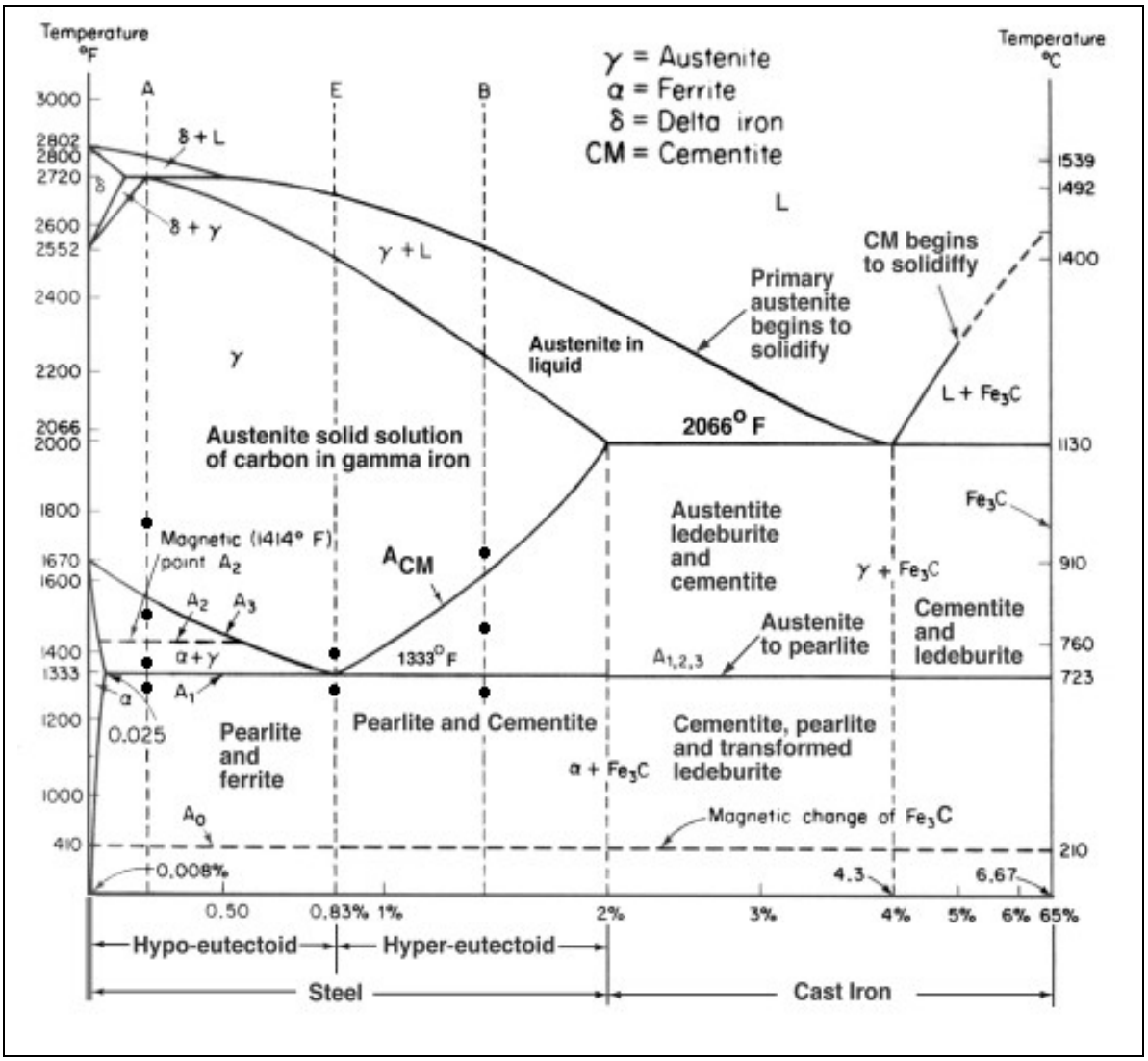

Fig.2.5: Ferrite –Cementite Phase Diagram (Source:Ferrous Alloy Diagrams)

In practice, the pyrometer reading of steel is raised after initial heat that is applied, to an elevated value than the readingat which one state transforms to the other. This rise in elevation in values is done because steel contains other alloys in addition to carbon, which alter the reading at which steel changes from one state to another.

Hot rolling takes place through a number of stands during which billet is decomposed as it being hot-rolled. The final draft is at a temperature higher than the recrystalisation temperature. Accordingly the cold stock is heated to a much higher value than the pyrometer reading for changing steel to austenite. Therefore, the final reading at which the work piece is heated is a function of the amount of total draft, the number of steps or sequences (Figure 2.6) where the drafting is offered and thechemical composition of the steel stock. Billets are heated inside the reheating furnace to the pyrometer reading that is ideal for every hot-rolling operation. This is the starting point of every hot rolling mill practice(Figure 2.7)

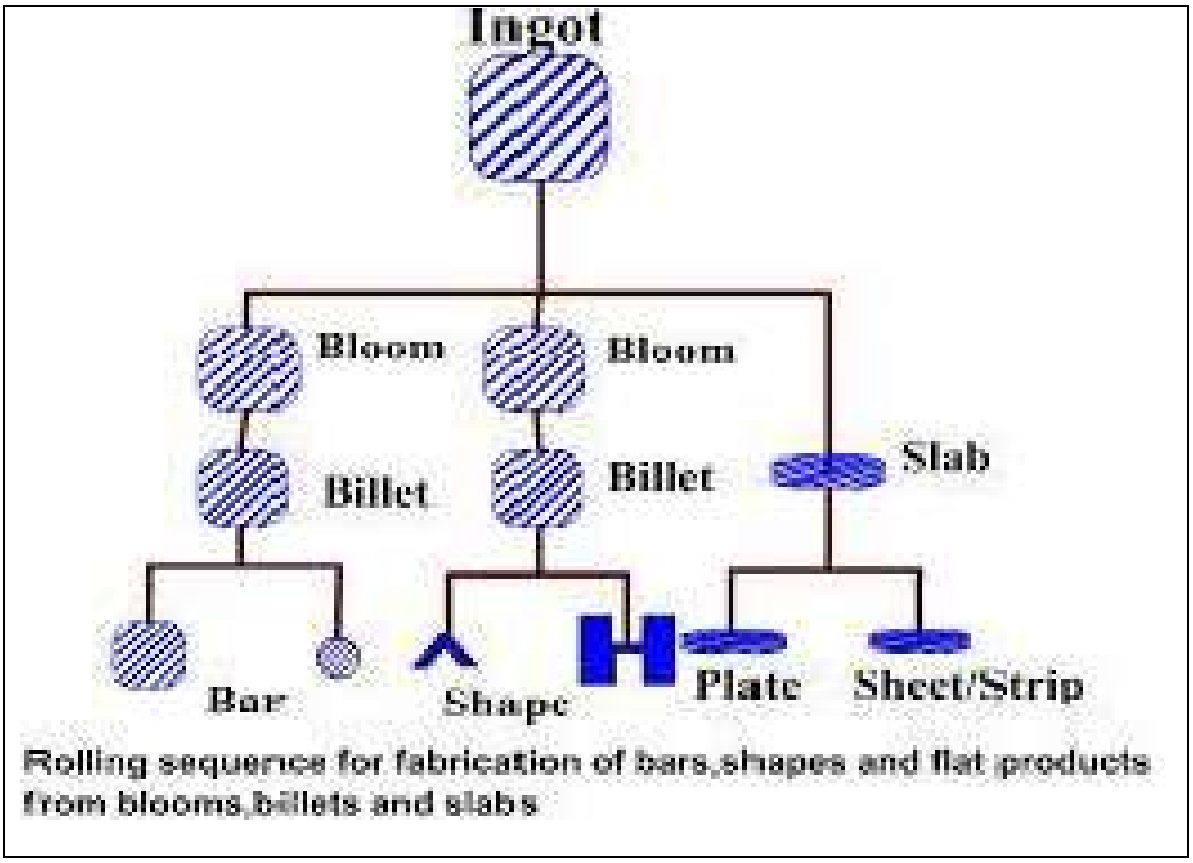

Fig.2.6:Rolling Sequence for Bars, Shapes and Flat Shapes (Source: Mallesham *et al., 2016)*

.

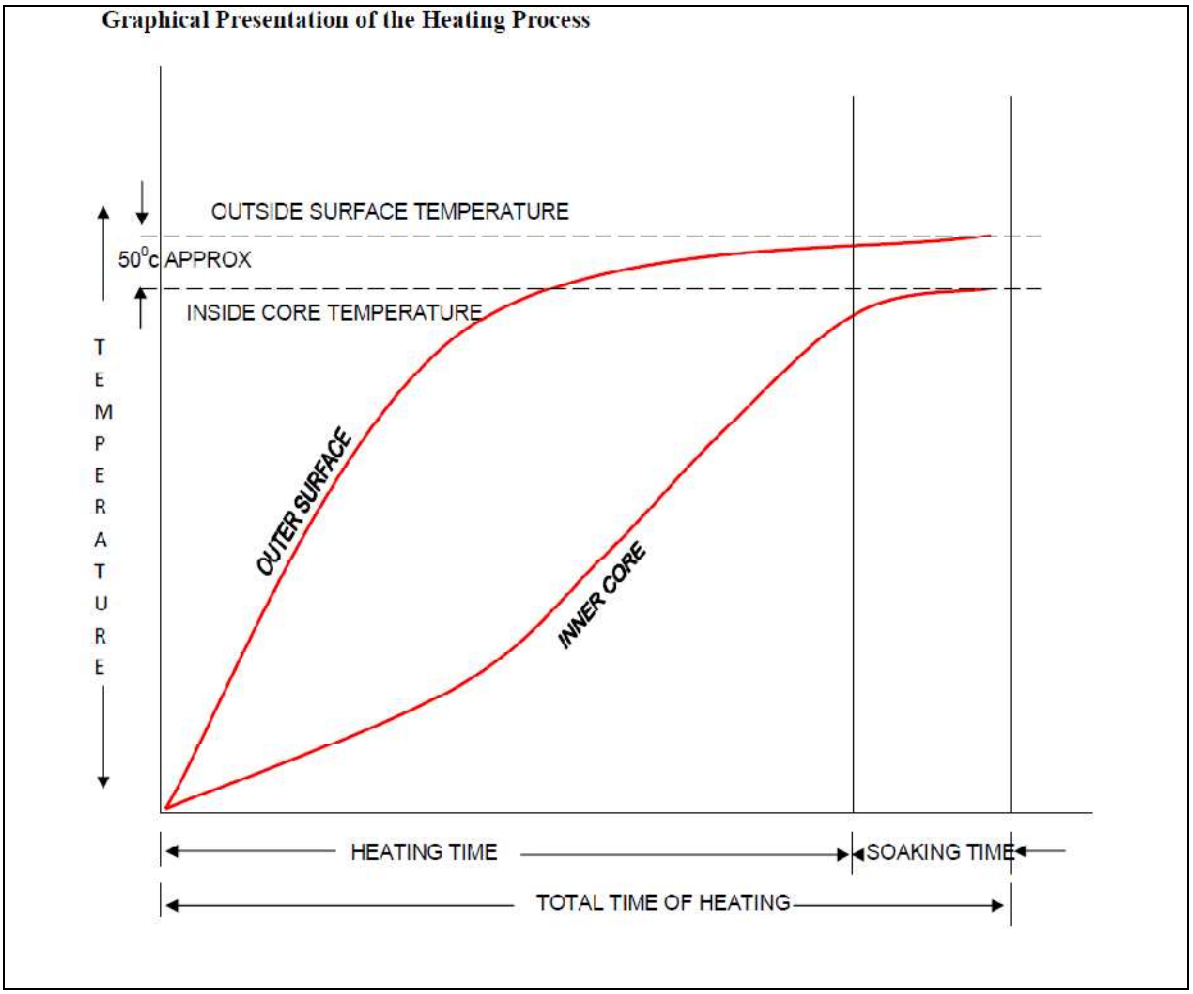

Fig.2.7:Heating Profile In a Reheating Furnace (Source: Dutta, 1986)

When a piece of billet is hot-rolled between two rolling stands, the billetexperiences vertical and horizontal stresses simultaneouslyand these stresses are caused by the vertical load from the rolling stands and at the same time, the part of the billet that is touching the rolling stands and the one that is not touching the stands react in opposition to the influence of this load (Dutta ,1986).

As the rolls offers a vertical stress on the billet, the latter offers the same amount of opposite stress back onto the rolling stand itself. As such the rolling stands are under the influence of stresses offered by the billets and it is shown as a two-dimensional % total deformation in the thickness in length directions or changes its cross sectional area.This deformation influences the mechanical properties of the hot-rolled steel(Ashrafi *et al.*,2015).In the deformation zone, the size of the billet inserted into the rolling stands diminishes in size and it elongates. This increases the linear speed of the billet as it goes out of the rolling mill.

The shape of the rolling space controls the geometry of the product (Dutta,1986).

The term, Draft describes a cutting action of the parts of the rolling stock, which is the billet as it moves through the rolling standswith highly elevated rate of movement. This cutting action of the rolls is accompanied by the linear enlongation of the billet and subsequent decrease in the size of the billet.

There are two types of cutting action, such as straight and non-straight cutting action. Non-straight cutting action is developed when the rolling stand pushes on the billet stock in non-vertical direction. Basically, one rolling stand grinds on the other rolling stand while rotating in the opposite direction.When part of the pass profile is slanted at an angle in between the vertical and horizontal, the % total deformation is caused by a combination of straight as well as non-straight cutting action. The straight cutting action that acts horizontally has a dominant effect as degree rises to 45°. However, when the degree goes higher than 45°, the effects of non-straight cutting action takes over from that of straight cutting action. On reaching a degree of 90° , the percentage total deformation depends almost entirely on non-straight cutting action (Dutta,1986).The rate of reduction or cutting action of the rolls also affect the mechanical properties and grain sizes of hot-rolled products (Aoda *et al*,, 2012; Song *et al.,* 2004). The billet enlongates and at the same time reduces in its cross sectional area, as the volume of billet

that leaves the rolling stands and the one that enters them is equal. What aid the billet to enlongate, otherwise expressed as the ratio of the final length to the initial length, is always greater than unity (Dutta,1986);and this enlongation decreases as the deformation increases(Hutchinson *et al.*,2015).When billet or material is compressed between two rolling stands, it obviously moves in the direction of smaller opposition. There is not only a longitudinal movement of parts but also some sideways movement, which is called 'Spread' (Dutta,1986). Hot-rolling is a one process, which represesnts or gives rise to two opposite movements. The rolling stands give a force that reduces the size of the billets and enlongates the length and sideways movement of the billet, which is known as spread.

The billet stock undergoes spread sideways when pressed by the two rolling stands and obstructed in the linear direction such that enlongation is interrupted.Spread is the flow of material at right angles to the directions of vertical force and elongation. The representation of spread is the ratio obtained when exit width is divided by the entry width. As the friction increases, the resistance to linear flow increases and therefore spread also increases. The quantity of spread can never be estimated accurately. There is no known method through, which an accurate value of spread can be obtained. People that design rolls only rely on estimation to counteract the problem, but accuracy of such guess work is not only extremely necessary but is needed. Practically, it is discovered that the rolling process parameters affect the amount of spread.Thus, rolling temperature of the billet has a prominent effect on spread. When the pyrometer reading of the billet that is inside the furnace is decreased, the spread and the strength of the hot-rolled billet grows higher.In the same vein, when the reading for the hot-rolling climbs up,the spread and the tensile strength of the billet goes down.Also, the higher the rolling strain rate,the greater is the spread and the strength of the steel and the lower the enlongation of the hot-rolled steel.The lower the rolling strain rate, the smaller is the spread and vice versa (Sierakowski,1997;Fahker *et* al.,2014;Mihalikova *et al.,*2007;Song *et al.,*2004). Smaller speed of rolling results in greater spread and vice-versa.

The size of the diameter of the rolling stands that deforms the billets also has a profound effect in assessing the amount of spread. As the diameter of the production rolling

standsincreases in magnitude, the spread gets smaller. Similarly, lower diameter results in higher spread.

The nature of the surfaces of the production rolling stands(i.e the roughness of the roll surfaces) is a major contributor to finding the amount of spread . As the surface of the production rolling stands gets rougher, the spread diminishes in magnitude, but the more smooth the surfaces of the production rolling stands appear, the higher in amount is the spread.The height of the billet or bloom or ingot has a prominent effect on spread.Higher cutting action and wider stock symbolises greater spread. When rectangular billet goes through plain rolling stands, then the spread is said to be undisturbed.

However, if the billet goes inside stock grooved rolling stands, then the form of the gap keeps the spread within certain limits. This means that the spread has been disturbed.

Because of this restricted spread the width of an entering stock is smaller than the width of the pass groove.

It is established that as the value obtained when the value of the wideness of the billetis divided by the value of the thickness of the billet becomes high enough, spread becomes diminished in size and value (Dutta,1986).

Hunter *et al.,*(2015) studied the co-ordinatedalloyed steel and concluded that the cooling mode during the co-ordination is faster than in the sample during the experimentation.

Fotovvati *et al.,*(2016) conducted a research on amount of meltingexperienced during welding of metals and concluded that their result would form a starting point for future research in this area that could be used to verify and validate other results in similar fields.

Kolli *et al.,* (2008) investigated that a special grade of steel that contains many components, evolves immediately after being decomposed and discovered that dispersion of the three constituent elements in the precipitate is a function of increased time.

Kolli *et al.,*(2014) worked on the evolution and combination of one notable constituent and other constituents of a special grade of steel that was investigated by looking into its atomic components and discovered that the precipitate containing notable dispersed at the outside of the parent metal while at the grain outskirts, they are larger than the ones scattered in the crystal lattice of the parent metal.

2.2. Effect of Controlled Hot-Rolling Parameters on the Mechanical and Microstructural Properties of Hot-Rolled Steel

A lot of hot-rolling plants in the third world countries presently make use of the usual production methods, which lack the necessary machines obtainable in monitored rolling.The results on the modelling of tensile strength and grain sizes of steel showed that common plastic deformation operations during rolling failed to comply with the needed pyrometer readings, which would ensure the evolvement of right mean grain size (Obikwelu, 1987). Rebars obtained from the usual production method have extremely poor yield strength and poor grain size most of the times. How fast the hot-rolling heating equipment work should be checked regularly during in-process, so that the steel undergoes complete austenitisation. This will definitely make sure that suitable conversion to good microstructures is achieved (Saroj*et al.,*2000).

Holscher *et al,.*(1991) in their study of the effect of hot-rolling parameters, investigated hot-rolling,structural and physical feeling of crystal lattice of steels and made an extensive research on this topic, which improved the properties of the steels.

In another study, an arithmetic program that is made up of programs for stationary and quasidynamic crystal formation and microstructural development was achieved. This could foretell the end mechanical properties of hot-rolled steels and is needful for the assessment of steel categories (Hodgson *et al*, 1992).

Raabe (1995) studied the non-uniformity of the surface structure of formed products in a hot-rolled steel of special grade and discovered that a surface structure gradient occurred between the structures at the centre and those at surface.

2.3. Effects of hot-rolling Process Parameters and chemical composition on the Mechanical and Microstructural Properties of Hot-Rolled Steel

Akpan *et al.,*(2012) studied how structures and mechanical properties of hot-rolled steel alloys evolved.It was discovered that as the grain size increases, the tensile, yield and fracture strength decrease respectively.

Akiyama *et al.,*(2002), in their study of effect of chemical composition, researched on the effect of constituent elements in carbon steels on stress –strain curve, especially on yieldstrength and explained the stress-strain curve qualitatively, pointing out the existence of strains in the ferrite predicted by the homogenisation method.

Alkhader *et al.,*(2012) in another study of the effect of rolling process parameter, studied the mechanical behaviour of a special grade of steel under the effect of tremendous manner of straining through an extensive spread of straining values and concluded that it has acknowledged tremendous manner at the climax.

Alafaghani *et al.,*(2018) studied the effects of some phenomena that aid in producing the grain sizes and mechanical propertiesof metals that can be hardened by the addition of precipitates and discovered that they have high modulus of elasticity and tensile strength.

Arabshahi *et al.,*(2010) studied the effects of some phenomena used to produce special grade of steel and alloying on the grain sizes and mechanical properties of medium carbon steel and discovered that increasing the reheating temperature above the readings obtained when alloyed steel dissolves, improved the toughness values.

Ashrafi *et al.,*(2016) studied a new and simple method for production of double state steels with perfect ductility and found that the grain sizes of the newly formed steel is made up of martensitic state inside ferritic matrix .

Baker (2013) studied procedures, grain sizesand properties of an alloyed steels and had an indepth considerationof the nucleation sequence and composition of hot-rolled alloyed steel which has a relationship between them.

Baker (2015) studied the alloyed steels and stated that the compositions, main production routes, grain sizes and structural properties of the alloyed steels have effect on each other.

Barranco (1992) worked on the effects of tempering for bainitic low values, martensitic values and mixed grain sizes on toughness, fracture and related mechanical properties of a special grade of steel and discovered that optimum tempering occurred at fairly high temperature.

Dongytian *et al.,*(2004) investigated the fatigue behaviour of 1500 MPa Bainitic/Martensitic Duplex-phase high strength steel and discoveredthat fatigue strength and crack increased .

It was discovered from the study of hot-rolling of steel that temperature is one of the most important parameters that co-ordinates the movement of other parameters like flow pressure. The mechanical properties of steel are decided by a number of microstructural variations given by heat application (Perelomaet *al.,* 2001). It was further discovered from an investigation on rolling of low carbon steel that the final zone heating and cutting plan are necessary for hot-rolling. They monitored movement of other phenomena such as formation of austenites, formation of crystals and formation of precipitates. The produced grain sizes are functions of these phenomena and their reactions (Panigrahi, 2001).

Chang *et al.,*(2017) investigated that the interaction of wheel and rail results into wear as a result of internal change in structures and discovered an increase in hardness.

Chen *et al.,*(2001) investigated on the effect that low yield strength have on steel with a controlled ductility and found that it is able to prevent early enlargement and development of cracks that occur in common braces.

It was also discovered that phenomena, which are functions of processed billets are functions of the final pyrometer readings (Choi, 2002). This initiative was used in the beginning of 1980s, to obtain a ferrite that does not contain interstices to remove challenges facing pyrometer readings. This was achieved by lowering the final pyrometer readings from usual higher values to lower values less than the liquidus temperature (Wilshire *et al.,*2002). This shows that increasing or decreasing the final pyrometer readings has an optimum effect on the mechanical properties of hot-rolled products, depending on the particular property one wants to optimize. There was a similarity between strain-rate and the flow pressure. According to a study of hot-rolling, the rolling temperature affected these two parameters so that improved temperature resulted in improved strain rate, this affected the austenite grain size (Choi, 2002).

Daramola *et al*.,(2010) investigated on the application of high temperature during the hot-rolling of steels and its implication on their tensile properties. The outcome of the

steel was a perfect blend of three mechanical properties that are very good for construction purposes. Balogun *et a*l., (2011) studied the effects of final pyrometer readings on the tensile properties of processed billet and concluded that comprehensive record of pyrometer reading improved the tensile and yield strength of the steel to temperature below 900^{o}C.Mertman *et al*., (2011) investigated on thermal application to steels and found that there was a considerable effect on the ability of the material to perform under fatigue.

Deardo *et al.,*(2013) studied metallurgical basis for TMT of alloyed steels and researched on the basic physical metallurgy of TMT and discussed various aspects of alloy design.

Dennis (1996) studied the relationship between the transformed phases and stress in a bid to determine remaining stresses and discovered that there is a relationship between the stress and the phases developed.

Dennis (2011) investigated on the issues of change in pressure in the computation of internal thermal pressure, which has made a proposal that can be applied in computing internal thermal pressure and explain thermal treatment of steel in its conversion. Zhang *et al*., (2012) investigated on the effects of TMT on the tensile strength of a special grade of steel and found out that its hardness showed a hardened precipitate at a very high temperature. Mechanical measurement indicated that TMT increased the tensile properties and enlongation of the steel more than those with only chemical composition.

Dorbrzanski *et al.,*(2009) studied how grain sizes of high-manganese steel evolved during the TMT processing and found that the steel has high values of compressive forces.

Ebrahimi *et al.,*(2010) studied the effects of factors of heat treatment on grain sizes and mechanical properties of alloyed steels and discovered that increasing the reheating temperature above the dissolution temperature of a special constituent element, increases the mechanical properties of the steel.

Ehinger *et al.,*(2018) studied the grain sizes and how a special grade of steel respond to deformation and discovered that the outside remained stable while the inside disintergrated by forming irregular inclusions.It was therefore, concluded that this grade

of steel showed higher compressive stress level and energy absorption capability when compressed .

Fakher *et al.,*(2012) studied the effects of the route, which hot-rolling takes and the effect of cutting by the rolls, on some of the mechanical properties for medium carbon steel and found that the route of rolling process as the degree rises to 90°, assumes a circular shape as the compressive force and hardness is less than the values in the vertical and horizontal direction.

Gorks *et al.,*(2018) investigated the grain sizes and mechanical properties of Welded Joints in Thermo-mechanical control processed steel and discovered that such weld were characterized by tensile strength similar to that of the base metal.

From an investigation on the effects of heat treatment conditions on the structures and mechanical properties of Dual Phase-type steel, it was discovered that a different initial structure affected the presence of martensites in a Dual Phase-type steel structure. This exists as a group of ropes in an iron body that deforms at high degree in the area of unmovable mass of austenite (Grajcar, 2006).This showed that the initial grain size given to the hot-rolled products at the last gap decided the tensile properties and grain sizes. Normalising temperature reduced with rising time of cooling; also mechanical properties reduced with reducing normalising temperature, which indicated that various steel categories could be produced from billets of identical composition by high rate of water flow (El-Mahallawi*et al.,* 2007).

Gajda *et al.,*(2008) studied grain sizes and how different states of a special grade of steel transform between each other and discovered that specially assisted grain sizesis made up of ferritic body, bainitic ferrite and remnants of austenite.

Gladman (2013) studied how precipitates can be used to harden metals and found that contribution to strength is derived from change in the amount or ratio of volume precipitates that can be used .

Ghosh (1977) studied a numerical analysis of the tensile test for sheet metals and discovered that the result agrees well with experiments conducted on a number of test materials.

Grajcar *et al.,*(2009) investigated on the effects of keeping temperature constant during bainitic transformation temperature on remnants of austenitic fraction on a special grade of steel and discovered that as the temperature reaches a certain value, remained austenites will be equated to a certain critical value , while the carbon content reduces to a certain critical value; there is the largest grains of retained austenite in the ferritic body because of large amount of martensitic transformation temperature.

Grajcar *et al.,*(2011) designed the cooling condition for a special grade of alloyed steel on the basis of direct controlled cooling transformation diagrams (Figure 2.9), and found that the amount or value of ferrite and remained austenite is a function of direction of cooled parts given in the transformation region. It was also discovered that the highest quantity of retained austenite was obtained as irregular grains from the ferrite matrix and fine islands .

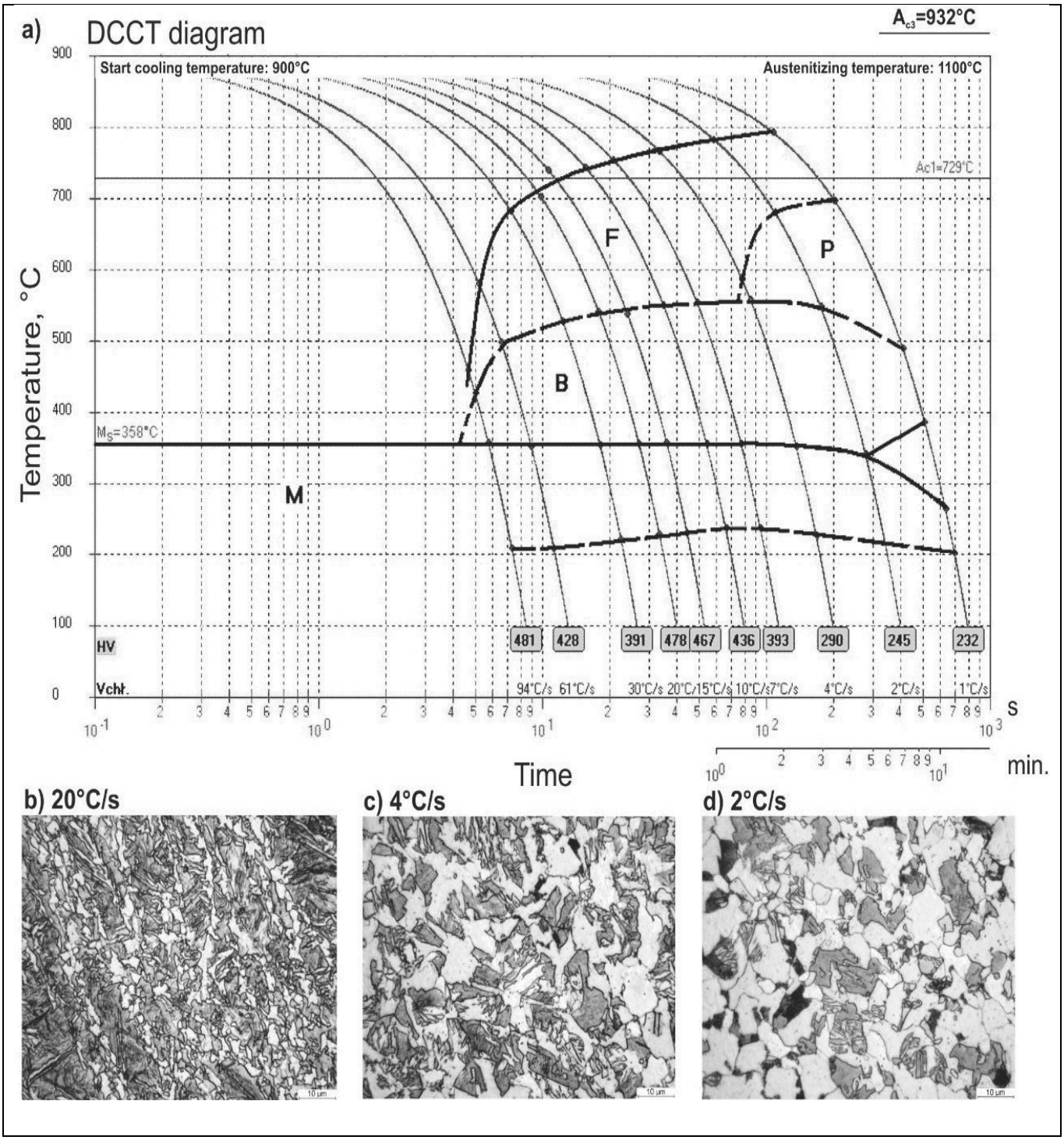

Fig.2.9:The DCCT Diagram of Si-Al Microalloyed TRIP Steel (Source :Grajcar *et al.,*2011)

Grajcar *et al.,*(2008) investigated on how plastic deformation influences low and medium carbon steel as these steadily cools and transforms. It was found that the developed steel possess ferrite and bainitic sections that extended only few inches in the time axis and section of pearlites sent out. It was also discovered that the plastic deformation of steel has a profitable influence on the shape of supercooled austenite curves.

Homma *et al.,* (2008) worked on the creation of methods of applying the evaluation on how steels used in constructing bridges performs and discovered that it contributed to the economical design, efficient fabrication and high performance of steel bridges.

Hutchinson *et al.,*(1977) studied the effect of degree of sensitive straining rises on thinning of metal at a spot under rectilinear tension and discovered that a relatively small amount of degree of straining dependence is known to lead to substantially increased straining prior to thinning down.

Furthermore, it was discovered that monitoring of temperature during hot-rolling was more essential at the end of rolling than at the end of hot-rolling. The proper thing usually done was to ensure that there was a reduction in the final pyrometer readings, as this could completely lower microstructural sizes as the pyrometer readings dropped (Laasraoui*et al.,*2007).This would also make it possible that small grains are produced ,which would give more desirable tensile strength and acceptable grain size (Plate 2.1). Granbom (2010) researched on the composition and tensile strength of DP-billets and discovered a modification in grain sizes and tensile strength caused by both constituent elements and hot-rolling phenomena such as pyrometer readings obtained while billets were evenly heated, degree of reduction and increase in pyrometer readings respectively.

Hutchinson *et al.,*(2013) studied products of a special steel grade with high values of ultimate tensile strength and discovered that alloying is important for obtaining good strength values that do not depend on the cooling temperature.

Harbib *et al.,*(2002) studied the effects of a heat treatment method upon the formation of grain sizes and mechanical properties of special type of stainless steel and found out that there was the formation of a unique structure of a special constituent element and precipitate of critical size in the samples.

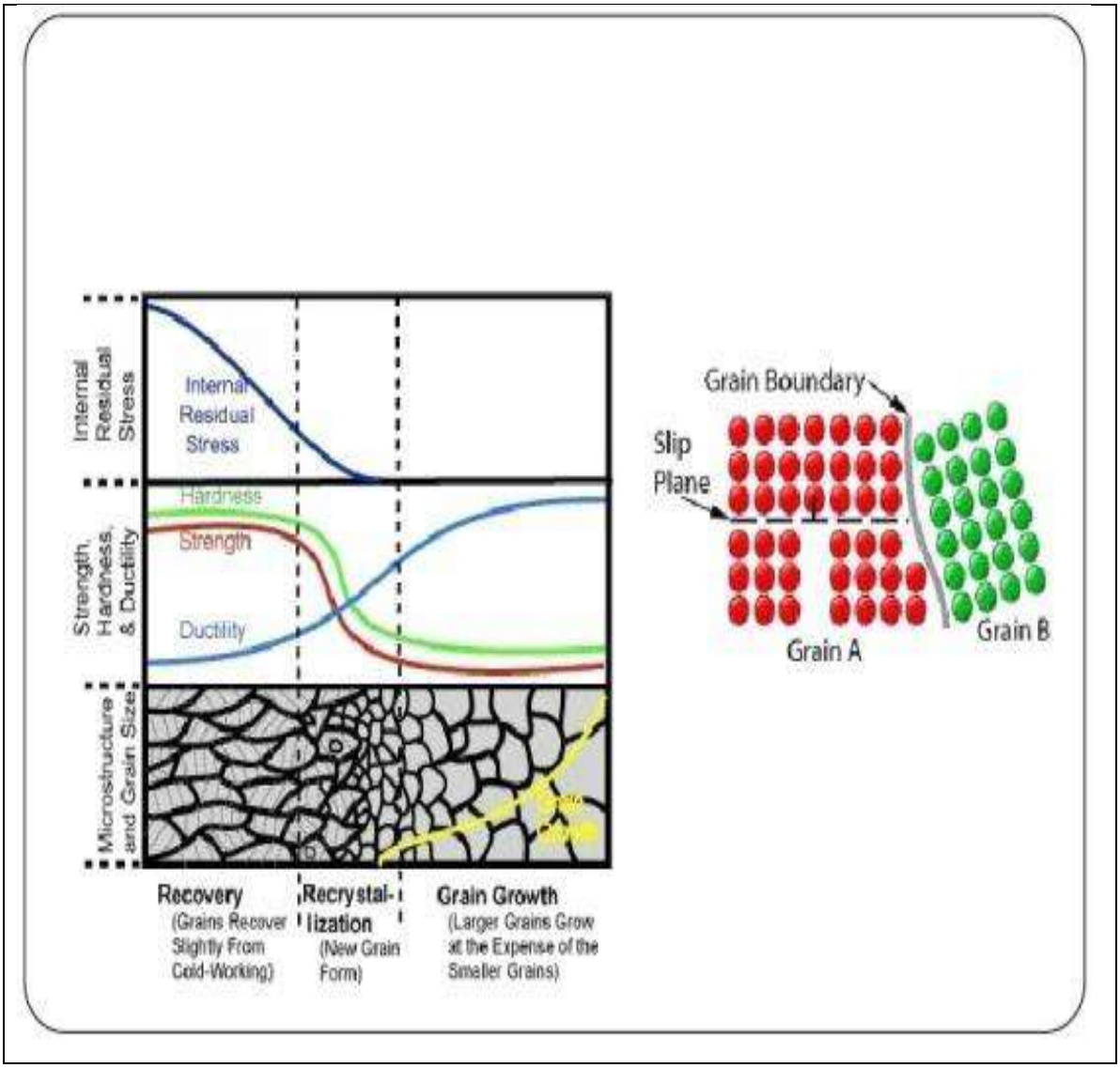

Plate 2.1: Grain structure (Source : Mallesham *et al .,2016)*

Holappa *et al.,*(2013) examined how to modify precipitates using those things that entered during a special treatment and discovered the condition in which those things that were in liquid form when they entered can be found with the special treatment.

Jena *et al.,*(1988) studied the effect of parts of the entire size of martensite on tensile strength of dual phase steel and discovered a non-linear relationship between strength and volume fraction of martensite.

Jing *et al.,*(2006) investigated the effects of a special heat treatment on impact toughness of precipitation hardening of a special grade of steel and discovered that increase in the pyrometer value during this treatment decreases the strength of the steel gradually while its toughness gradually increases.

Kabir *et al.,*(2014) studied the properties developed during case-hardeninig of metals and tensile behaviours of TMT steel bars and discussed the methods in which they shatter in terms of how they are made chemically and with elemental constituents.

Mallesham *et al.,*(2016) studied sheet metal rolling using two roller powered machine and discovered that as the gap between rollers decreases, the length of materials increased;also as the number of gaps increase, the length of materials also increase (Plate 2.2).

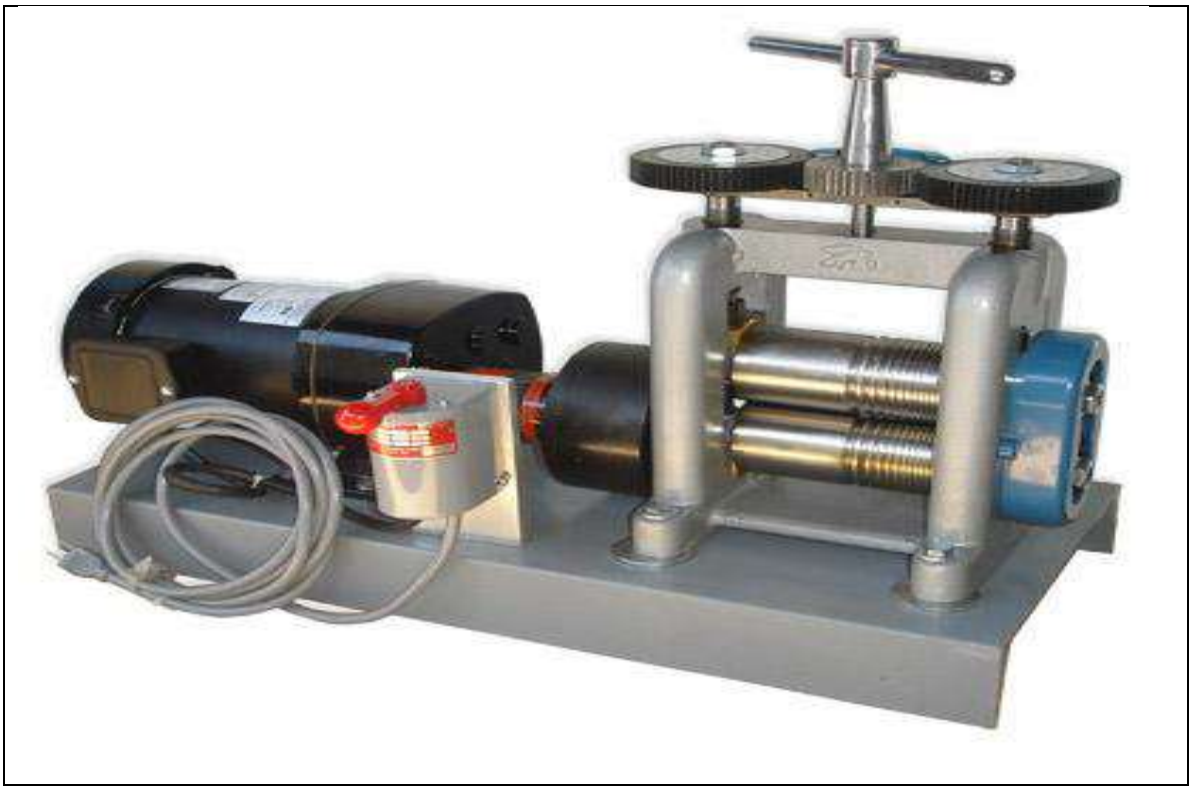

Plate 2.2: Electrical rolling machine (Source: Mallesham *et al., 2016)*

Mengtian *et al.,*(2017) investigated on the effect of faster reduction of temperature of metalwith the aid of special substance and dividing of grain sizes and mechanical properties of a special grade of steel and discovered that better grain sizes and mechanical properties were achieved.

Mihalikova *et al.,*(2007) studied the influence of degree of loading and hot-rolling straining on strength properties and ductilities of steels that have optimum mechanical properties and found that the combination of the degree of loading and category of test rebar made it possible to obtain the relationships of monitored variables in straining periods .

Nakagawa *et al.,*(1981) studied the effect of a special elemental constituent on how body crystals influence the mechanical and microstructural properties of double phase steels and found out that the element is not useful to these special grade of low carbon steel when quickly applied.

Kafi *et al.,*(2013) organised a comparison of the tensile strength, fatigue and fracture behaviour of a special grade ofsteel parts made by careful collection of special metal forming methods with respect to building orientation and discovered that horizontal orientation revealed better tensile strength properties when compared with the vertical orientation.

Kwon (1992) researched on a technology used to predict and control microstructural changes and mechanical properties in steel and established a new technology that predicts the microstructural changes that occur during hot-rolling to control the mechanical properties for optimization of the hot-rolling process.

Lakal *et al.,* (2012)studied the improvement in yield strength of deformed steel bar by quenching using a special statistical tool of optimization and found that the yield strength of the bar has been improved by controlling the quenching process parameters at optimum level, which was found from influence of variables by the tools.

Lawrynowicz *et al.,*(2002) studied the features of bainitic transformation in steels and discovered that there is a substantial information on the mechanism of bainitic

transformation in steel including the methods that are not clearly described as mobile and that can displace.

Lememoto *et al.,*(1992) studied computer modelling of phase transformation from work hardened austenite and discovered a mathematical model of transformation kinetics.

Nakagawa *et al.,* (1985) investigated on how the mechanical properties of dual phase steel relate to each other and discovered that there was a reduction in the carbon level from a higher to a lower value,which give maximum performance to bridge structure.

Nguyen *et al.,*(2019) investigated on the improvement for grain sizes of severely deformed steel of a special grade after hot-rolling process and improved the strong texture of the steel using special heat treatment method.

Mistry (2003) investigated on excellent quality steels for highway bridges and discovered that excellent quality steels has an optimized balance.

Peng *et al.,(2015)*studied the effects of a special heat treatment on strengthening character of a special grade of steel and discovered that it consists special precipitate and martensitic state that is highly densed with a high degree to dislocate.

Rao *et al.,*(1982) worked on the effect of the equipment used to lower the temperature on the grain sizes and remaining austenite in a special heat treated grade of steel that contains special element and obtained improved grain sizes.

Rashid (1980) studied alloyed steels that have High Strength values and showed that alloyed steels with highly placed values of strength,, have nearly same composition as plain carbon steels.

Safi *et al.,*(2013) compared and contrasted tensile strength and impact energy of specially heat treated steels and discovered that the best combination of strength and ductility can be achieved by the mixed structure of tempered martensite and lower bainite.

Shekher *et al.,*(2014) studied the effects of the path followed during hot-rolling and found that there is proportional relation between the degree of hot-rolling and the tensile strength.

Sierakowski *et al.,*(1997) studied how compounded reinforcements dynamically deforms and fractures the dynamic deformation and fracture and found that as the degree of loading is increased, the corresponding failure methods changes.

Simm *et al.,*(2017) studied the effect of a two-stage heat-treatment on the microstructural and mechanical properties of a maraging steel and showed that such a combination of characterization method is necessary to quantify this complex alloy and relate the microstructural changes to mechanical properties.

Singh *et al.,*(2014) developed dual phase steel with its its mechanical properties compared with low carbon steel.The intercritical annealing was found to assist the improvement in its mechanical properties.

Shoushtari *et al.,*(2011) studied the influence of heat treatment that takes place after welding on corrosive attack of zinc of a special grade of steel put in a salt medium and discovered that it improved the passivity of weld region by raising the pitting potential.

Shoushtari (2010) studied the effects of a special kind of heat treatment on corrosive tendency of a special grade and type ofsteel in a salt medium and discovered that when the pyrometer reading is raised to an immediate higher value,the power to pit is also raised;but on further increase,the pitting potential is reduced.

Song *et al.,*(2014) studied how to classify the outskirts of grain and measure their sizes in a special type of steel and discovered that the resulting microstructures showed very fine ferrite grains and homogenous distributed cementite particles.

Sujit *et al.,*(1994) investigated on a new criterion to predict effect or thinning failure under two way extension and found out that a new criterion that can be used under a wide range of forming conditions to predict limit strains has been developed.

Tiao *et al.,*(2016) worked on the effects of a joining process and heat treatment that takes place after joining on a very small size of precipitate and mechanical properties of an highly strengthened steel made strnnger by the addition of very small particles of special constituents elements and compounds and indicated that the welding process dissolves all pre-existing nanoparticles and causes grain coarseninig in the mixing zones.

Timokhina (2004) studied the effects of grain sizes on the stability of remained austenite in the plasticity caused by its ability to transform from one form to another and found out that their mechanical properties dependednot only on the individual behaviour of all the phases during deformation, but also on the rolling parameters.

Tomita *et al.,*(1985) studied mechanical properties of a special grade of high strength steel having a mixed structure of martensite and bainite, and discovered that it provided a better combination of strength and fracture ductility.

Vaynman *et al.,*(2008) investigated the chemical composition of Highly-Strengthened Steel that is made of special elemental constituents and showed that the increase in strength is brought about by high density of these special elemental constituents.

Wright (1997) investigated excellent property steel and discovered that the steel has superior weldability and toughness to ordinary steels.

Wang *et al.,*(2016) also investigated the effects of chemical composition, especially an uncommon element, on the properties of steels that evolve many constituents that richlycontain special elements and established a fact that the effects of one of these elements is multiple when other special constituent elements in steel are viewed.

Wang (2012) investigated on the influence of alloying on grain sizes and tensile strength of a dual phase steel and found out that the alloys have effects on the ferritic and martensitic grain sizes. Mathew *et al*., (2013) studied the effect of heat-treatment on medium carbon steel and found out that the mechanical properties of air cooled products were better than those without the treatment. They also suggested pure molten metal as feasible option. They found out that the tensile properties could be improved by thermal application treatment.

Xiong (2015) investigated the grain sizes and mechanical properties of dual phase steel produced by a controlled process of casting in the laboratory and said that grain sizes made of multifaceted ferrites, and other special and unique metallic phases and states were observed which had tensile strength in the optimum range

.

Senfuka *et al*., (2013) worked on TMT rebars produced by recycled steels and found out that there is unbalanced sharing of properties. Grajcar *et al.,* (2013) studied an ideal hot rolling operation of a special grade of steel and found that the rolling line was made up of rolling equipment and machines that expressed the effects of hot-rolling parameters fully. Mahmood *et al.,*(2014) studied the effect of residual thermal application on tensile strength of medium carbon steel and discovered an improved property.Alharbi, *et al*.,(2014) investigated on the effects of process parameters on the grain size and tensile strength of a special grade of steel and discovered that TMT process improved the mechanical properties and ductility.

Young *et al.,*(1994) investigated on the strength of mixtures of bainite and martensite and showed that a quantitative interpretation of peaked strength and mixed microstructure was achieved.

Zeng *et al.,*(2014) studied the effects of small particle inclusions on subsurface-initiated rolling contact fatigue of a railway wheel and found that the larger size of the inclusion gives rise to higher fatigue.

Zhuang *et al.,* (2008) worked on the influence of hot-rolling conditions on the mechanical properties of hot-rolled TRIP steel and found out polygonal ferrite, granular bainite and larger amount of retained austenite, which were obtained from the controlled hot-rolling processes.

Ausforming is the breaking down or austenitizing of steel after the ferrites but before the bainitic part of the Time Temperature Transformation curves (Figure 2.10). It was also shown that steels are fully austenitized when they are fully deformed without changing to other forms. There is martensitic transformation of steel when cooled to 25^{o}C temperature and tensile properties evenly conferred on it during cooling.

Also according to Total Materials Database, during iso-forming process the deformation of steel in the metastable austenite region was fully transformed. The ausforming treatment needed close monitoring to be achieved and steels are fully deformed during the process. And with these, improved properties would be conferred without lowering enlongation and impact strength. It was discovered that steels that involves quick

transformation at slight ausforming should be alloyed with certain special alloying elementsto create a far reaching austenitization by shifting the time temperature transformation curve to high values of time.

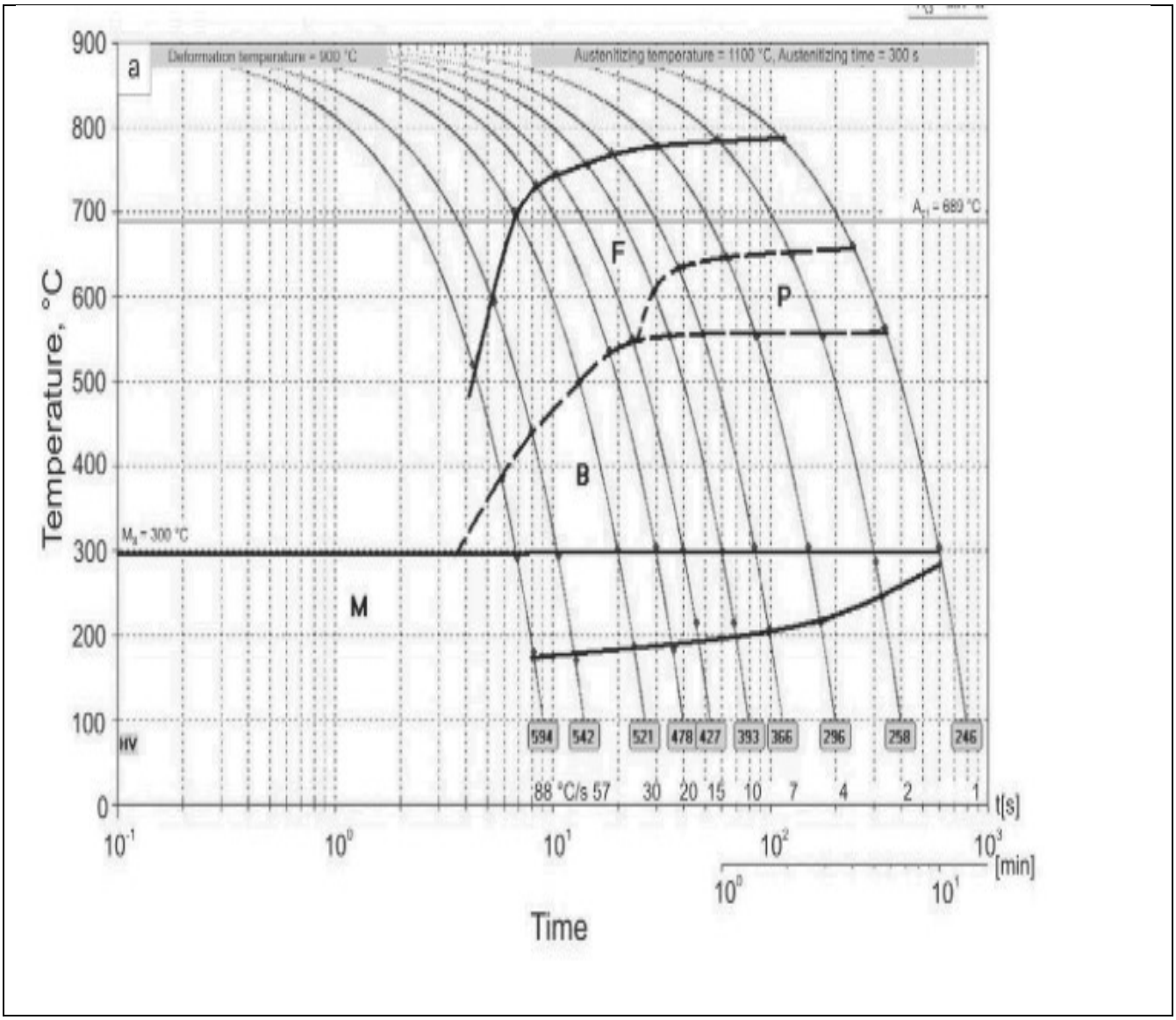

Fig.2.9: Continous Cooling Transformation Diagrams for TRIP Steel(Source:Grajcar *et al.,2008)*

It was also discovered that austenitization has to be as small as possible to cause increased degree of deformation. It had also been discovered that the change of austenite has to be done quickly to stop transformation to other steel compositions. This would ensure that the properties conferred during ausforming improved as they deform at a high rate as strain hardening developed. It had also been discovered that the rate of deformation of the steel is directly proportional to the tensile properties conferred on the steel.

Jing *et al.,*(2015) investigated on the influence of cold working deformation on dissolution density of a special grade of steel and concluded that cold working deformation influenced the properties of the materials appreciably.

Opiela *et al.,*(2012) worked on the influence of plastic deformation on Continous Cooling Transformation-diagrams of newly developed microalloyed steel and discovered that plastic deformation of steel at a certain specific temperature with respect to the beginning of state change results to distinct acceleration of pearlitic transformation and slight translation to bainitic transformation towards shorter time.

2.4 Optimization Models

Optimization or modelling is a way of using control algorithm or modules to control or co-ordinate a system or process of interest.It is a process used to represent or produce a construction or working of a system of interest (Maria, 1997). Models are verified by adding inputs and comparing their outputs with the system's outputs (Kleijnen, 1995).

Models are controlled or operated using well arranged computer languages, which can be re-interpreted(Rivet,1971). For example, an engineering model can be operated or simulated to explainhow microstuctural evolution affect the mechanical properties of a particular hot-rolling process by solid solution, ferrite formation, dislocation and austenitization (Majta *et al.,* 1996) For all industrial processes, modelling, optimization and control are the keys to enhance productivity and ensure product quality (Ashengroph *et al*., 2015)

2.4.1.Optimization models and simulation of hot-rolling processes

The design of control algorithm or software for control and monitoring of engineering processes is now in vogue as many available tools can be used to control them either graphically or otherwise, and hence design and develop a model of the specific problem (Malinov and Sha,2003; Oluwole,2009).

Optimization and control of grain growth, grain outskirts formation and nucleation are used to understand how the microstructure is evolved, as well as the mechanical properties (Zurob *et al.,2002; Zhang, 2001)*

Designining optimized rolling schedule is helpful for a good evolution of grain sizes and mechanical properties.Before a rolling plan is designed, comprehensive understanding of chemical composition and hot-rolling process is important.Mathematical models are commonly used to explain hot-deformation behaviour of steels.These model are results of experimental studies, which are limited to certain experimental conditions or steel compositions.They can be tested, validated and compared with the industrial data for them to be applicable. Hodgson (1993) in addition to the above, also stated that mathematical model have the advantages of reducing the cost or capital intensiveness or expensive industrial trials, improving rolling practices, developing new modules, saving hundreds of hours of lost time in designinig, helping one to understand the combined effect of variable hot-rolling parameters on the mechanical and microstructural properties, foretelling variables. From the work, some examples of mathematical models include empirical models, one dimensional models, artificial neural network (ANN), and Extremum theorems are given. One example of empirical model is the one by Schey (2004), which calculates the forces that distinguish the rolls using manual, spread sheet or simple computer programs.Example of one dimensional models are the Orowan classical models (Orowan, 1946), Bland and Ford model or technique which can be used to cold draw (Bland, 1948), Sim's model for hot-rolling (Sims, 1954)), Cook and McCrum model which enhances accuracy of rolls flattening (Cook, 1938) and Sellars models for description of microstructural evolution and meta-dynamic recrystallization, grain size and strain (Sellars, 1990; Beynon, 1992).

2.4.2. Classical Orowan Models

Finite element approach has been used to explain many optimization methods. A method that can compute dispersion of the roll force by mechanical perspective with many optimization methods for inhomogenous deformation as a function of different exponents of friction was suggested by Orowan (Orowan, 1946).A lot of researchers have proposed theories on approximations of Orowan method (Sims, 1954; Ford, 1964)

2.4.3.Sims Model

Sim's optimization proposes that angles in the roll gap are negligible .When this angle is multiplied by the stress due to shear, the answer is so infinitesimal. It also proposed that there is a friction that sticks to the rolls. Also, it states that the Hitchcock radius consists of the effect of flatness of roll and that this rolled material is so stiff (Sims,1954). Sim's model is commonly used in steel industry.Mean flow stress variables are computed with the aid of Sim's model. This is done by substituting the values of entry and exit thickness of the strip, its width, rolling force and work roll radius into the equation.

2.4.4. Ford and Alexander Model

Ford and Alexander proposed a modified Sim's model for average shear yield strength.

i.e. Fys = $\frac{P/W}{\sqrt{R(ho-h1)}[1.57+\frac{\sqrt{R(h0-h1)}}{(h0-h1)}}$…….2.9

i.e. MFs sims = $(\sqrt{3} \times Fys)$……..2.10

where Fys = Flow Yield Stress and

MFS = Mean Flow Stress respectively.

2.4.5.Friction-Hill Model

Friction hill model employs the assumed straight strain force of a slab.

The mean flow stress is given by Hill (1998)

MFSfriction-$_{Hill}$= $\frac{\sqrt{3P}}{2[\frac{1}{q(E-1)WLp}]}$……..2.11

Where Q = μlP$\sqrt{h}$……..2.12

H = $\frac{(h_o+h_1}{2}$ …….2.13

2.4.6.The General Model

The General Model(Figure 2.11) by Siciliano (2005) is shown below with the following inputs:

1. First size of Austenitic grain = 100μm
2. Niobium and (Ceq) wt%
3. The Reheating temperature = 1 200°C
4. The chemical composition
5. The Deformation schedule

Whenever there is deformation, the developed grain size, the strain, the new initial grain size, the amount of Niobium in solution and the addition of $t_{lp}/t_{0.05ps}$are taken as inputs for the next deformation.

This model can predict the following points:

1.Formation of crystals to solute drag

2. Even formation of crystals followed by grain nucleation

3. Formed precipitates due to strain rate that does not support crystal production

4. Weight of the precipitate

5.Temperature when there is no crystal formed

6. Active formation of crystals.

7. Mean Grain size

8.Mean flow stress

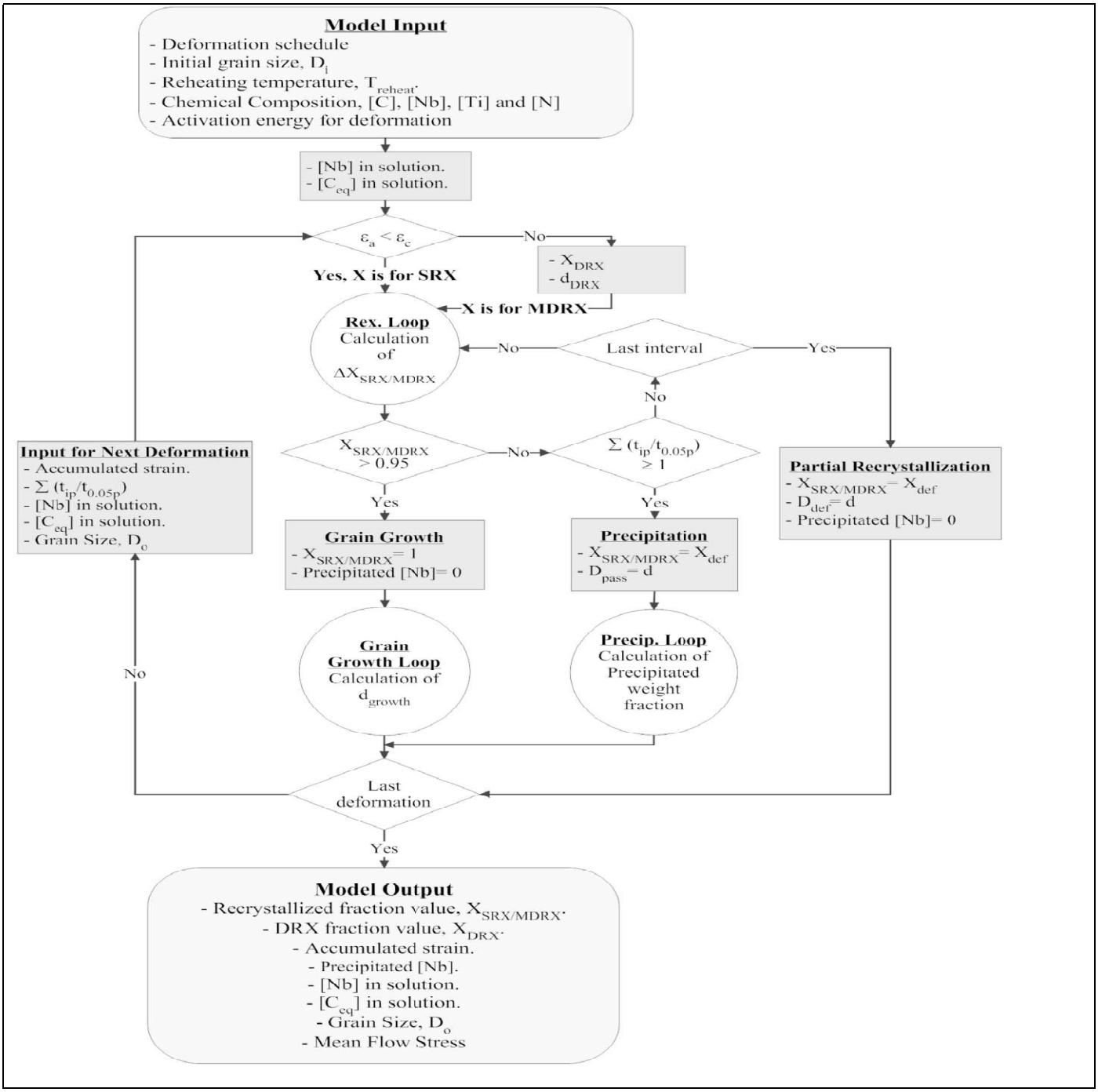

Fig.:2.10:General Model Flow Chart for MFS calculation (Source: Sicilian, 2005)

2.4.7.Response Surface Methodology in Hot-Rolling Processes

Response Surface Model (RSM) is a comprehensive method of modelling that explainshow the objective function responds to the design variables by using both the mathematical and statistical algorithms. Response Surface Methodology uses an assumed model on the basis of function fitting concept to replace experimental and numerical models (Myers, 1990; Bucher, 1999).Response Surface Methodology has been in all kinds of areas of study such as where processes are analysed to know if they are reliable, where research is donevigorously and in engineering control.Based on experimental data, response model is developed and normalized by significance analysis and analysis of variance (ANOVA).Finally, effects of different variables on optimization objective or goals are explained comprehensively based on the response model.This developed approach can be suitably used in the optimization with multiple variables and objectives. In general, Response Surface Model design is carried out by designing variables and objective function,designing of experiment (DOE),establishment of the response model, analysis of the direct and interactive effects and optimization of the response model (Cui *et al.,* 2018). Permanasari *et al.,*(2018) investigated on the modelling and optimization of hot-rolling process of A36 structural steelby using Response Surface Methodology and obtained optimum properties of the steel.Cui *et al.,*(2018) investigatedhow the surface can be work-hardened and optimized by the use of coldroll-beating splines based on an improved double-response satisfaction function methods and discovered that the satisfaction degree of the improved response model is an optimized value. The optimized parameters are roll speed or certain specific value, degree of feeding of a particular value and work rate of a certain value.Ashengrroph *et al.,*(2013) investigated on the application of special optimization tool and Response Surface Methodology for improving conversion of a special substance into another special substance using a specially sophisticated technique and obtained an optimum conversion.

Peasura *et al.,*(2019) studied the use of Response Surface Methodology for modelling of heat treatment done after welding in a steel pressure vessel of a special grade and discovered that the time is the dominant mechanism

Benuwa *et al.,*(2016) carried out a comprehensive research of particle swarm optimization and was able to present a comprehensive investigation of Particle Swam Optimization, as well as a proposed theoretical framework to improve its implementation

Liu *et al.,*(2017) carried out a research of optimization techniques used in the composite recycling area, especially on the state-of-the-art steps towards a research agenda and was able to apply the methods in the design of experimental methods to improve the quality of recyclates.

Venter (2010) reviewed optimization methods and focused on techniques that are commonly used in engineering optimization applications with suggestions to the designer to select an appropriate technique for a specific problem at hand.

Ghasetemalizadeth *et al*., (2016) reviewed optimization procedures in Artificial networks, and introduced optimization techniques in neural networks, comparing the methods to three problems of parity.

Amaran *et al.,* (2016) also reviewed co-ordination of optimization, focusing on algorithms and applicationsand laid emphasis on the stresses involved in the co-ordination of optimization when examined relatively with algebraic model-based mathematical programming.

Andrei *et al., (*2010) conducted an overview of the Response Surface Methodology and carried out a complete review of basic experimental designs for fitting linear response surface models, discussed more recent modelling techniquesin Response Surface Models with emphasis on Taguchi's robust parameter design.

William *et al.,*(1996) carried out a detailed review of Response Surface Methodology and emphasized on the practical applications of the methods.

Behera *et al.,*(2018) experimented on the application of response surface methods (RSM) for optimization of leaching parameters for ash reduction from low-grade coal and proposed a quadratic model for best results.

Mohktar *et al.,* (2013) investigated on how to analyse by comparing the effects of Response Surface Methodology and Artificial Neural Network on medium optimization for a special substance under certain condition and suggested a quadratic regression model.

Quadros *et al.,*(2014) worked on analysis of variance (ANOVA) and Response Surface Analysis of pulling force and toque in drilling granite fiber reinforced epoxy composites by using special method and proposed a mathematical model.

Analysis of Variance (ANOVA) is an analytical tool used in statistics that breaks down varied observation found inside a set of data into two parts known as sophisticated factors and experimental factors (Wil Kenton,2019). ANOVA is used to determine the influence that independent variables have on the dependent variables in a regressive study.

Nist *et al.,* (2012) in their Engineering Statistics Handbook, stated that a contour plot is a statistical tool used as a graphical method for showing the x, y and z axis of a surface by plotting constant z lines, called contours on a two –dimensional format..

2.5. Filling the Research Gap

The present study is undertaken to address the limitation of lower yield strength and coarse grain size, conferred by chemical composition on the tensile and grain sizes of the steel grade during conventional hot-rolling process. The study is designed to investigate on how best to improve the yield strength and grain size of the hot-rolled steel grade using the effects of finish rolling temperature, percentage total deformation and rolling strain rate; and to further understand how best to optimise these rolling process parameters for simultaneously improved properties of the steel, and successful and cheaper hot-rolling operations.

CHAPTER THREE
MATERIALS AND METHODS

3.1 Materials

The billets used in this research wasof St60Mn steel grade measuring 12 x 12 x 1200 cm. The source was from DangoteIntergrated Steel Rolling Company. The chemical constituents are shown in Table 3.1. The mechanical properties of the control sample of the material is also presented in Table 3.2 .

3.2 Determination of PTD

3.2.1 Measurement of draft and controlof PTD during hot-rolling process

The adjustable height of the exit roller guide or roll grooves (h_i/h_f), was used to control the drafts (Δh) and the percentage total deformation (PTD) during the hot-rolling process.

$$\Delta h = h_i - h_f \quad (3.1)$$

Where h_i and h_f are initial and final heights of the roll grooves respectively and

$$PTD = \frac{A_i - A_f}{A_i} x\ 100\% \quad (3.2)$$

Where A_i and A_f are initial and final cross-sectional areas of the billets respectively. The initial height (h_i) and final height (h_f)of the exit roller guides were measured with the vernier callipers and filler gauges, and varied by using exit roller guides of different heights or kept constant by using exit roller guides of the same height, during the hot-rolling process.

Table 3.1: Chemical Composition of ST60Mn Steel

Chemical Compositions (%)									
Steel Grade	**C**	**Si**	**Mn**	**P**	**Cr**	**Ni**	**Cu**	**S**	**N**
ST60Mn	0.41	0.24	1.12	0..021	0.008	0.02	0.03	0.03	0.010

Table 3.2 Mechanical Properties of the as-cast Control Sample

Steel grade	Tensile strength (MPa)	Yield strength (MPa)	Percentage enlongation (%)	Bendability	Impact strength (joules/mm²)	Hardness (HB)
ST60Mn steel	500	420	10	Mandrel 48/180°	0.4000	140

3.2.2 Calculation of PTD

Calculation of the PTD of the samples from the billets was done using equation 3.2,

$$PTD = \frac{Cross\ sectional\ area\ of\ the\ billet - Cross\ sectional\ area\ of\ rolled\ sample}{Cross\ sectional\ area\ of\ the\ billet}\ x\ 100\%$$

$$\text{PTD} = \frac{A_i - A_f}{A_i} \text{ x } 100\%$$

Where

A_i =Cross sectional area of the billet,

A_f=cross sectional area of the hot-rolled sample.

3.3 Determination of the RSR

3.3.1 Measurement and calculation of RSR

Calculation of RSR of the samples from the billet was done with the relation,

$$\text{RSR } (\epsilon) = V_r\left(\frac{1}{R\Delta h}\right) \ln \frac{h_i}{h_f} \quad (3.3)$$

Where V_r= (Velocity ratio) =2πRn

R = average roll radius,

Δh = draft during rolling

h_i = Initial thickness of the billet before rolling

h_f =final thickness of the billet after rolling

v_r =velocity ratio of the rolls during rolling

n = speed of the rolls in revolutions per seconds.

3.3.2 Control of the RSR during Hot-Rolling

The RSR, (ϵ),were controlled by increasing or decreasing the roll speed (V_r) and rolling time through the HMI (computer) by using a lever device in a machine panel, called the joy stick. The measured roll speed is substituted in the rolling strain equation to get the value of the rolling strain rate (see equation 3.3).

$$RSR\ (\in) = V_r\left(\frac{1}{R\Delta h}\right) ln\frac{h_i}{h_f}$$

So the roll speed was increased by raising up the joy stick and decreased by lowering it in this manner the rolling strain rate was either kept constant or varied and their values calculated using the equation of hot-rolling above.

3.4 Determination of FRT

3.4.1 Tracking of FRT

The Jenway digital pyrometer model 220k, was used to monitor the process temperature at the furnace area and finishing stands. The points at which temperature readings were obtained include the finishing stands respectively.

3.4.2 Control of FRT during hot-rolling

The furnace reheat temperature was increased or decreased by opening or closing the air and oil valves of the reheat furnace through the computer respectively. In this way, the FRT was controlled through the HMI computer, at the furnace pulpit. Since the air and oil ratio in the furnace controlled the strength of the flame used to reheat the billets, the valves were closed or opened to low or high percentages respectively and the strength of the flame was decreased or increased respectively, thereby affecting the FRT

3.5 Research Experimental Procedures

Three hundred and twenty four samples of the steel billet grade measuring12 x 12 x 1200 cm were loaded into a reheating furnace at 1230°C and hot-rolled into 12, 14, 16 and 25 mm of rebars, at FRT of 915, 917, 919, 921, 923, 925, 927 and 929°C, RSR of 4000, 4500, 5000, 5500,6000, 6500, 7000 and 7500 S^{-1}, and PTD of 96.0, 96.5, 97.0, 97.5 , 98.0, 98.5 , 99.0 and 99.5 percent respectively. Factorial experimental design was used as shown in Tables 3.3, 3.4 and 3.5 respectively.

.

Table 3.3: Changing FRT and keeping RSR constant at each PTD.

PTD	**RSR (S^{-1})**																							
(%)	5000								6000								7000							
	FRT (°C)								**FRT (°C)**								**FRT (°C)**							
96.0	915	917	919	921	923	925	927	929	915	917	919	921	923	925	927	929	915	917	919	921	923	925	927	929
98.0	915	917	919	921	921	925	927	929	915	917	919	921	923	925	927	929	915	917	919	921	923	925	927	929
99.0	915	917	919	921	921	925	927	929	915	917	919	921	923	925	927	929	915	917	919	921	923	925	927	929

Table 3.4: Changing RSR and keeping FRT constant at each PTD.

PTD	**FRT (°C)**																							
(%)	915								917								919							
	RSR X 10^3 (S^{-1})								**RSR X 10^3 (S^{-1})**								**RSR X 10^3 (S^{-1})**							
96.0	4.0	4.5	5.0	5.5	6.0	6.5	7.0	7.5	4.0	4.5	5.0	5.5	6.0	6.5	7.0	7.5	4.0	4.5	5.0	5.5	6.0	6.5	7.0	7.5
98.0	4.0	4.5	5.0	5.5	6.0	6.5	7.0	7.5	4.0	4.5	5.0	5.5	6.0	6.5	7.0	7.5	4.0	4.5	5.0	5.5	6.0	6.5	7.0	7.5
99.0	4.0	4.5	5.0	5.5	6.0	6.5	7.0	7.5	4.0	4.5	5.0	5.5	6.0	6.5	7.0	7.5	4.0	4.5	5.0	5.5	6.0	6.5	7.0	7.5

Table 3.5: Changing PTD and keeping FRT constant at each RSR.

RSR	**FRT (°C)**																							
X	915								917								919							
10^3(S^{-1})	**PTD (%)**								**PTD (%)**								**PTD (%)**							
96.0	96	96.5	97	97.5	98	98.5	99	99.5	96	96.5	97	97.5	98	98.5	99	99.5	96	96.5	97	97.5	98	98.5	99	99.5
98.0	96	96.5	97	97.5	98	98.5	99	99.5	96	96.5	97	97.5	98	98.5	99	99.5	96	96.5	97	97.5	98	98.5	99	99.5
99.0	96	96.5	97	97.5	98	98.5	99	99.5	96	96.5	97	97.5	98	98.5	99	99.5	96	96.5	97	97.5	98	98.5	99	99.5

3.7 Equipment

The following equipment were used for the study.

(i) Hardness Tester Metatest 38456 as shown in Plate 3.8 was used to test the hardenability of the samples.

(ii) Metallographic Microscope Metallux 2 shown in Plate 3.14, and the Optical Microscope with image capturing device, obtained from the Materials Testing Laboratory of ObafemiAwolowo University Ile-Ife were used to test the samples micrographs in the laboratory.

(iii) Metaserve Cut-off Machine as shown in Plate 3.9 was used for sectioning the samples.

(iv) Mounting Press Model Minor as shown in Plate 3.10 was used for the mounting of the samples.

(v) Metaserve Rotary Polisher as shown in Plate 3.13 was used to polish the selected sample surfaces.

(vi) Alba Automatic Bar Bender as shown in Plate 3.7was used to test the ductility of the samples.

(vii) Universal Materials Testing Machine Type UPD 100S shown in Plate 3.5 obtained in the Quality Control laboratory of DangoteIntergrated Steel Company PLC, was used for the samples TS, YS, PE, PRA and YME.

(viii) Pendulum Impact Testing Machine PSW 300 as shown in Plate 3.6 was used to test the impact energy of the samples.

(ix) Belt Grinding Machine Type I-VIS as shown in Plate 3.11 was used for the rough grinding of the samples' surfaces.

(x) Metaserve Rotary Pregrinder as shown in Plate 3.12, was used for smooth grinding of the samples' surfaces.

(xi) Coulmat 702 as shown in Plate 3.1 was used to determine the chemical composition of the steel grade sample.

(xii) Roughing Mill Section of the rolling line in Plate3.2 shows where the first phase of the plastic deformation of the billets takes place, as they leave the reheating furnace.

(xiii) Loopers Stand in Plate 3.3 was used to control the tension in the billets during rolling.

3.7. DETERMINATION OF THE CHEMICAL COMPOSITION OF BILLET

A sample of the billet is cut with a gas cutter and taken to the laboratory for chemical test. The chemical analysis of the billet sample was done using the Coulmat 702 in Plate 3.1 .

Plate 3.1: Coulmat 702

3.8. HOT-ROLLING OF BILLETS

The steel billet grade measusring 12 x 12 x 1200 cm, were loaded into a reheating furnace at 1230^{o}C and hot-rolled into 12 , 14, 16 and 25 mm diameters of rebars, using the roughing mill shown in plate 3.2, looper's stand in Plate 3.3 and the intermediate and finishing mill in Plate 3.4 .

The billets were heated to the temperature inside the reheating furnace and subsequently pushed out through the exit of the furnace, into the roughing stand. The initial deformation of the billets started at the roughing stand.Here as the billets passed through the roll grooves, passes and the roller tables between the mill stands, they were subjected to enormous strain, tension and compression, which aided its hot-working. The looper's stand helped to reduce tension in the billets as they passed through roll grooves in the mill stands.

Plate 3.2: Exit end of Reheating Furnace and The Roughing Mill.

Plate 3.3: looper's stand.

Plate 3.4: Intermediate and Finishing Mill.

3.9 Mechanical Test

3.9.1. Testing for tensile properties

Tensile properties of the hot-rolled samples were measured in accordance with internationally recognized standardization. Eight mechanical properties were measured with the aid of the U.T.S.machine shown in Plate 3.5 .

A sample of the hot-rolled rebar is cut and taken to the laboratory for mechanical test.The rib size and the diameter of the test samples are measured with the vernier caliper.The length of the samples were measured with a meter rule .All measurements were done according to the British Standard (BS 4449). .The samples were marked with a punch and inserted into the clamp of the U.T.S machine, which pulls the test sample under tension until it undergoes necking and breaks.The broken samples were then collected for subsequent measurements and calculation of the above mechanical properties.

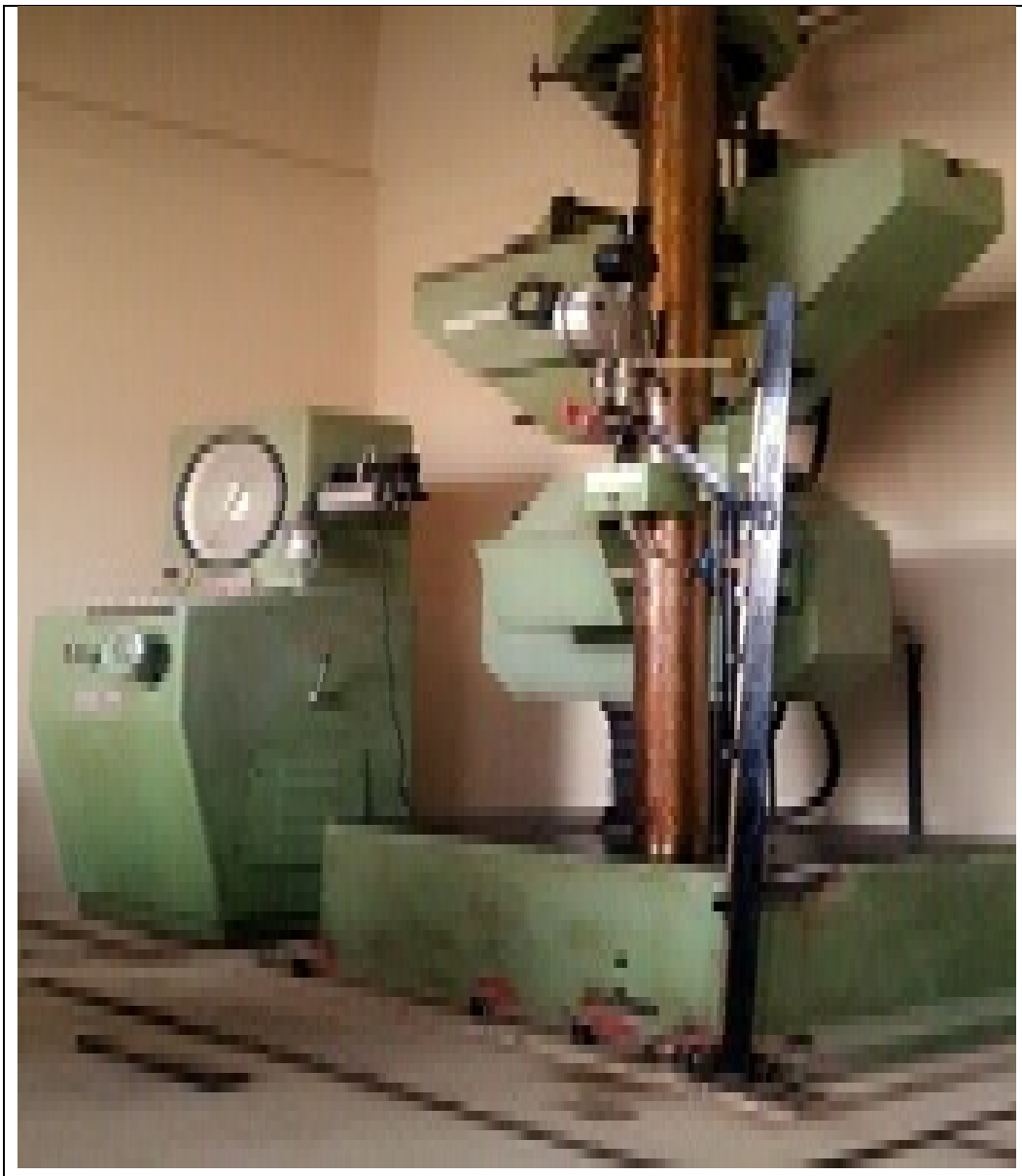

Plate3.5: Universal Materials Testing Machine.

3.9.2 Measurement of Impact Energy

The hot-rolled samples were sectioned into small lengths of certain values and four equal-sized shapes of certain measurements using the lathe machines. These were bevel-marked centrally. The samples were positioned at the horizontal before crushing. The impact energy measuring instrument shown in Plate 3,6 was used to crush them. The test samples were crushed by releasing the swinging arm of the impact energy measuring instrument in Plate 3.6 on the test sample, which breaks. The final value is read from the calibration of the machine as indicated by the pointer.

Plate 3.6: Pendulum Impact Testing Machine

3.9.3. Measurement of bendability or ductility

Test samples were determined in accordance with the internationally recognized standardization, using specific dimensions of the instrument that measures ductility shown in Plate 3.7 . For smaller rebars like 12 and 14 mm, 4 x dimension, was used, while for larger dimensions above 16 mm, 7 x dimension, was used;'dimension' represent the diameter of the bar. Angles less than 90^{o} were chosen by the machine because of the grade of the billet, which is a medium carbon steel. Ductility test checks for the presence of cracks in the rebar and helps to determine the formability or ductility of the material

Plate 3.7: Alba automatic Bar Bending Machine

3.9.4. Measurement of Hardness

The samples were tested for hardness using hardness tester shown in Plate 3.8. Load or force was applied for a certain duration of time and an impression was made on the specimen by the spindle of the machine, which was later measured. The values of the force and the dimension of the small impression were substituted in a standard equation to calculate the values of the material.Brinell test method was employed.

Plate 3.8 Hardness Testing Machine

3.10 Metallographic Examination

3.10.1. Selection of Samples

Samples of rolled rebars that passed the dimensional tests of quality control, were selected at the end of each rolling cycle, cut with gas cutters and taken to the laboratory for further metallographic procedures as in the following sections.

3.10.2 Sectioning the Specimens

After selecting the areas of interest, specimens were sectioned with Aluminium Oxide (Al_2O_3) abrasives and water-base additive containing soluble oil as coolant, using the metaserve cut-off machine shown in Plate 3.9..

Plate 3.9: Metaserve Cut-Off Machine

3.10.3 Mounting the Specimens

Specimens were mounted with special polymers such as Bakelite and Acrylic moulding powder, by applying heat and pressure using the Mounting Press Model Minor shown in Plate 3.10. This was done to provide the specimens with good edge retention during subsequent processes.

Plate 3.10: Mounting Press Model Minor

3.10.4 Grinding

The specimens were ground in series of steps using successively finer abrasives such as silicon carbides and aluminium oxide with grit sizes of 240,320,400 and 600 grit, and water as coolant, which was used to flush the surface debris. The grinding was done manually on a single specimen, one after the other, using the belt Belt Grinding Machine shown in Plate 3.11 and the Metaserve Rotary Pregrinder shown in Plate 3.12

Plate 3.11: Grinding Machine

Plate 3.12: Metaserve Rotary Pregrinder

3.10.5 Polishing

The test specimens were polished to give them fine smooth finish, using the Metaserve Rotary Polisher shown in Plate 3.13, by rotating them on cloths impregnated with aluminium oxide. The specimens were then etched with 2% nital and dried with a specimen dryer.

Plate 3.13: Metaserve Rotary Polisher

3.10.7 Optical Microscopy

The specimens were then viewed with the Metallographic Optical Microscope metallux 2 shown in Plate 3.14, a metallograph which depended on light and a lens system to reproduce the polished and etched specimens surfaces and a camera that made photomicrographs of the surface replica.

Plate 3.14: Metallographic Optical Microscope

3.11. Microstructure Characterization

The microstructure evolution during hot rolling of the steel grade was characterized in terms of the mean grain size. The Gwyddion software for grains size analysis of microstructures was employed to determine the mean grain sizes of the hot-rolled samples. The relative measurement of the grains and grains statistical procedure of Gwyddion, using edge detecton method, which was used to study grain properties, by the simplest function. The procedure is from Data Process→Grains→Statistics. This function calculates the total number of grains, their total projected area, both as an absolute value and as a fraction of total data field area, total grain volumes, total length of grain boundaries and the mean area and equivalent square size of one grain. The mean size is calculated by averaging the equivalent square sides so its square is not, in general, equal to the mean area. Overall, characteristics of the marked area can be obtained with Statistical Quantities tool when its use mask option is switched on. By inverting the mask the same information can be obtained for the non-grain area.

3.12. Optimization Method

The Response Surface Methodology (RSM) was used to model the properties relationship with the rolling process parameters. The Response surface methodology, which relied on statistical principle was used to study the combined influence of the hot-rolling process parameters on the properties.

3.12.1 Response Surface Methodology

Response surface methodology was employed for the optimization of the YS, TS and Impact energy of the hot rolled steel grade. Actual data from the experiment were used for the RSM experimental design. The behaviour of the YS(σ_y,), TS(σ_T),and Impact energy(E_{ImT}), as obtained in the experimental data were modelled as functions of the FRT and RSR using the Response Surface Methodology (RSM).The response functions/equation was obtained from the design expert software .

The objective of the Response Surface Methodology is to decide the optimum settings for the variables and to see how the variables perform over the whole experimental domain, including any interactions such as the combined effect of the hot-rolling process parameters on the properties of the hot rolled steel grade. The FRT and rolling strain rate

were taken as two independent variables, which determine the response of the YS (σ_y), TS(σ_T) and Impact energy (E_{ImT}) of the steel to the hot-rolling process parameters. The experimental design and statistical analysis were done according to the response surface analysis method using Design Expert 6.0.8 software. Data obtained from the experiments was used to study the combined effect of the FRT (x_1) and RSR (x_2).The dependent variables (y) measured were the YS(σ_y), TS (σ_T) and Impact energy(E_{ImT}) of the hot-rolled steel grade. These dependent variables were shown individually as a function of the independent variables known as response function.

The cubic order three dimensional surface model was used to describe the relationship between each of the properties y, and the two independent variables (FRT; x_1, and RSR; x_2).The model was able to explain the curvature of the response and the relationship of the independent variables in the response surface. The data point (y, x_i, x_j) defines a curved surface in 3D space shown by the following polynomial (Karuppaiya *et al*., 2010; Lazic, 2004; Man *et al*., 2010). Constant coefficients are the parameters β_i, which are regressive. These coefficients are used to find the expected change in the response y per unit increase in x_i when the x_j is held constant and vice versa and are set up by regression analysis in the RSM programme.

$\Sigma\beta_j x_j$ is the main/individual effect, $\Sigma\beta_{jj}x_j^2$ are the curvature, $\Sigma_{i<j}\Sigma\beta_{ij}x_i x_j$ is the combined/interactive effect and e is the error. The design expert software package was used to obtain all the coefficients. The R^2 values and the probability obtained from the analysis of variance (ANOVA) was used to confirm the goodness of fit. The optimum values of the hot-rolling process parameters and the properties were obtained from the numerical analysis of the RSM package.

CHAPTER FOUR

RESULTS AND DISCUSSION

This chapter contains the results and discussions for influence of RSR, FRT and PTD on the tensile and grain sizes of the steel grade and the results and discussions of optimization of the hot-rolling process parameters. The eight mechanical properties considered include Tensile Strength (TS), Yield Strength (YS), hardness, ductility or bendability, impact energy, Percentage Enlongation (PE), Percentage Reduction in Area (PRA) and Young Modulus of Elasticity (E).

4.1 Results and Discussion for Influence of RSR at FRT of 915°C.

Table 4.1 displays the impacts that RSRhave on the mechanical properties of the steel grade. Figures 4.1-4.7displays the impacts that RSRhave on the above tensile properties at FRT of 915°C and variable PTD of 99.0 percent, 98.0 percent and 96 .0 percent respectively..

When the PTDwas recorded as 99.0 percent and FRT was recorded as 915°C , as the RSR increased from 4000 to 4500 S^{-1}, the TS increased from 611.3 to 614 MPa (Fig.4.1), YS increased from 432.1 to 432.2 MPa (Fig.4.2), PE decreased from 16.6 to 16 percent (see Fig.4.6), impact energy decreased from 0.48 J/mm^2 to 0.4606 J/mm^2 (Fig.4.4), Ductility increased from 45.95° to 46° (Fig.4.3), PRA decreased from 30.2 to 30 percent (Fig.4.7), hardness increased from 222 to 224 HB (Fig.4.5), E increased from 57 to 60 GPa (Fig.4.8). At 98.0 percent and 915°C FRT, as the RSR increased from 4000 to 4500 S^{-1},TS increased from 569 to 569.6 MPa (see Fig.4.1),YS increased from 418MPa to 419MPa (Fig.4.2), PE decreased from 19 to 18.7 percent (Fig.4.6), impact energy decreased from 0.5089to 0.5086 J/mm^2(see Fig.4.4), Ductility increased from 44.48° to 44.49° (Fig.4.3), PRA decreased from 36 to 34.9 percent (Fig.4.7), hardness increased from 222 to 223 BH (see Fig.4.5), E increased from 53.2 to 53.21 GPa (Fig.4.8).

At 96.0 percent PTD and 915°C constant FRT, as the RSR increased from 4000 to 4500 S^{-1}, TS increased from 509.5 to 511 MPa (Fig.4.1), YS increased from 411 to 417 MPa (Fig.4.2), PE decreased from 19.5 to 19.2 percent (Fig.4.6), impact energy decreased from

0.5195 to 0.519 J/mm^2(Fig.4.4), Ductility increased from 42.75º to 42.78º (Fig.4.3), PRA decreased from 40 to 39 percent (Fig.4.6), hardness increased from 216 to 217 HB (Fig.4.2), E increased from 40.83 to 40.98 GPa (Fig.4.8). The above same property trend is also applicable to the other RSR of 5000, 5500, 6000, 6500, 7000, and 7500 S^{-1}, and FRTof 917 and 919ºC,and the other constants of PTD of 98.0 and 96.0 percent.

As expressed above, if the RSR rises, the TS, YS, hardness, E and ductility also rise, while impact energy, PRA and PE decrease. The billets were completely broken down and yielded within the stands, which gave rise to maximally displaced mass of constituents and scattered smooth carbon particles.The billets were yielded because of a stoppage from components in the matrix and other related components. There was an inextensible relationship between the displaced components and other related components which stopped some movement in the matrix.. Because of these, TS, YS, hardness, E and ductility were increased in value. The increased E as RSR increased, showed how bulky the hot-rolled billets were. The same trend was also repeated by the values of ductility. At the same time, lower values of impact energy, PRA and PE was caused by tension in the lattice and uneven dislocated atoms, which gave rise to larger microstructural sizes and longer movement and as the pyrometer readings got higher, the microstructural sizes grew larger.

Table **4.1:** Effect of RSR at Constant FRT and variable PTD.

RSR (S^{-1})	PTD (%)	FRT (°C)	Hardness (HB)	E (GPa)	Ductility or Bendability (°)	TS (MPa)	YS (MPa)	PE (%	PRA (%)	Impact Energy (J/mm^2)
4000	99.0	915	222	57	45.95	611.3	432.1	16.6	30.2	0.4800
4000										
4000	98.0	915	221	53	44.48	569.0	418.0	19.0	36.0	0.5089
4000	96.0	915	216	40	42.75	509.5	411.0	14.8	40.0	0.5195
4500	99.0	915	224	60	46.00	614.0	432.2	16.0	30.0	0.4606
4500	98.0	915	223	53	44.49	569.6	419.0	18.7	34.9	0.5086
4500	96.0	915	217	40	42.78	511.0	417.0	19.2	39.0	0.5190
5000	99.0	915	229	61	46.05	614.6	442.0	18.5	29.8	0.4605
5000	98.0	915	224	53	44.50	570.0	418.0	18.4	34.5	0.5076
5000	96.0	915	218	42	42.90	512.8	417.0	18.9	39.9	0.5185
5500	99.0	915	229	61	46.25	622.0	445.0	15.0	26.8	0.4605
5500	98.0	915	225	55	44.53	572.3	420.0	17.3	34.2	0.5020
5500	96.0	915	220	42	43.45	520.1	419.0	17.7	39.8	0.5135
6000	99.0	915	230	62	46.28	629.0	449.0	14.6	26.3	0.4527
6000	98.0	915	226	55	45.00	580.0	420.0	16.0	34.1	0.5010
6000	96.0	915	221	44	43.52	539.0	419.0	16.9	39.0	0.5127
6500	99.0	915	231	65	46.34	635.7	450.0	14.4	26.0	0.4525
6500	98.0	915	227	56	45.20	600.0	421.0	15.9	33.5	0.4980
6500	96.0	915	222	44	43.6	598.6	420.0	16.3	37.8	0.512
7000	99.0	915	232	66	46.93	635.8	450.0	14.0	25.5	0.4508
7000	98.0	915	229	63	45.47	625.0	424.0	15.0	33.0	0.4505
7000	96.0	915	224	45	43.74	547.0	423.0	16.0	37.0	0.5110
7500	99.0	915	225	69	47.00	697.2	455.8	17.5	25.0	0.4200
7500	98.0	915	230	64	45.48	635.4	427.0	16.5	32.0	0.4207
7500	96.0	915	226	46	43.77	551.0	426.8	15.4	35.0	0.5090

Table 4.1 (continued): Effect of RSR at Constant FRT, variable PTD.

RSR (S^{-1})	PTD (%)	FRT (^oC)	Hardness (HB)	E (GPa)	Ductility or Bendability (^{o})	TS (MPa)	YS (MPa)	PE (%)	PRA (%)	Impact Energy (J/mm^2)
4000	99.0	917	227	60	46.04	614.0	456.0	15.0	29.9	0.4606
4000	98.0	917	223	53	44.49	572.0	428.4	18.5	34.7	0.5077
4000	96.0	917	217	41	42.8	512.7	424.0	19.9	40.0	0.5186
4500	99.0	917	228	60	46.24	621.0	464.0	14.5	26.9	0.4605
4500	98.0	917	224	54	44.52	579.0	436.0	17.4	34.3	0.5030
4500	96.0	917	219	41	43.00	520.0	428.0	17.9	39.9	0.5136
5000	99.0	917	229	61	46.27	628.0	476.0	14.3	26.5	0.4528
5000	98.0	917	225	54	44.98	583.0	443.2	16.3	34.2	0.5020
5000	96.0	917	220	43	43.51	538.0	440.0	17.0	39.0	0.5128
5500	99.0	917	230	64	46.33	634.7	480.0	14.0	26.0	0.4526
5500	98.0	917	226	55	45.10	598.0	444.0	16.0	33.8	0.4990
5500	96.0	917	221	43	43.50	580.0	442.0	16.5	37.9	0.5130
6000	99.0	917	231	65	46.91	634.8	481.0	13.5	25.8	0.4510
6000	98.0	917	227	61	45.40	599.0	445.0	15.2	33.7	0.4980
6000	96.0	917	222	47	44.60	571.0	443.0	16.4	37.6	0.5120
6500	99.0	917	222	68	47.00	635.0	482.0	13.2	25.7	0.4400
6500	98.0	917	228	62	45.80	599.3	446.0	14.7	33.8	0.4810
6500	96.0	917	223	49	44.70	572.0	444.0	16.3	37.8	0.5110
7000	99.0	917	233	69	47.20	636.0	483.0	12.6	28.5	0.4300
7000	98.0	917	229	62	46.00	599.7	447.0	14.6	33.4	0.4700
7000	96.0	917	224	50	44.80	573.0	445.0	16.2	37.4	0.5080
7500	99.0	917	234	69	47.50	637.0	485.0	12.1	23.0	0.4200
7500	98.0	917	230	63	46.50	601.0	449.0	14.2	43.0	0.4500
7500	96,0	917	225	50	44.90	574.0	447.0	16.0	37.0	0.5050

Table 4.1 (continued): Effect of RSR at Constant FRT, variablePTD.

RSR (S^{-1})	PTD (%)	FRT (°C)	Hardness (HB)	E (GPa)	Ductility or Bendability (°)	TS (MPa)	YS (MPa)	PE (%)	PRA (%)	Impact Energy (J/mm^2)
4000	99.0	919	235	70	47.51	638	486	12.0	22.0	0.4100
4000	98.0	919	231	64	46.90	602	450	14.1	32.0	0.4470
4000	96.0	919	226	51	45.00	575	448	15.8	36.0	0.4800
4500	99.0	919	226	71	48.00	689	487	11.8	21.0	0.4000
4500	98.0	919	222	65	47.00	603	451	13.7	31.0	0.4300
4500	96.0	919	227	52	45.20	576	449	15.6	35.0	0.4700
5000	99.0	919	220	55	44.91	508	443	19.4	30.8	0.4610
5000	98.0	919	219	51	43.47	566	423	20.4	39.0	0.5150
5000	96.0	919	214	39	42.72	507	419	21.2	48.0	0.5199
5500	99.0	919	222	58	44.00	611	446	19.1	30.5	0.4609
5500	98.0	919	221	52	43.50	568	424	19.6	37.0	0.5096
5500	96.0	919	215	39	42.75	505	420	20.5	45.0	0.5197
6000	99.0	919	226	59	45.00	613	454	18.9	30.0	0.4608
6000	98.0	919	222	52	44.46	570	427	19.4	34.8	0.5085
6000	96.0	919	216	40	42.80	511	422	20.2	43.0	0.5187
6500	99.0	919	227	59	45.23	620	463	18.0	28.6	0.4607
6500	98.0	919	223	53	44.50	577	435	18.6	34.4	0.5039
6500	96.0	919	218	40	43.00	518	425	19.8	41.1	0.5156
7000	99.0	919	228	60	46.24	626	475	17.7	26.6	0.4530
7000	98.0	919	224	53	44.90	582	442	18.3	34.3	0.5029
7000	96.0	919	219	43	43.49	536	439	19.2	40.0	0.5135
7500	99.0	919	229	63	46.30	633	478	17.3	26.1	0.4528
7500	98.0	919	225	54	45.00	596	443	17.9	33.9	0.5010
7500	96.0	919	220	43	43.50	570	441	18.6	38.8	0.5131

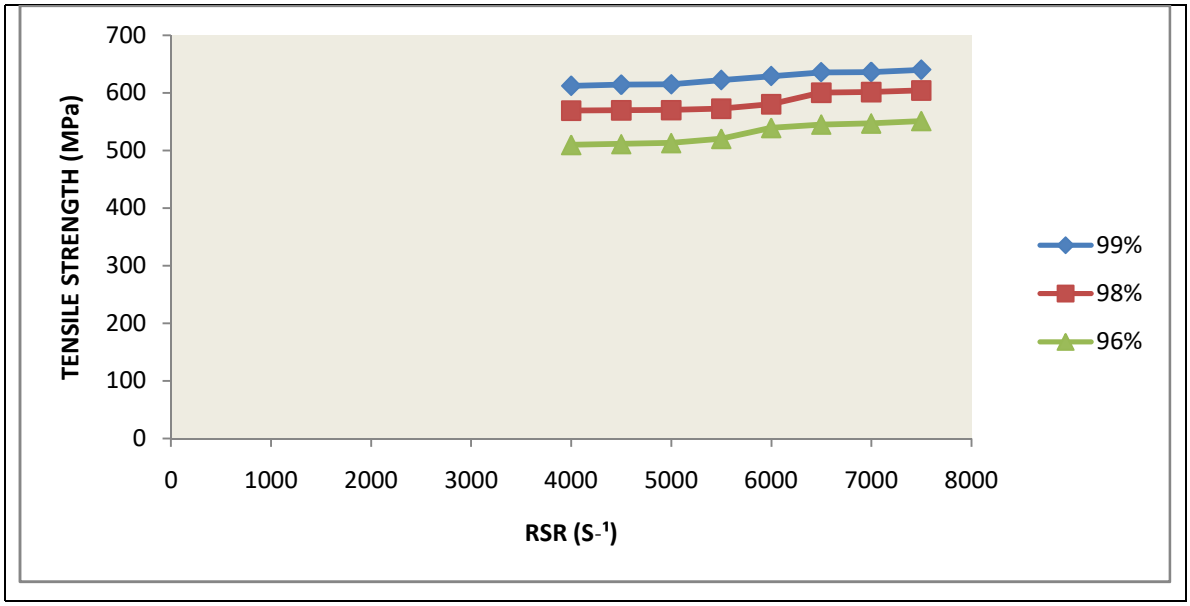

Figure 4.1: Effect of RSRon TS atFRT of 915°C and Variable PTD

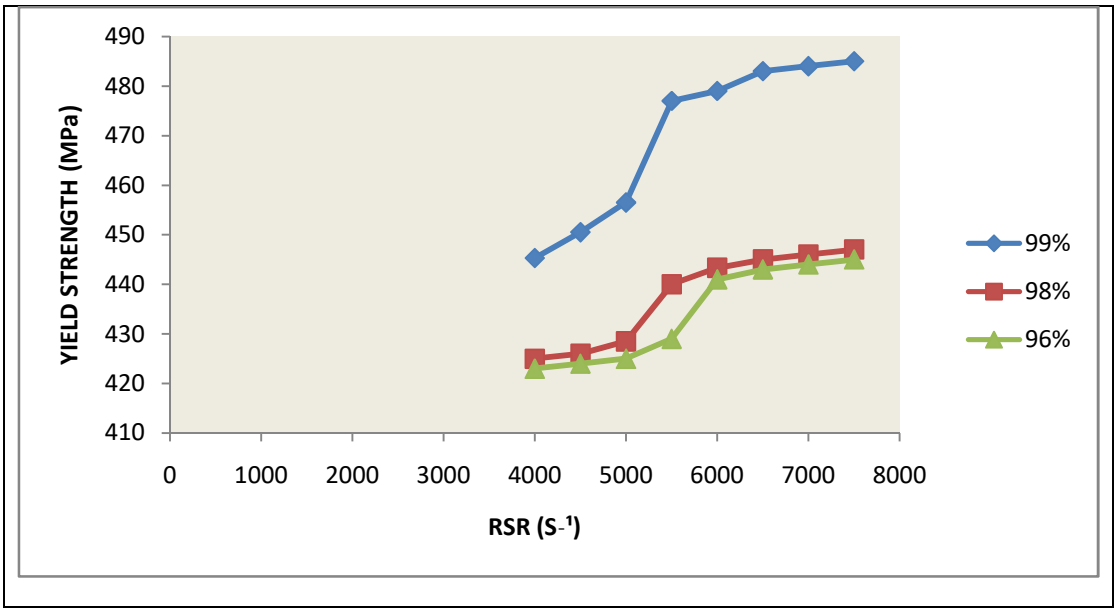

Figure 4.2: Effects of RSR on YS at Constant FRT of 915°C

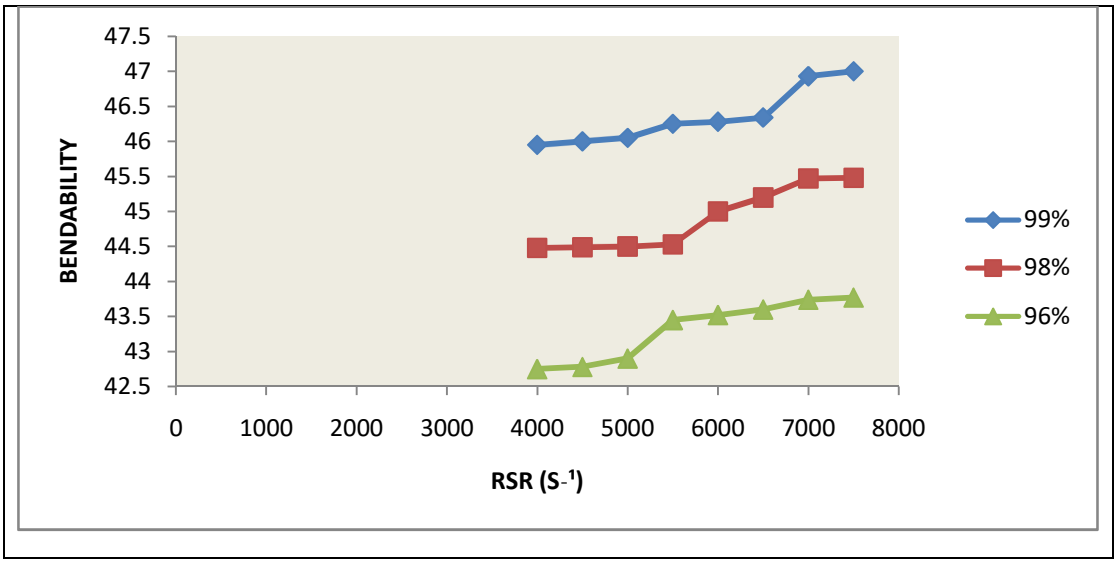

Figure 4.3: Effect of RSR on ductility at Constant FRT of 915°C and Variable PTD.

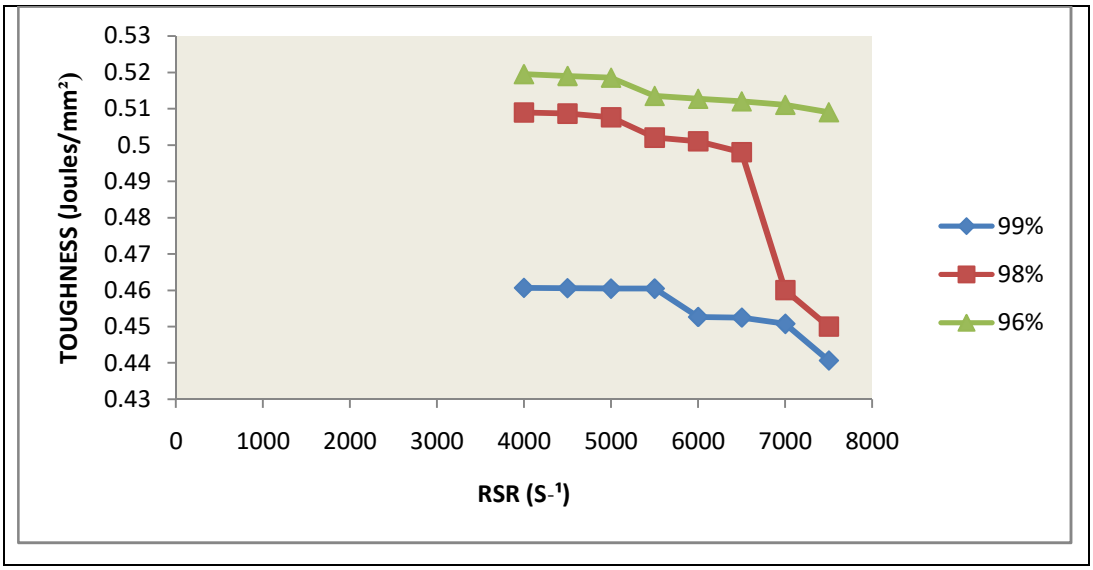

Figure 4.4:Effect of RSR on Impact Energy at FRT of 915°C and Variable PTD

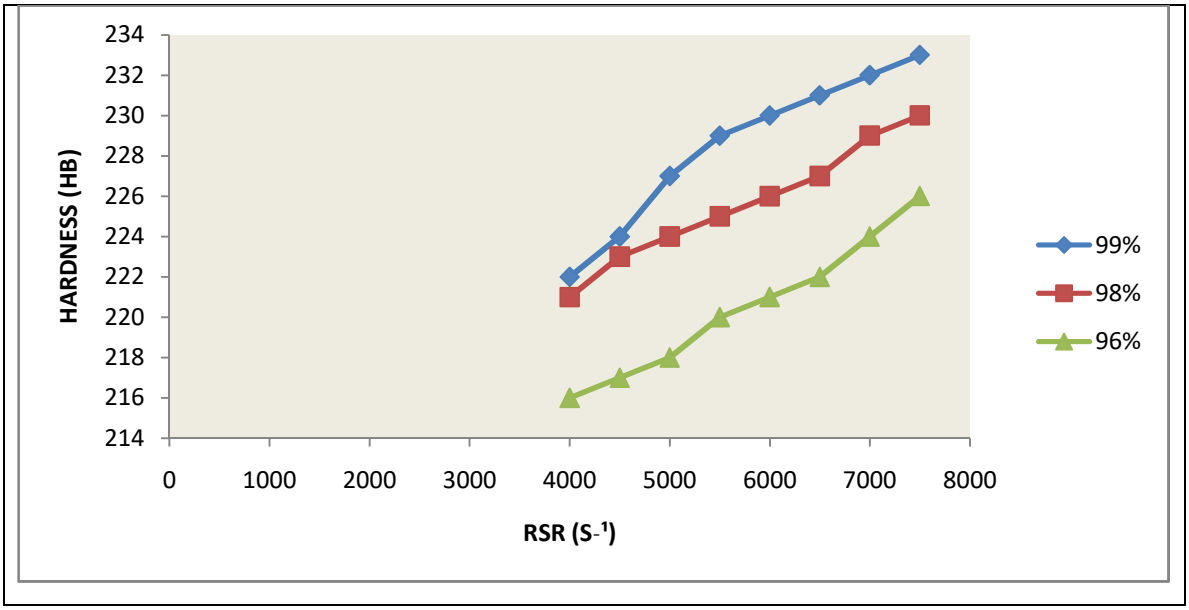

Figure 4.5:Effect of RSR on Hardness at Constant FRT of 915°C and Variable PTD

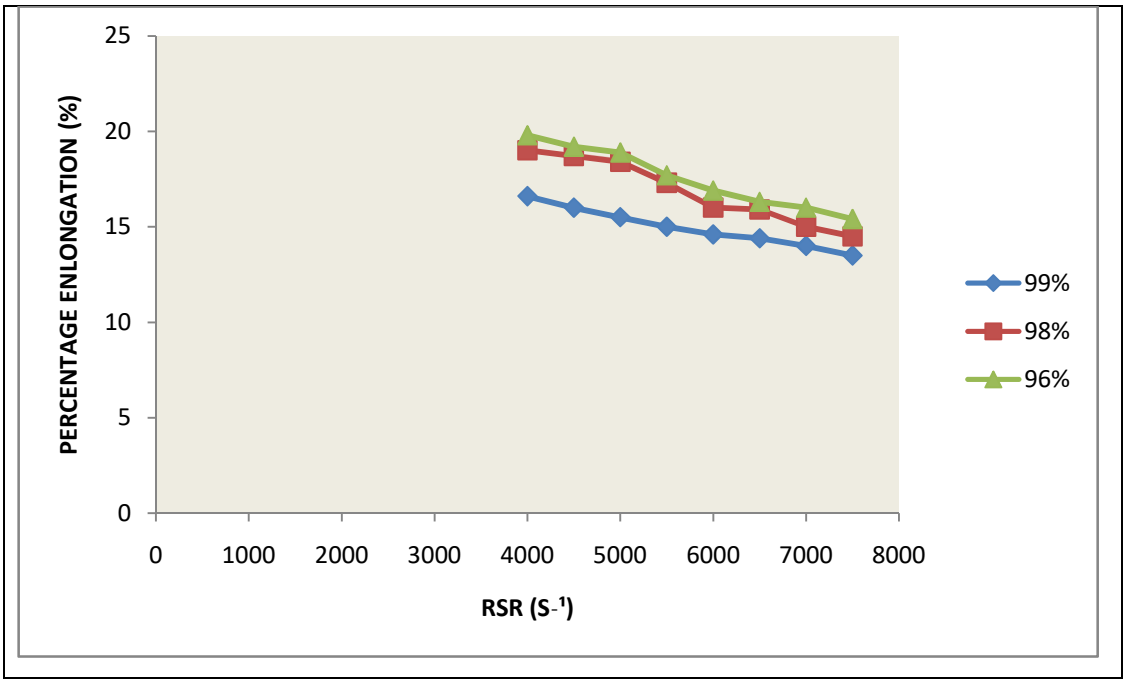

Figure 4.6: Effect of RSR on PE at FRT of 915°C and Variable PTD

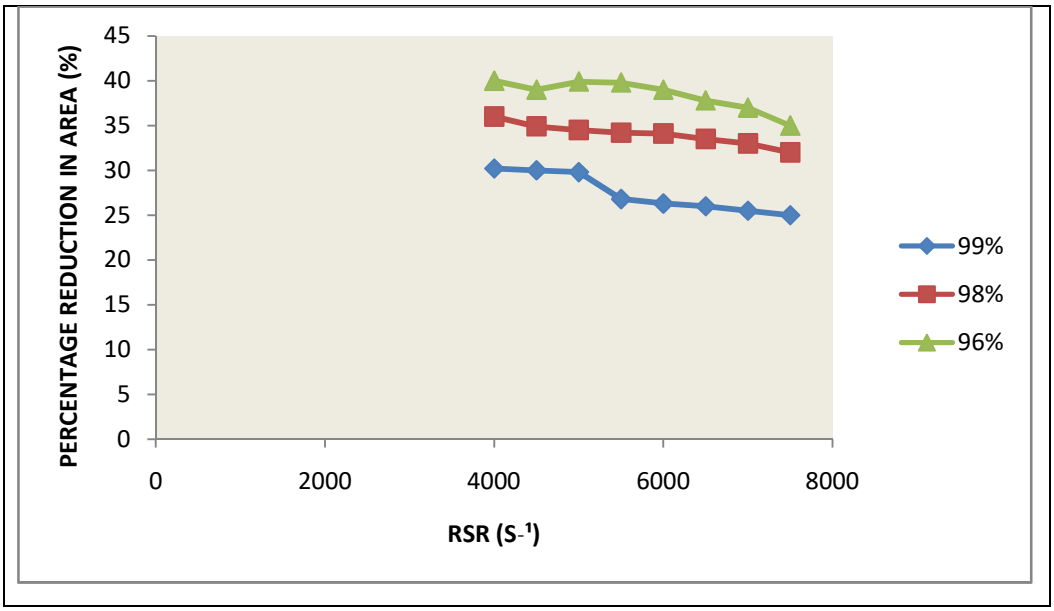

Figure 4.7: Effect of RSR versus PRA at FRT of 915°C

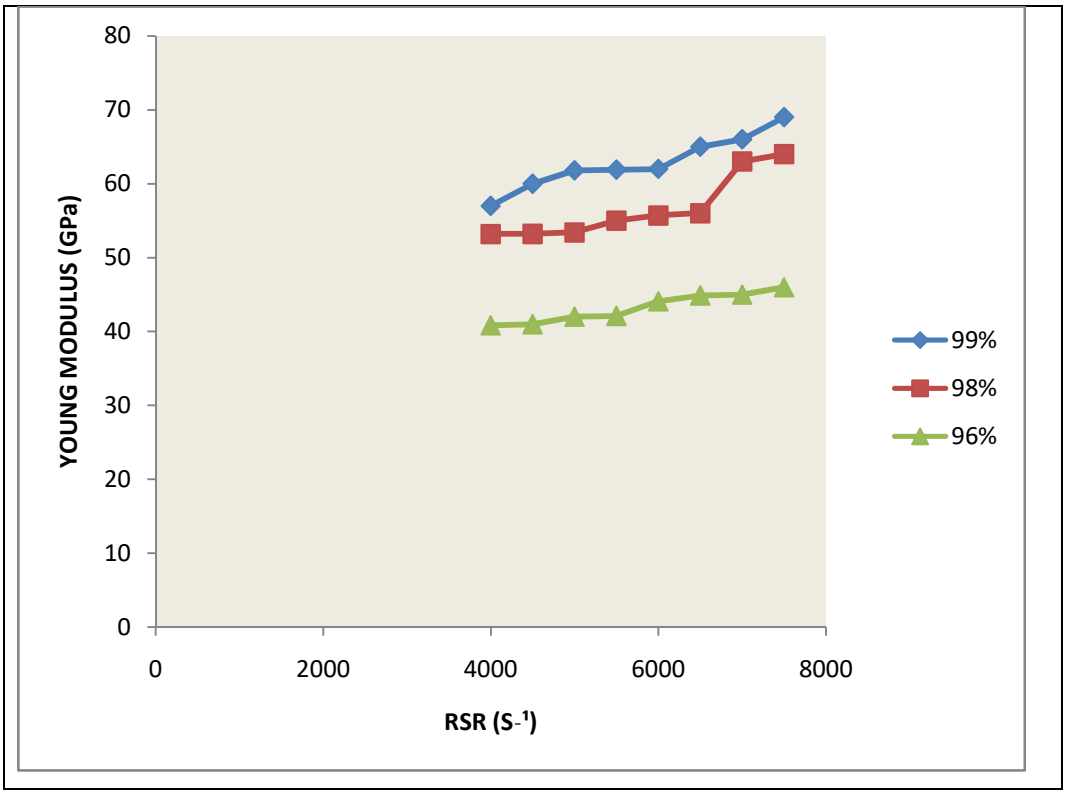

Figure 4.8: Effect of RSR versus E at FRT of 915°Cand variable PTD

4.2 Results and Discussions For Influence of RSR at FRT of 917 °C

Figures 4.9-4.16 show the influence of RSR on the mechanical properties at constant FRT at 917°C and variable PTD**.**

At 99.0 percent PTD and 917 °C FRT, when the RSR increased from 4000 to 4500 S^{-1},the TS increased from 614 to 621MPa (Fig.4.9), YS increased from 456 to 464MPa (Fig.4.10), PE decreased from 15 to 14.5 percent (fig.4.14), impact energy decreased from 0.4606 to 0.4605 J/mm^2(fig.4.12), Ductility increased from 46.04 to 46.24 °(fig.4.11), PRA decreased from 29.9 to 26.9 percent (fig.4.15), hardness increased from 227 to 228 HB (fig.4.13), E increased from 60 to 61 GPa (fig.4.16). At 98.0 percent and 917 °C FRT, as the RSR increased from 4000 to 4500 S^{-1}, TS increased from 572 to 579 MPa (Fig.4.9), YS increased from 428.4 to 436MPa (Fig.10). PE decreased from 18.5 to 17.4 percent (Fig.4.14), impact energy decreased from 0.5077 to 0.503 J/mm^2 (Fig.4.12). Ductility increased from 44.49 to 44.52° (Fig.4.11), PRA decreased from 34.7% to 34.3%(Fig.4.15),hardness increased from 223 to 224 HB (Fig.4.13), E increased from 53 to 54 GPa (Fig.4.16). At 96.0 percent PTD and 917 °C FRT, as the strain rate increased from 4000 to 4500 S^{-1}, TS increased from 512.7 to 520 MPa (Fig.4.9), YS increased from 424 to 428 MPa (Fig.4.10). PE decreased from 19.9 to 17.9 percent(Fig.4.15), impact energy decreased from 0.5186 to 0.5136 J/mm^2 (Fig.4.12). Ductility increased from 42.8 to 43° (Fig.4.11), PRA decreased from 40 to 39.9 percent (Fig.4.15), hardness increased from 217 to 219 HB (Fig.4.13), E increased from 41 to 41 GPa (Fig.4.16).The above same property trend is also applicable to the other constants of FRT of 917 Celsius Degrees and 919 Degrees Celsius,and the other constants of PTD of 98 and 96 percent respectively.

As could also be observed from the above trend, the higher the value of the rolling strain rate of the rolled stock, the higher and better the ultimate tensile strength, yield strength, hardness, modulus of elasticity and bendability of the rolled samples; while the toughness, percentage reduction in area and percentage elongation decreased. The billet underwent deformation as it passed through the rolls, and the effects of strain hardening gave rise to a very high dislocation and there was even distribution of carbides of alloy throughout the billets. The dislocated atoms were hinderedby various obstructions like

atoms in the interstices, foreign precipitates, which made the billets to strain harden. The interaction between the dislocated atoms and the obstructions were totally non-plastic and prevented the atoms from slipping. Therefore tensile strength, yield strength, hardness, modulus of elasticity and bendability increased. Particularly, increase in modulus of elasticity as rate of strain increased indicated how stiff the billets were at the same time, there was increased toughness, percentage reduction in area and percentage elongation, as a result of inner stress, uneven dislocation structures and ϵ-phase, that gave rise to larger grain sizes and lengthy slippage; and this increased as the temperature increased.

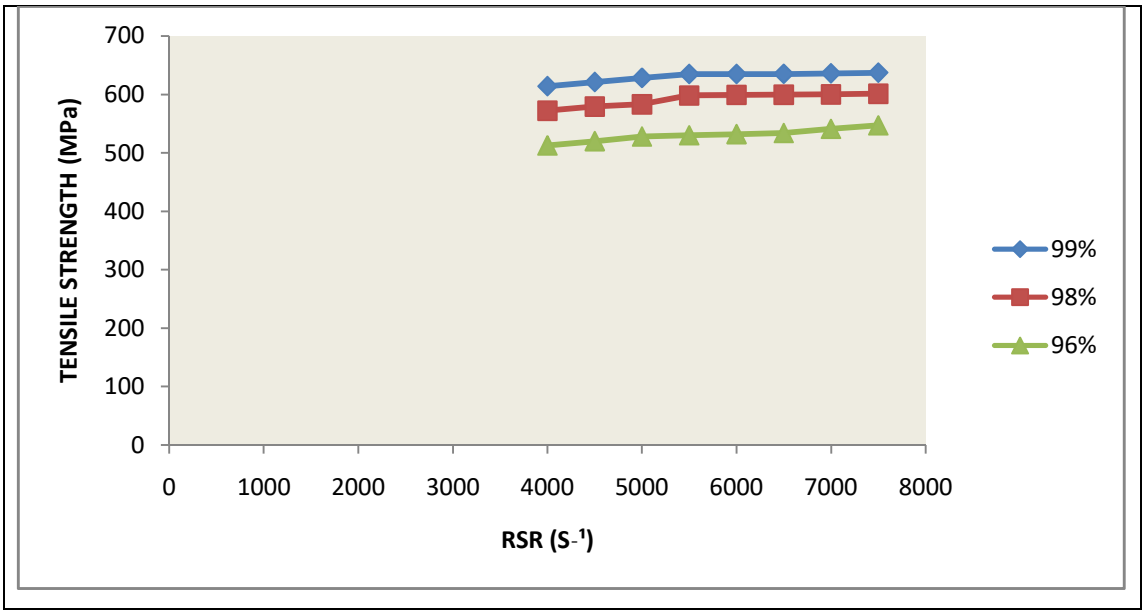

Figure 4.9: Effect of RSR versus TS at a Constant FRT of 917°C and Variable PTD.

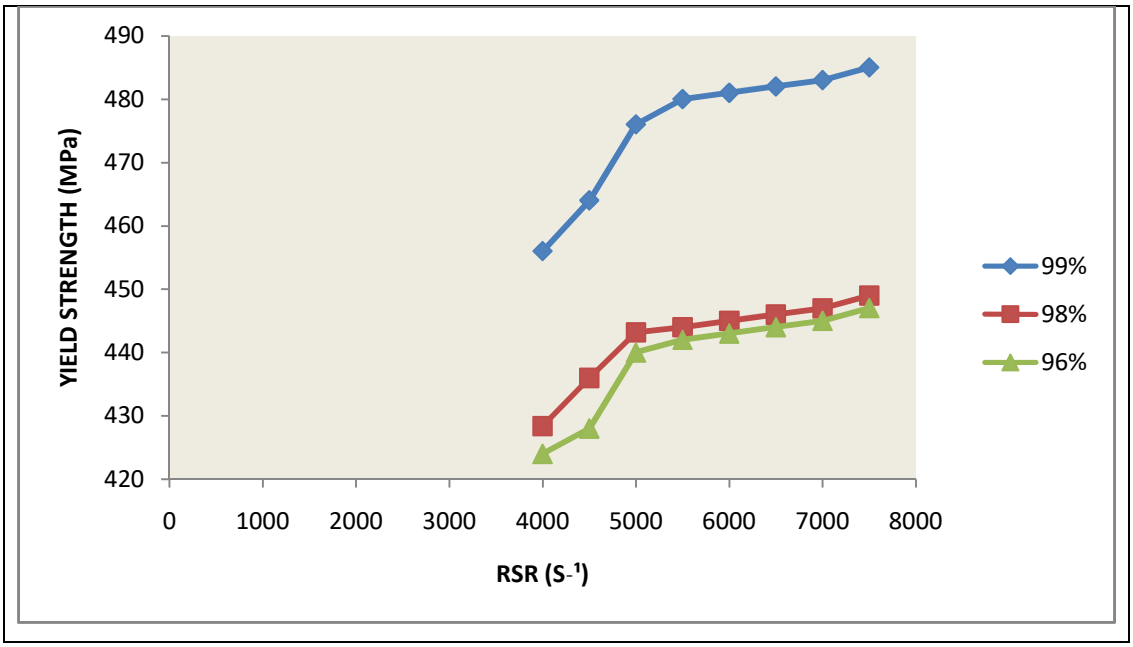

Figure 4.10: Effect of RSR Versus YS at a Constant FRT of 917°C and variable PTD.

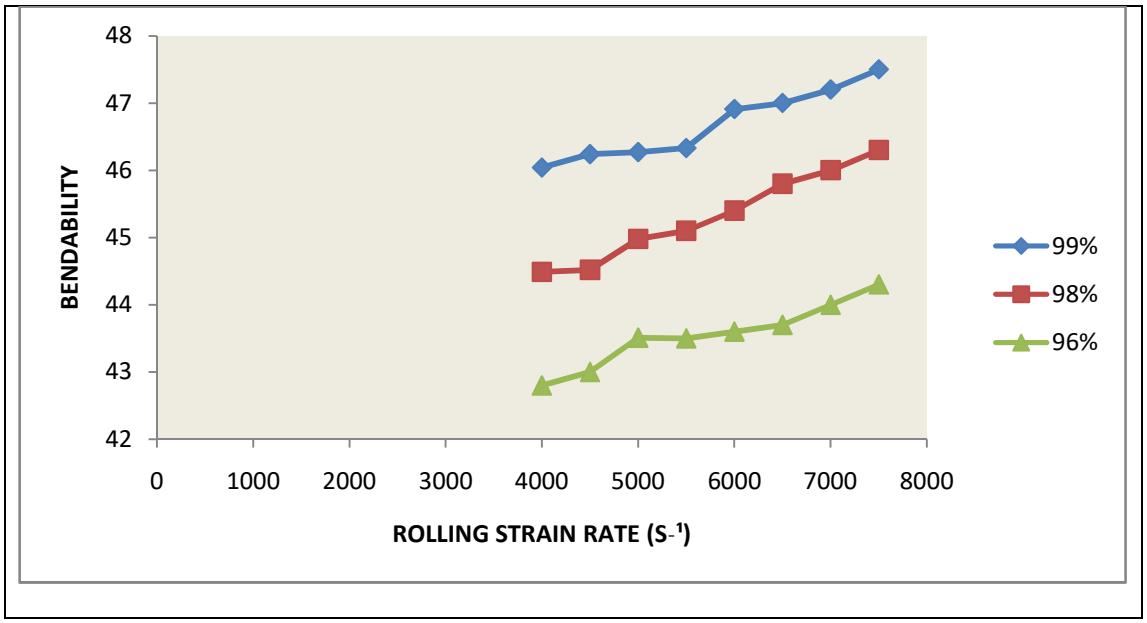

Figure 4.11: Effect of RSR versus ductility at a Constant FRT of 917°C and Variable PTD

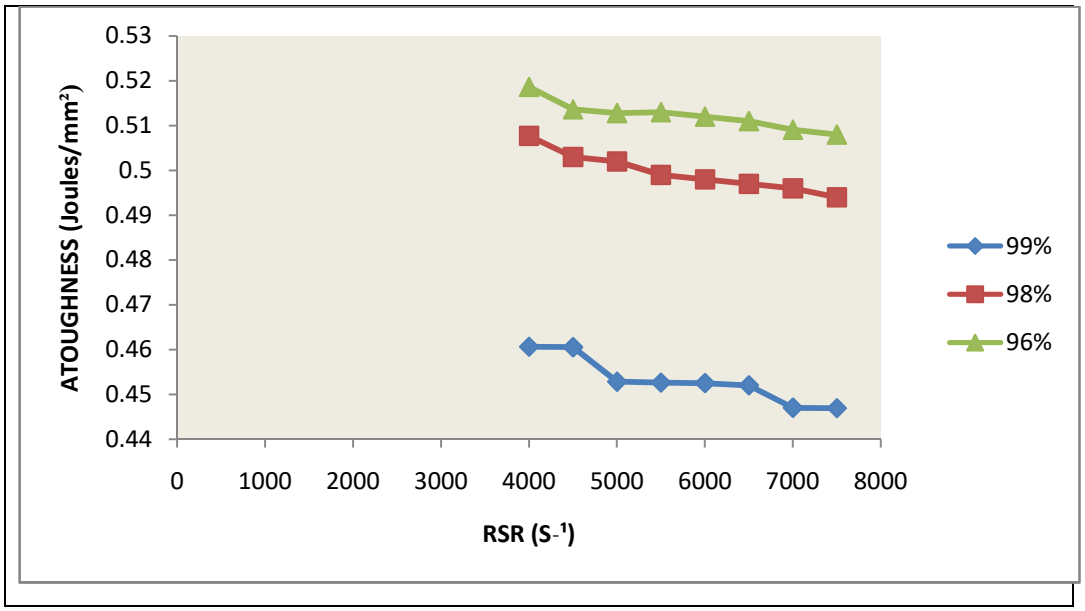

Figure 4.12: Effect of RSR versus Impact Energy at a Constant FRT of 917°C and Variable PTD

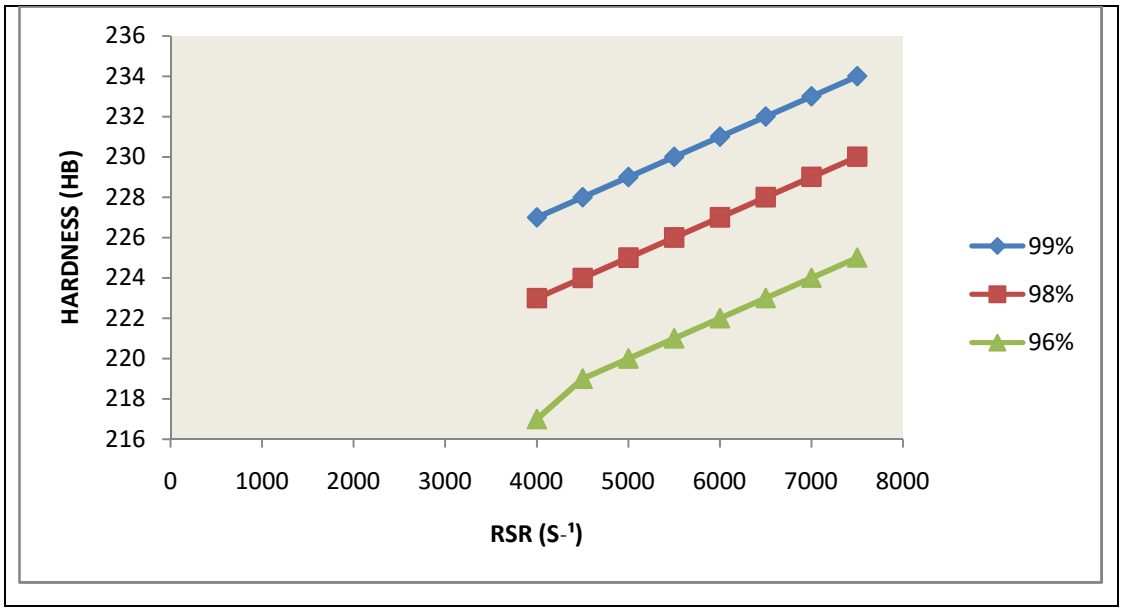

Figure 4.13: Effect of RSR versus Hardness at a Constant FRT of 917°C and Variable PTD

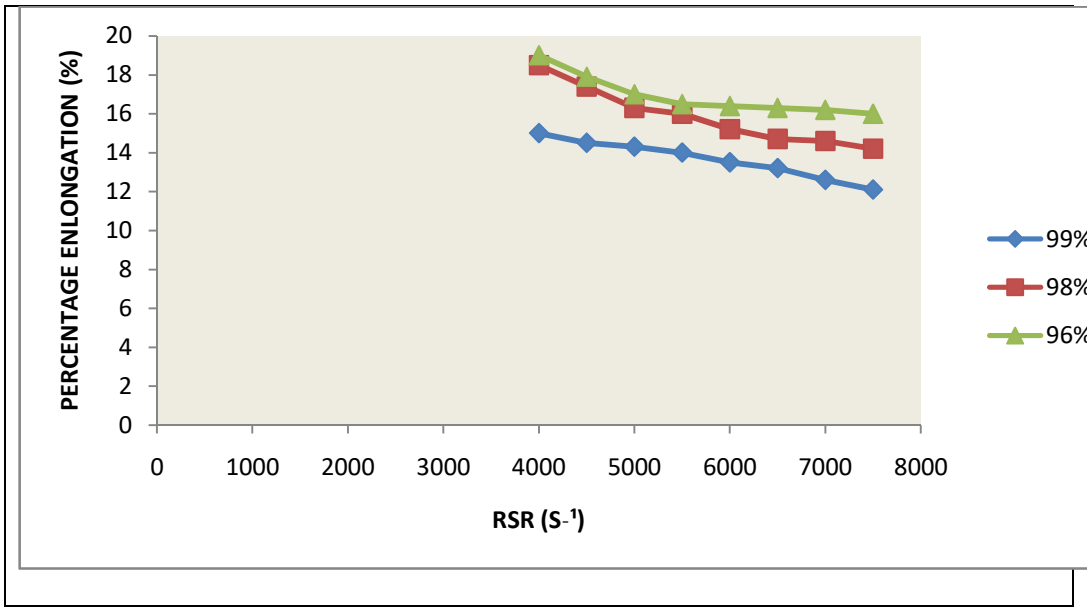

Figure 4.14:Effect of RSR on PE at a FRT of 917°C

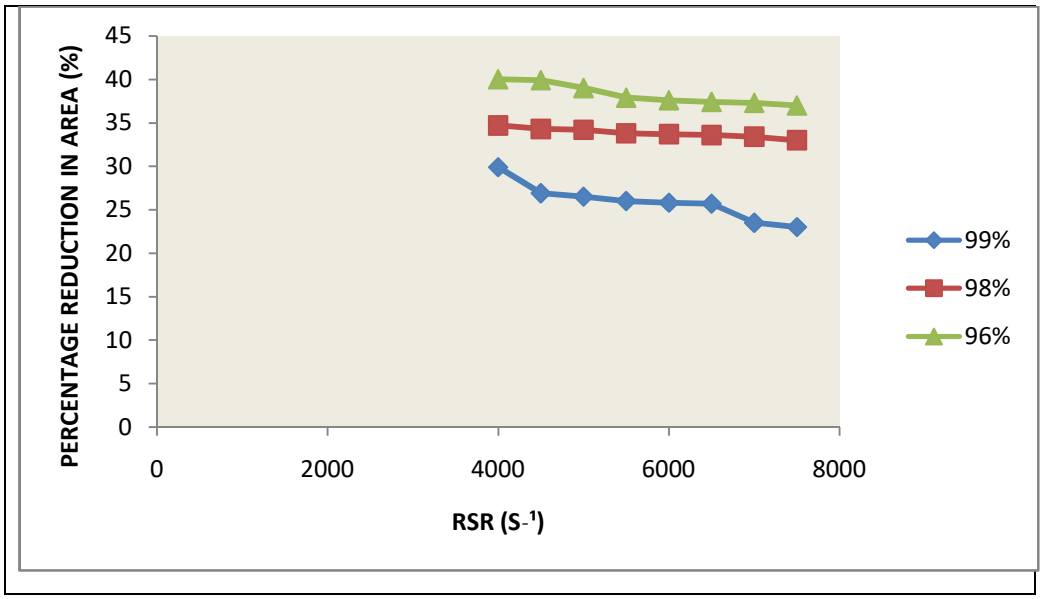

Figure 4.15: Effect of RSR on PRA at a Constant FRT of 917°C

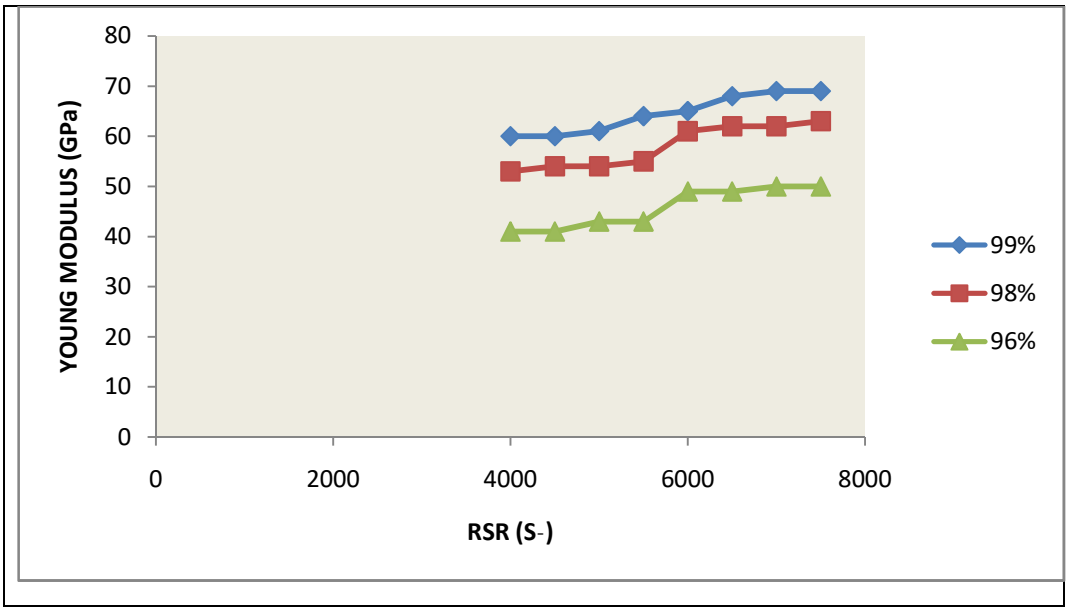

Figure 4.16: Effect of RSR onE at a constant FRT of 917°C .

4.3 Results and Discussion For influence of RSR at FRT of 919°C

Figures 4.17-4.24 show the influence of RSR on the mechanical properties at a FRT of 919°Cand variable PTD.

At 99.0 percent PTD, and 919 FRT, when the RSR increased from 4000 to 4500 S^{-1}, the TS increased from 638 to 689MPa (Fig.4.17),YS increased from 486 to 487 MPa (Fig.4.18) PE decreased from 12 to 11.8 percent(Fig.4.22), impact energy decreased from 0.41 to 0.40 J/mm^2 (Fig.4.20), Ductility increased from 47.51 to 48° (Fig.4.19), PRA decreased from 22 to 21% (Fig.4.23),hardness increased from 225 to 226 HB (Fig.4.21) E increased from 70 to 71 GPa (Fig.4.24). At 98.0 % PTD and 919°C FRT, as the RSR increased from 4000 to 4500 S^{-1}TS increased from 602 to 603MPa (Fig.4.17), YS increased from 450 to 451MPa (Fig.4.18). PE decreased from 14.1 to 13.7% (Fig.4.22)Impact energy decreased from 0.447 to 0.43 J/mm2 (Fig,4.20), Ductility increased from 46.9 to 47° (Fig.4.19), PRA decreased from 32 to 31% (Fig.4.23), hardness increased from 231 to 222 HB (Fig.4.21), E increased from 64 to 65 GPa (Fig.4.24). At 96.0 perecnt PTD and 919°CFRT, as the RSR increased from 4000 to 4500 S^{-1}, TS increased from 575 to 576MPa (Fig.4.17), YS increased from 448 to 449 MPa (Fig.4.18). PE decreased from 15.8 to 15.6%(Fig.4.22), impact energy decreased from 0.48 to 0.47 J/mm^2 (Fig.4.20). Ductility increased from 45 to 45.2°(Fig.4.19), PRA decreased from 36 to 35% (Fig.4.23), hardness increased from 226 to 227 HB (Fig.4.21), E increased from 51 to 52GPa(Fig.4.24).The above same property trend is also applicable to the other constants of FRT of 917 and 919,and the other constants of PTD of 98 and 96 percent respectively.

As illustrated above, if the RSR rises, the TS, YS, hardness, E and ductility also rise and impact energy, PRA and PE lower. The billets were completely broken down and yielded within the stands, which gave rise to maximally displaced mass of constituents and scattered smooth carbon particles.. The billets were yielded because of a stoppage from components in the matrix and other related components. There was an inextensible relationship between the displaced components and other related components which stopped some movement in the matrix.Because of these, TS, YS, hardness, E and

ductilitywere increased in value. The increased E as RSR increased, showed how bulky the hot-rolled billets were. The same trend was also repeated by the values of ductility. At the same time, lower values of impact energy, PRA and PE was caused by tension in the lattice and uneven dislocated atoms, which gave rise to larger microstructural sizes and longer movement and as the pyrometer readings got higher, the microstructural sizes grew large

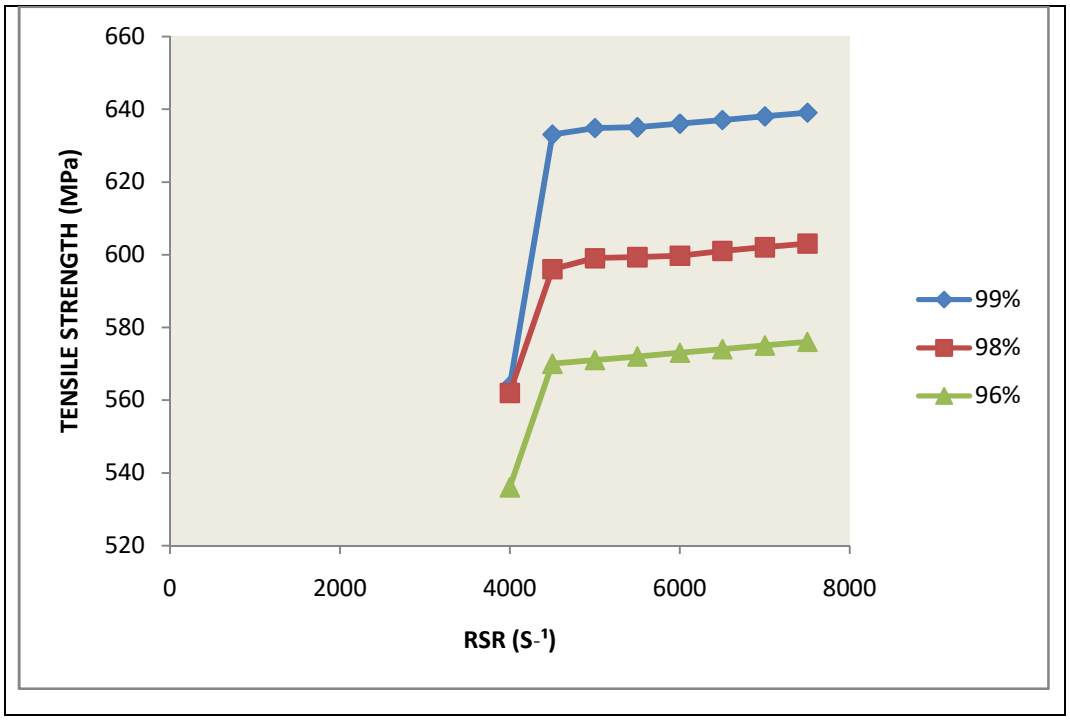

Figure 4.17: Effect of RSR on TS at a constant FRT of 919°C and variable PTD

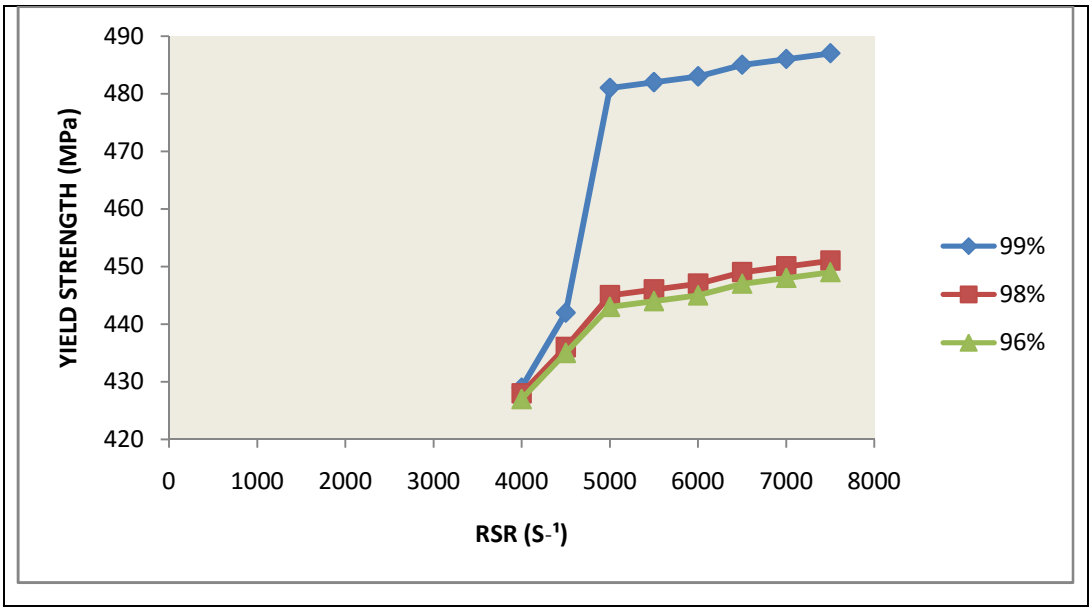

Figure 4.18: Effect of RSR on YS at a constant FRT of 919°C and variable PTD

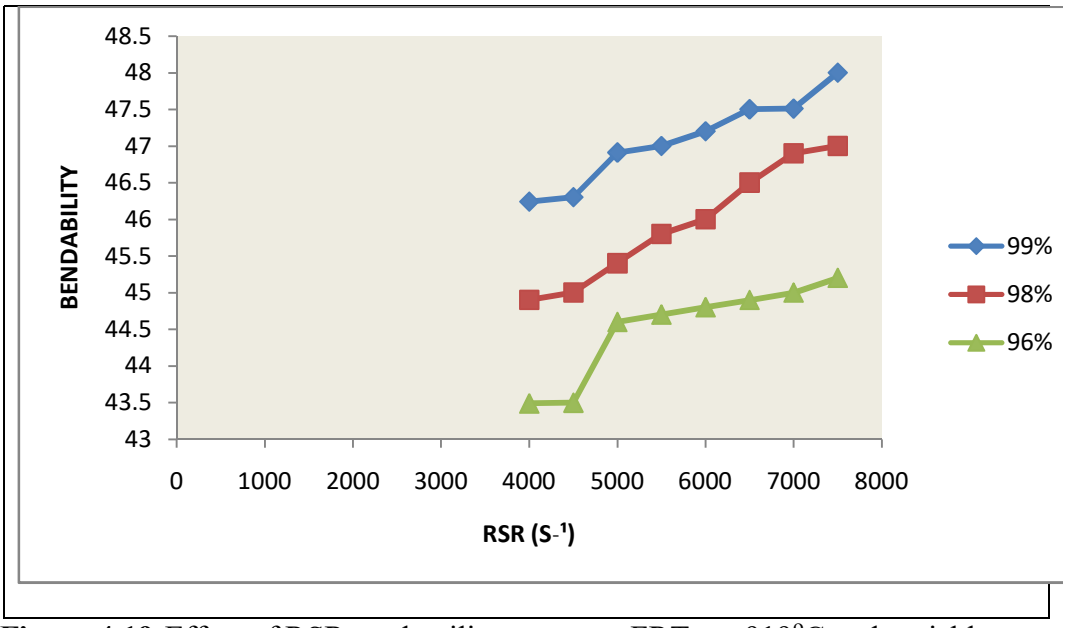

Figure 4.19: Effect of RSR on ductility constant FRT at 919^{o}C and variable PTD,

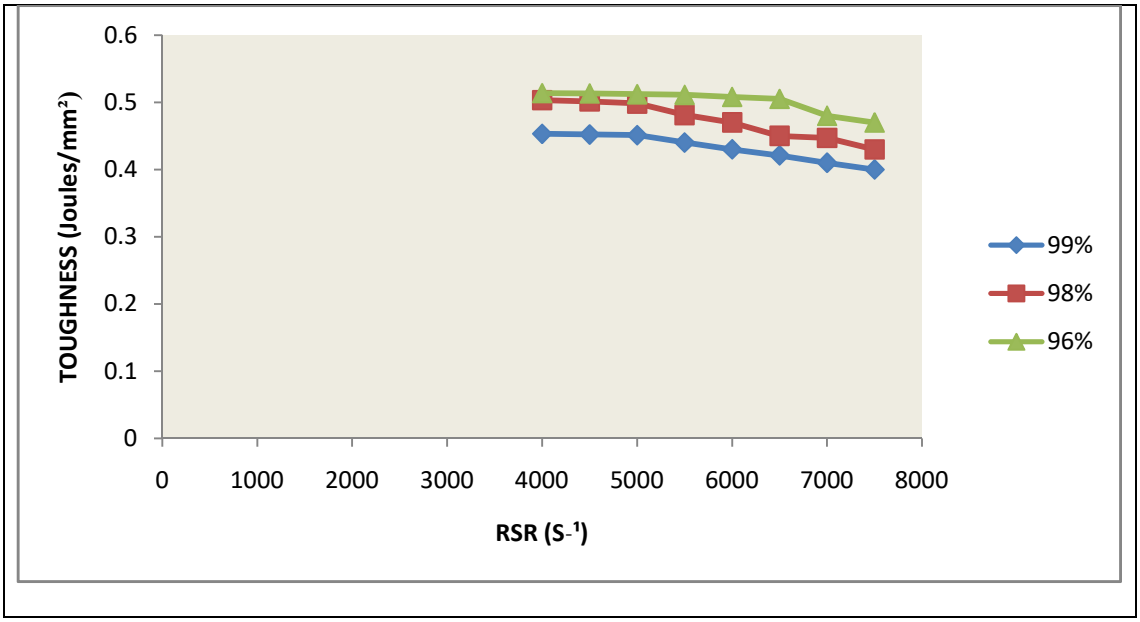

Figure 4.20: Effect of RSR on Impact Energyat a constant FRT of 919°C and variable PTD.

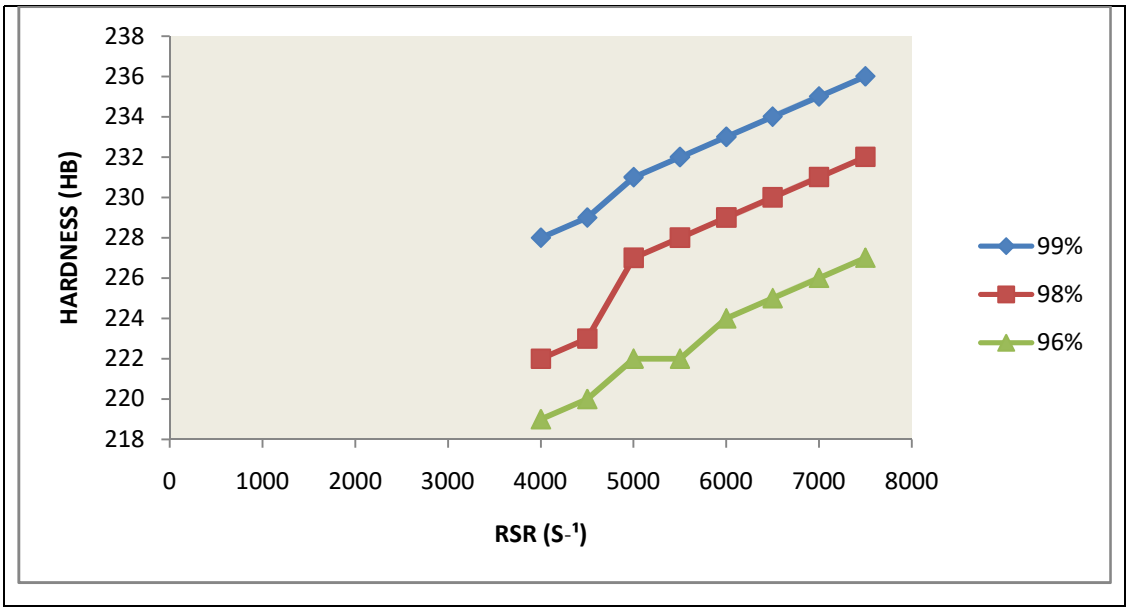

Figure 4.21:Effect of RSR on hardness at a constant FRT of 919°C and variable PTD

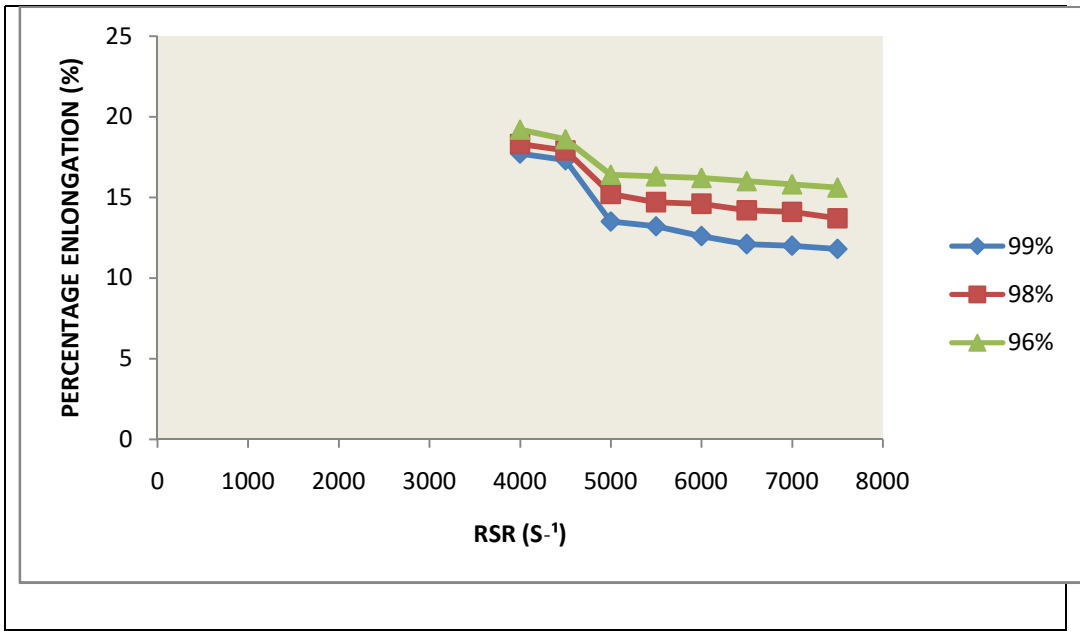

Figure 4.22: Effect of RSR on PE at a FRT of 919°C

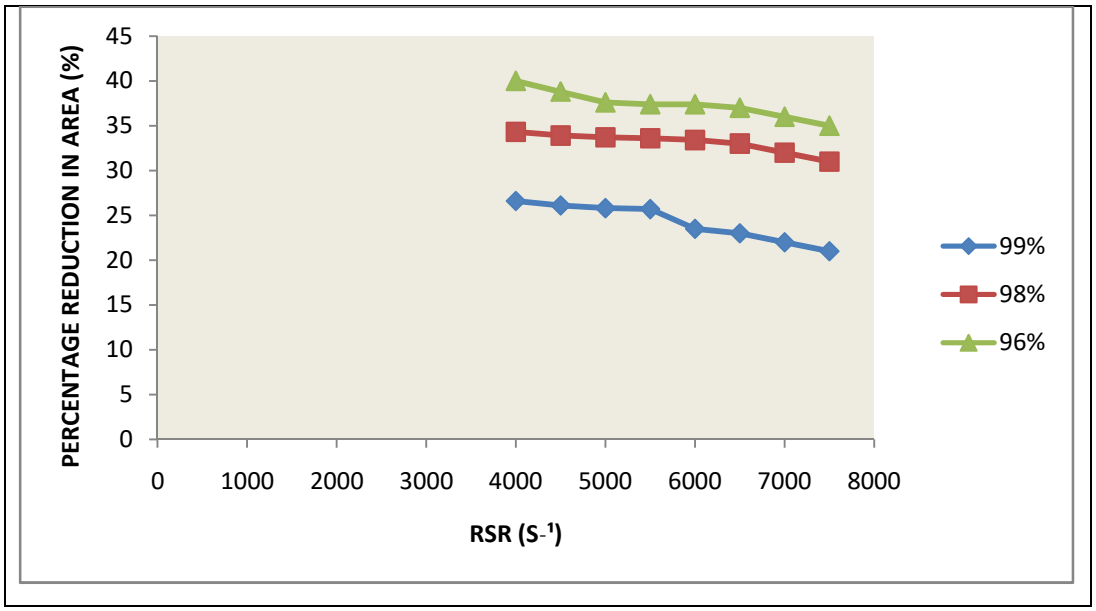

Figure 4.23:Effect of RSR on PRA at a FRT of 919°C

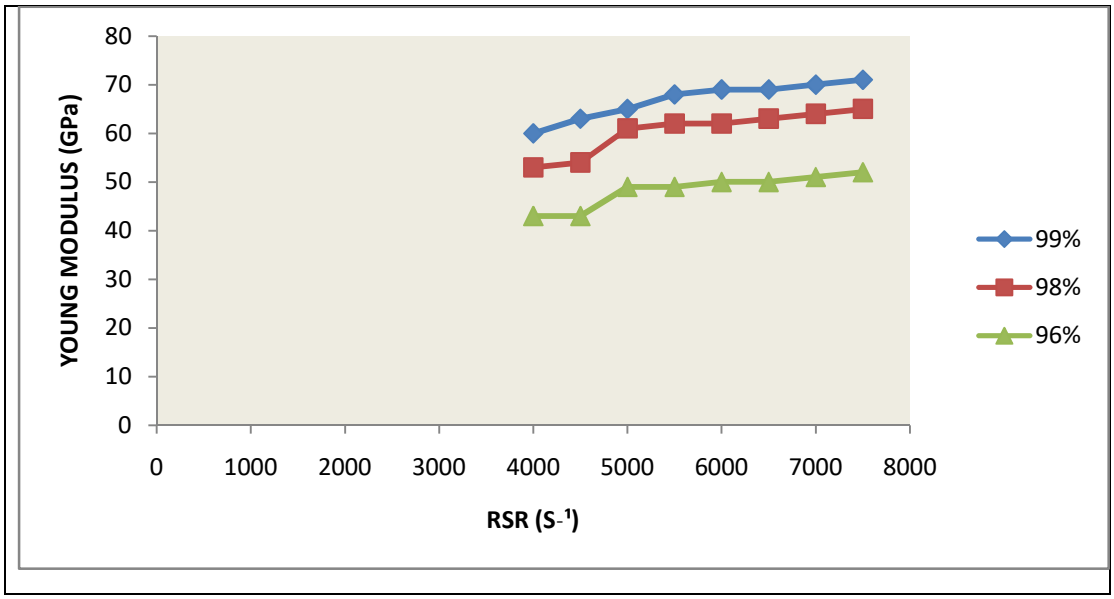

Figure 4.24:Effect of RSR on E at a constant FRTof 919°C and variable PTD.

4.4 Results and Discussion For influence of RSR at PTD of 99.0 percent

Table 4.2shows the influence of RSR on the mechanical properties of St60Mn steel. Figures 4.25-4.32 show the influence of RSR on the above mechanical properties at constant FRT of 915,varying PTD of 99.0, 98.0 and 96.0 percent respectively..

At 915°C FRT and 99 percent PTD, when the RSR increased from 4000 to 4500 S^{-1}, the TS increased from 611.3 to 614 MPa (Fig.4.26), YS increased from 432.1 to 432.2 MPa (Fig.4.27), PE decreased from 16.6 to 16% (see Fig.4.30), Impact Energy decreased from 0.48 to 0.4606 J/mm^2 (Fig.4.28), Ductility increased from 45.95 to 46º (Fig.4.27), PRA decreased from 30.2% to 30% (Fig.4.31), hardness increased from 222 to 224 HB (Fig.4.29), E increased from 57 to 60 GPa (Fig.4.32). At 917°C FRT and 99 percent PTD, as the RSR increased from 4000 to 4500 S^{-1}, TS increased from 569 to 569.6 MPa (see Fig.4.25), YS increased from 418MPa to 419MPa (Fig.4.26), PE decreased from 19% to 18.7% (Fig.4.30),Impact energy decreased from 0.5089 to 0.5086 J/mm^2 (see Fig.4.28), Ductility increased from 44.48 to 44.49º (Fig.4.27), PRA decreased from 36% to 34.9% (Fig.4.31), hardness increased from 222 to 223 HB (see Fig.4.29), E increased from 53.2 GPa to 53.21 GPa (Fig.4.32).

At 919°C FRT and 99.0 percent PTD, as the RSR increased from 4000 to 4500 S^{-1} , TS increased from 509.5 to 511 MPa (Fig.4.25), YS increased from 411 to 417 MPa (Fig.4.26), PE decreased from 19.5% to 19.2% (Fig.4.30), impact energy decreased from 0.5195 to 0.519 J/mm^2 (Fig.4.28), Ductility increased from 42.75 to 42.78 (Fig.4.27), PRA decreased from 40% to 39% (Fig.4.31), hardness increased from 216 to 217 HB (Fig.4.29), E increased from 40.83 GPa to 40.98 GPa (Fig.4.32). The above same property trend is also applicable to the other RSR of 5000, 5500, 6000, 6500, 7000, and 7500 S^{-1}, and FRTof 917°C and 919°C,and the other values of PTD of 98 and 96 percent

As stated above, if the RSR rises, the TS, YS, hardness, E and ductility also rise and impact energy, PRA and PE lower. The billets were completely broken down and yielded within the stands, which gave rise to maximally displaced mass of constituents and scattered smooth carbon particles.. The billets were yielded because of a stoppage from components in the matrix and other related components. There was an inextensible relationship between the displaced components and other related components, which

stopped some movement in the matrix.Because of these, TS, YS, hardness, E and ductility were increased in value. The increased E as RSR increased, showed how bulky the hot-rolled billets were. The same trend was also repeated by the values of ductility. At the same time, lower values of impact energy, PRA and PE was caused by tension in the lattice and uneven dislocated atoms, which gave rise to larger microstructural sizes and longer movement and as the pyrometer readings got higher, the microstructural sizes grew larger.

Table 4.2: InfluenceofRSR at Constant PTD and variable FRT.

RSR(S^{-1})	PTD (%)	FRT (°C)	Hardness (HB)	E (GPa)	Ductility or Bendability (°)	TS (MPa)	YS (MPa)	PE (%)	PRA (%)	Impact Energy (J/mm^2)
4000	99.0	915	222	57	45.95	611.3	432.1	16.6	30.2	0.4800
4000	99.0	917	221	53	44.48	569.0	418.0	19.0	36.0	0.5089
4000	99.0	919	216	40	42.75	509.5	423.0	14.8	40.0	0.5195
4500	99.0	915	224	60	46.00	614.0	432.2	16.0	30.0	0.4606
4500	99.0	917	223	53	44.49	569.6	418.0	18.7	34.9	0.5086
4500	99.0	919	217	40	42.78	511.0	424.0	19.2	39.0	0.5190
5000	99.0	915	229	61	46.05	614.6	442.0	18.5	29.8	0.4605
5000	99.0	917	224	53	44.50	570.0	418.0	18.4	34.5	0.5076
5000	99.0	919	218	42	42.90	512.8	425.0	18.9	39.9	0.5185
5500	99.0	915	229	61	46.25	622.0	445.0	15.0	26.8	0.4605
5500	99.0	917	225	55	44.53	572.3	420.0	17.3	34.2	0.5020
5500	99.0	919	220	42	43.45	520.1	429.0	17.7	39.8	0.5135
6000	99.0	915	230	62	46.28	629.0	449.0	14.6	26.3	0.4527
6000	99.0	917	226	55	45.00	580.0	420.0	16.0	34.1	0.5010
6000	99.0	919	221	44	43.52	539.0	441.0	16.9	39.0	0.5127
6500	99.0	915	231	65	46.34	635.7	450.0	14.4	26.0	0.4525
6500	99.0	917	227	56	45.20	600.0	421.0	15.9	33.5	0.4980
6500	99.0	919	222	44	43.60	598.6	443.0	16.3	37.8	0.5120
7000	99.0	915	232	66	46.93	635.8	450.0	14.0	25.5	0.4508
7000	99.0	917	229	63	45.47	625.0	424.0	15.0	33.0	0.4505
7000	99.0	919	224	45	43.74	547.0	444.0	16.0	37.0	0.5110
7500	99.0	915	225	69	47.00	697.2	455.8	17.5	25.0	0.4200
7500	99.0	917	230	64	45.48	635.4	427.0	16.5	32.0	0.4207
7500	99.0	919	226	46	43.77	551.0	455.8	15.4	35.0	0.5090

Table 4.2 (continued): Influence of RSR at Constant PTD and variable FRT.

RSR (s^{-1})	PTD (%)	FRT (°C)	Hardness (HB)	E (GPa)	Ductility or Bendability (°)	TS (MPa)	YS (MPa)	PE(%)	PRA (%)	Impact Energy (J/mm^2)
4000	98.0	915	227	60	46.04	614.0	456.0	15.0	29.9	0.4606
4000	98.0	917	223	53	44.49	572.0	428.4	18.5	34.7	0.5077
4000	98.0	919	217	41	42.80	512.7	424.0	19.9	40.0	0.5186
4500	98.0	915	228	61	46.24	621.0	464.0	14.5	26.9	0.4605
4500	98.0	917	224	54	44.52	579.0	436.0	17.4	34.3	0.503
4500	98.0	919	219	42	43.00	520.0	428.0	17.9	39.9	0.5136
5000	98.0	915	229	61	46.27	628.0	476.0	14.3	26.5	0.4528
5000	98.0	917	225	54	44.98	583.0	443.2	16.3	34.2	0.5020
5000	98.0	919	220	43	43.51	538.0	440.0	17.0	39.0	0.5128
5500	98.0	915	230	64	46.33	634.7	480.0	14.0	26.0	0.4526
5500	98.0	917	226	55	45.10	598.0	444.0	16.0	33.8	0.4990
5500	98.0	919	221	43	43.50	580.0	442.0	16.5	37.9	0.5130
6000	98.0	915	231	65	46.91	634.8	481.0	13.5	25.8	0.4510
6000	98.0	917	227	61	45.40	599.0	445.0	15.2	33.7	0.4980
6000	98.0	919	222	47	44.60	571.0	443.0	16.4	37.6	0.5120
6500	98.0	915	222	68	47.00	635.0	482.0	13.2	25.7	0.4400
6500	98.0	917	228	62	45.80	599.3	446.0	14.7	33.8	0.4810
6500	98.0	919	223	49	44.70	572.0	444.0	16.3	37.8	0.5110
7000	98.0	915	233	69	47.20	636.0	483.0	12.6	28.5	0.4300
7000	98.0	917	229	62	46.00	599.7	447.0	14.6	33.4	0.4700
7000	98.0	919	224	50	44.80	573.0	445.0	16.2	37.4	0.5080
7500	98.0	915	234	69	47.50	637.0	485.0	12.1	23.0	0.4200
7500	98.0	917	230	63	46.50	601.0	449.0	14.2	43.0	0.4500
7500	98.0	919	225	50	44.90	574.0	447.0	16.0	37.0	0.5050

Table 4.2 (continued): Influence of RSR at Constant PTD and variable FRT.

RSR (S^{-1})	PTD (%)	FRT (°C)	Hardness (HB)	E (GPa)	Ductility or Bendability (°)	TS MPa)	YS (MPa)	PE (%)	PRA (%)	Impact Energy (J/mm^2)
4000	96.0	915	235	70	47.51	638	486	12.0	22.0	0.4100
4000	96.0	917	231	64	46.90	602	450	14.1	32.0	0.4470
4000	96.0	919	226	51	45.00	575	448	15.8	36.0	0.4800
4500	96.0	915	226	71	48.00	689	487	11.8	21.0	0.4000
4500	96.0	917	222	65	47.00	603	451	13.7	31.0	0.4300
4500	96.0	919	227	52	45.20	576	449	15.6	35.0	0.4700
5000	96.0	915	220	55	44.91	508	443	19.4	30.8	0.4610
5000	96.0	917	219	51	43.47	566	423	20.4	39.0	0.5150
5000	96.0	919	214	39	42.72	507	419	21.2	48.0	0.5199
5500	99.0	915	222	58	44.00	611	446	19.1	30.5	0.4609
5500	96.0	917	221	52	43.50	568	424	19.6	37.0	0.5096
5500	96.0	919	215	39	42.75	505	420	20.5	45.0	0.5197
6000	96.0	915	226	59	45.00	613	454	18.9	30.0	0.4608
6000	96.0	917	222	52	44.46	570	427	19.4	34.8	0.5085
6000	96.0	919	216	40	42.80	511	422	20.2	43.0	0.5187
6500	96.0	915	227	59	45.23	620	463	18.0	28.6	0.4607
6500	96.0	917	223	53	44.50	577	435	18.6	34.4	0.5039
6500	96.0	919	218	40	43.00	518	425	19.8	41.1	0.5156
7000	96.0	915	228	60	46.24	626	475	17.7	26.6	0.4530
7000	96.0	917	224	53	44.90	582	442	18.3	34.3	0.5029
7000	96.0	919	219	43	43.49	536	439	19.2	40	0.5135
7500	96.0	915	229	63	46.30	633	478	17.3	26.1	0.4528
7500	96.0	917	225	54	45.00	596	443	17.9	33.9	0.5010
7500	96.0	919	20	43	43.5	570	441	18.6	38.8	0.5131

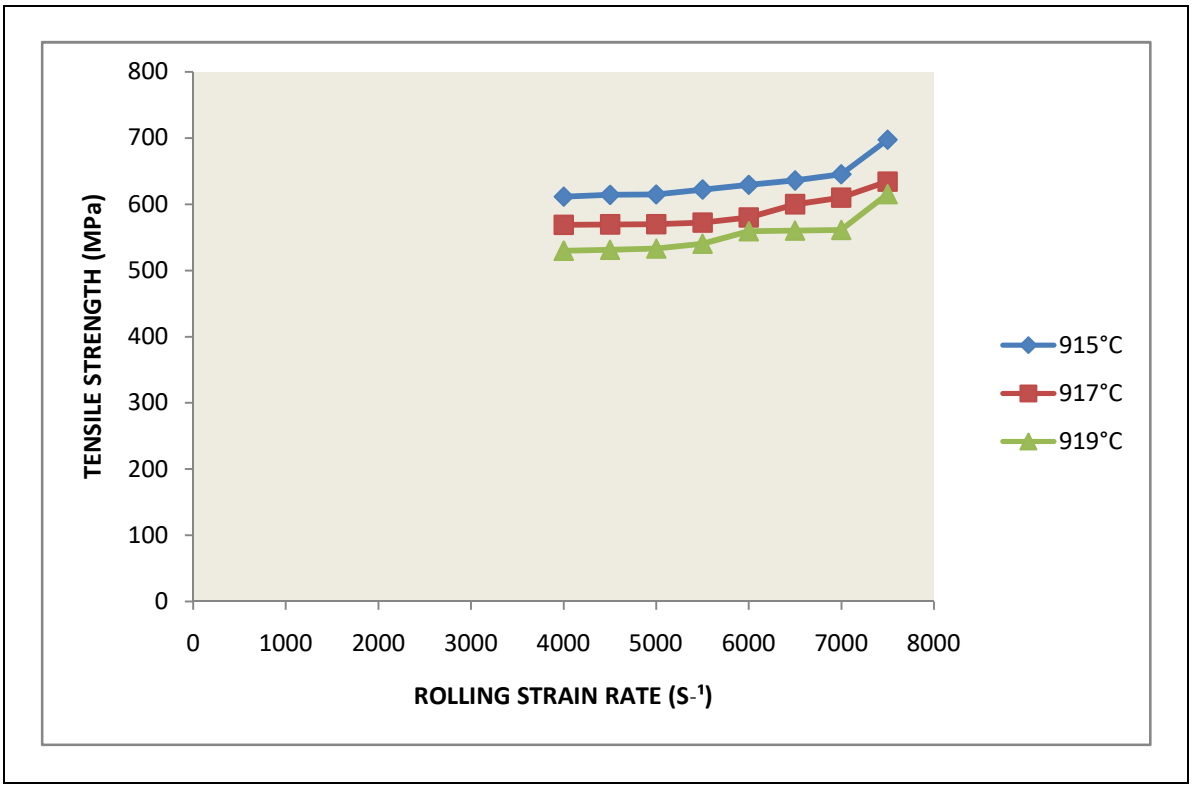

Figure 4.25: Effect of RSR on TS at a PTD of 99.0 % and Variable FRT

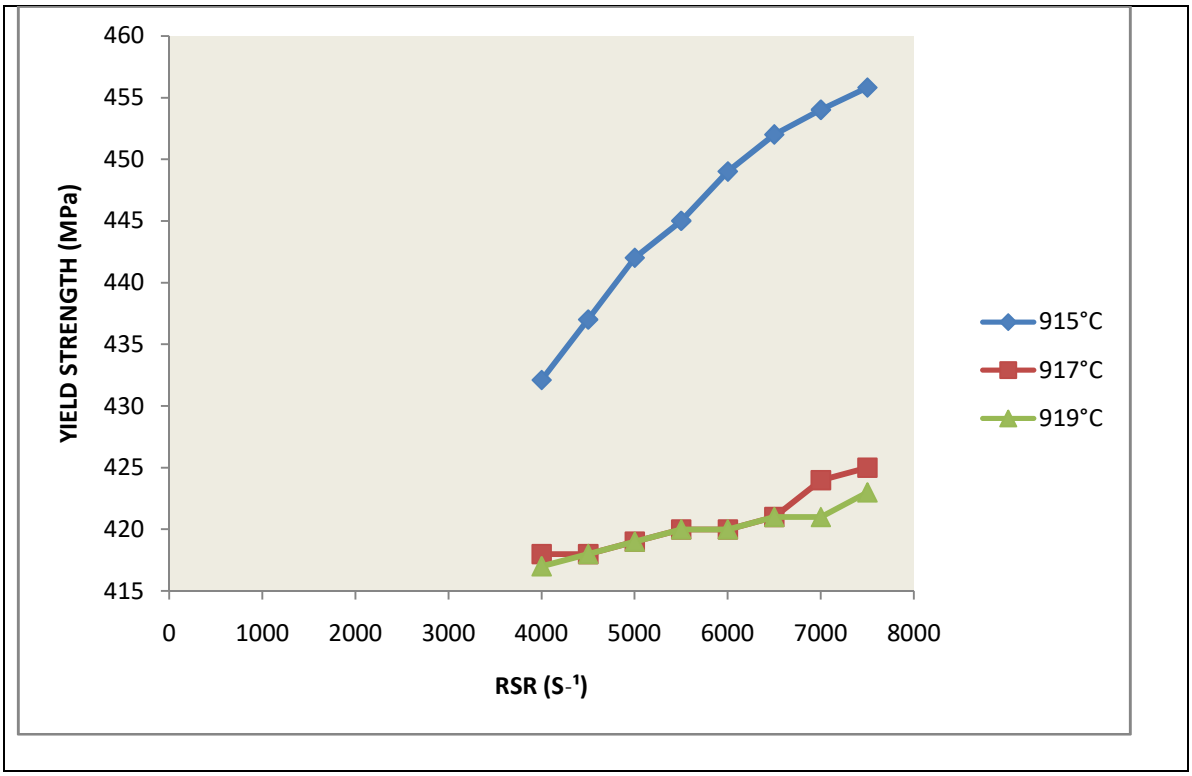

Figure 4.26: Effect of RSR on YS at Constant PTD of 99.0% and Variable FRT

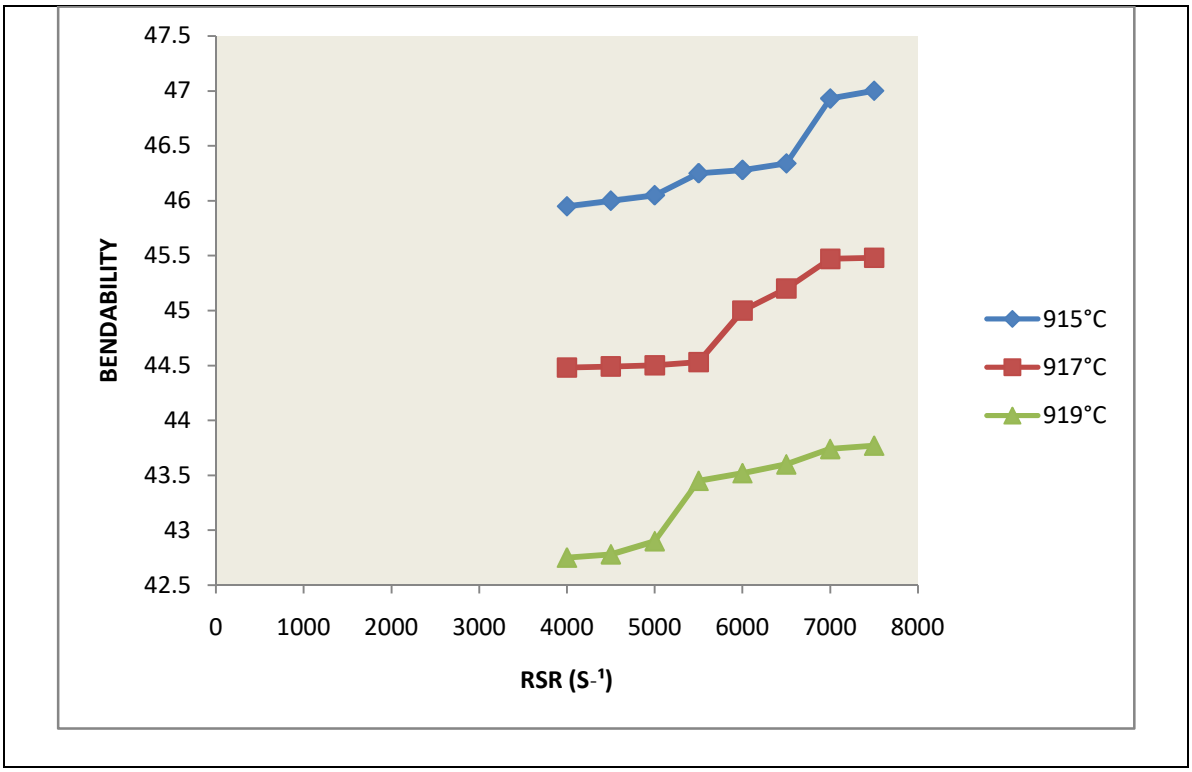

Figure 4.27: Effect of RSR on ductility at Constant PTD of 99.0% and Variable FRT

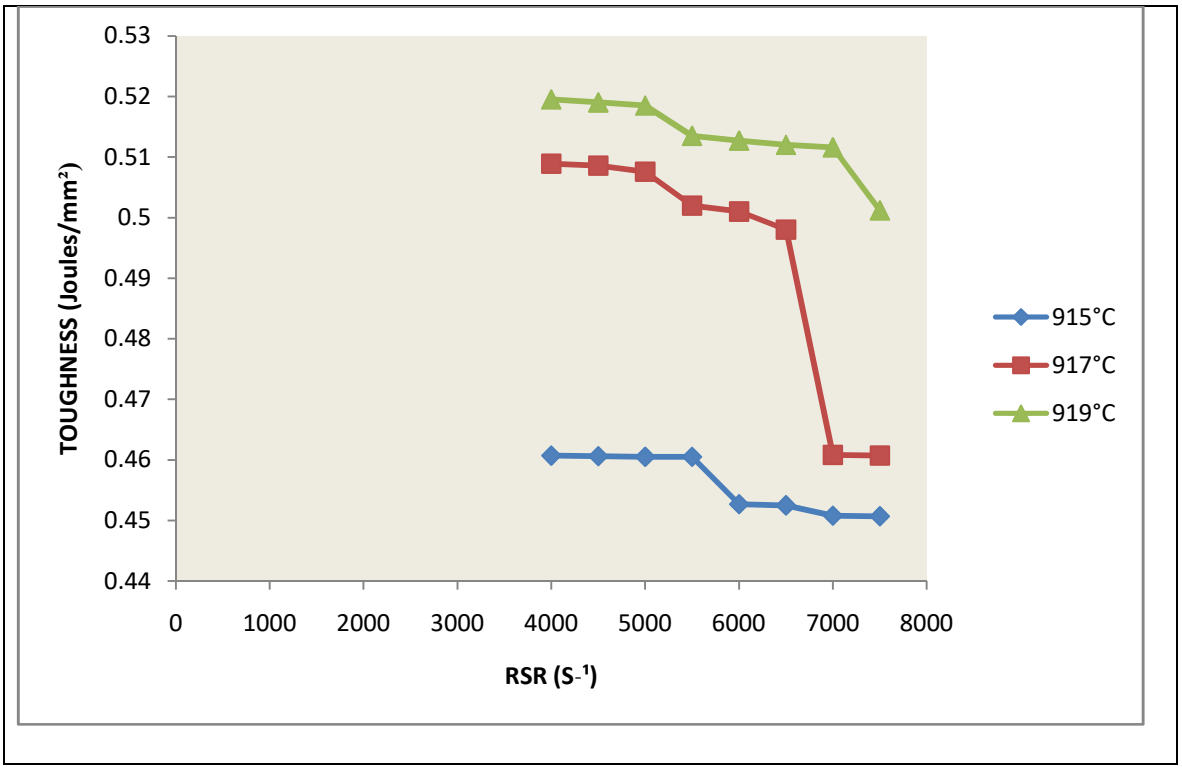

Figure 4.28:Effect of RSR on Impact Energy at Constant PTD of 99.0 % and Variable FRT

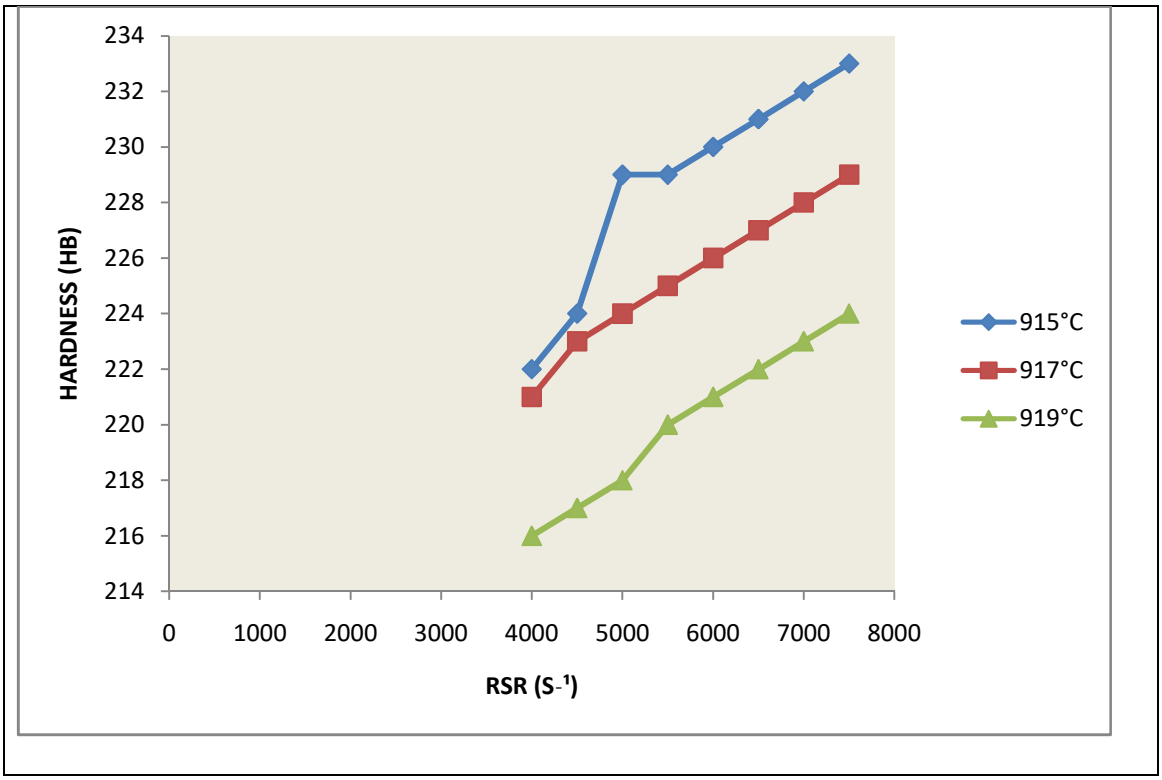

Figure 4.29: Effect of RSR on Hardness at Constant PTD of 99.0% and Variable FRT

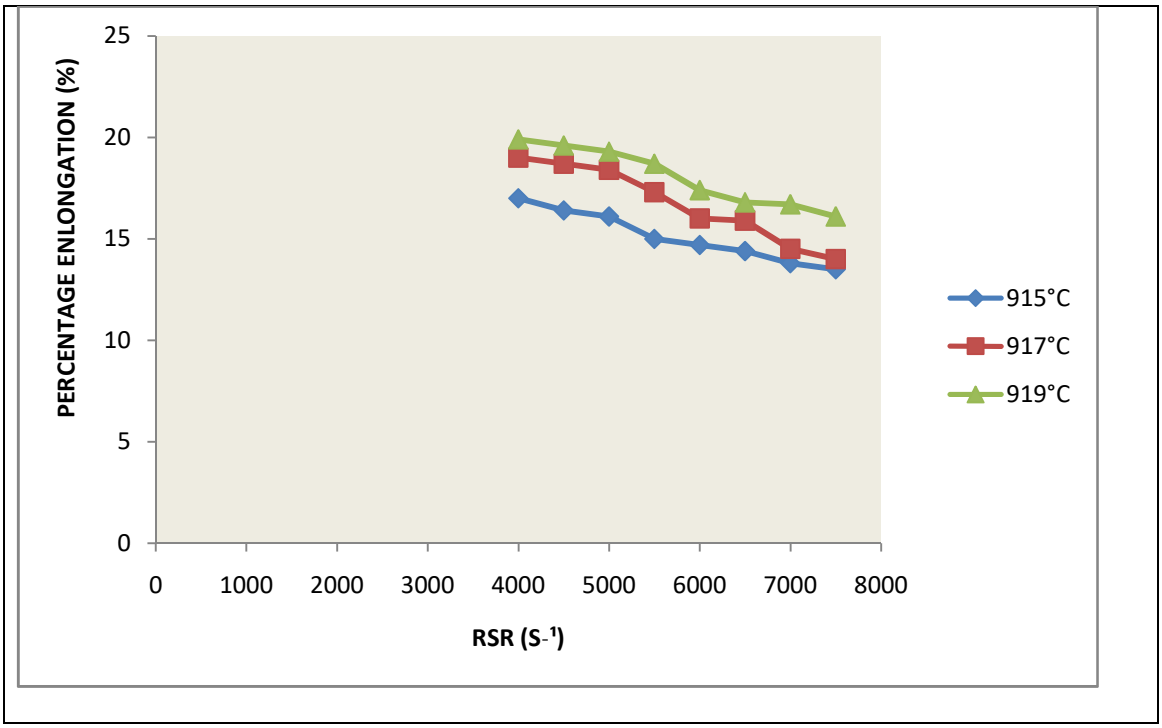

Figure 4.30: Effect of RSR on PE at Constant PTD of 99.0 % and Variable FRT.

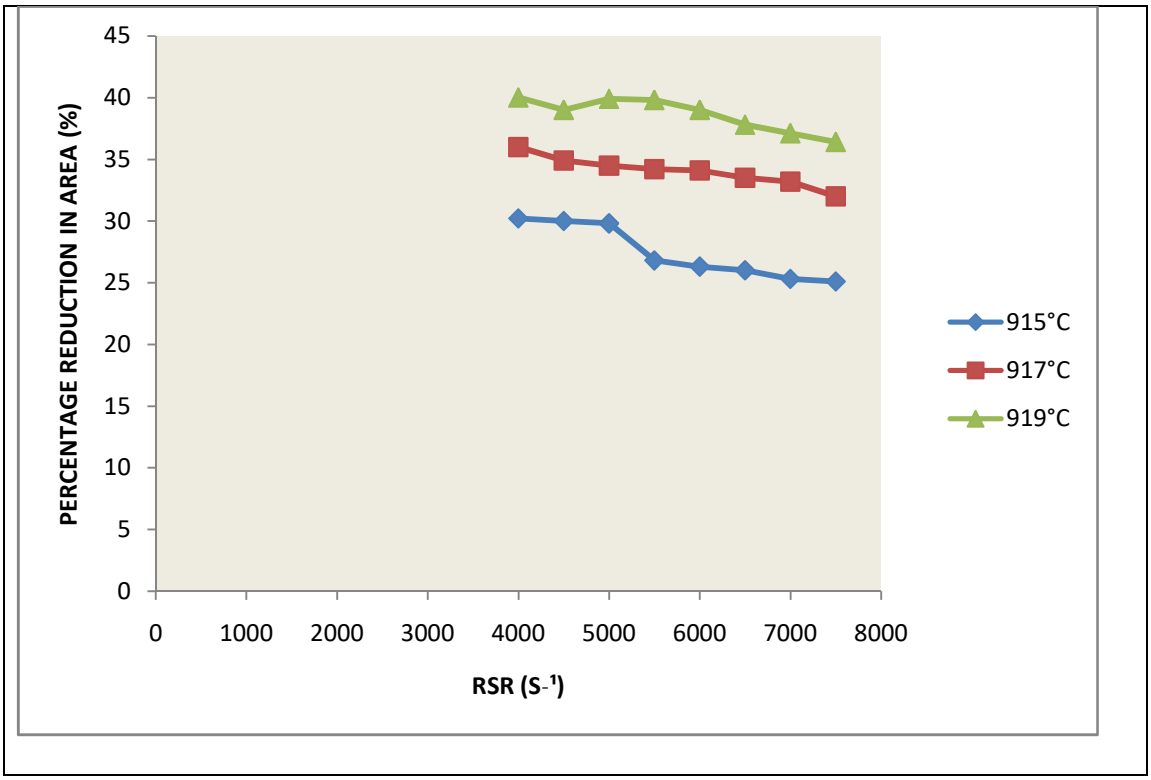

Figure 4.31: Effect of RSR on PRA at Constant PTD of 99.0% and Variable FRT

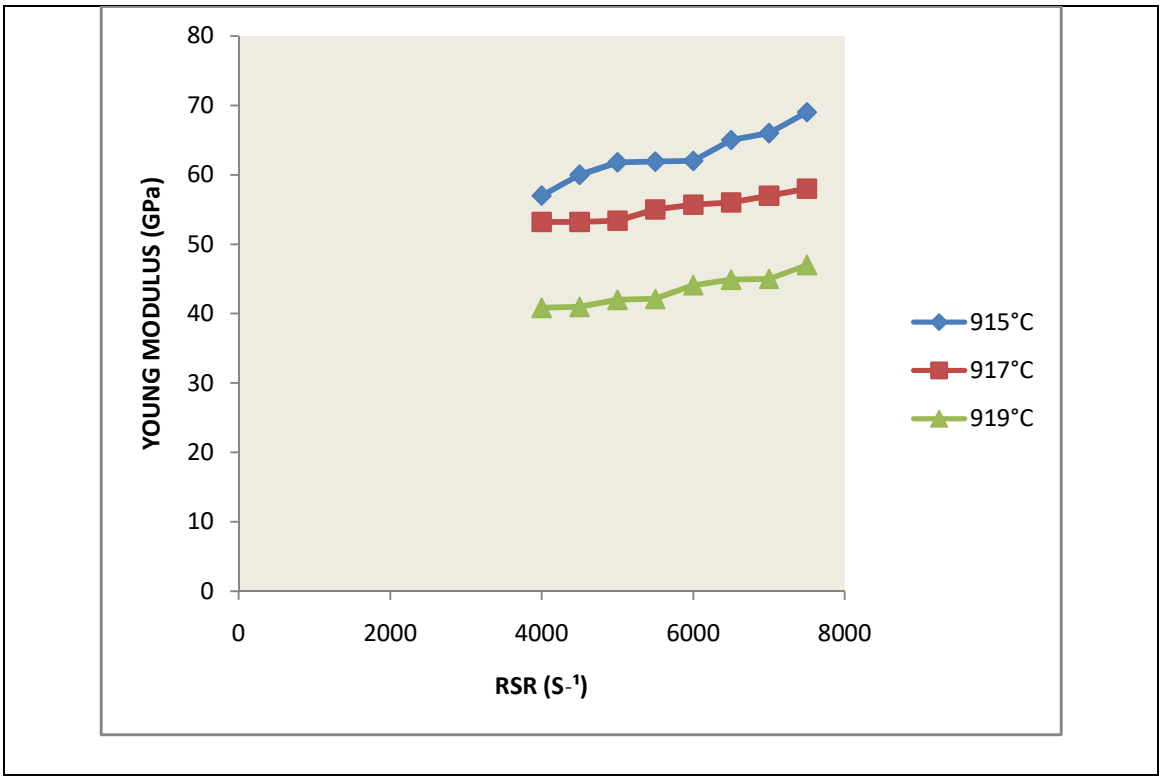

Figure 4.32: Effect of RSR on E at Constant PTD of 99.0% and Variable FRT

4.5 Results and Discussions For RSR at PTD of 98.0 percent

Figures 4.33-4.40 show the influence of RSR on the mechanical properties at constant PTD of 98 percent, varying FRT.

At 915°C FRT and 98.0 percent PTD, when the RSR increased from 4000 to 4500 S^{-1},the TS increased from 614 to 621MPa (Fig.4.33), YS increased from 456 to 464MPa (Fig.4.34), PE decreased from 15% to 14.5% (Fig.4.38), Impact energy decreased from 0.46 to 0.4605 J/mm^2 (Fig.4.36), ductility increased from 46.04 to 46.24 (Fig.4.35), PRA decreased from 29.9% to 26.9% (Fig.4.39), hardness increased from 227 to 228 HB (Fig.4.37), E increased from 60 to 61 GPa (Fig.4.40). At 917°C FRT and 98 percent PTD, as the RSR increased from 4000 to 4500 S^{-1},TS increased from 572 to 579 MPa (Fig.4.33),YS increased from 428.4 to 436 MPa(Fig.34). PE decreased from 18.5% to 17.4%(Fig.4.38), impact energy decreased from 0.5077 to 0.503 J/mm^2(Fig.4.36). ductility increased from 44.49 to 44.52° (Fig.4.35), PRA decreased from 34.7% to 34.3%(Fig.4.39),hardness increased from 223 to 224 HB (Fig.4.37), E increased from 53 to 54 GPa (Fig.4.40). At 919°C FRT and 98.0%PTD, as the RSR increased from 4000 to 4500 S^{-1}, TS increased from 512.7 to 520 MPa (Fig.4.33), YS increased from 424 to 428 MPa (Fig.4.34). PE decreased from 19.9% to 17.9%(Fig.4.38), impact energy decreased from 0.5186 to 0.5136 J/mm^2 (Fig.4.36). Ductility increased from 42.8 to 43° (Fig.4.35), PRA decreased from 40% to 39.9% (Fig.4.39), hardness increased from 217 to 219 HB (Fig.4.37), E increased from 41 to 42GPa (Fig.4.40).The above same property trend is also applicable to the other constants of FRT of 917°C and 919°C,and the other constants of PTD of 98.0 and 96.0 percent respectively.

As stated above, if the RSR rises, the TS, YS, hardness, E and ductility also rise and impact energy, PRA and PE lower. The billets were completely broken down and yielded within the stands, which gave rise to maximally displaced mass of constituents and scattered smooth carbon particles.. The billets were yielded because of a stoppage from components in the matrix and other related components. There was an inextensible relationship between the displaced components and other related components which stopped some movement in the matrix.Because of these, TS, YS, hardness, E and ductility were increased in value. The increased E as RSR increased, showed how bulky the hot-

rolled billets were. The same trend was also repeated by the values of ductility. At the same time, lower values of impact energy, PRA and PE was caused by tension in the lattice and uneven dislocated atoms, which gave rise to larger microstructural sizes and longer movement and as the pyrometer readings got higher, the microstructural sizes grew larger.

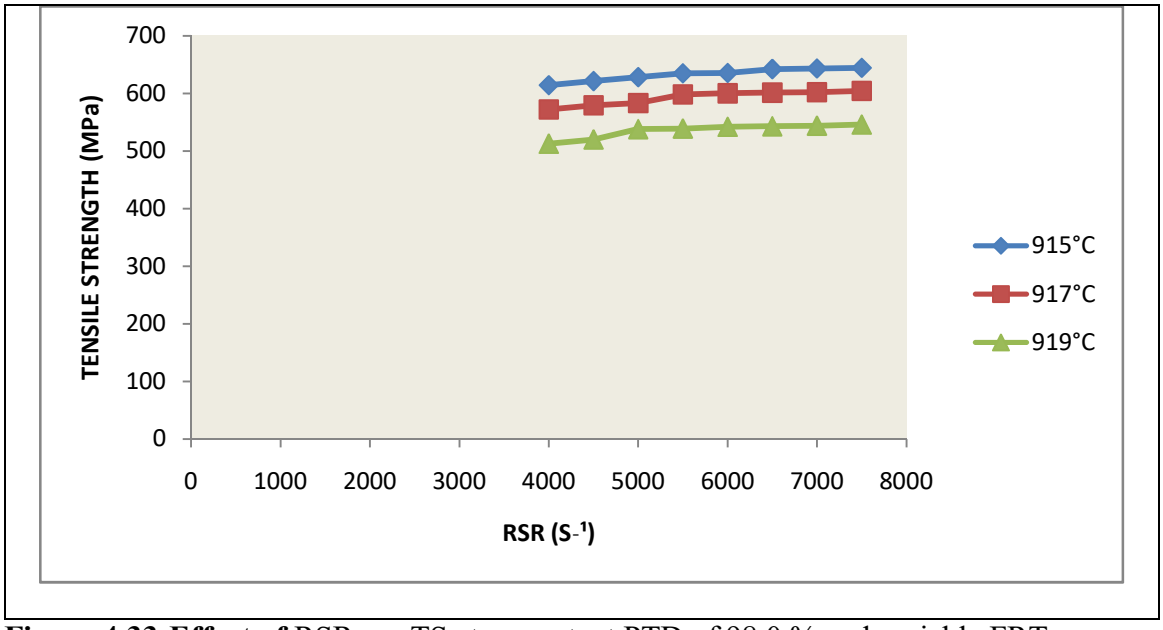

Figure 4.33:Effect of RSR on TS at a constant PTD of 98.0 % and variable FRT.

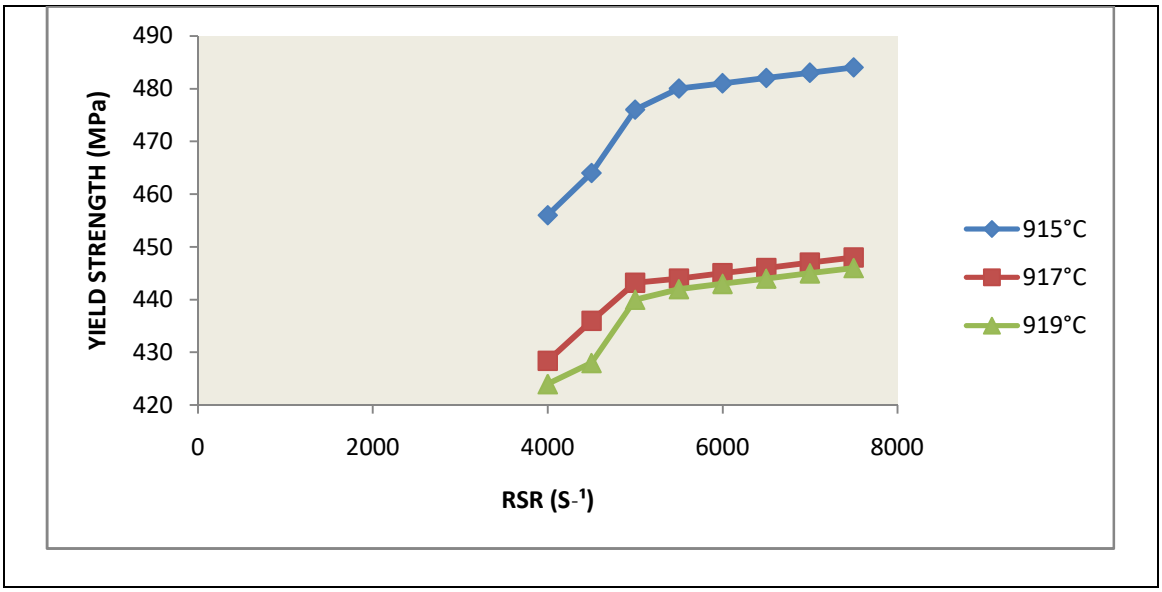

Figure 4.34: Effect of RSR on YSat a Constant PTD of 98.0 % and Variable FRT

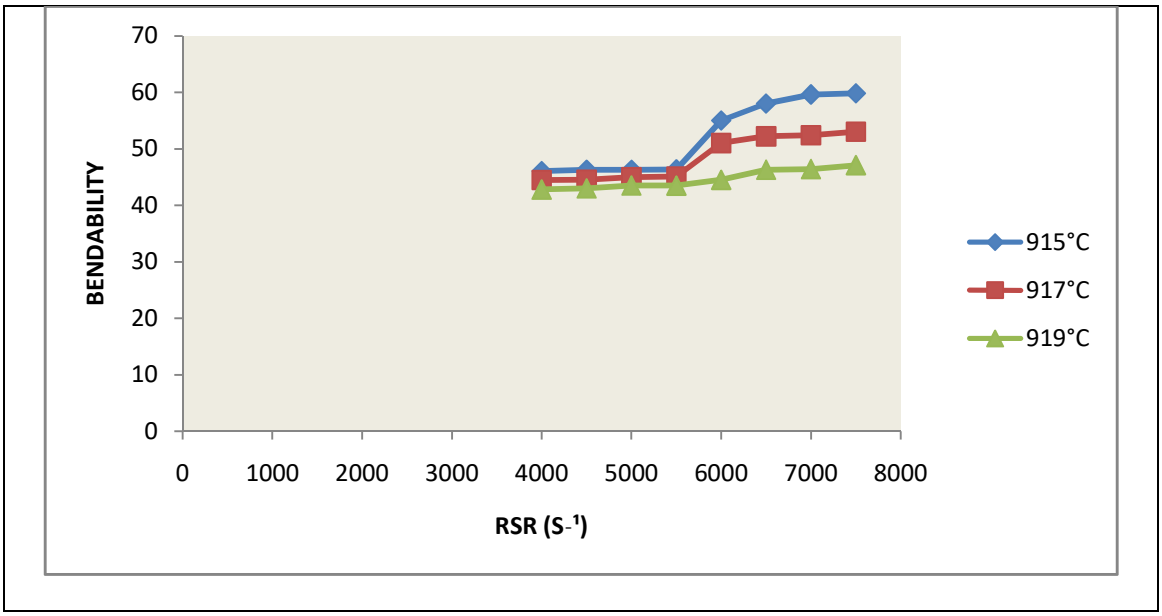

Figure 4.35: Effect of RSR on ductility at a Constant PTD of 98.0 % and Variable FRT

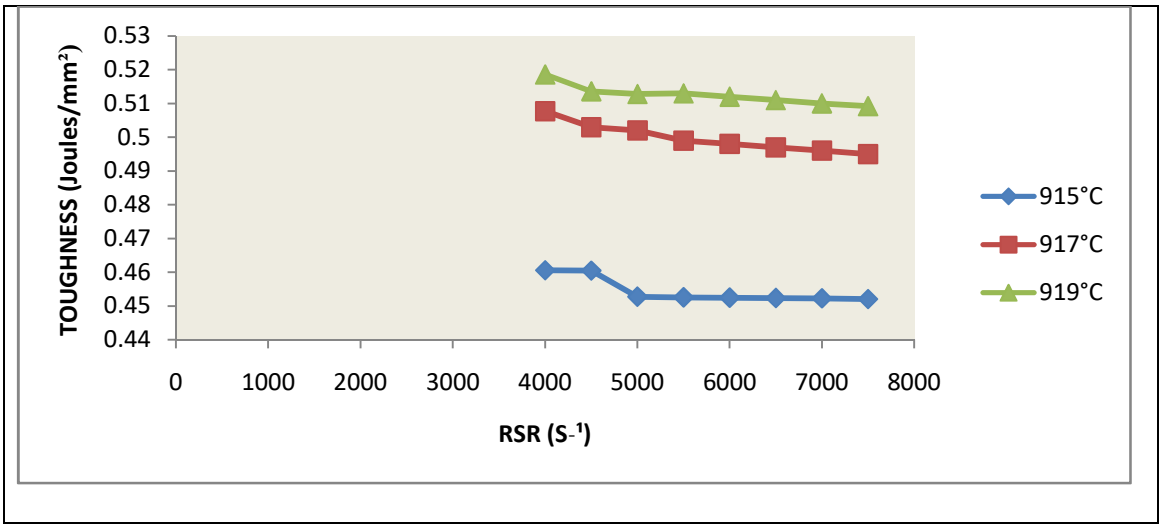

Figure 4.36: Effect of RSR on Impact Energy at a constant PTD of 98.0 % and variable

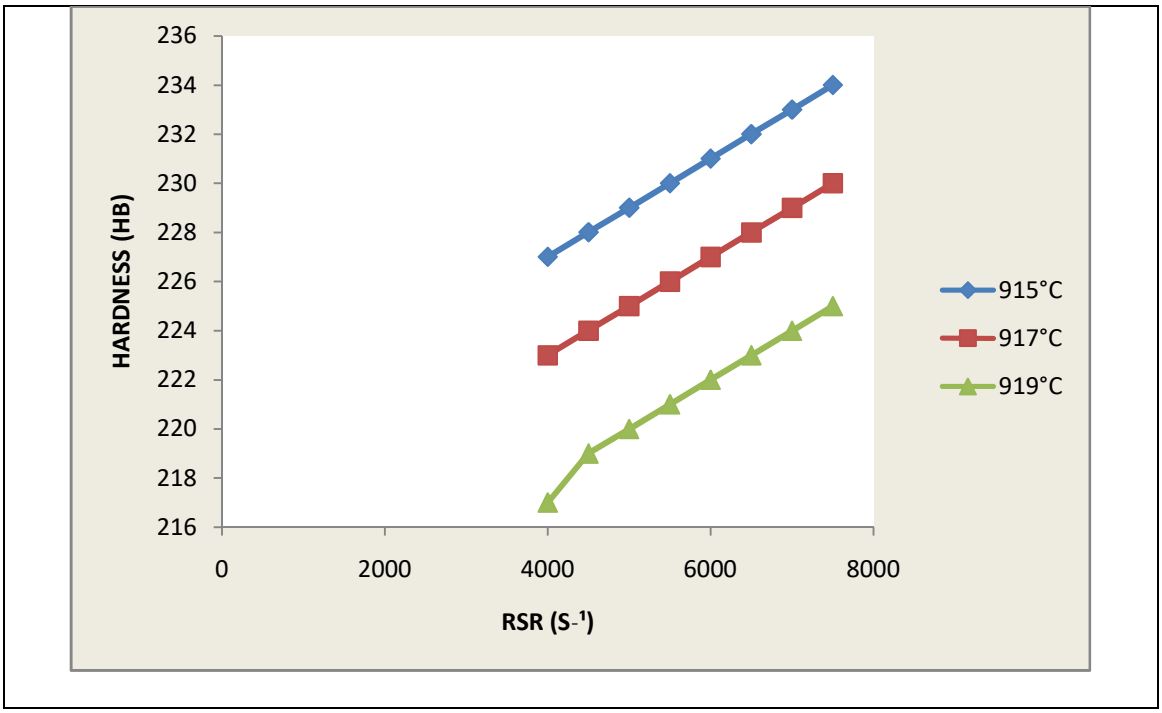

Figure 4.37: Effect of RSR on Hardness at a Constant PTD of 98.0 % and Variable FRT

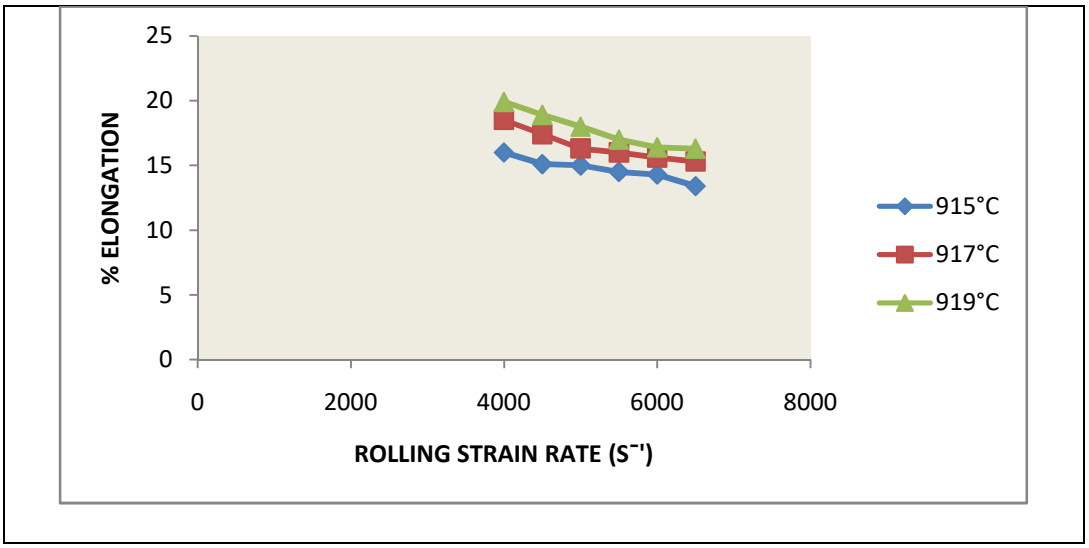

Figure 4.38: Effect of RSR on PE at a Constant PTD of 98.0 % and Variable FRT.

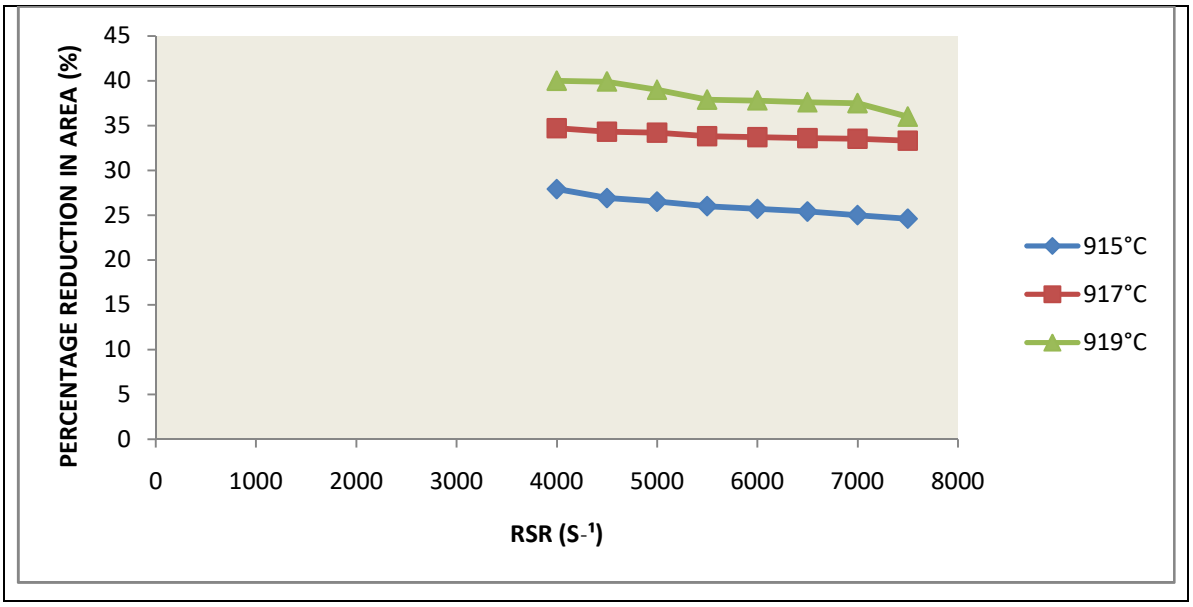

Figure 4.39: Effect of RSR on PRA at a constant PTD of 98.0 % and variable FRT.

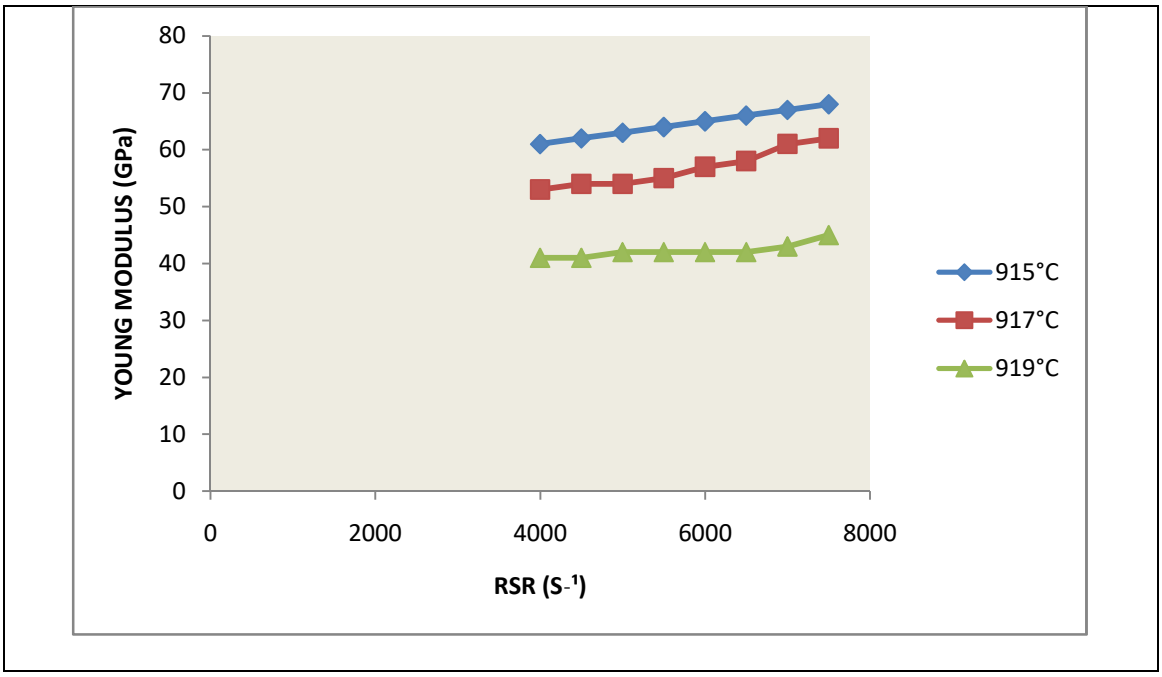

Figure 4.40: Effect of RSR onE at a constant PTD of 98.0 % and variable FRT

4.6 Results and Discussions For RSR at PTD of 96.0 percent

Figures 4.41-4.48 show the influence of RSR on the mechanical properties at a PTD of 96.0 percent and variable FRT.

At 915°C FRT, and 96.0 percent PTD, when the RSR increased from 4000 to 4500 S^{-1} the TS increased from 638 to 689 MPa (Fig.4.41), YS increased from 486 to 487MPa (Fig.4.42) PE decreased from 12 to 11.8%(Fig.4.46), impact energy decreased from 0.41 to 0.40 J/mm^2 (Fig.4.44),ductility increased from 47.51 to 48° (Fig.4.43), PRA decreased from 22 to 21%% (Fig.4.47), hardness increased from 225 to 226 HB (Fig.4.45), E increased from 70 to 71 GPa (Fig.4.48).At 917°C FRT and 96.0 percent PTD, as the RSR increased from 4000 to 4500 S^{-1},TS increased from 602 to 603 MPa (Fig.4.41) YS increased from 450 to 451 MPa (Fig.4.42). PE decreased from 14.1 to 13.7%(Fig.4.46),impact energy decreased from 0.4470 to 0.4300 J/mm^2(Fig,4.44),ductility increased from 46.90 to 47.00° (Fig.4.43), PRA decreased from 32 to 31% (Fig.4.47), hardness increased from 231 to 222 HB (Fig.4.45), E increased from 64 to 65 GPa (Fig.4.48). At 919°C FRT and 96.0 percent PTD, as the RSR increased from 4000 to 4500 S^{-1},TS increased from 575 to 576 MPa(Fig.4.41), YS increased from 448 to 449 MPa (Fig.4.42). PE decreased from 15.8 to 15.6%(Fig.4.46), Impact energy decreased from 0.4800 to 0.4700 J/mm² (Fig.4.44), ductility increased from 45.0 to 45.2°(Fig.4.43), PRA decreased from 36 to 35%(Fig.4.47), hardness increased from 226 to 227 HB (Fig.4.45), E increased from 51 to 52 GPa (Fig.4.48).The above same property trend is also applicable to the other constants of FRT of 917 and 919°C,and the other constants of PTD of 98.0 and 96.0 percent respectively.

As expressed above, if the RSR rises, the TS, YS, hardness, E and ductility also rise and impact energy, PRA and PE lower. The billets were completely broken down and yielded within the stands, which gave rise to maximally displaced mass of constituents and scattered smooth carbon particles.. The billets were yielded because of a stoppage from components in the matrix and other related components. There was an inextensible relationship between the displaced components and other related components which stopped some movement in the matrix.Because of these, TS, YS, hardness, E and ductility were increased in value. The increased E as RSR increased, showed how bulky the hot-

rolled billets were. The same trend was also repeated by the values of ductility. At the same time, lower values of impact energy, PRA and PE was caused by tension in the lattice and uneven dislocated atoms, which gave rise to larger microstructural sizes and longer movement and as the pyrometer readings got higher, the microstructural sizes grew larger

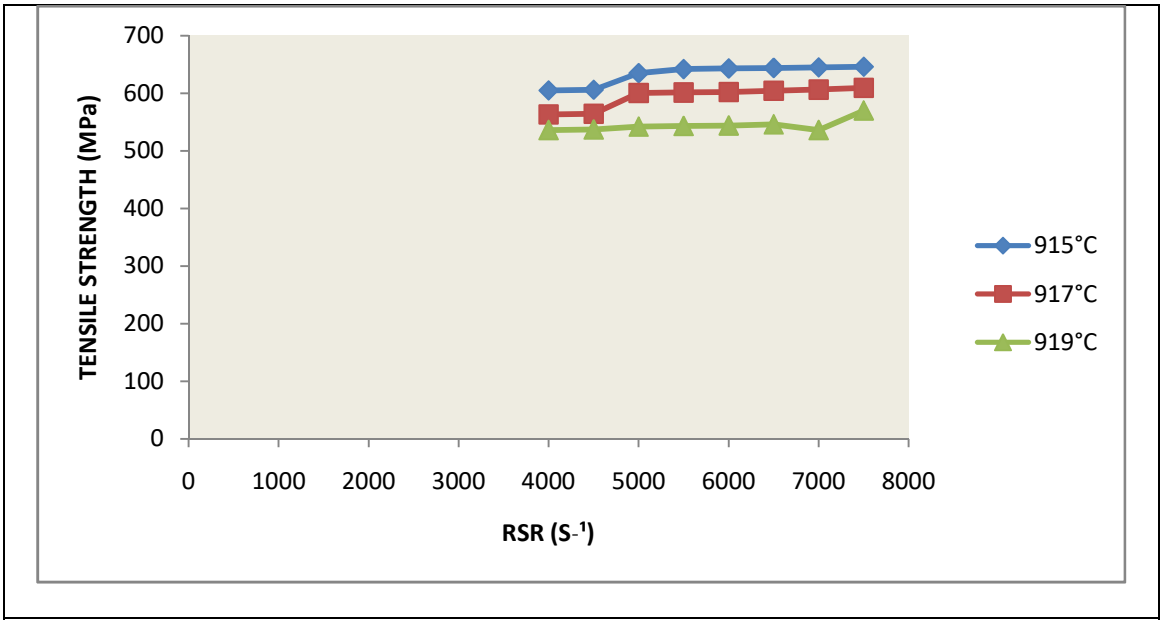

Figure 4.41: Effect of RSR on TS at a constant PTD of 96.0 % and variable FRT.

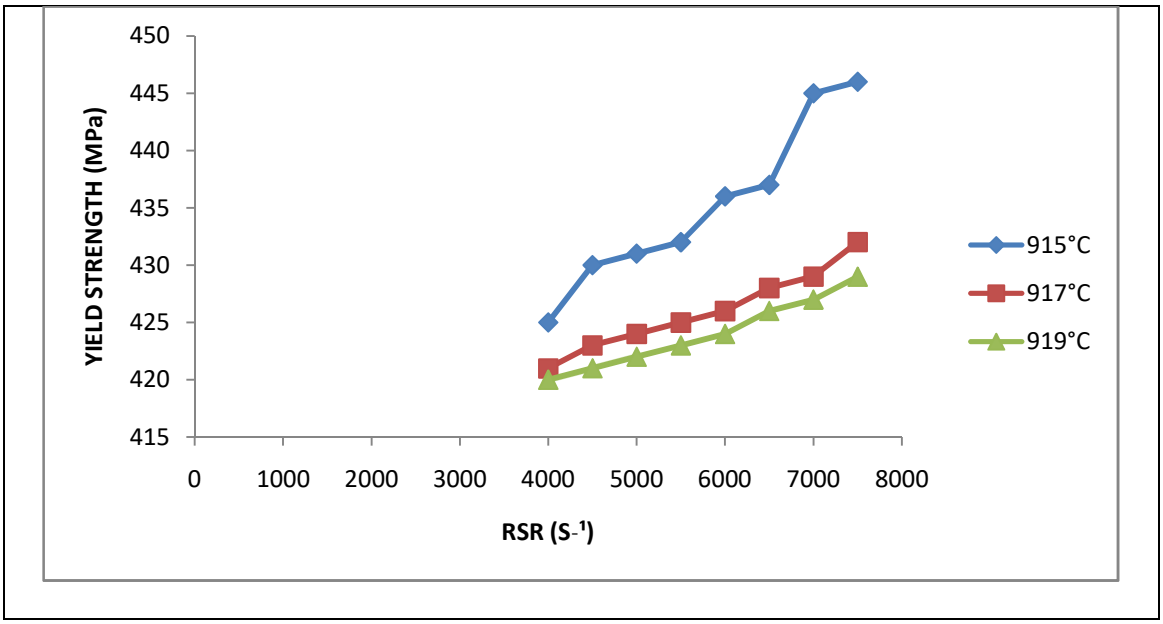

Figure 4.42: Effect of RSR on YS at a constant PTD of 96.0 % and variable FRT.

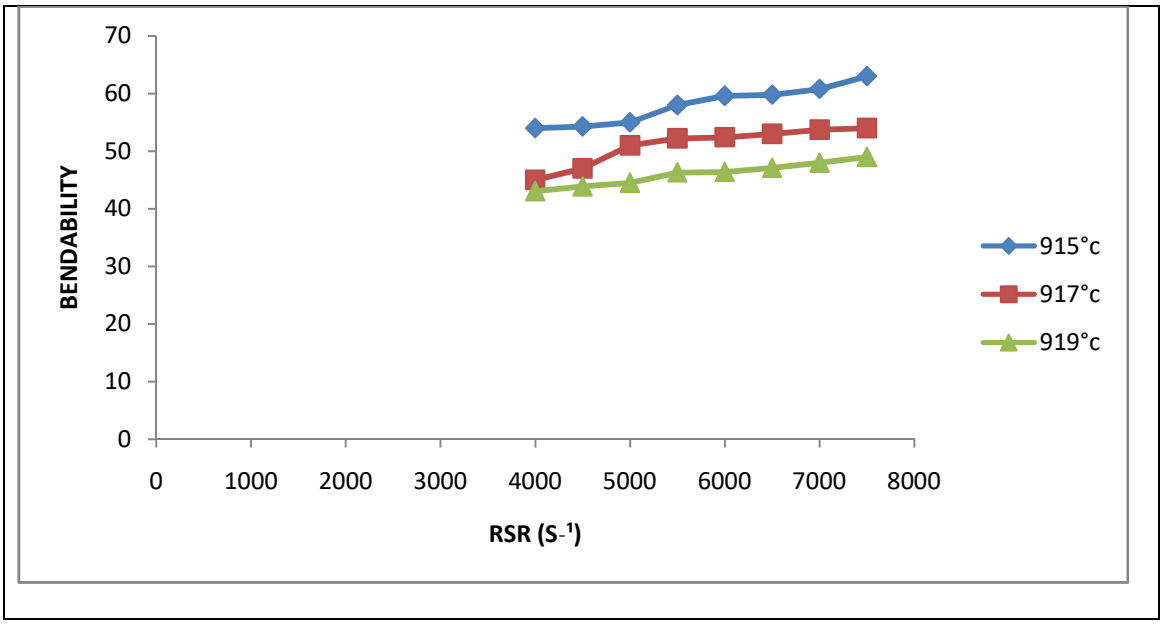

Figure 4.43:Effect of RSR on ductility at a constant PTD of 96.0% and variable FRT.

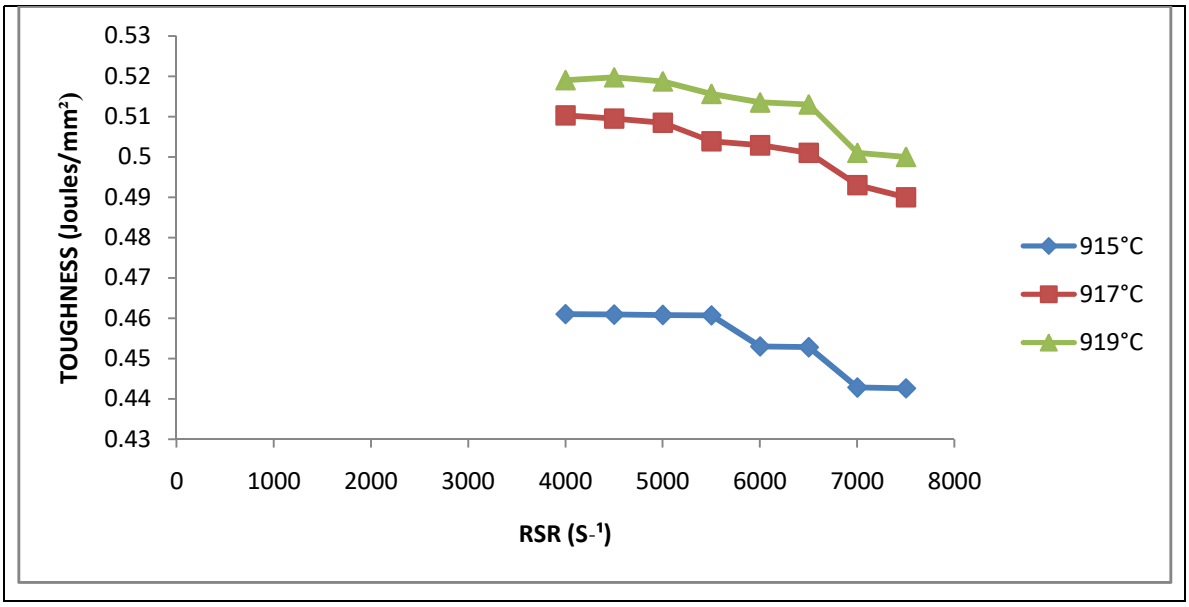

Figure 4.44: Effect of RSR on Impact Energy at a constant PTD of 96.0 % and variable FRT.

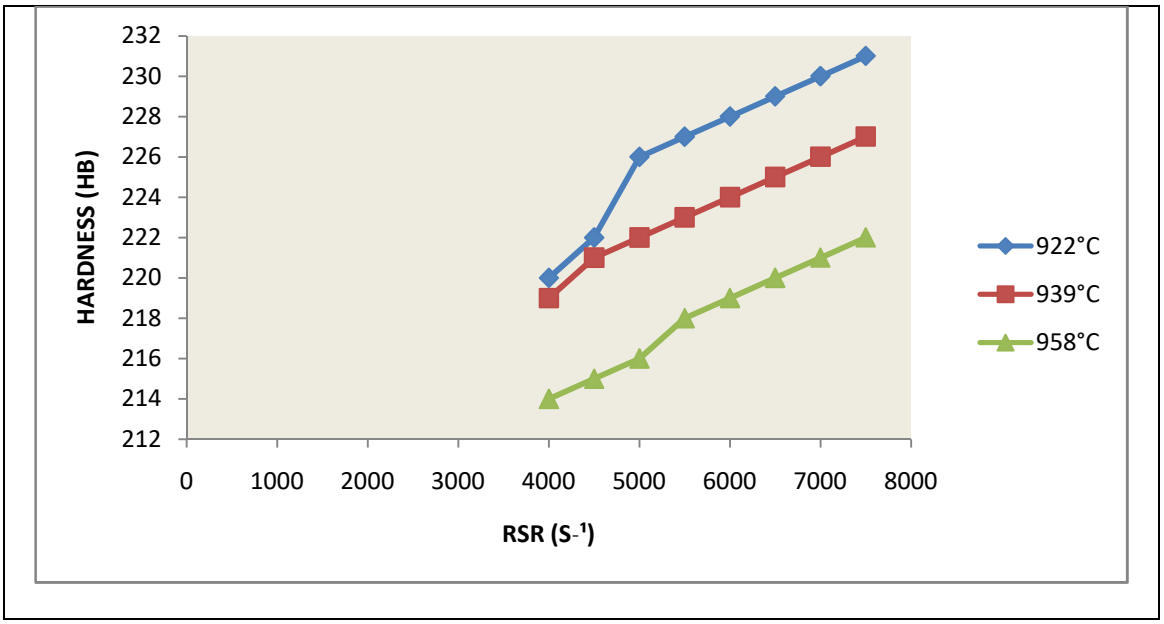

Figure 4.45:Effect of RSRon hardness at a constant PTD of 96.0% and variable FRT.

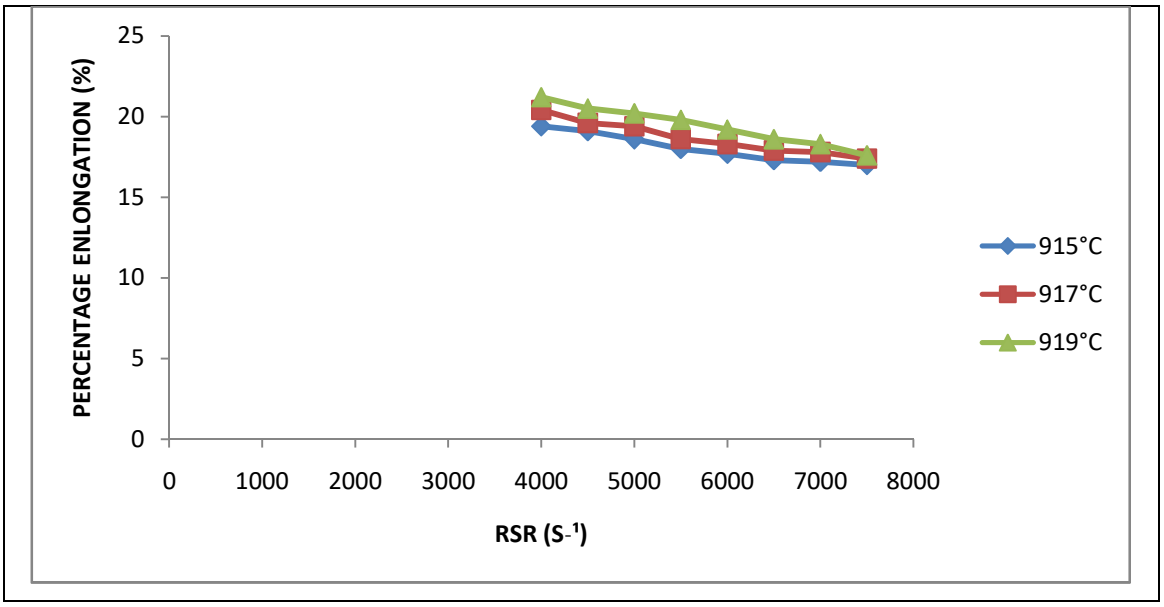

Figure 4.46: Effect of RSR on PE at a constant PTD of 96.0% and variable FRT.

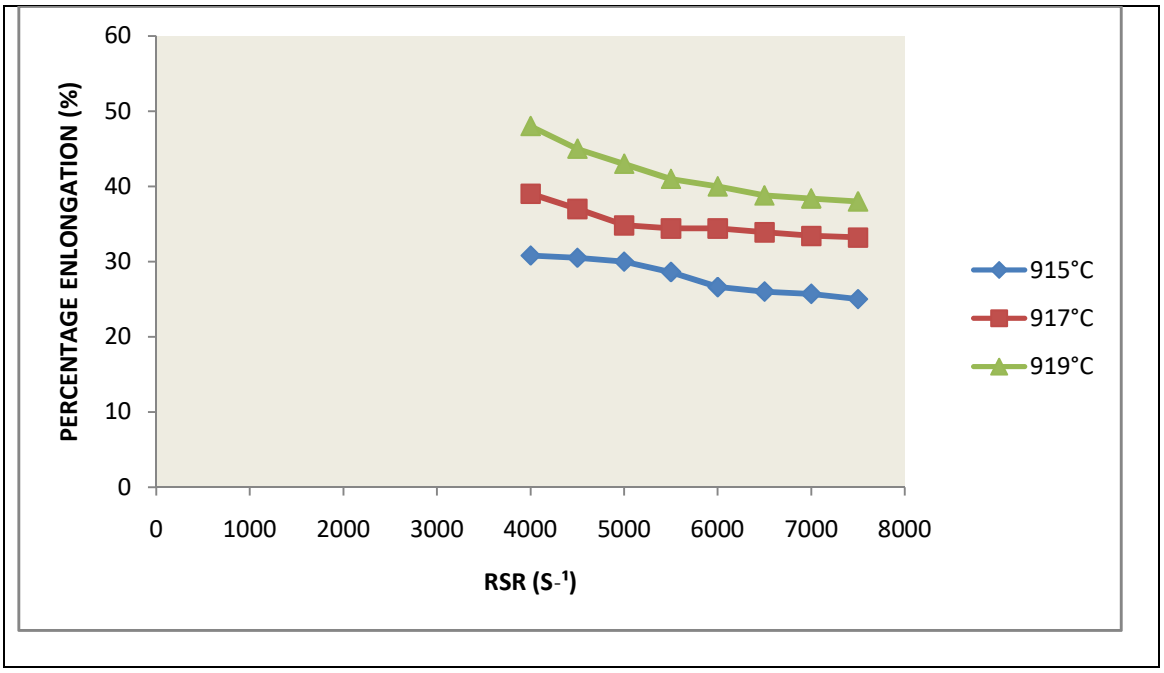

Figure 4.47: Effect of RSR on PRA at a constant PTD of 96.0 % and variable FRT.

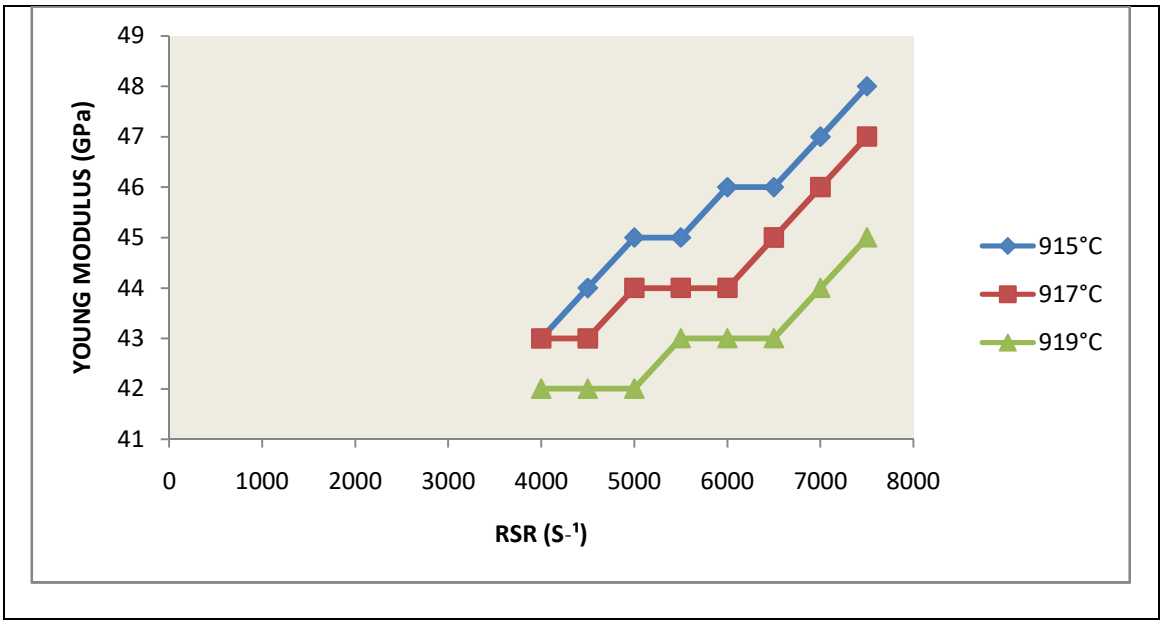

Figure 4.48: Effect of RSR on E at a constant PTD of 96.0% and variable FRT.

4.7 Results and Discussions For FRT at RSR of 7000 S^{-1}

Results of the influence of FRT on the mechanical properties at constant RSR are tabulated in Table 4.3.

The graphs of FRT versus YS, TS, PE, PRA, E, ductility, hardness and impact energy at constant RSR of 7000 S^{-1}, varying with three different PTD of 99.0, 98.0 and 96.0 percent respectively, are shown in Figures 4.49-4.56 .

The TS, YS, hardness, E and ductility reduced with increasing FRT, while the impact energy,PRA and PE increased with increasing FRT for all the degrees of PTD and RSR observed, in the above two cases.

From Tables 4.3 and Figures 4.49 to 4.56, at 99.0 percent PTD and 7000 S^{-1}RSR ,when the FRT increased from 915°C to 921°C, the TS reduced from 611 to 607 MPa, YS reduced from 432 to 429 MPa (Fig.4.49), hardness reduced from 231 to 229 HB (Fig.4.53), E reduced from 42..0 to 41.3GPa (Fig.4.55), ductility reduced from 50 to 48° (Fig.4.50) while impact energyincreased from 0.4480 to 0.4580 J,mm^2 (Fig.4.52), PRA increased from 7.9 to 23.3%(Fig.4.56), PE increased from 10.3 to 15%(Fig.4.54).At 98.0 percent PTD and 7000 S^{-1} RSR ,as the FRT increased from 915 to 921°C,the TS reduced from 610 to 606 MPa, YS reduced from 431 to 422 MPa (Fig.4.49), hardness reduced from 2230 to 227 HB (Fig.4.53), E reduced from 42.1 to 41.2 GPa (Fig.4.55) and ductility reduced from 49.2 to 39°(Fig.4.50);while impact energy increased from 0.44 to 0.52 J/mm^2 (Fig.4.52), PRA increased from 7.7 to 23.2%(Fig.4.56) and PE increased from 10.2 to 14%(Fig.4.56) .

At 96.0 PTD and 7000 S^{-1} RSR ,as the FRT increased from 915 to 921°C, TS reduced from 608 to 594 MPa, YS reduced from 428 to 424 MPa (Fig.4.49), hardness reduced from 227 to 224 HB (Fig.4.53), E reduced from 41.6 to 39.2 GPa (Fig.4.55) and ductility reduced from 46.9 to 44.7°(Fig.4.50);while impact energy increased from 0.5000to 0.5100J/mm^2(Fig.4.52),percentage reduction in area increased from 9.2 to 24.1% (Fig.4.56) PE increased from 15.1 to 17.8%(Fig.4.54) .

The above property trend is also applicable to valuesof RSR at 6000 and 5000 S^{-1} and PTD of 98.0 and 96.0 percent respectively.Similar trend was observedas increased values

of the FRT of the rolled stock gave rise to higher and better TS, YS, hardness, E and ductility of the hot-rolled samples; while the impact energy ,PRA and PE get lower. This was as a result of similar even working of the billet that occured which made them to yield and increase the amount of displaced component. The billets yielded because they were stopped by solidification of another component. All these increased the values of TS, YS, hardness, E and ductility. At the same time, impact energy, PRA and PE decreased.

Table 4.3: Influence of FRT at constant RSR and variable PTD.

FRT (°C)	PTD (%)	RSR (S^{-1})	Hardness (HB)	E (GPa)	Ductility or Bendability (°)	TS (MPa)	YS (MPa)	PE (%)	PRA(%)	Impact Energy (J/mm^2)
915	99.0	7000	231	42.8	50.25	611	432	10.3	7.9	0.48
915	98.0	7000	228	42.2	47.30	610	429	13.1	8.1	0.49
915	96.0	7000	227	41.6	46.90	608	428	15.1	9.2	0.50
917	99.0	7000	231	41.7	48.25	610	431	13.3	12.2	0.48
917	98.0	7000	227	40.9	45.00	609	427	16.2	12.8	0.49
917	96.0	7000	226	40.7	44.80	600	426	17.1	13.5	0.50
919	99.0	7000	230	41.4	48.20	609	430	14.2	21.7	0.51
919	98.0	7000	226	40.7	45.00	608	426	17.2	22.5	0.52
919	96.0	7000	225	40.0	44.80	596	425	17.5	23.3	0.52
921	99.0	7000	229	41.3	48.15	607	429	15.0	23.3	0.49
921	98.0	7000	225	40.5	44.90	597	425	17.3	23.8	0.50
921	96.0	7000	224	39.2	44.70	594	424	17.8	24.1	0.51
923	99.0	7000	229	41.1	46.05	606	428	26.8	16.0	0.50
923	98.0	7000	225	40.0	44.0	595	424	17.4	28.2	0.52
923	96.0	7000	223	38.7	43.8	592	423	17.9	29.0	0.53
925	99.0	7000	229	40.5	45.8	606	427	18.3	32.7	0.51
925	98.0	7000	224	38.0	43.8	594	423	17.9	33.0	0.52
925	96.0	7000	222	36.3	43.6	611	422	18.8	34.4	0.53
927	99.0	7000	228	40.4	45.7	606	426	18.4	32.8	0.55
927	98.0	7000	223	37.0	43.7	594	422	18.6	33.4	0.56
927	96.0	7000	221	36.2	43.5	589	421	18.9	34.5	0.58
929	99.0	7000	227	40.3	45.6	605	425	18.3	32.9	0.59
929	98.0	7000	222	36.0	43.6	589	421	18.7	33.7	0.60
929	96.0	7000	220	36.0	43.4	585	420	19.1	34.6	0.63

Table 4.3 (continued): Effect of FRT at constant RSR and variable PTD.

FRT (°C)	PTD (%)	RSR (S^{-1})	Hardness (HB)	E (GPa)	Ductility or Bendability (°)	TS (MPa)	YS (MPa)	PE (%)	PRA (%)	Impact Energy (J/mm^2)
915	99.0	6000	230	42.8	42.6	610	426	10.2	7.8	0.44
915	98.0	6000	227	42.1	42.1	609	425	13.0	8.0	0.49
915	96.0	6000	226	41.5	41.3	608	424	15.0	9.1	0.50
917	99.0	6000	229	41.6	41.6	609	425	13.1	12.1	0.51
917	98.0	6000	226	40.8	41.9	608	424	16.1	12.7	0.50
917	96.0	6000	225	40.6	39.6	607	423	17.0	13.4	0.51
919	99.0	6000	228	41.3	41.9	608	424	14.1	21.6	0.52
919	98.0	6000	225	40.6	40.7	607	423	17.1	22.3	0.51
919	96.0	6000	224	39.0	40.0	606	422	17.4	23.2	0.52
921	99.0	6000	227	41.2	41.3	607	423	14.0	23.2	0.53
921	98.0	6000	224	40.4	43.4	606	422	17.2	23.7	0.52
921	96.0	6000	223	38.2	38.0	605	421	17.7	24.0	0.53
923	99.0	6000	226	41.0	43.0	606	422	15.0	26.6	0.54
923	98.0	6000	223	38.0	40.0	605	421	17.3	28.0	0.53
923	96.0	6000	222	37.7	37.0	604	420	17.8	28.0	0.54
925	99.0	6000	225	40.3	41.0	605	421	17.2	32.6	0.57
925	98.0	6000	223	37.0	38.0	604	420	17.8	32.0	0.61
925	96.0	6000	221	35.7	35.0	603	419	18.6	34.2	0.61
927	99.0	6000	224	40.0	44.8	604	420	17.3	32.7	0.57
927	98.0	6000	222	36.0	42.5	603	418	17.9	33.0	0.59
927	96.0	6000	220	34.0	41.5	602	417	18.7	34.3	0.61
929	99.0	6000	223	39.7	44.7	603	417	17.4	32.8	0.61
929	98.0	6000	221	35.0	42.4	602	413	18.1	34.0	0.62
929	96.0	6000	219	33.0	41.3	601	414	18.9	34.4	0.65

Table 4.3 (continued): Effect of FRT at constant RSR and variable PTD.

FRT (°C)	PTD (%)	RSR (S^{-1})	Hardness (HB)	E (GPa)	Ductility or Bendability (°)	TS (MPa)	YS (MPa)	PE (%)	PRA (%)	Impact Energy (J/mm^2)
915	99.0	5000	229	42.5	49.1	609	425	10.5	8.0	0.56
915	98.0	5000	226	42.0	46.8	608	424	13.6	9.3	0.50
915	96.0	5000	228	41.4	45.7	607	423	15.5	10.3	0.51
917	99.0	5000	228	41.5	48.0	608	424	13.4	12.4	0.57
917	98.0	5000	225	40.6	45.4	607	423	16.4	12.9	0.51
917	96.0	5000	224	40.5	44.4	606	422	17.3	13.8	0.52
919	99.0	5000	227	41.2	47.0	607	423	14.4	21.8	0.58
919	98.0	5000	224	40.5	44.9	606	422	17.3	22.8	0.52
919	96.0	5000	223	40.0	43.7	605	421	18.0	23.5	0.53
921	99.0	5000	226	41.0	46.15	606	422	14.5	23.3	0.59
921	98.0	5000	223	39.4	43.8	605	421	17.4	23.9	0.53
921	96.0	5000	222	38.1	42.6	599	420	18.1	25.0	0.54
923	99.0	5000	225	40.2	45.0	605	421	16.0	26.7	0.60
923	98.0	5000	222	37.8	43.1	604	420	17.5	29.0	0.54
923	96.0	5000	221	37.0	41.7	593	419	18.3	30.0	0.55
925	99.0	5000	224	40.0	43.9	604	420	17.4	32.7	0.61
925	98.0	5000	221	36.7	42.5	593	419	18.6	34.0	0.56
925	96.0	5000	220	35.6	41.5	582	418	19.8	35.3	0.59
927	99.0	5000	223	39.0	43.8	591	419	17.5	32.8	0.62
927	98.0	5000	220	36.6	42.4	586	417	18.2	33.0	0.58
927	96.0	5000	219	35.3	41.4	577	416	19.9	35.6	0.60
929	99.0	5000	222	36.0	43.7	585	417	17.6	32.9	0.63
929	98.0	5000	219	36.0	42.3	580	416	18.8	36.0	0.59
929	96.0	5000	218	35.0	41.3	575	415	20.0	37.0	0.61

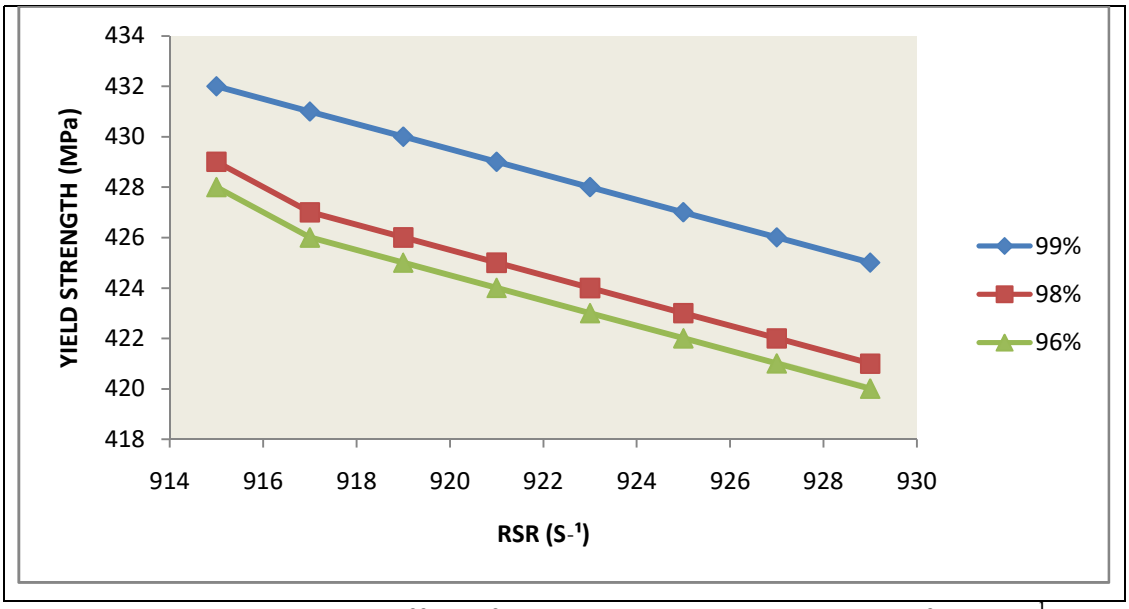

Figure 4.49: Effect of FRT on YS at a constant RSR of 7000 S^{-1}

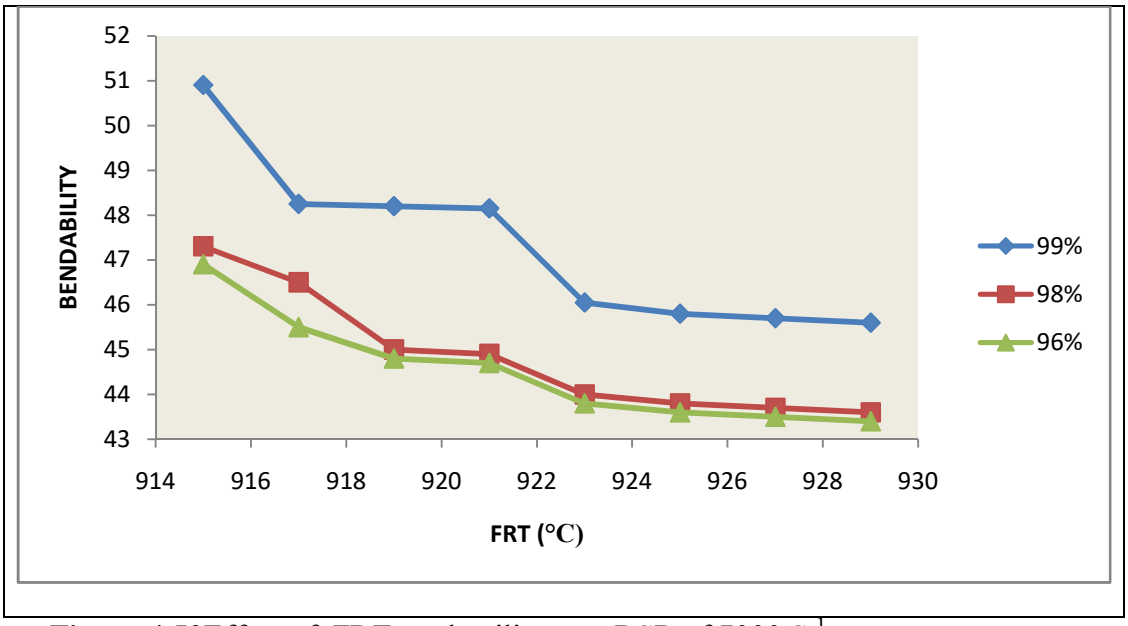

Figure 4.50 Effect of FRT on ductility at a RSR of 7000 S^{-1}

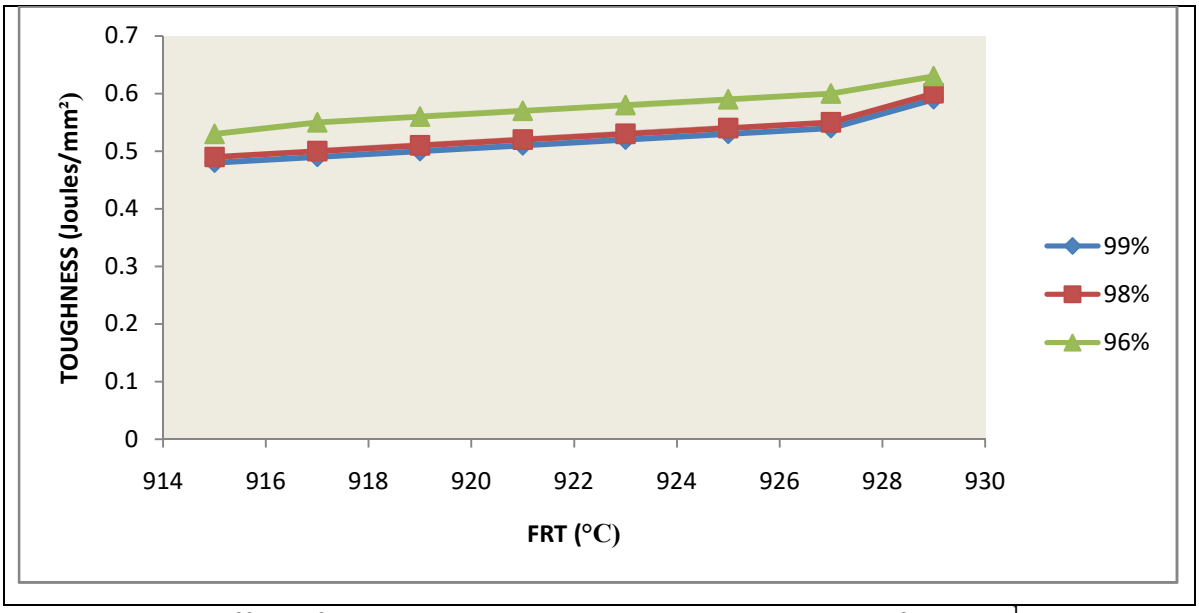

Figure 4.51: Effect of FRT on Impact Energy at a constant RSR of 7000 S^{-1}

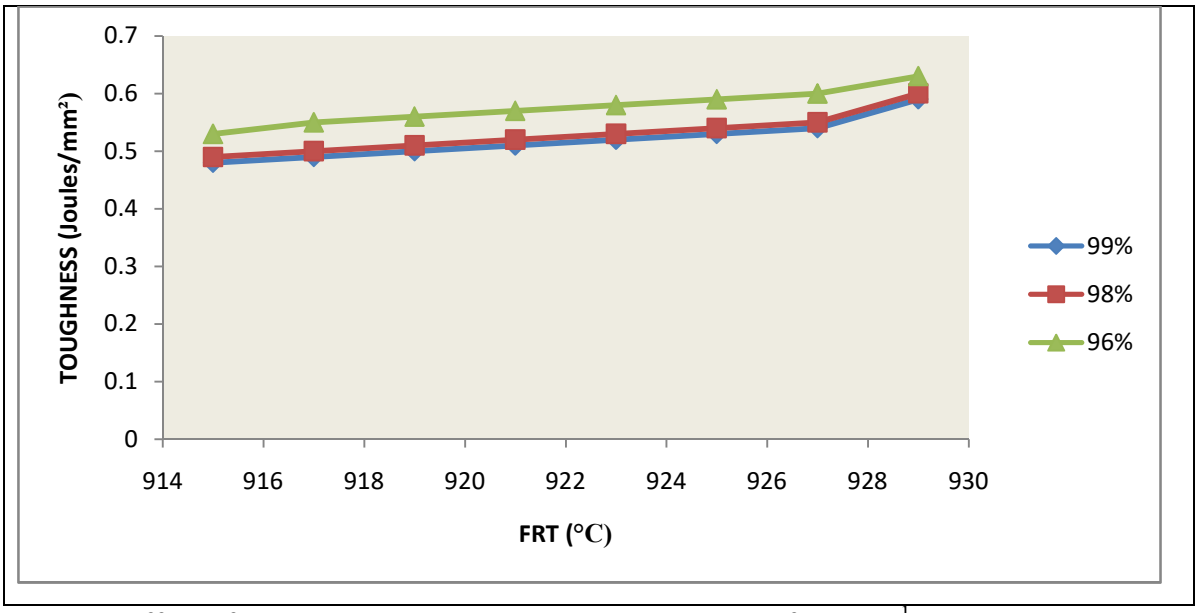

Figure 4.52: Effect of FRT on Impact Energy at constant RSR of 7000 S^{-1}

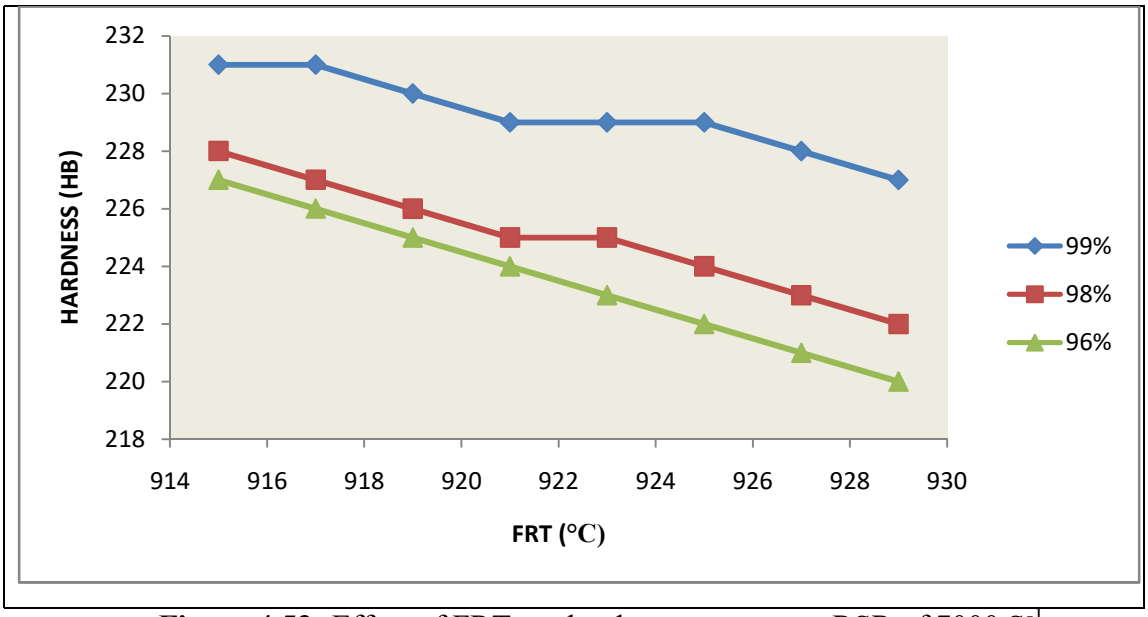

Figure 4.53: Effect of FRT on hardness at constant RSR of 7000 S^{-1}

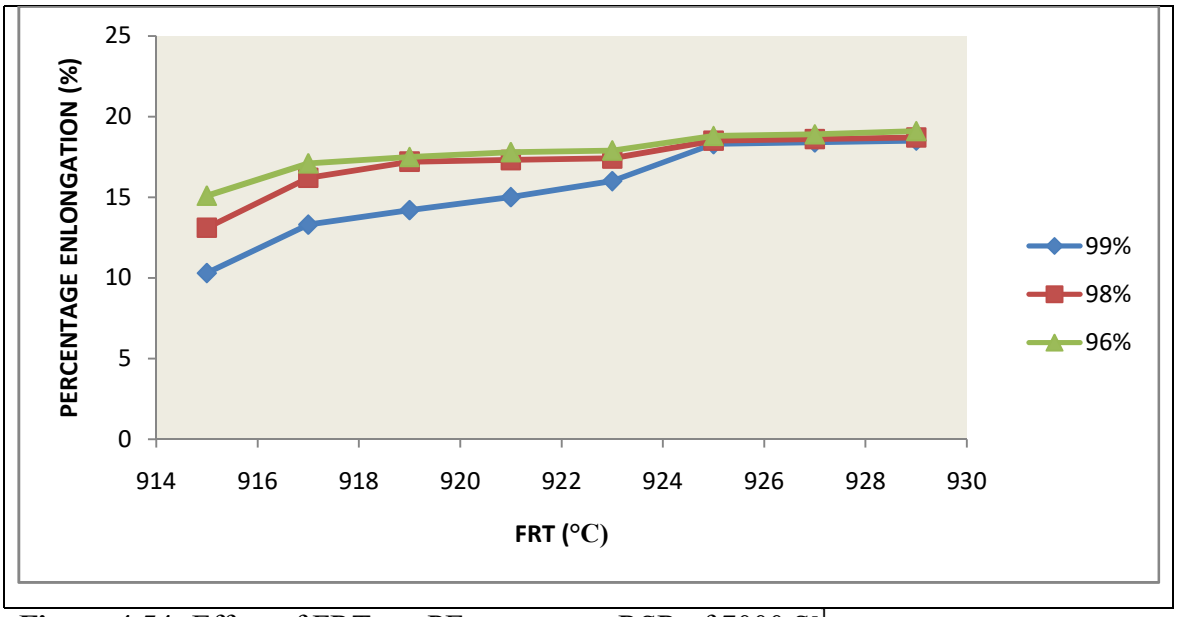

Figure 4.54: Effect of FRT on PE at constant RSR of 7000 S^{-1}

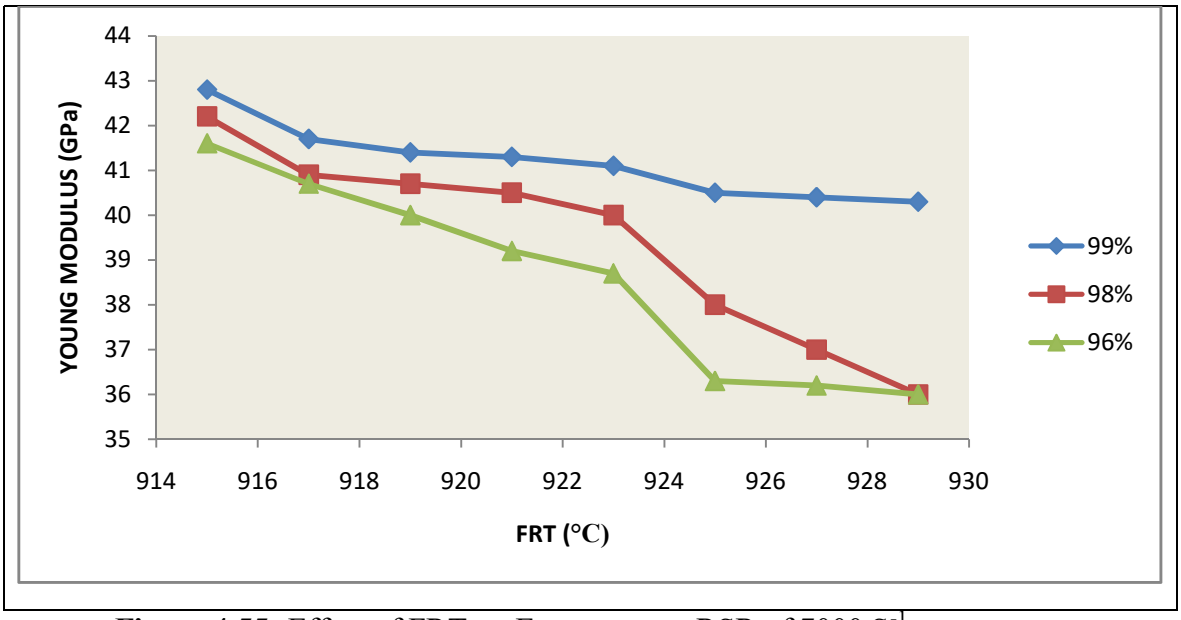

Figure 4.55: Effect of FRT on E at constant RSR of 7000 S^{-1}

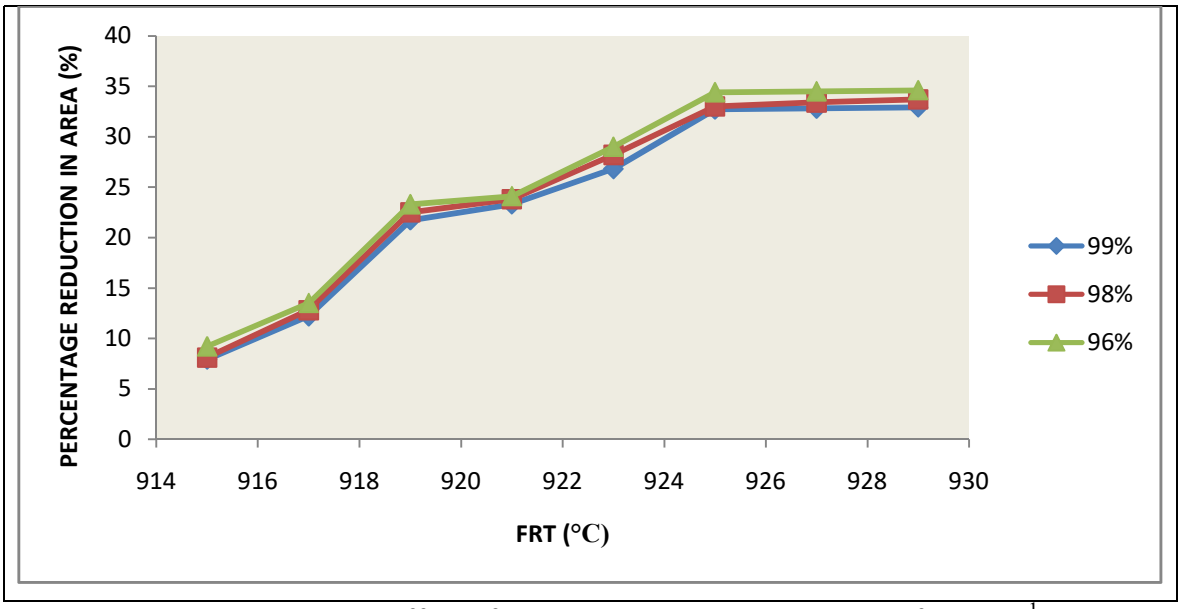

Figure 4.56: Effect of FRT on PRA at constant RSR of 7000 S^{-1}

4.8 Results and Discussion For influence of FRT at RSR of 6000 S^{-1}

The graphs of FRT versus YS, TS, PE, PRA, E, ductility, hardness and impact energy at constant RSR of 6000 S^{-1},at different PTD of 99.0, 98.0 and 96.0 percent respectively, are shown in Figures 4.57-4.64 .

The TS, YS, hardness, E and ductility reduced with increasing FRT, while the impact energy, PRA and PE increased with increasing FRT for all the degrees of PTD and RSR observed, in the above two cases.

From Figures 4.57 to 4.64 ,at 99 PTD and 6000 S^{-1} and RSR ,when the FRT increased from 915°C to 921°C,the UTS reduced from 610 to 607 MPa (Fig.4,57), YS reduced from 426 to 423 MPa (Fig.4.58), hardness reduced from 230 to 227 HB (Fig.4.61), E reduced from 42.8 GPa to 41.2 GPa (Fig.4.63), ductility reduced from 42.6 to 41.3°(Fig.4.59) while impact energy increased from 0.4400 to 0.5300 J/mm^2 (Fig.4.60), PRA increased from 7.8 to 23.2%(Fig.4.64), PE increased from 10.2% to 14%(Fig.4.62).At 98% PTD and 6000 s^{-1}RSR ,as the FRT increased from 915 to 921°C,the TS reduced from 609 to 606 MPa (Fig.4.57) YS reduced from 425 to 422 MPa (Fig.4.58), hardness reduced from 227 to 224 HB (Fig.4.61), E reduced from 42.1 to 40.4 GPa (Fig.4.63) and ductility reduced from 42.1 to 43.4°(Fig.4.59);while impact energy increased from 0.49 to 0.52 J/mm^2 (Fig.4.60), PRA increased from 8 to 23.7%(Fig.4.64) and PE increased from 13 to 17.2%(Fig.4.62) .

At 96.0 percent PTD and 6000 S^{-1} RSR ,as the FRT increased from 915 to 921°C ,the TS reduced from 608 to 605MPa (Fig.4.570, YS reduced from 424 to 421 MPa (Fig.4.58), hardness reduced from 226 to 223 HB (Fig.4.61), E reduced from 41.5 to 38.2 GPa (Fig.4.63) and ductility reduced from 41.3 to 38°(Fig.4.59);while impact energy increased from 0.50 to 0.53 J/mm^2(Fig.4.60), PRA increased from 9.1 to 24%(Fig.4.64) and PE increased from 15 to 17.7%(Fig.4.62) .

The above property trend is also similar to constants of RSR at 6000 and 5000 S^{-1} and constants of PTD of 98.0 and 96.0 percent respectively. It was a similar trend also, as it was observed that increased values of the FRT of the rolled stock also gave rise to higher and better TS, YS, hardness, E and ductility of the hot-rolled samples; while the impact

energy PRA and PE get lower. This was as a result of similar even working of the billet that took place, which made them to yield and increase the amount of displaced component. The billets yielded because they were stopped by solidification of another component. All these increased the values of TS, YS, hardness, E and ductility; while, impact energy, PRA and PE decreased.

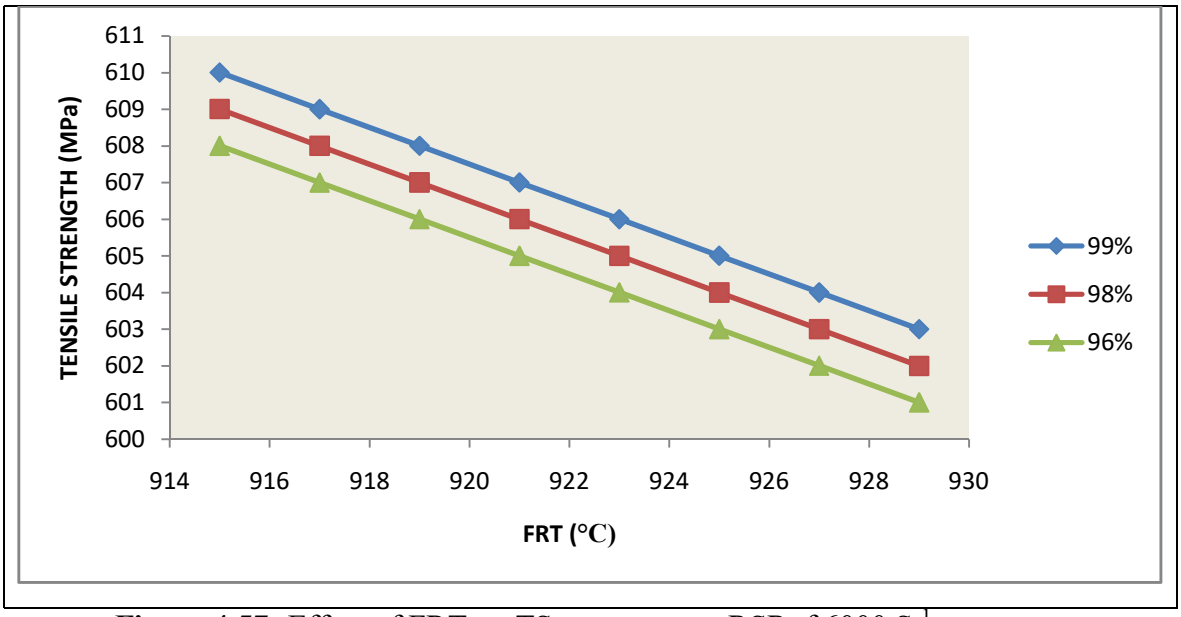

Figure 4.57: Effect of FRT on TS at a constant RSRof 6000 S^{-1}.

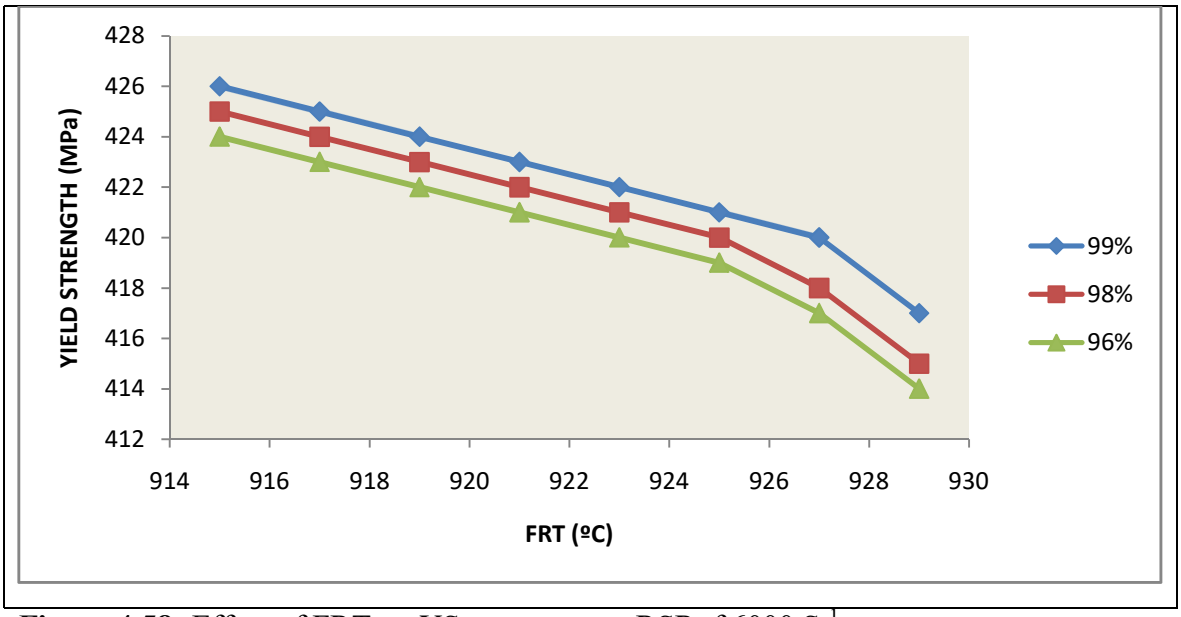

Figure 4.58: Effect of FRT on YS at a constant RSRof 6000 S^{-1},

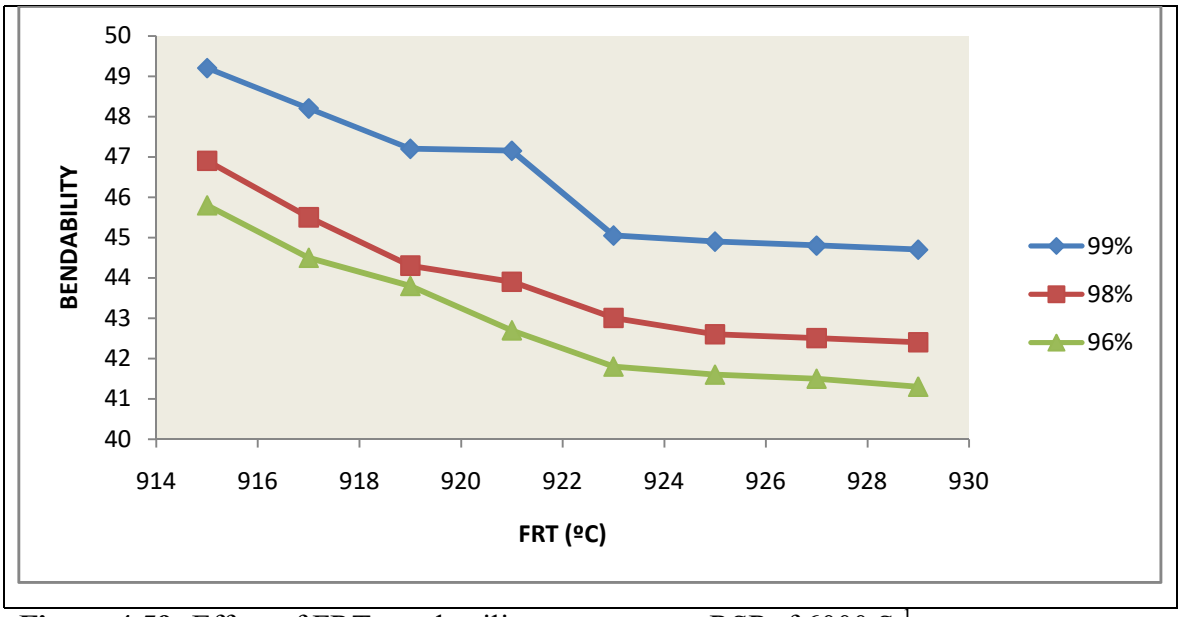

Figure 4.59: Effect of FRT on ductility at a constant RSRof 6000 S^{-1},

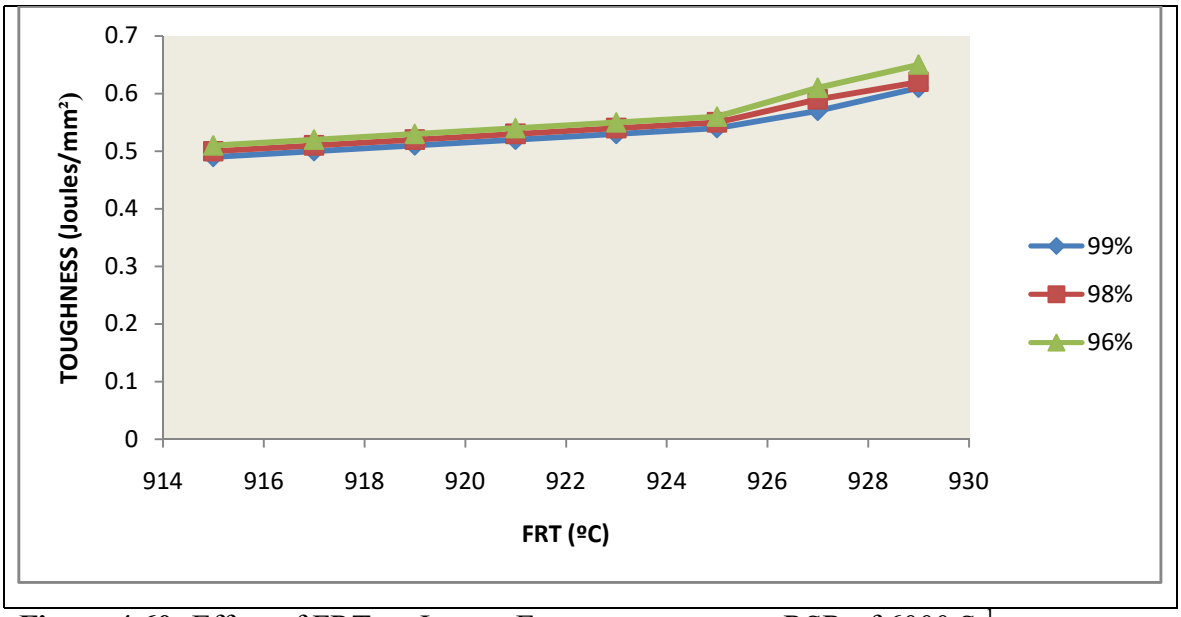

Figure 4.60: Effect of FRT on Impact Energy at a constant RSR of 6000 S^{-1},

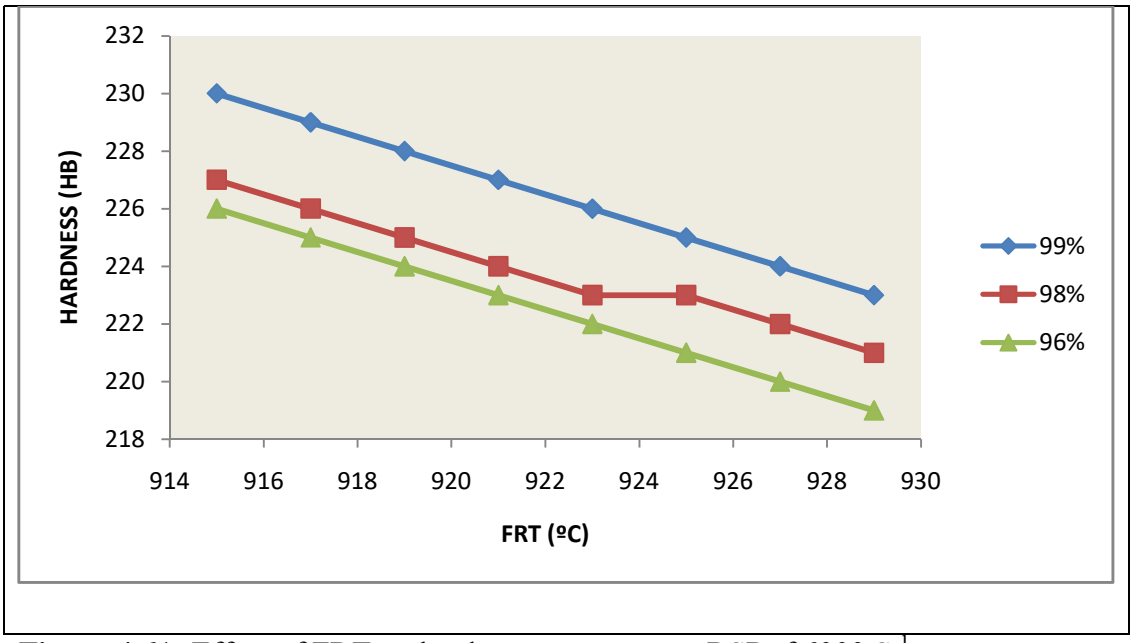

Figure 4.61: Effect of FRT on hardness at a constant RSRof 6000 S^{-1}

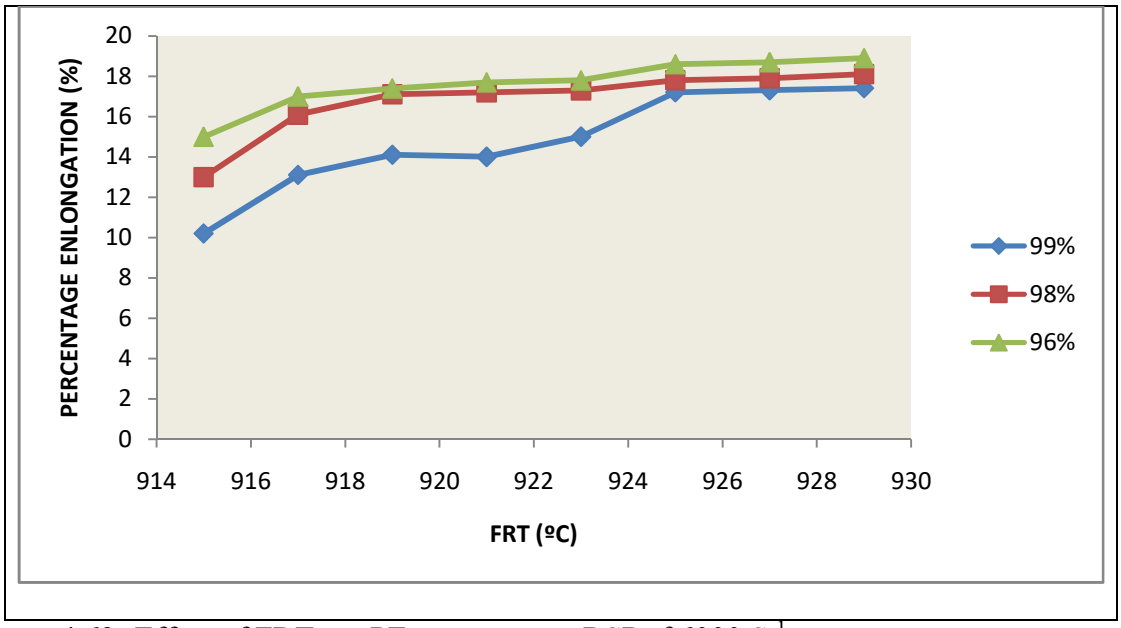

Figure 4.62: Effect of FRT on PE at a constant RSRof 6000 S^{-1},

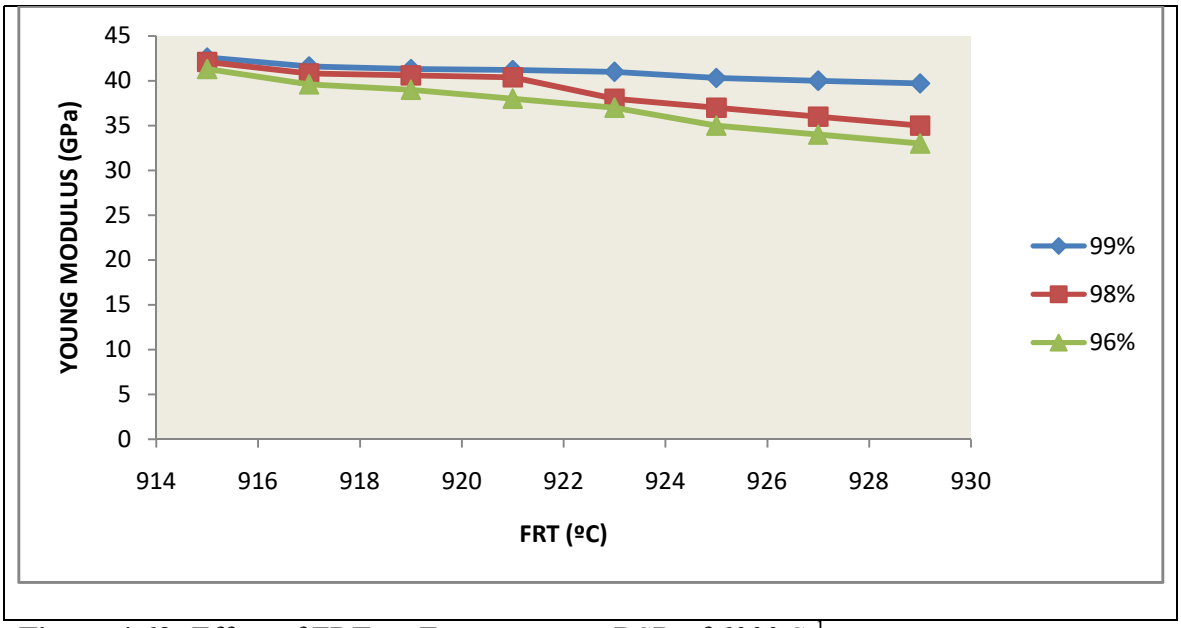

Figure 4.63: Effect of FRT on E at a constant RSR of 6000 S^{-1},

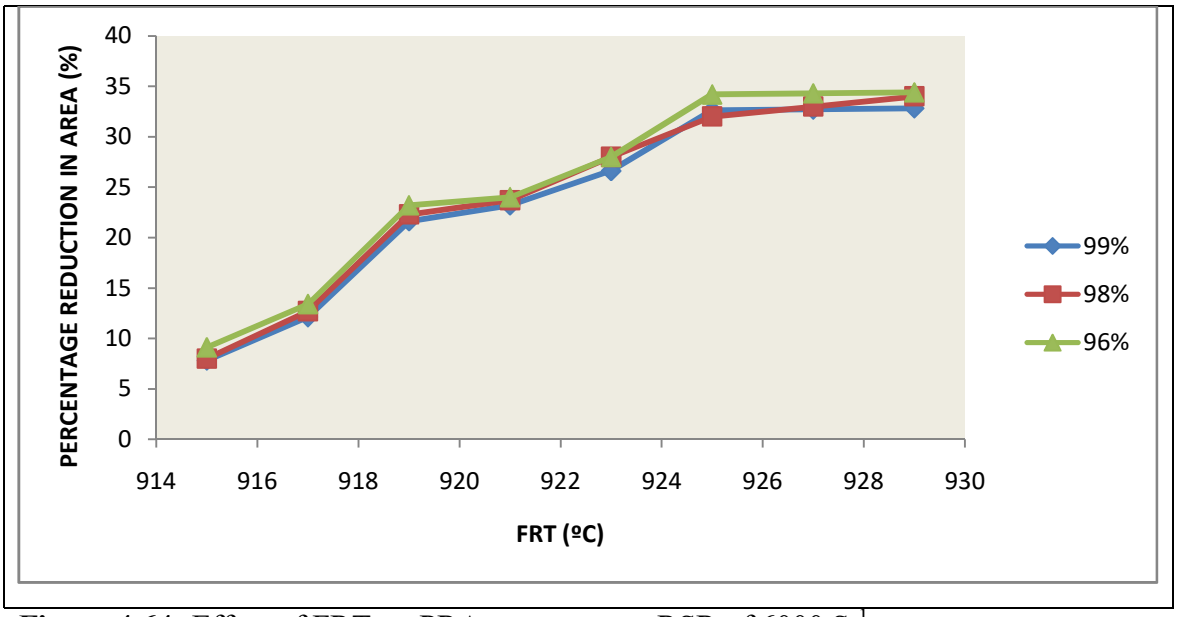

Figure 4.64: Effect of FRT on PRA at a constant RSR of 6000 S^{-1}

4.9 Results and Discussion For Effects of FRT Temperature at RSR of 5000 S^{-1}

The plots of FRT versus YS, TS, PE, PRA, E, ductility, hardness and impact energy at RSR of 5000 S^{-1}, varying as different PTD of 99.0 ,98.0 and 96.0 percent respectively, are shown in Figures 4.65-4.72 .

The TS, YS, hardness, E and ductility reduced with increasing FRT, while the impact energy, PRA and PE increased with increasing FRT for all the degrees of PTD and RSR observed, in the above two cases.

From Tables 4.3 and Figures 4.65 to 4.72 ,at 99.0% PTD and 5000 s^{-1} RSR ,when the FRT increased from 915°C to 921°C, the TS reduced from 609 to 606MPa (Fig.4.65), YS reduced from 425 to 422MPa (Fig.4.66), hardness reduced from 229 to 226 HB (Fig.4.69), E reduced from 42.5 to 41 GPa (Fig.4.71),ductility reduced from 49.1 to 46.15°(Fig.4.67) while impact energy increased from 0.56 to 0.59 J/mm^2 (Fig.4.68), PRA increased from 8 to 23.3%(Fig.4.72), PE increased from 10.5 to 14.5%(Fig.4.70). At 98 percent PTD and 5000 S^{-1} RSR,as the FRT increased from 915 to 921°C the TS reduced from 608 to 605MPa (Fig.4.65), YS reduced from 424 to 421 MPa (Fig.4.66), hardness reduced from 226 to 223 HB (Fig.4.69), E reduced from 42 to 39.4GPa (Fig.4.71) and ductility reduced from 46.8 to 43.8°(Fig.4.67);while impact energy increased from 0.50 to 0.53 J/mm^2(Fig.4.68), PRA increased from 9.3 to 23.9%(4.72) and PE increased from 13.6 to 17.4%(Fig.4.70).

At 96.0 percent PTD and 5000 S^{-1}RSR ,as the FRT increased from 915 to 921°C,the TS reduced from 607 to 599 MPa (Fig.4.65), YS reduced from 423 to 420 MPa (Fig.4.66), hardness reduced from 228 to 222 HB (Fig.4.69), E reduced from 41.4 to 38.1GPa (Fig.4.71) and ductility reduced from 45.7 to 42.6°(Fig.4.67);while impact energy increased from 0.51 to 0.54 J/$mm^{2(}$ (Fig.4.68), PRA increased from 10.3 to 25%(Fig.4.72) and PE increased from 15.5 to 18.1%(Fig.4.72) .

The above property trend is also applicable to constants of RSR of 6000 and 5000 S^{-1} and constants of PTD of 98.0 and 96.0 percent respectively. It was a similar trend also, as it was observed that increased values of the FRT of the rolled stock also gave rise to higher and better TS, YS, hardness, E and ductility of the hot-rolled samples; while the impact

energy PRA and PE get lower. This was as a result of similar even working of the billet that took place above which made them to yield and increase the amount of displaced component. The billets yielded because they were stopped by solidification of another component. All these increased the values of TS, YS, hardness, E and ductility. At the same time, impact energy, PRA and PE decreased.

.

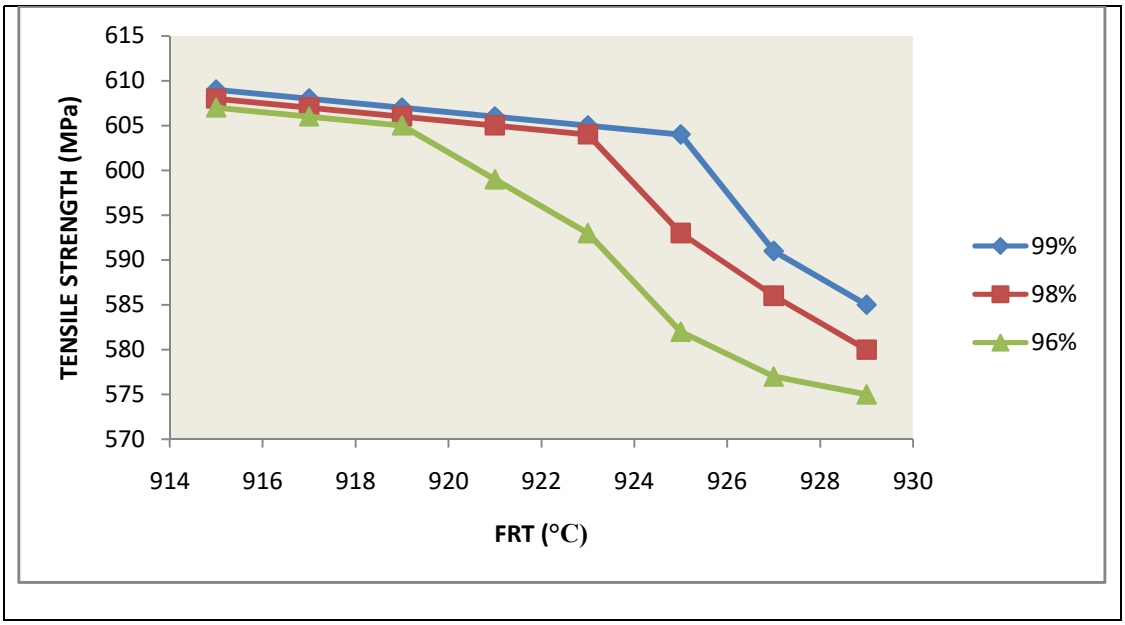

Figure 4.65: Effect of FRT on TS at a constant RSR

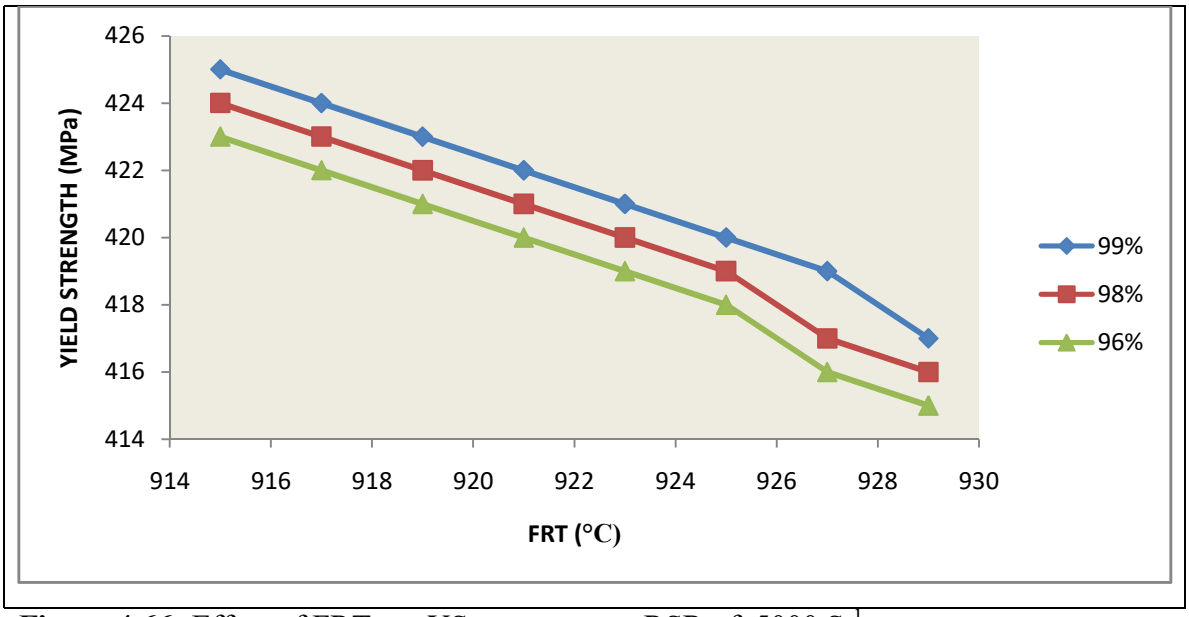

Figure 4.66: Effect of FRT on YS at a constant RSR of 5000 S^{-1}

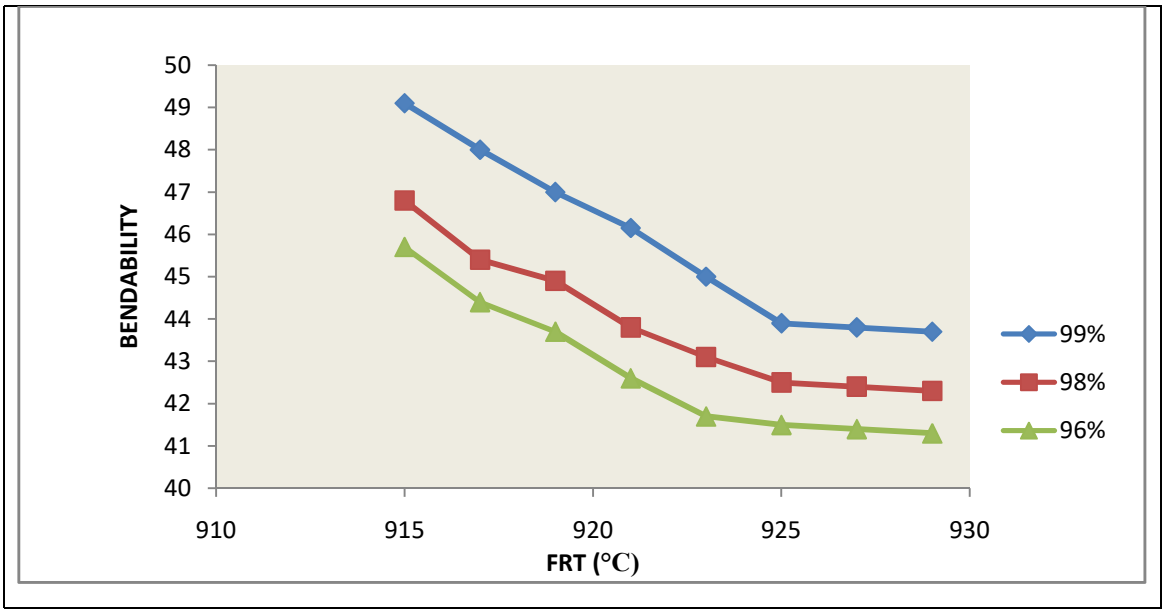

Figure 4.67: Effect of FRT on ductilityat a constant RSR

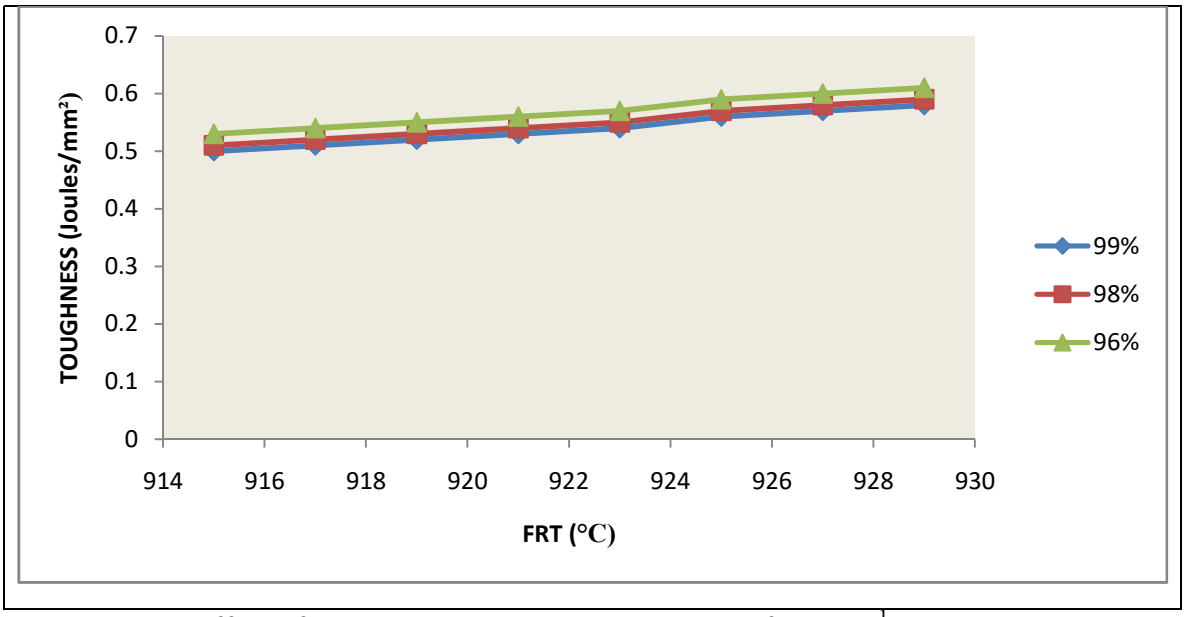

Figure 4.68: Effect of FRT on Impact Energy at a RSR of 5000 S^{-1},

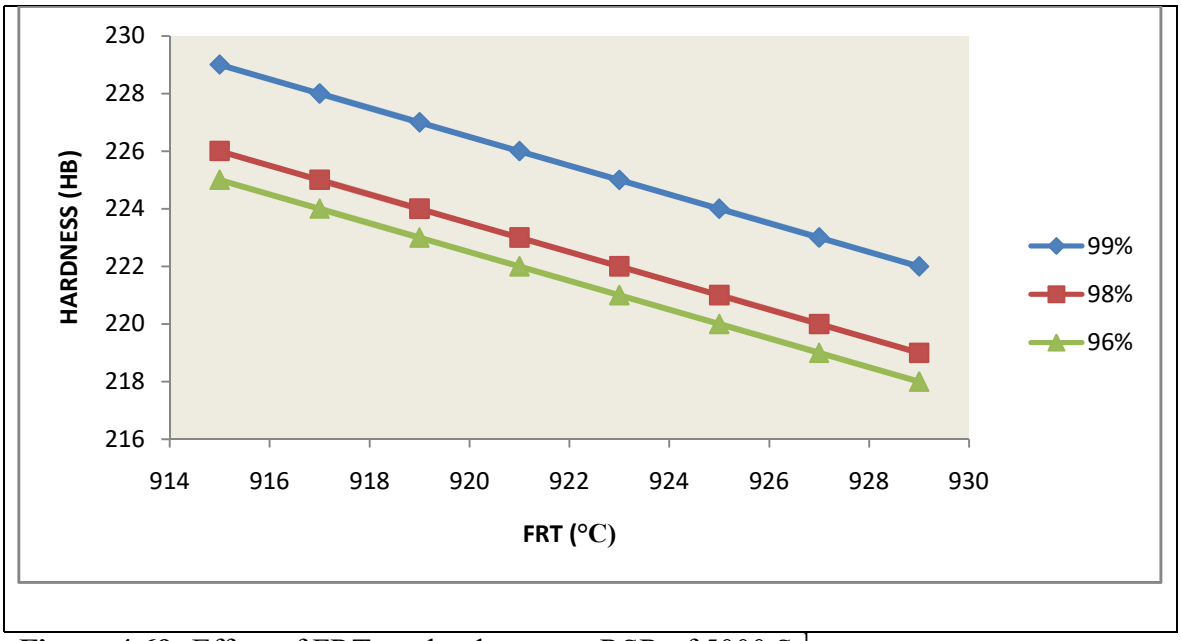

Figure 4.69: Effect of FRT on hardness at a RSR of 5000 $S^{-1,}$

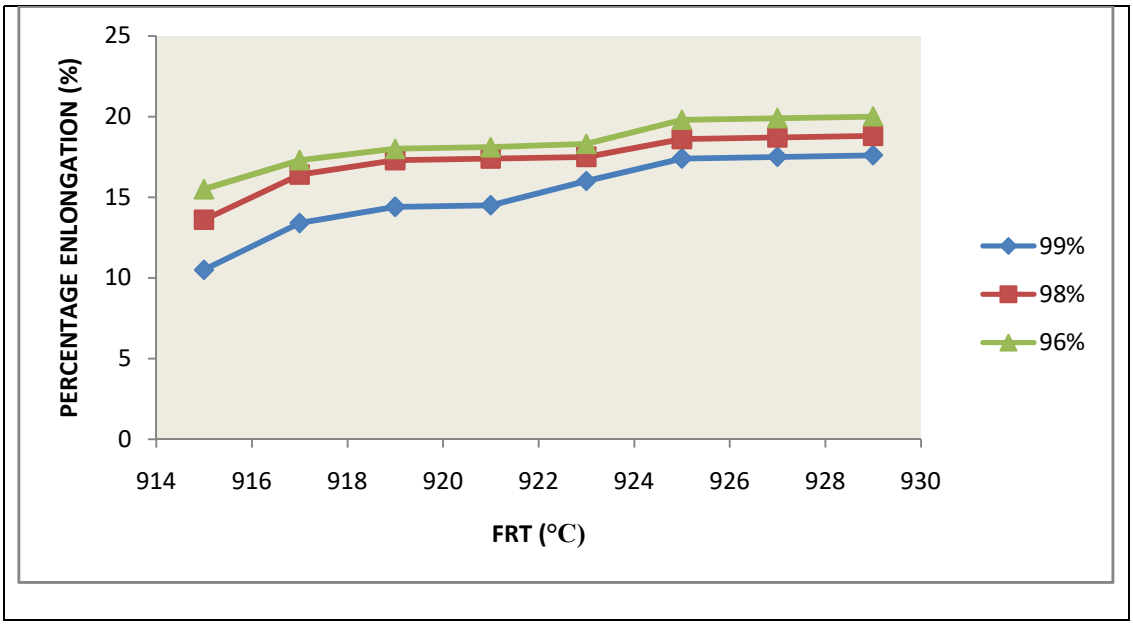

Figure 4.70: Effect of FRT on PE at a constant RSR

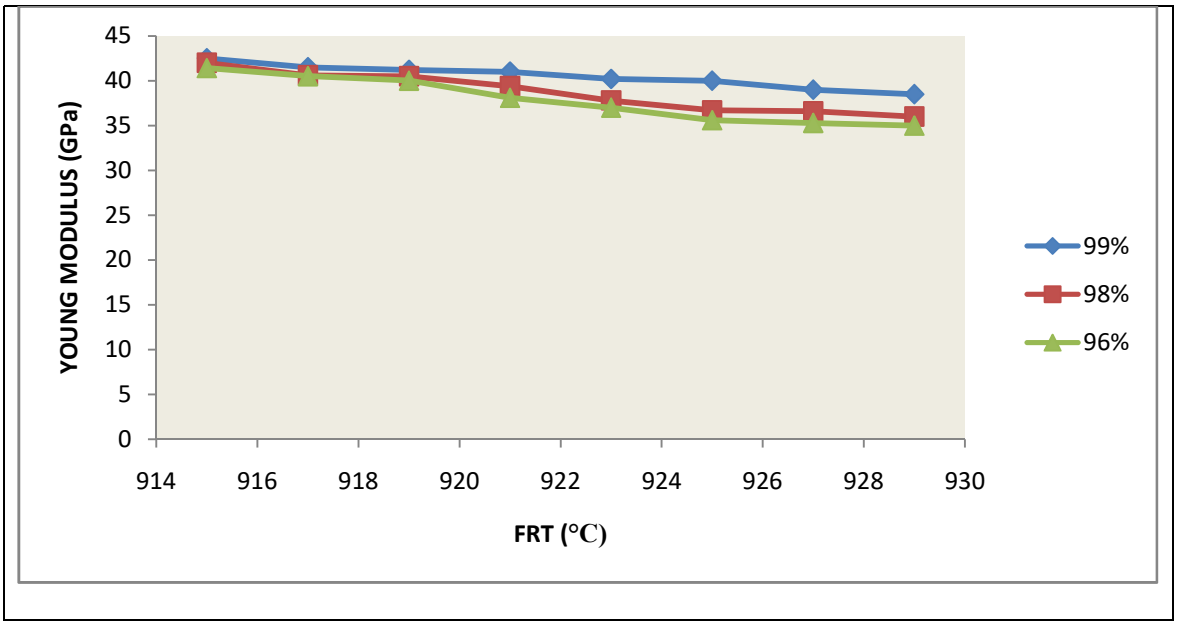

Figure 4.71: Effect of FRT on E at a constant RSR

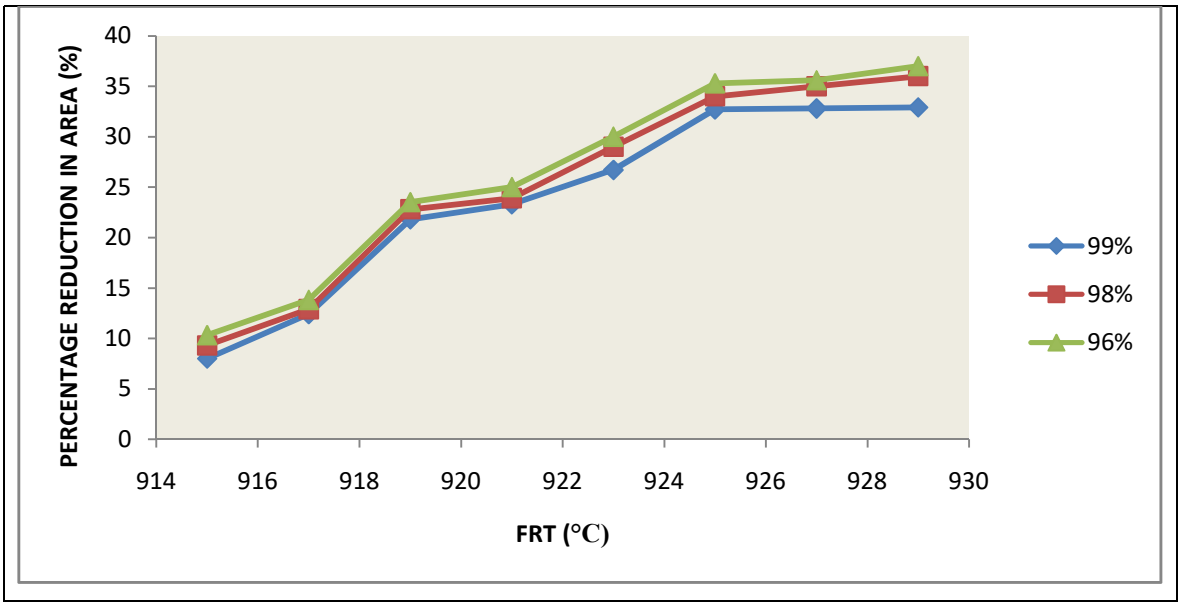

Figure 4.72: Effect of FRT on PRAat a constant RSR

4.10 Results and Discussions For Effects of FRT at PTD of 99.0 percent

Results of the effects of FRT on the tensile properties at constant RSR are tabulated in Table 4.4.

The plots of FRT versus YS, TS, PE, PRA, E, ductility, hardness and impact energy at constant PTD of 99.0%, varying at three different RSR of 5000, 6000 and 7000S^{-1}, respectively, are shown in Figures 4.73-4.80 .

The TS, YS, hardness,E and ductility reduced with increasing FRT, while the impact energy, PRA and PE increased with increasing FRT for all the degrees of PTD and RSR observed, in the above two cases.

From Tables 4.3 and Figures 4.73 to 4.80, at 7000 S^{-1} and constant PTD of 99 %,when the FRT increased from 915°C to 921°C,the TS reduced from 611 to 607 MPa (Fig.4.73), YS reduced from 432 to 429 MPa (Fig.4.74), hardness reduced from 231 to 229 HB (Fig.4.77), E reduced from 42..0 to 41.3GPa (Fig.4.79), ductility reduced from 50 to 48°(Fig.4.75) while impact energy increased from 0.4480 J/mm^2 to 0.4580 J/mm^2(Fig.4.76), PRA increased from 7.9 to 23.3%(Fig.4.80), PE increased from 10.3 to 15%(Fig.4.78). At 6000 S^{-1}RSRand PTD of 99.0%,as the FRT increased from 915 to 921°C, the TS reduced from 610 to 606 MPa (Fig.4.73), YS reduced from 431 to 422 MPa (Fig.4.74), hardness reduced from 2230 to 227 HB (Fig.4.77) E reduced from 42.1 to 41.2 GPa (Fig.4.79) and ductility reduced from 49.2 to 39.0°(Fig.4.75);while impact energy increased from 0.44 to 0.52 J/mm^2(Fig.4.76), PRA increased from 7.7 to 23.2%(Fig.4.80) and PE increased from 10.2 to 14%(Fig.4.78) .

At RSR of 5000 $S^{-1}$and PTD of 99.0% ,as the FRT increased from 915 to 921°C, the TS reduced from 608 to 594 MPa (Fig.4.73), YS reduced from 428 to 424 MPa (Fig.4.74), hardness reduced from 227 to 224 HB (Fig.4.77), E reduced from 41.6 to 39.2 GPa (Fig.4.79) and ductility reduced from 46.9 to 44.7°(Fig.4.75);while impact energy increased from 0.50 to 0.51 J/mm^2(Fig.4.76), PRA increased from 9.2 to 24.1%(Fig.4.80) and PE increased from 15.1 to 17.8%(Fig.4.78) .

The above property trend is also applicable to RSR of 6000 and 5000 S^{-1} and constants of PTD of 98.0 and 96.0 percent respectively. It was observed that increased values of the

FRT of the rolled stock also gave rise to higher and better TS, YS, hardness, E and ductility of the hot-rolled samples; while the impact energy PRA and PE get lower. This was as a result of similar even working of the billet that took place which made them to yield and increase the amount of displaced component. The billets yielded because they were stopped by solidification of another component. All these increased the values of TS, YS, hardness, E and ductility. At the same time, impact energy, PRA and PE decreased.

Table 4.4: Influence of FRT at constant PTD and variable RSR.

FRT (°C)	PTD (%)	RSR(S^{-1})	Hardness (HB)	E (GPa)	Ductility or Bendability (°)	TS (MPa)	YS (MPa)	PE (%)	PRA (%)	Impact Energy (J/mm)
915	99.0	7000	231	42.8	50.25	611	432	10.3	7.9	0.48
915	99.0	6000	228	42.2	47.3	610	429	13.1	8.1	0.49
915	99.0	5000	227	41.6	46.9	608	428	15.1	9.2	0.50
917	99.0	7000	231	41.7	48.25	610	431	13.3	12.2	0.48
917	99.0	6000	227	40.9	45.0	609	427	16.2	12.8	0.49
917	99.0	5000	226	40.7	44.8	600	426	17.1	13.5	0.50
919	99.0	7000	230	41.4	48.2	609	430	14.2	21.7	0.51
919	99.0	6000	226	40.7	45.0	608	426	17.2	22.5	0.52
919	99.0	5000	225	40.0	44.8	596	425	17.5	23.3	0.52
921	99.0	7000	229	41.3	48.15	607	429	15.0	23.3	0.49
921	99.0	6000	225	40.5	44.9	597	425	17.3	23.8	0.50
921	99.0	5000	224	39.2	44.7	594	424	17.8	24.1	0.51
923	99.0	7000	229	41.1	46.05	606	428	26.8	16.0	0.50
923	99.0	6000	225	40.0	44.0	595	424	17.4	28.2	0.52
923	99.0	5000	223	38.7	43.8	592	423	17.9	29.0	0.53
925	99.0	7000	229	40.5	45.8	606	427	18.3	32.7	0.51
925	99.0	6000	224	38.0	43.8	594	423	17.9	33.0	0.52
925	99.0	5000	222	36.3	43.6	611	422	18.8	34.4	0.53
927	99.0	7000	228	40.4	45.7	606	426	18.4	32.8	0.55
927	99.0	6000	223	37.0	43.7	594	422	18.6	33.4	0.56
927	99.0	5000	221	36.2	43.5	589	421	18.9	34.5	0.58
929	99.0	7000	227	40.3	45.6	605	425	18.3	32.9	0.59
929	99.0	6000	222	36.0	43.6	589	421	18.7	33.7	0.60
929	99.0	5000	220	36.0	43.4	585	420	19.1	34.6	0.63

Table 4.4 (continued): Effect of FRT at constant PTD and variable RSR.

FRT (°C)	PTD (%)	RSR (S^{-1})	Hardness (HB)	E (GPa)	Ductility or Bendability (°)	TS (MPa)	YS (MPa)	PE (%)	PRA (%)	Impact Energy (J/mm^2)
915	98.0	7000	230	42.8	42.6	610	426	10.2	7.8	0.44
915	98.0	6000	227	42.1	42.1	609	425	13.0	8.0	0.49
915	98.0	5000	226	41.5	41.3	608	424	15.0	9.1	0.50
917	98.0	7000	229	41.6	41.6	609	425	13.1	12.1	0.51
917	98.0	6000	226	40.8	41.9	608	424	16.1	12.7	0.50
917	98.0	5000	225	40.6	39.6	607	423	17.0	13.4	0.51
919	98.0	7000	228	41.3	41.9	608	424	14.1	21.6	0.52
919	98.0	6000	225	40.6	40.7	607	423	17.1	22.3	0.51
919	98.0	5000	224	39.0	40.0	606	422	17.4	23.2	0.52
921	98.0	7000	227	41.2	41.3	607	423	14.0	23.2	0.53
921	98.0	6000	224	40.4	43.4	606	422	17.2	23.7	0.52
921	98.0	5000	223	38.2	38.0	605	421	17.7	24.0	0.53
923	98.0	7000	226	41.0	43.0	606	422	15.0	26.6	0.54
923	98.0	6000	223	38.0	40.0	605	421	17.3	28.0	0.53
923	98.0	5000	222	37.7	37.0	604	420	17.8	28.0	0.54
925	98.0	7000	225	40.3	41.0	605	421	17.2	32.6	0.57
925	98.0	6000	223	37.0	38.0	604	420	17.8	32.0	0.61
925	98.0	5000	221	35.7	35.0	603	419	18.6	34.2	0.61
927	98.0	7000	224	40.0	44.8	604	420	17.3	32.7	0.57
927	98.0	6000	222	36.0	42.5	603	418	17.9	33.0	0.59
927	98.0	5000	220	34.0	41.5	602	417	18.7	34.3	0.61
929	98.0	7000	223	39.7	44.7	603	417	17.4	32.8	0.61
929	98.0	6000	221	35.0	42.4	602	413	18.1	34.0	0.62
929	98.0	5000	219	33.0	41.3	601	414	18.9	34.4	0.65

Table 4.4 (continued): Effect of FRT at constant PTD and variable RSR.

FRT (°C)	PTD (%)	RSR (S^{-1})	Hardness (HB)	E (GPa)	Ductility or Bendability (°)	TS (MPa)	YS (MPa)	PE (%)	PRA (%)	Impact Energy (J/mm)
915	96.0	7000	229	42.5	49.1	609	425	10.5	8.0	0.56
915	96.0	6000	226	42.0	46.8	608	424	13.6	9.3	0.50
915	96.0	5000	228	41.4	45.7	607	423	15.5	10.3	0.51
917	96.0	7000	228	41.5	48.0	608	424	13.4	12.4	0.57
917	96.0	6000	225	40.6	45.4	607	423	16.4	12.9	0.51
917	96.0	5000	224	40.5	44.4	606	422	17.3	13.8	0.52
919	96.0	7000	227	41.2	47.0	607	423	14.4	21.8	0.58
919	96.0	6000	224	40.5	44.9	606	422	17.3	22.8	0.52
919	96.0	5000	223	40.0	43.7	605	421	18.0	23.5	0.53
921	96.0	7000	226	41.0	46.15	606	422	14.5	23.3	0.59
921	96.0	6000	223	39.4	43.8	605	421	17.4	23.9	0.53
921	96.0	5000	222	38.1	42.6	599	420	18.1	25.0	0.54
923	96.0	7000	225	40.2	45.0	605	421	16.0	26.7	0.60
923	96.0	6000	222	37.8	43.1	604	420	17.5	29.0	0.54
923	96.0	5000	221	37.0	41.7	593	419	18.3	30.0	0.55
925	96.0	7000	224	40.0	43.9	604	420	17.4	32.7	0.61
925	96.0	6000	221	36.7	42.5	593	419	18.6	34.0	0.56
925	96.0	5000	220	35.6	41.5	582	418	19.8	35.3	0.59
927	96.0	7000	223	39.0	43.8	591	419	17.5	32.8	0.62
927	96.0	6000	220	36.6	42.4	586	417	18.2	33.0	0.58
927	96.0	5000	219	35.3	41.4	577	416	19.9	35.6	0.60
929	96.0	7000	222	36.0	43.7	585	417	17.6	32.9	0.63
929	96.0	6000	219	36.0	42.3	580	416	18.8	36.0	0.59
929	96.0	5000	218	35.0	41.3	575	415	20.0	37.0	0.61

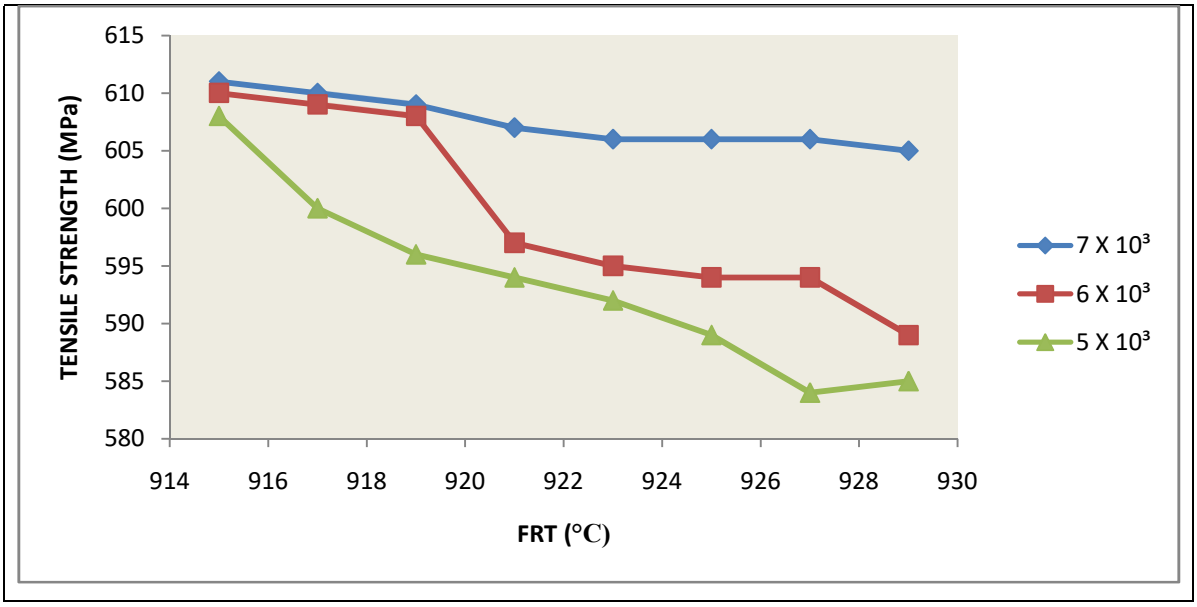

Figure 4.73: Effect of FRT on TS at constant PTD of 99.0 % varying RSR

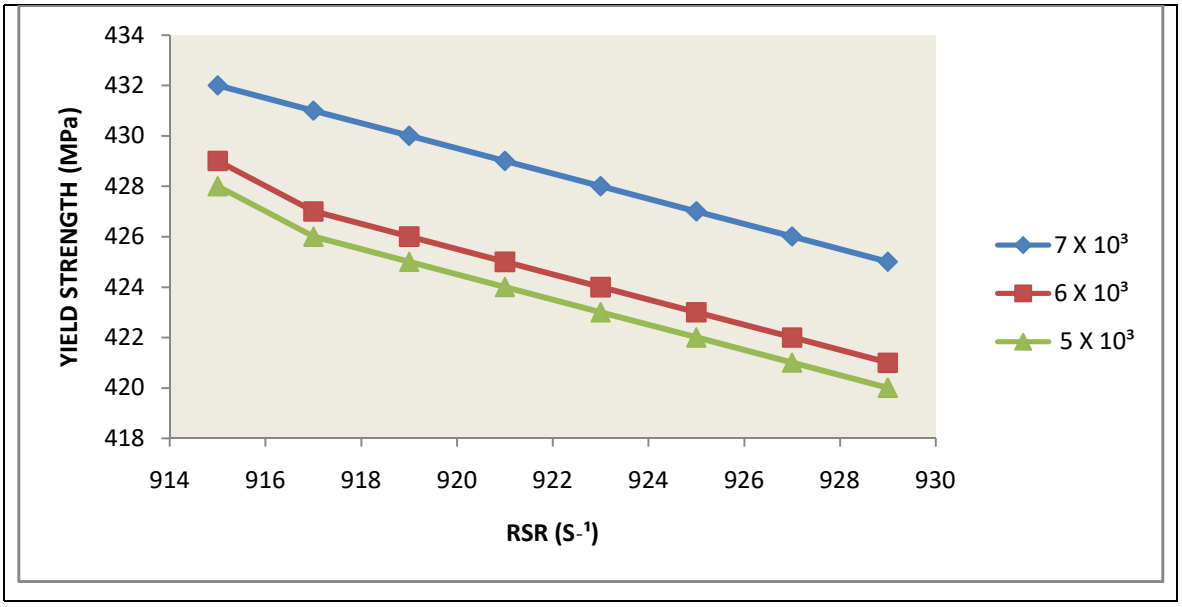

Figure 4.74: Effect of FRT on YS at constant PTD of 99.0 % varying RSR

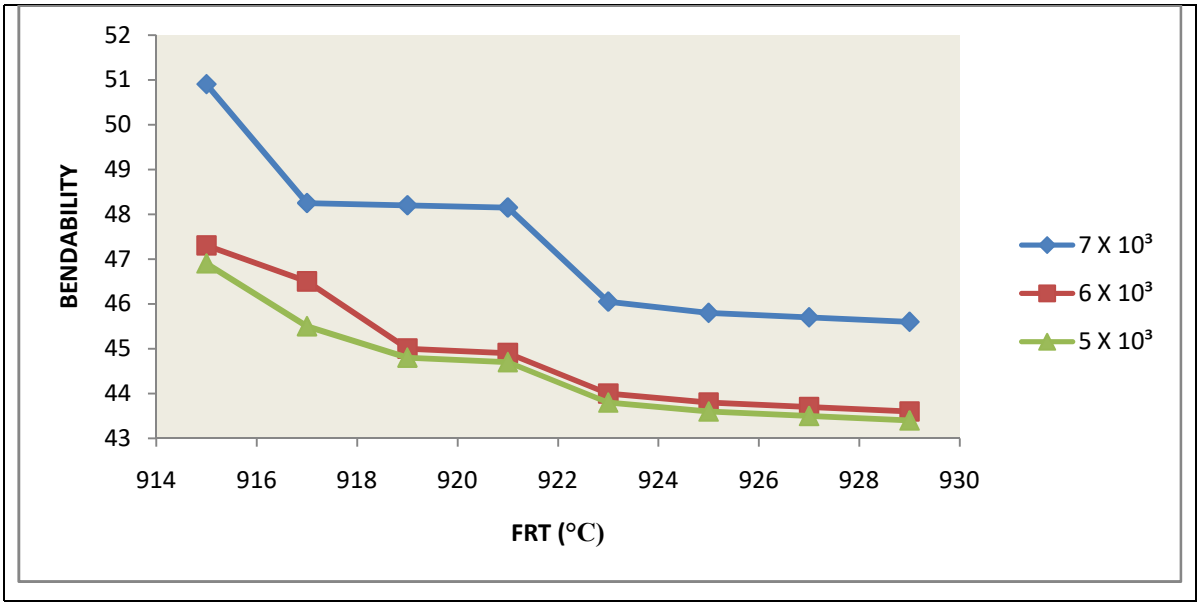

Figure 4.75: Effect of FRT on ductility at constant PTD of 99.0 % varying RSR.

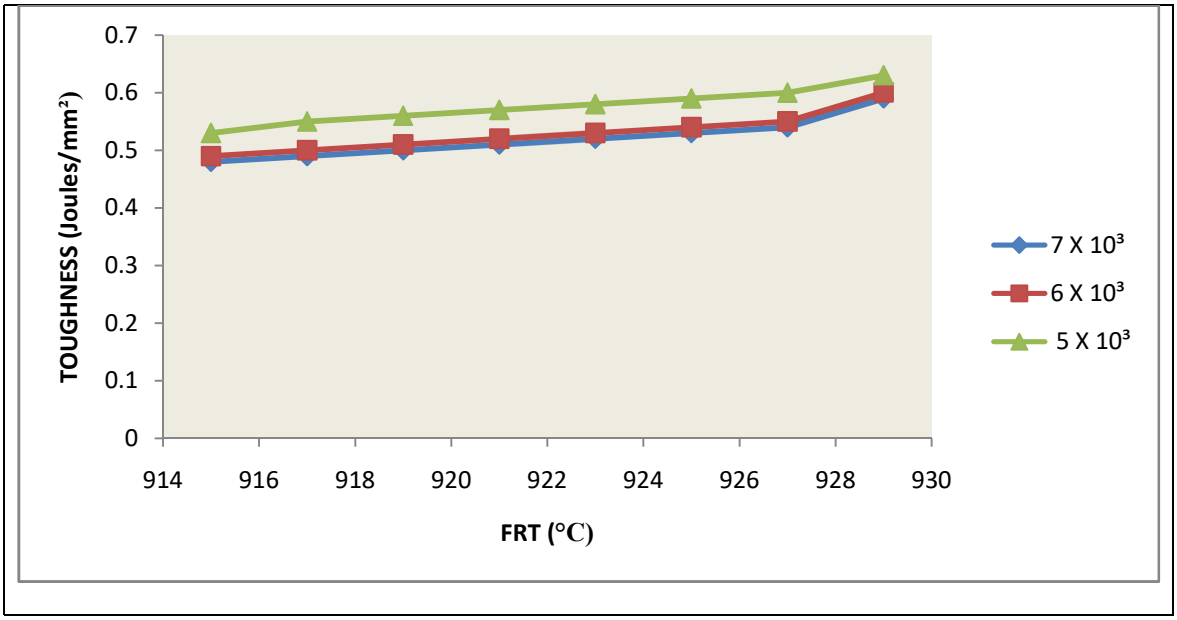

Figure 4.76: Effect of FRT on Impact Energy at constant PTD of 99.0% varying RSR.

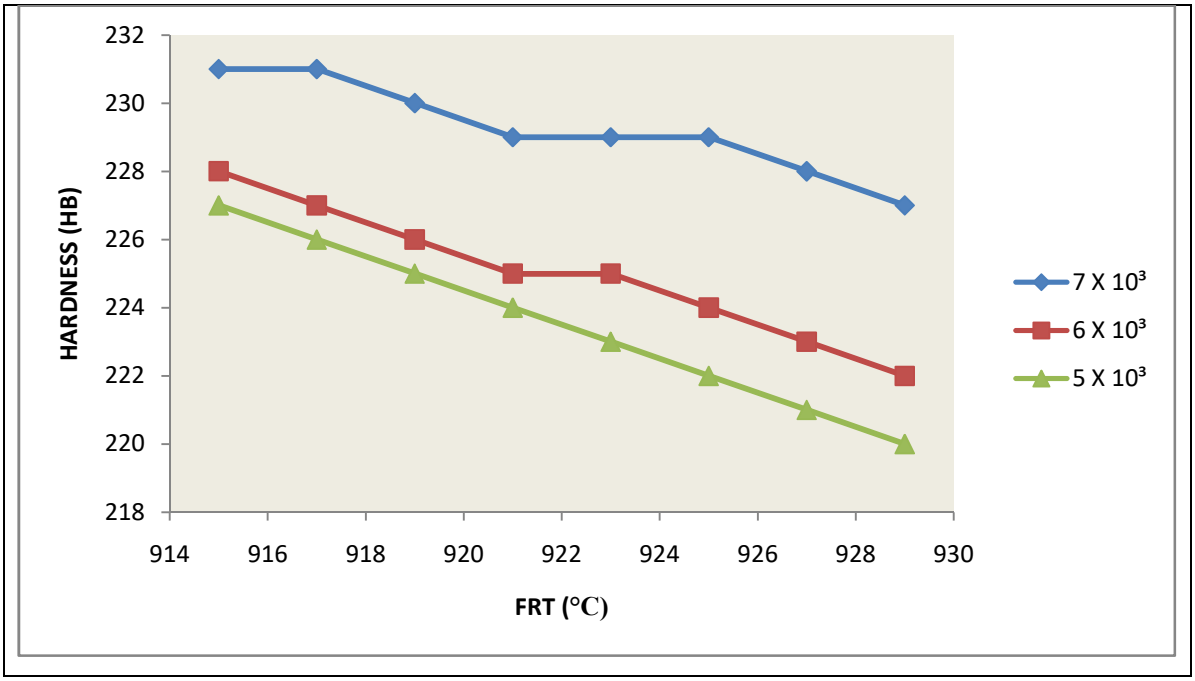

Figure 4.77: Effect of FRT on hardness at constant PTD of 99.0% varying RSR.

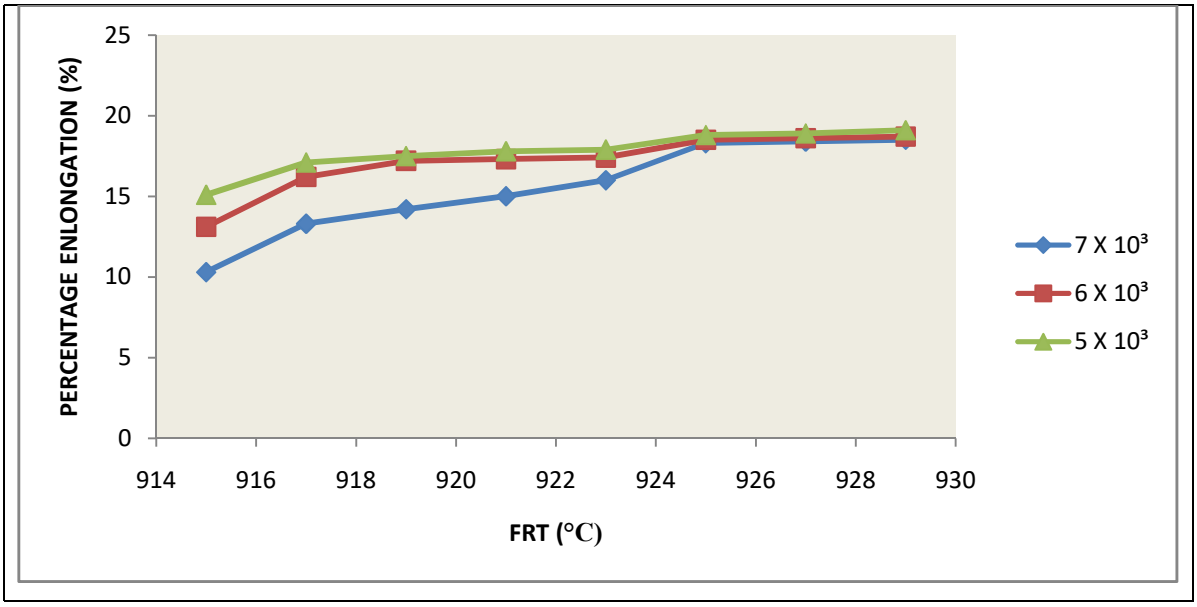

Figure 4.78: Effect of FRT on PE at constant PTD of 99.0 % varying RSR.

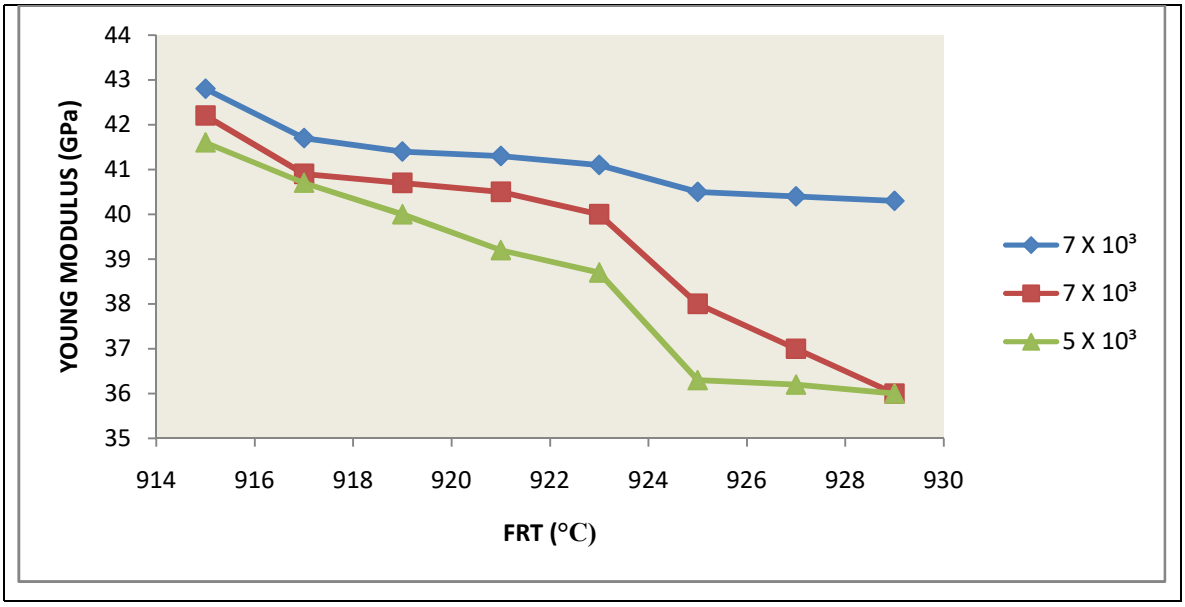

Figure 4.79: Effect of FRT on E at constant PTD of 99.0 % varying RSR.

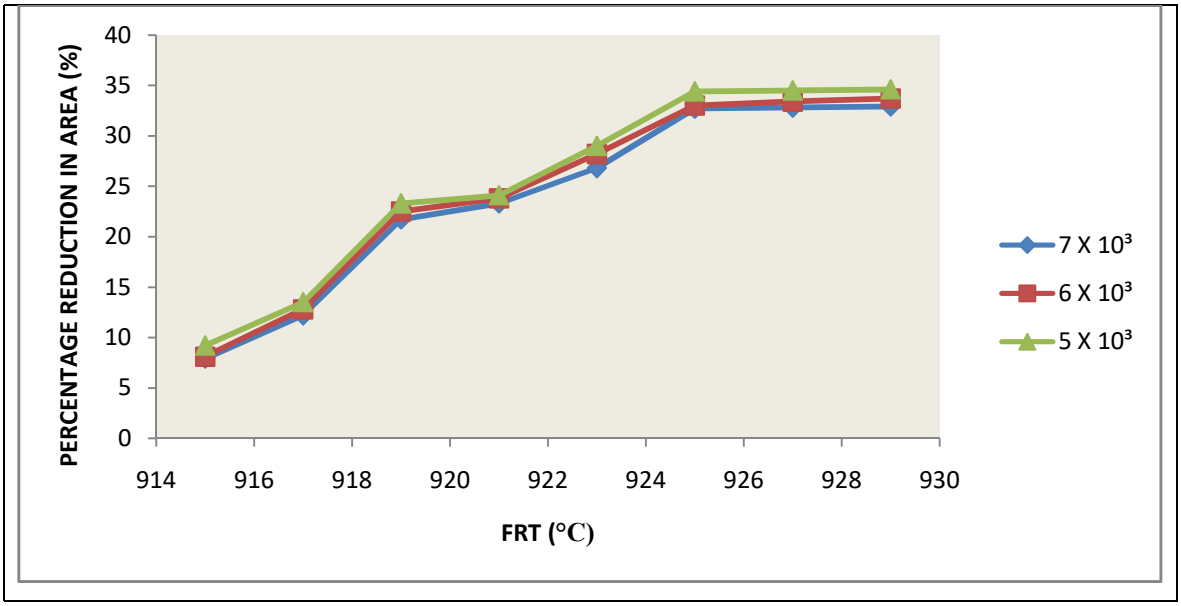

Figure 4.80: Effect of FRT on PRA at constant PTD of 99.0 % varying RSR

4.11 Results and Discussions For Effects of FRT at PTD of 98.0 percent

The plots of FRT versus YS, TS, PE, PRA, E, ductility, hardness and impact energy atPTD of 98.0,varying to three different RSR of 7000, 6000 and 5000 S^{-1} respectively, are shown in Figures 4.81-4.88 .

The TS, YS, hard, E hardness ductility reduced with increasing FRT, while the impact energy, PRA and PE increased with increasing FRT for all the degrees of PTD and RSR observed, in the above two cases.

From Figures 4.81 to 4.88 , at 99.0% PTD and 6000 S^{-1} RSR,when the FRT increased from 915°C to 921°C, the TS reduced from 610 to 607 MPa (Fig.4.81) YS reduced from 426 to 423 MPa (Fig.4.82), hardness reduced from 230 to 227 HB (Fig.4.85), E reduced from 42.8 to 41.2GPa (Fig.4.87), ductility reduced from 42.6 to 41.3° (Fig.4.83) while impact energy increased from 0.44 to 0.53 J/mm^2(Fig.4.84), PRA increased from 7.8 to 23.2%(Fig.4.88), PE increased from 10.2 to 14%(Fig.4.86). At 98% PTD and 6000 S^{-1}RSR ,as the FRT increased from 915 to 921°C, the TS reduced from 609 to 606 MPa (Fig.4.82), YS reduced from 425 to 422 MPa (Fig.4.90), hardness reduced from 227 to 224 HB (Fig.4.85), E reduced from 42.1 to 40.4 GPa (Fig.4.87) and ductility reduced from 42.1 to 43.4°(Fig.4.83);while impact energy increased from 0.49 to 0.52 J/mm^2(Fig.4.84), PRA increased from 8 to 23.7%(Fig.4.88) and PE increased from 13 to 17.2% (Fig.4.86).

At 96.0% PTD and 6000 S^{-1}RSR ,as the FRT increased from 915 to 921°C,the TS reduced from 608 to 605 MPa (Fig.4.82), YS reduced from 424 to 421MPa (Fig.4.90),hardness reduced from 226 to 223 HB (Fig.4.85) E reduced from 41.5 to 38.2 GPa (Fig.4.87) and ductility reduced from 41.3 to 38°(Fig.4.83);while impact energy increased from 0.50 to 0.53 J/mm^2(Fig.4.84), PRA increased from 9.1 to 24%(Fig.4.88) and PE increased from 15 to 17.7%(Fig.4.86) .

The above property trend is also applicable atRSR of 6000 and 5000 S^{-1} and constants of PTD of 98.0 and 96.0 percent respectively. A similar trend was observed that increased values of the FRT of the rolled stock also gave rise to higher and better TS, YS, hardness, E and ductility of the hot-rolled samples; while the impact energy PRA and PE get lower. This was as a result of similar even working of the billet that took place which made them

to yield and increase the amount of displaced component. The billets yielded because they were stopped by solidification of another component. All these increased the values of TS, YS, hardness, E and ductility. At the same time, impact energy, PRA and PE decreased.

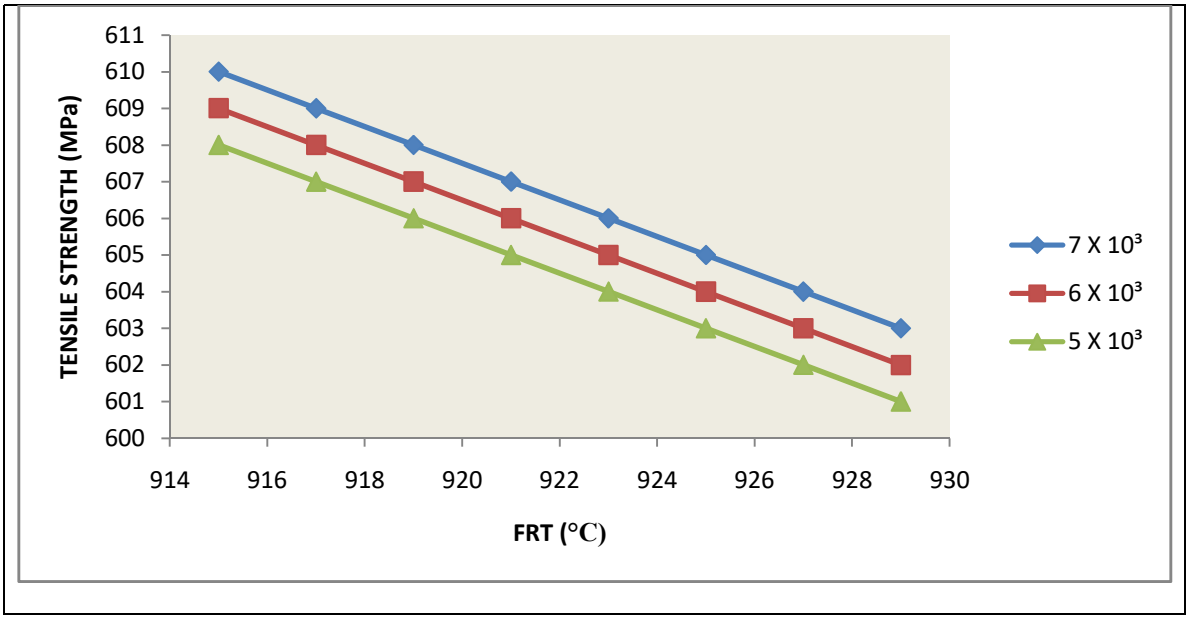

Figure 4.81:FRT versus TS at a constant PTD of 98.0% varying RSR.

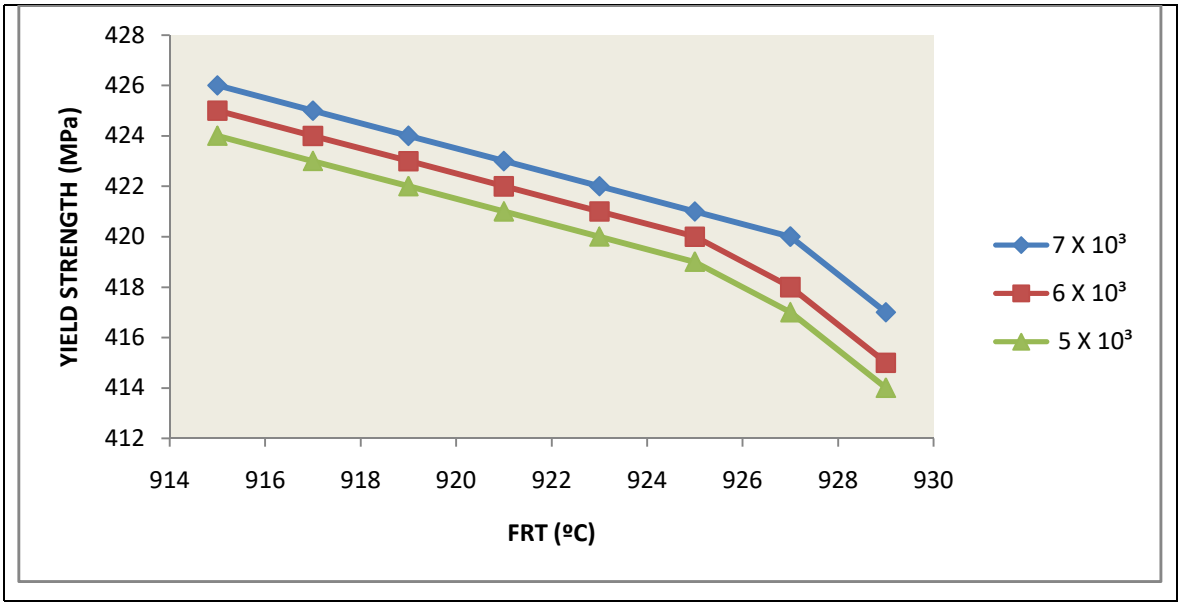

Figure 4.82: FRT versus YS at a PTD of 98.0 % varying RSR.

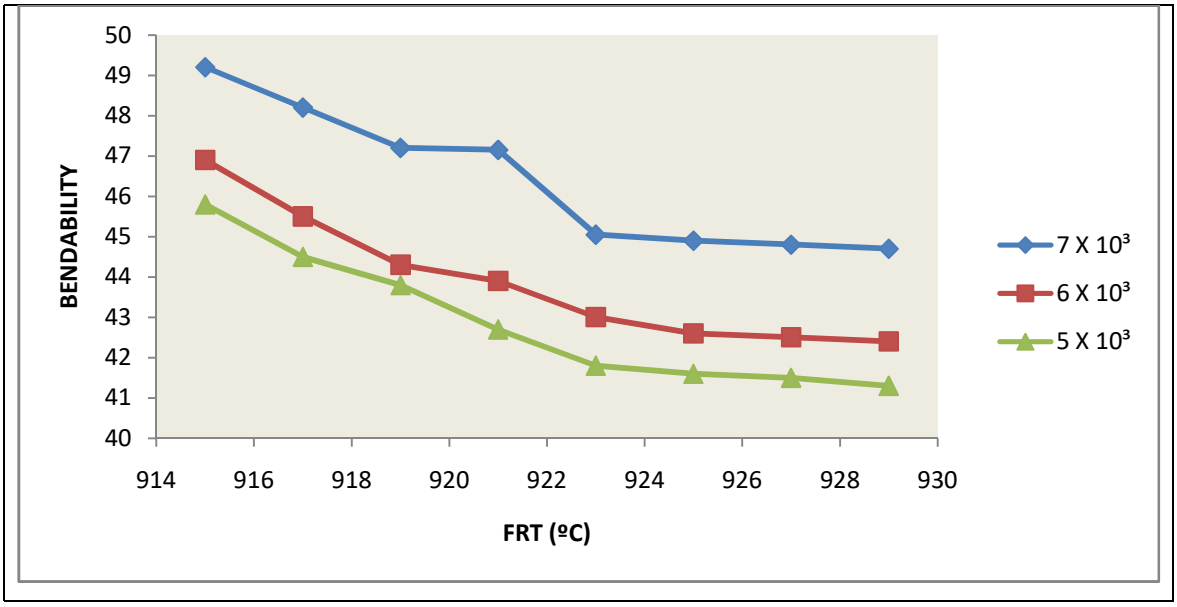

Figure 4.83: FRT versus ductility at a constant PTD of 98.0% varying RSR.

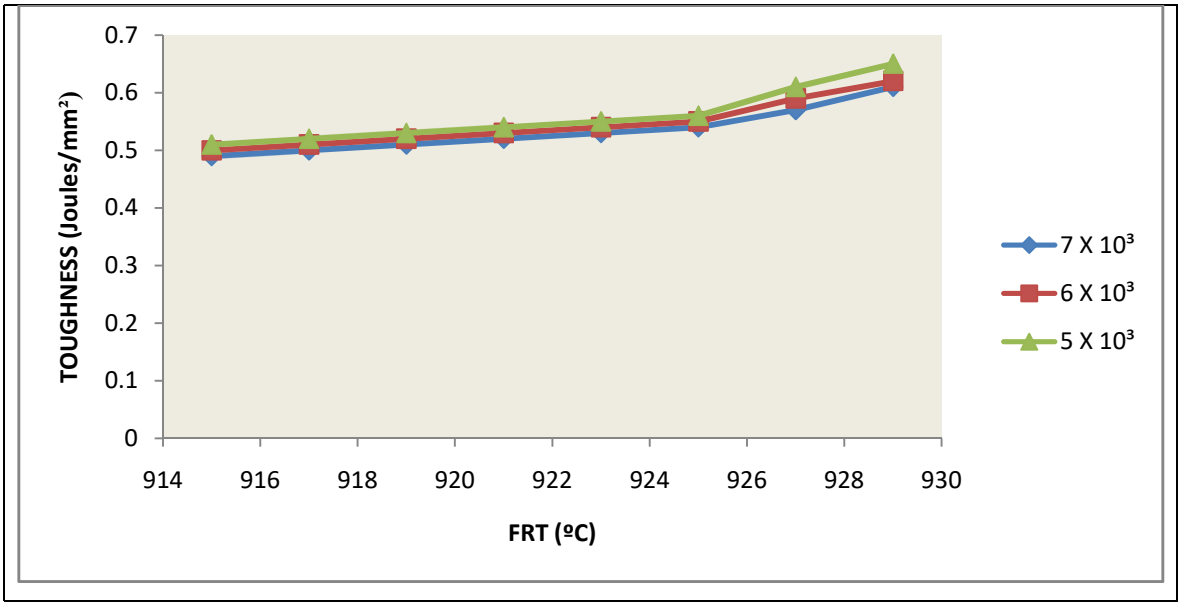

Figure 4.84: FRT versus Impact Energy at a constant PTD of 98.0% varying RSR

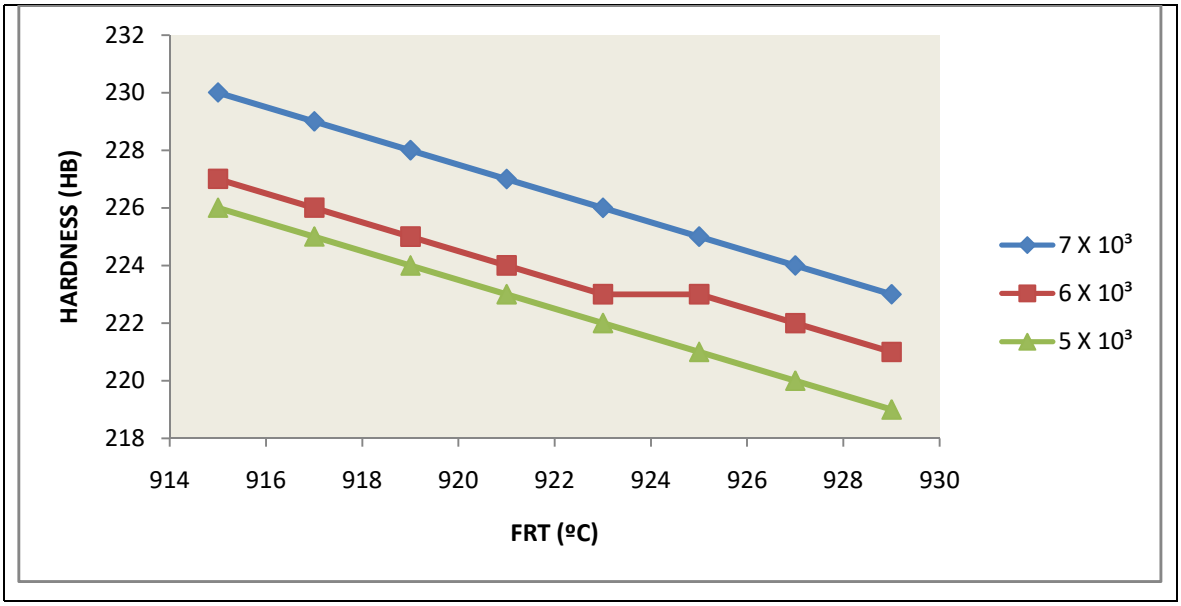

Figure 4.85: FRT versus hardness at a constant PTD of 98.0% varying RSR.

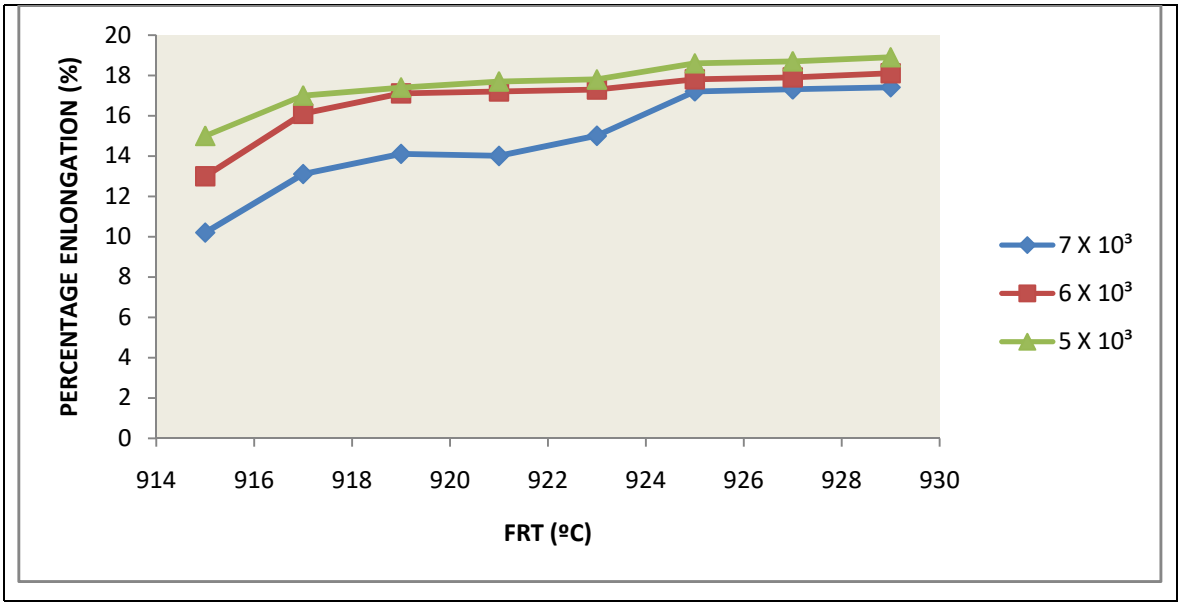

Figure 4.86: FRT versus PE at a constant PTD of 98.0 % varying RSR.

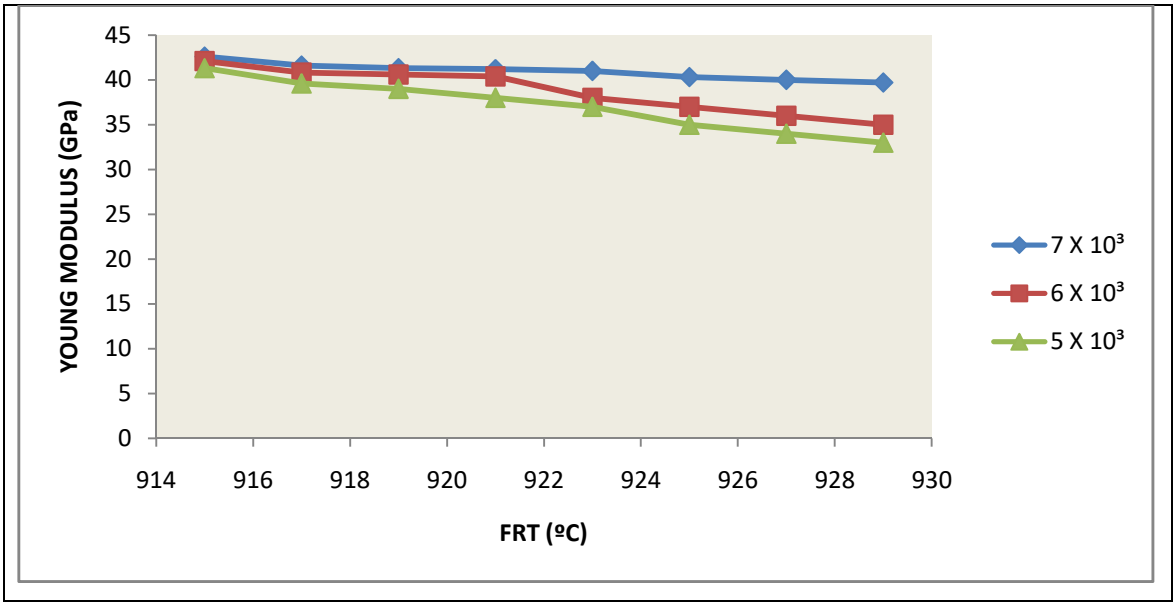

Figure 4.87: FRT versus E at a constant PTD of 98.0% varying RSR.

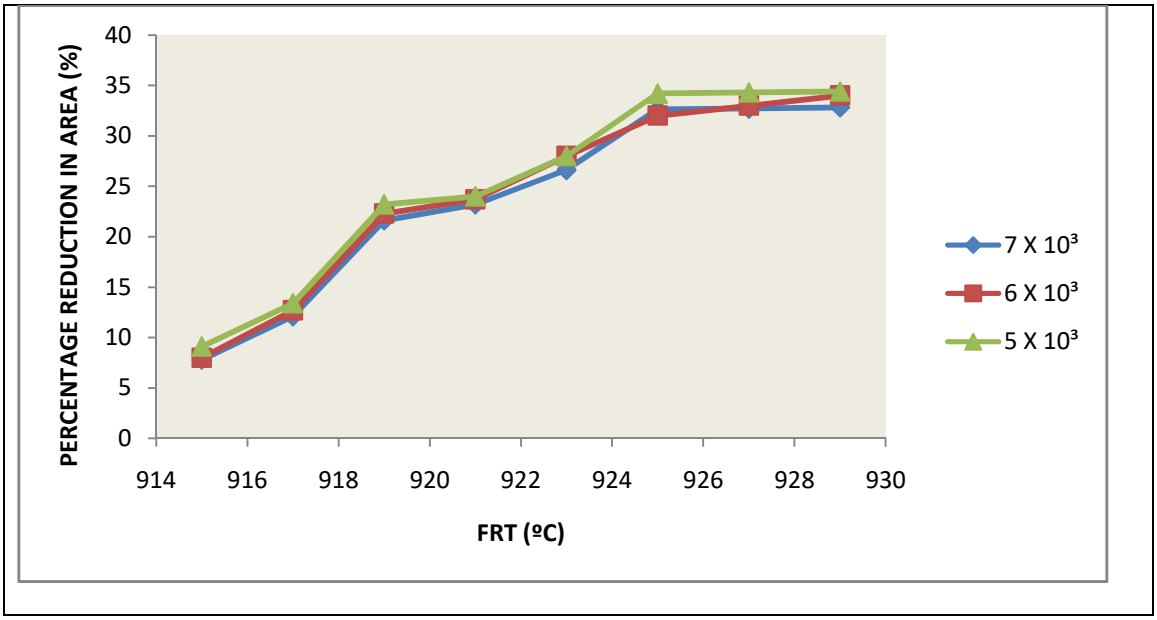

Figure 4.88: FRT versus PRA at a constant PTD of 98.0 % varying RSR

4.12 Results and Discussions For Effects of FRT at PTD of 96.0 percent

The plots of FRT versus YS, TS, PE, PRA, E, ductility, hardness and impact energy at constant PTD of 96.0%, varying at RSR of 7000, 6000 and 5000 S^{-1}, respectively, are shown in Figures 4.89-4.96 .

The TS, YS, hardness,E and ductility reduced with increasing FRT, while the impact energy, PRA and PE increased with increasing FRT for all the degrees of PTD and RSR observed, in the above two cases.

From Figures 4.89 to 4.96, at 7000 S^{-1}RSR and 96.0 % PTD, ,when the FRT increased from 915°C to 921°C, the TS reduced from 609 to 606 MPa (Fig.4.89), YS reduced from 425 to 422 MPa (Fig.4.90), hardness reduced from 229 to 226 HB (Fig.4.93), E reduced from 42.5 to 41 GPa (Fig.4.95), ductility reduced from 49.10 to 46.15° (Fig.4.91) while impact energy increased from 0.56 to 0.59 J/mm^2(Fig.4.92), PRA increased from 8 to 23.3%(Fig.4.96), PE increased from 10.5 to 14.5%(Fig.4.94).At 6000 S^{-1} RSR and 96.0% PTD ,as the FRT increased from 915 to 921°C,the TS reduced from 608 to 605 MPa (Fig.4.89), YS reduced from 424 to 421 MPa (Fig.4.90), hardness reduced from 226 to 223 HB l(Fig.4.93), E reduced from 42 to 39.4 GPa (Fig.4.95) and ductility reduced from 46.8 to 43.8°(Fig.4.91);while impact energy increased from 0.50 to 0.53 J/mm^2(Fig.4.92), PRA increased from 9.3 to 23.9%(Fig.4.96) and PE increased from 13.6 to 17.4%(Fig.4.94) .

At 5000 S^{-1} RSR and 96.0% PTD ,as the FRT increased from 915 to 921°C, the UTS reduced from 607 to 599 MPa Fig.4.89), YS reduced from 423 to 420 MPa (Fig.4.90), hardness reduced from 228 to 222 HB (Fig.4.93) E reduced from 41.4 to 38.1 GPa (Fig.4.95) and ductility reduced from 45.7 to 42.6°(Fig.4.91);while impact energy increased from 0.51 to 0.54 J/mm^2(Fig.4.92), PRA increased from 10.3 to 25%(Fig.96) and PE increased from 15.5 to 18.1%(Fig.4.94) .

The above property trend is applicable atRSR of 6000 and 5000 S^{-1} and constants of PTD of 98.0 and 96.0 percent respectively. A similar trend was observed that increased values of the FRT of the rolled stock also gave rise to higher and better TS, YS, hardness, E and ductility of the hot-rolled samples; while the impact energy PRA and PE get lower. This

was as a result of similar even working of the billet that occured which made them to yield and increase the amount of displaced component. The billets yielded because they were stopped by solidification of another component. All these increased the values of TS, YS, hardness, E and ductility. At the same time, impact energy, PRA and PE decreased.

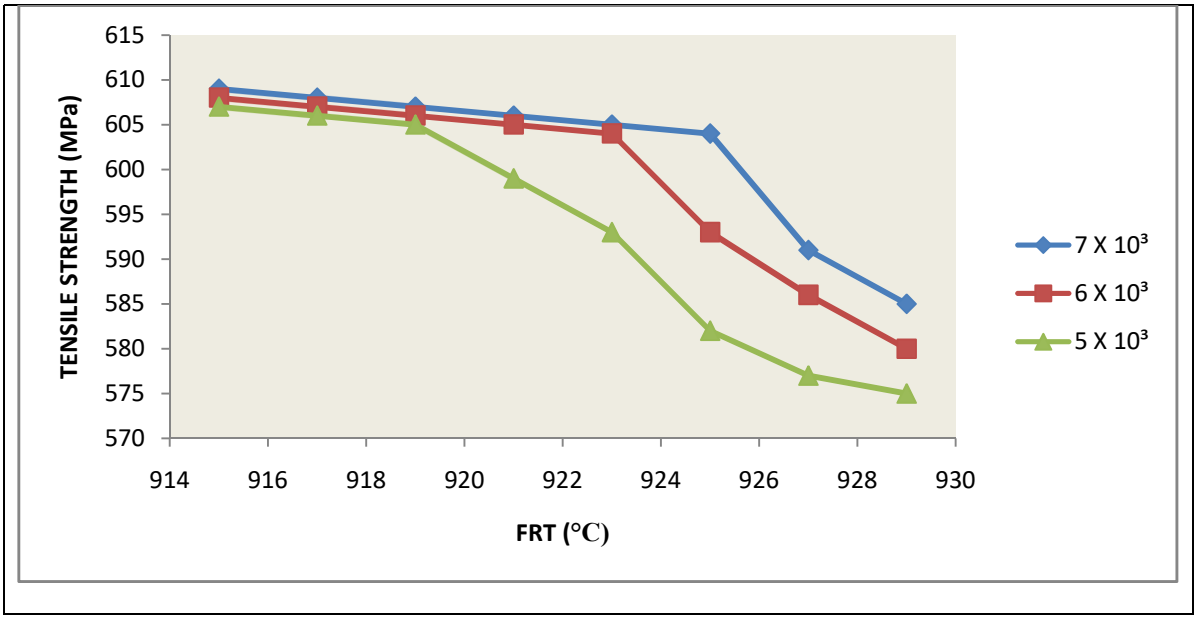

Figure 4.89: FRT versus TS at a constant PTD of 96.0% varying RSR

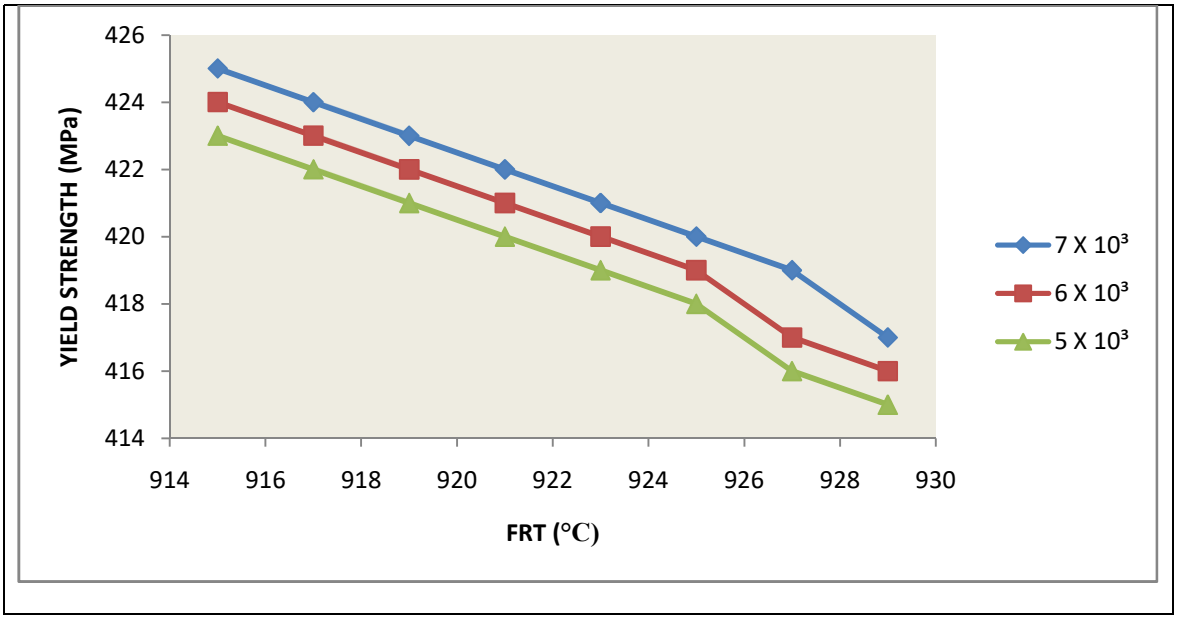

Figure 4.90: FRT versus YS at a constant PTD of 96.0 % varying RSR.

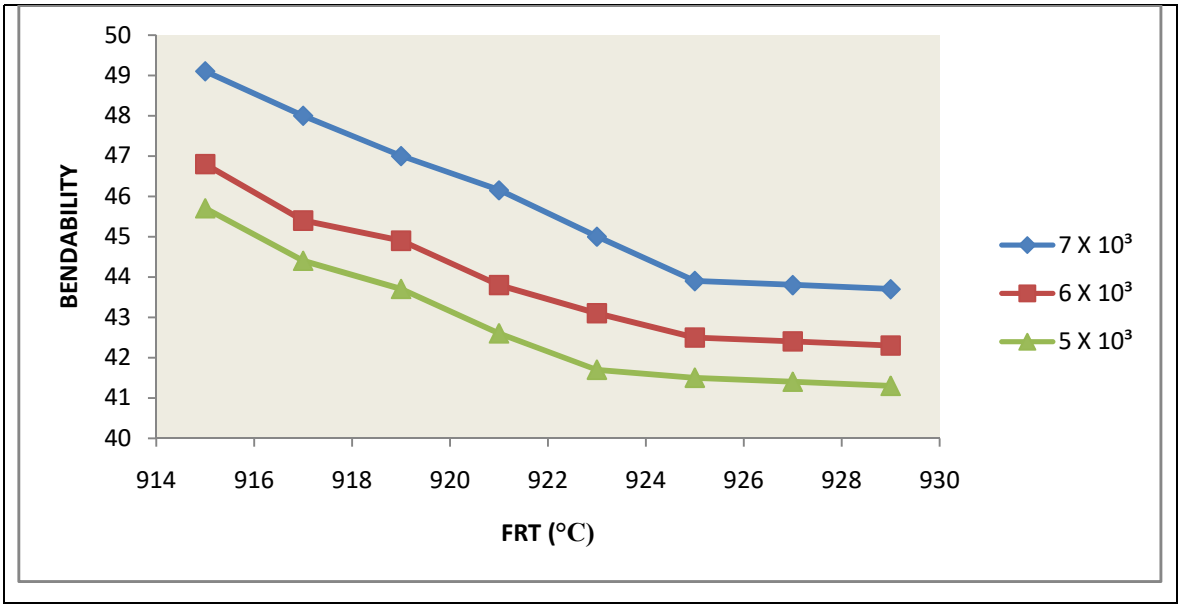

Figure 4.91: FRT versus ductility at a constant PTD of 96.0% varying RSR.

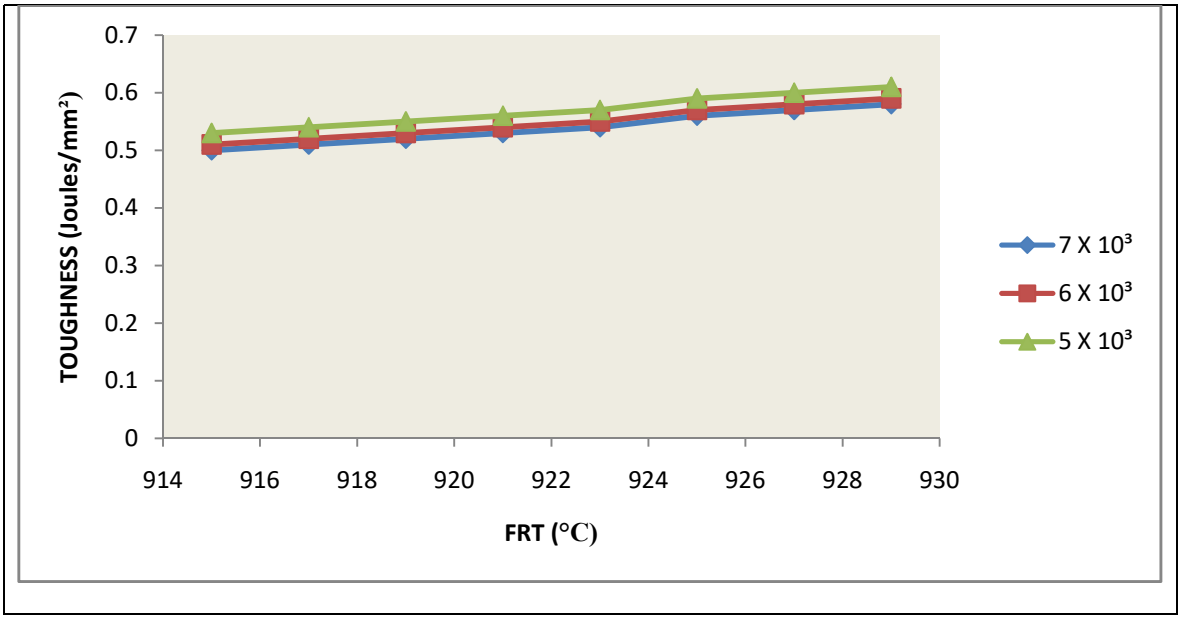

Figure 4.92: Effect of FRT on Impact Energy at a constant PTD of 96.0 % varying RSR.

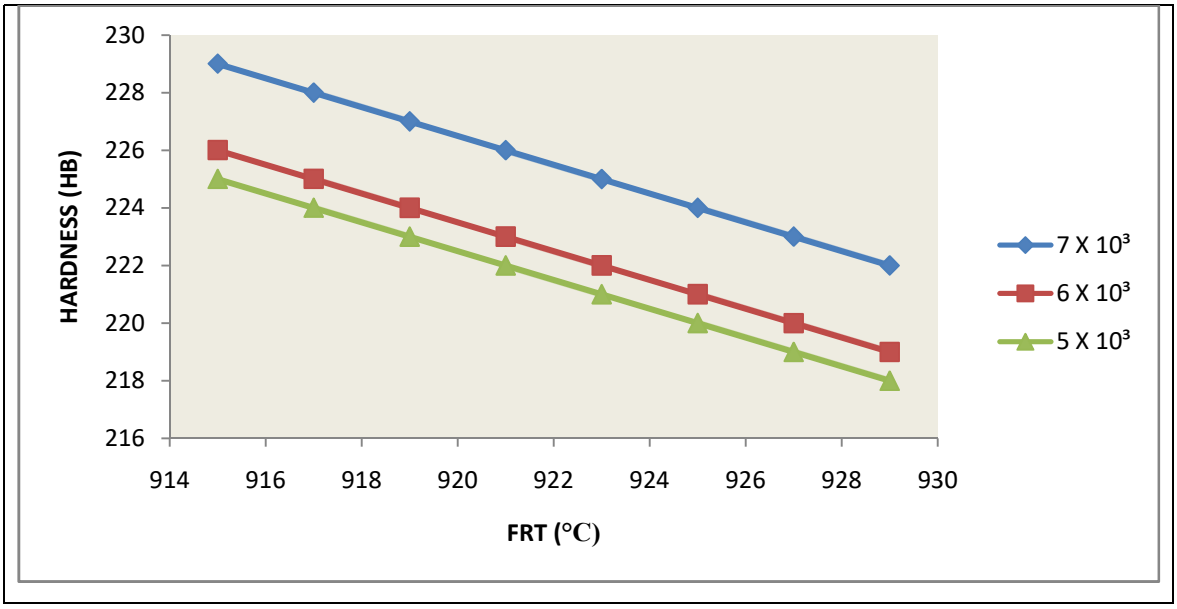

Figure 4.93: Effect of FRT on hardness at a constant PTD of 96.0 % varying RSR

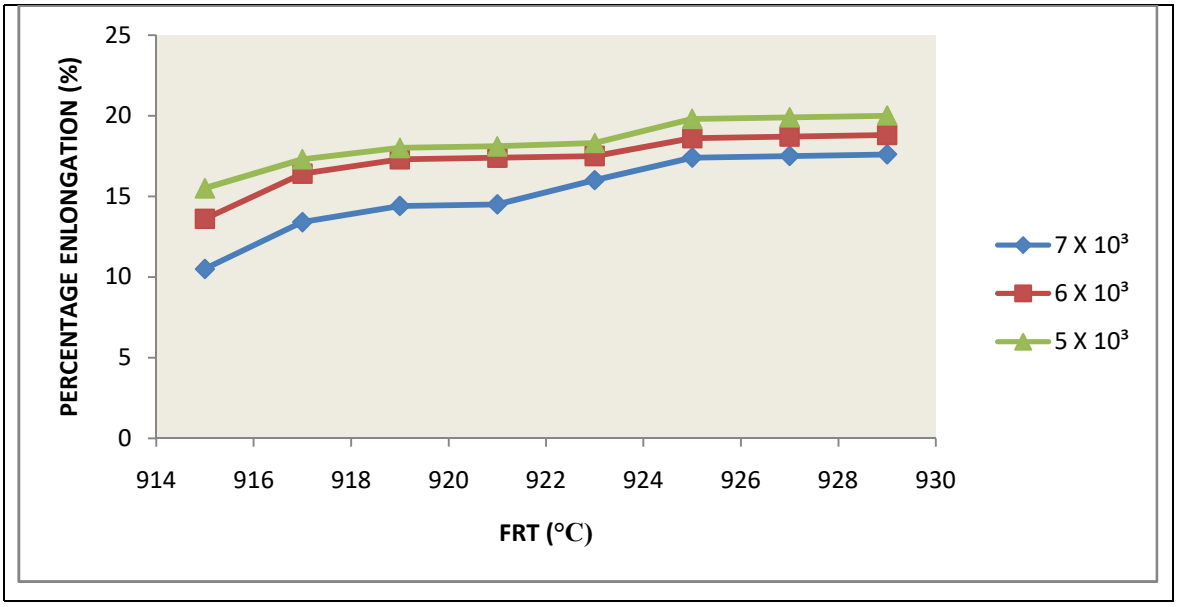

Figure 4.94: Effect of FRT on PE at a constant PTD of 96.0% varying RSR.

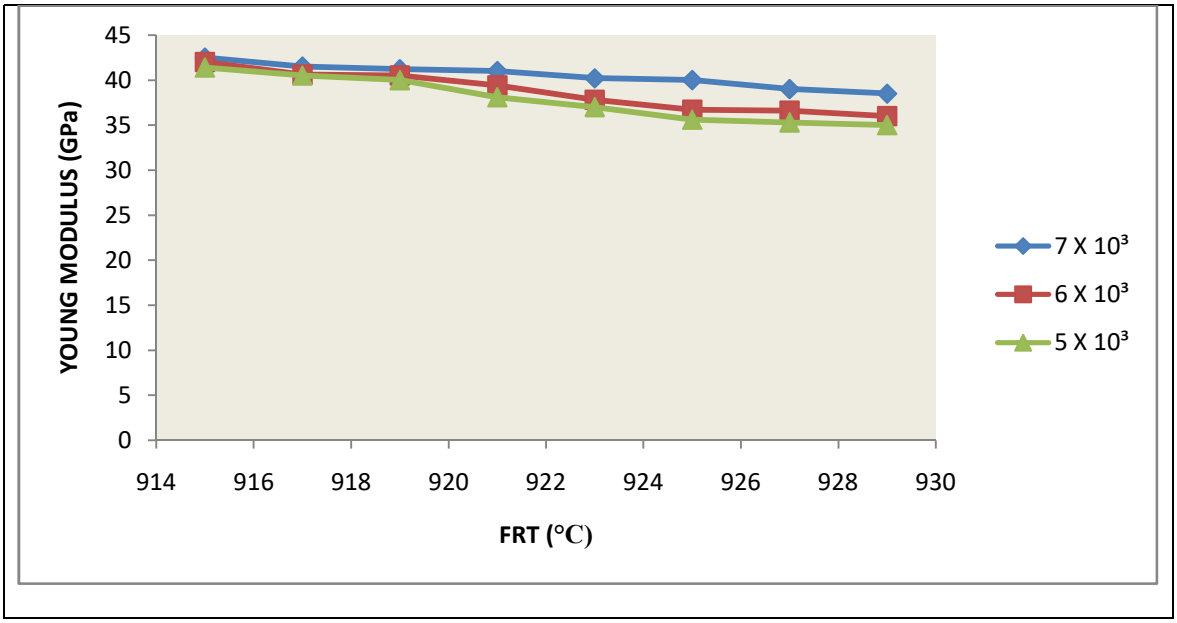

Figure 4.95: Effect of FRT on E at a constant PTD of 96.0% varying RSR.

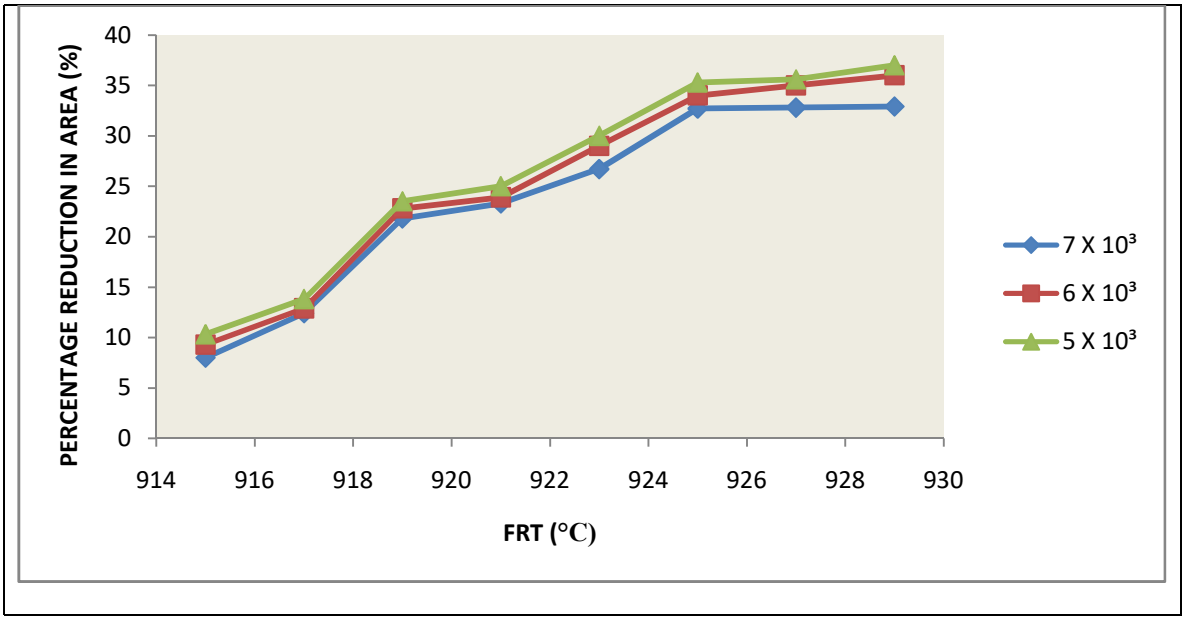

Figure 4.96: Effect of FRT on PRA at PTD of 96.0,% varying RSR

4.13 Results and Discussions For Effects of PTD at FRT of 915°C

Table 4.5 shows the effect of PTD on all the tensile propertiesof the steel grade investigated..Figures 4.97-4.103 show the effect of PTD on the tensile properties of the steel grade at constant FRT of 915°C,while changing to three different RSR of 7000, 6000 and 5000 S^{-1}respectively

After the analysis of the mechanical properties of the hot-rolled steel it may equally be reported that the tensile properties of the hot-rolled steel grade is substantially influenced by the PTD at 7000, 6000 , 5000 S^{-1} RSR. The TS, YS, hardness, E and ductility increased with increasing PTD, while the impact energy, PRA and PE decreased with increasing PTD for all the degrees of RSR and FRT observed.

From Tables 4.5 and Figures 4.97 to 4.103,at 7000 S^{-1}RSR and 915°C FRT ,when the PTD increased from 96.0 to 96.5%, the TS increased from 611.2 to 611.3 MPa (Fig.4.97),YS increased from 432 to 432.01 MPa (Fig.4.98), hardness increased from 224 to 225 HB (Fig.4.101), E increased from 56 to 60.1 GPa, bendability increased from 45.94 to 46.01°(Fig.4.99);while impact energy reduced from 0.4608 to 0.4607 J/mm^2 (Fig.4.100), PRA reduced from 30.3 to 30.1%(Fig.4.103), PE reduced from 18.3 to 18.1% (Fig.4.102). At 6000 S^{-1}RSR , and 915°C FRT, as the PTD increased from 96.0 to 96.5 percent, the TSincreased from 568.7 to 569.6 MPa (Fig.4.97), YS increased from 425.6 to 426 MPa (Fig.4.98), hardness increased from 221 to 229 HB (Fig.4.101, E increased from 53.1 to53.3GPa and ductility increased from44.49 to 44.5° (Fig.4.99);while impact energy reduced from 0.509 to 0.5085 J/mm^2 (Fig.4.100), PRA reduced from 35.7 to 34.8%(Fig.4.103) and PE reduced from 19 to 18.8% (Fig.4.103). At 5000 S^{-1} RSR and 915^{0}C FRT, as the PTD increased from 96.0 to 96.5 percent, TS increased from 568.7 to 512 MPa (Fig.4.97), YS increased from 423.5 to 423.9 MPa (Fig.4.98), hardness increased from 216 to 218HB(Fig.4.101),modulus of elasticity increased from 40.83 to 40.91GPa,bendability increased from 42.73 to 42.79°(Fig.4.99);while impact energy reduced from 0.5196 to 0.5188 J/mm^2(Fig.4.100), PRA reduced from 42 to 40.3%(Fig.4.103). PE reduced from 20.5 to 20.2%(Fig.4.102).

The effects of PTD on the rolled stock was very pronounced as the PTD increases,the TS, YS, hardness, E, and ductility of the hot-rolled samples increase; while the impact

energy, PRA and PE decrease. The workingof the billets within the stands gave rise to increased yielding and increased number of displaced components were transferred to the final hot-rolled rebar. The strengthening obtained came from smoothening of the microstructure of the austenites and displacement of layers of cementite by spheroidal particles.

This yielding was due to displacement movement occasioned by many stoppages like solidification of another components and this gave rise to increase in TS, YS, hardness, E and ductility. Impact energy, PRA and PE also decreased.

Table 4.5: Effect of PTD at Constant FRT and variable RSR.

PTD (%)	RSR (S^{-1})	FRT (°C)	Hardness (HB)	E (GPa)	Ductility or Bendability (°)	TS (MPa)	YS (MPa)	PE(%)	PRA (%)	Impact Energy (J/mm^2)
96.0	7000	915	224	56.00	45.94	611.2	432.00	18.3	30.30	0.4800
96.0	6000	915	221	53.10	44.49	568.7	425.60	19.0	35.70	0.5090
96.0	5000	915	216	40.83	42.73	568.7	423.50	20.5	42.00	0.5196
96.5	7000	915	225	60.10	46.01	611.3	432.01	18.1	30.10	0.4607
96.5	6000	915	222	53.30	44.50	569.6	426.00	18.8	34.80	0.5085
96.5	5000	915	218	40.30	42.79	512.0	423.90	20.2	40.91	0.5188
97.0	7000	915	228	61.60	46.06	614.0	432.04	17.7	30.00	0.4606
97.0	6000	915	224	53.40	44.51	570.0	428.40	18.6	34.60	0.5074
97.0	5000	915	219	40.98	42.91	512.9	425.20	19.9	39.90	0.5177
97.5	7000	915	229	61.80	46.25	615.0	432.05	16.6	26.90	0.4605
97.5	6000	915	225	54.00	44.53	572.0	428.50	17.3	34.30	0.5015
97.5	5000	915	220	42.11	43.44	522.0	425.60	18.9	39.80	0.5123
98.0	7000	915	230	63.00	46.28	616.0	432.06	15.5	26.30	0.4526
98.0	6000	915	226	55.60	45.10	581.0	428.50	15.9	34.20	0.4916
98.0	5000	915	222	43.08	43.53	540.0	425.70	18.3	39.00	0.5012
98.5	7000	915	231	65.00	46.35	617.0	432.07	15.0	25.90	0.4525
98.5	6000	915	228	56.00	45.20	598.0	428.70	15.3	33.80	0.4880
98.5	5000	915	225	45.30	43.63	579.0	426.70	17.3	37.60	0.3900
99.0	7000	915	232	66.00	46.36	618.0	432.08	14.8	25.80	0.4524
99.0	6000	915	229	57.00	45.40	599.0	429.00	15.2	33.50	0.4870
99.0	5000	915	224	45.20	43.62	570.0	426.00	17.4	37.70	0.4980
99.5	7000	915	233	67.00	46.37	620.0	432.20	14.5	25.70	0.4100
99.5	6000	915	230	58.00	45.50	600.0	429.50	15.1	33.40	0.4000
99.5	5000	915	225	45.30	43.63	579.0	426.70	17.3	37.60	0.3900

Table 4.5 (Continued): Effect of PTD At Constant FRT and variable RSR.

PTD (%)	RSR (S^{-1})	FRT (°C)	Hardness (HB)	E (GPa)	Ductility or Bendability (°)	TS (MPa)	YS (MPa)	PE (%)	PRA (%)	Impact Energy (J/mm^2)
96.0	7000	917	223	55.00	45.93	611.0	426.0	18.4	30.50	0.4609
96.0	6000	917	220	51.00	44.38	568.7	425.6	19.5	36.70	0.509
96.0	5000	917	215	41.00	40.82	509.0	423.5	21.0	43.00	0.5197
96.5	7000	917	224	60.00	46.00	612.0	427.0	18.3	30.30	0.4608
96.5	6000	917	221	52.20	44.40	569.6	426.0	18.8	34.90	0.5089
96.5	5000	917	217	40.90	42.78	512.0	423.9	20.8	41.30	0.5189
97.0	7000	917	227	61.50	46.05	613.0	428.0	17.8	30.20	0.4607
97.0	6000	917	223	52.30	44.50	570.0	427.0	18.5	34.70	0.5078
97.0	5000	917	218	40.79	42.90	512.9	425.2	40.0	39.00	0.5179
97.5	7000	917	228	61.00	46.24	614.0	429.0	16.7	28.00	0.4606
97.5	6000	917	224	53.00	44.78	572.0	428.5	17.4	34.40	0.5024
97.5	5000	917	219	42.10	43.33	522.0	425.3	19.2	39.90	0.5125
98.0	7000	917	229	62.00	46.27	613.0	430.0	15.6	27.40	0.4527
98.0	6000	917	225	54.60	45.00	581.0	428.6	16.6	34.30	0.4917
98.0	5000	917	221	39.00	43.52	540.0	425.6	19.0	43.07	0.5014
98.5	7000	917	230	63.00	46.34	617.0	430.4	15.3	25.00	0.4526
98.5	6000	917	227	55.00	45.20	598.0	428.7	16.0	33.70	0.4890
98.5	5000	917	222	45.00	43.60	542.0	426.3	18.0	37.90	0.4983
99.0	7000	917	232	66.00	46.36	618.0	430.6	14.7	25.70	0.4425
99.0	6000	917	229	57.00	45.40	599.0	428.8	15.2	33.40	0.4810
99.0	5000	917	224	45.30	43.62	543.0	426.4	17.4	35.50	0.4980
99.5	7000	917	233	67.00	46.37	619.0	431.0	14.0	25.00	0.4000
99.5	6000	917	230	58.00	45.50	600.0	429.0	15.0	33.00	0.4800
99.5	5000	917	225	45.50	43.63	545.0	427.0	17.0	37.00	0.4970

Table 4.5 (continued): Effect of PTD at constant FRT and variable RSR.

PTD (%)	RSR (S^{-1})	FRT (°C)	Hardness (HB)	E (GPa)	Ductility or Bendability (°)	TS (MPa)	YS (MPa)	PE (%)	PRA (%)	Impact Energy (J/mm)
96.0	7000	919	222	54.00	44.92	610.0	425.0	19.8	30.80	0.4635
96.0	6000	919	219	50.00	43.38	566.0	423.0	20.8	36.90	0.5099
96.0	5000	919	214	45.00	42.70	506.0	421.0	21.9	39.87	0.5190
96.5	7000	919	223	56.00	45.00	612.0	426.0	19.4	30.50	0.4626
96.5	6000	919	220	50.10	43.40	567.5	424.0	19.8	35.90	0.5091
96.5	5000	919	216	39.90	42.78	509.0	422.0	20.9	42.60	0.5190
97.0	7000	919	226	60.00	45.06	613.0	427.0	18.7	30.40	0.4619
97.0	6000	919	222	51.40	43.50	568.0	426.0	19.6	35.00	0.5079
97.0	5000	919	217	39.97	42.39	510.0	423.0	20.6	41.00	0.5180
97.5	7000	919	227	60.70	44.00	621.0	428.0	17.6	29.00	0.4607
97.5	6000	919	223	52.00	43.79	570.0	427.0	18.9	34.70	0.5025
97.5	5000	919	218	40.00	43.32	520.0	426.0	19.7	41.10	0.5126
98.0	7000	919	228	61.00	45.30	627.1	429.0	16.7	27.90	0.4559
98.0	6000	919	224	53.80	44.00	578.0	428.0	18.5	34.50	0.4957
98.0	5000	919	229	42.07	43.50	538.0	427.3	19.5	39.60	0.4528
98.5	7000	919	229	62.00	45.35	633.0	429.2	16.2	26.00	0.4528
98.5	6000	919	226	54.00	44.40	596.0	428.3	17.0	33.90	0.491
98.5	5000	919	221	43.00	43.60	550.0	427.9	18.8	38.00	0.4981
99.0	7000	919	230	63.00	43.36	617.0	429.5	16.1	25.50	0.4425
99.0	6000	919	227	55.00	44.50	599.0	428.5	16.7	33.80	0.4900
99.0	5000	919	222	44.00	43.70	551.0	427.8	18.7	37.00	0.4980
99.5	7000	919	231	64.00	45.37	618.0	430.0	16.0	25.00	0.3910
99.5	6000	919	228	56.00	44.60	600.0	429.0	16.5	23.60	0.4800
99.5	5000	919	223	45.00	43.80	556.0	428.0	18.6	36.00	0.4970

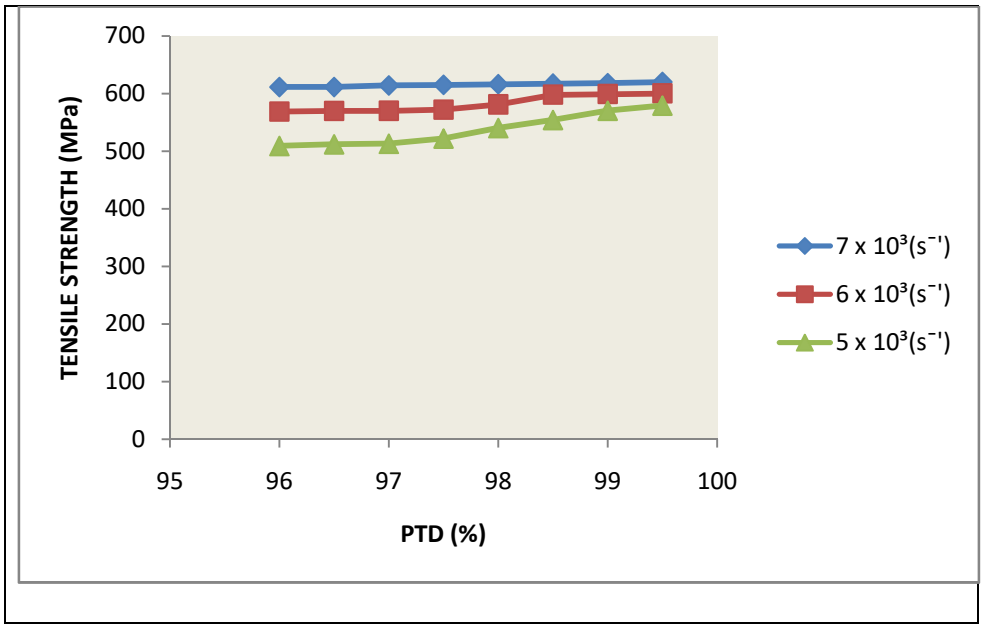

Figure 4.97: Effect of PTD on TS at FRT of 915°C.

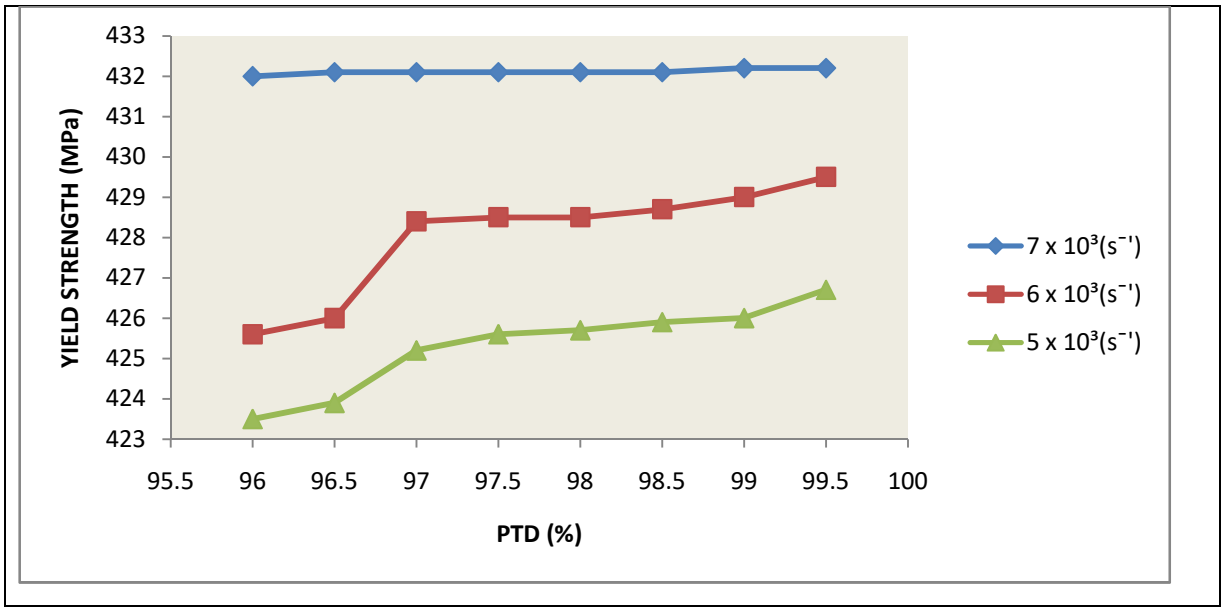

Figure 4.98: Effect of PTD on YS at FRT of 915°C

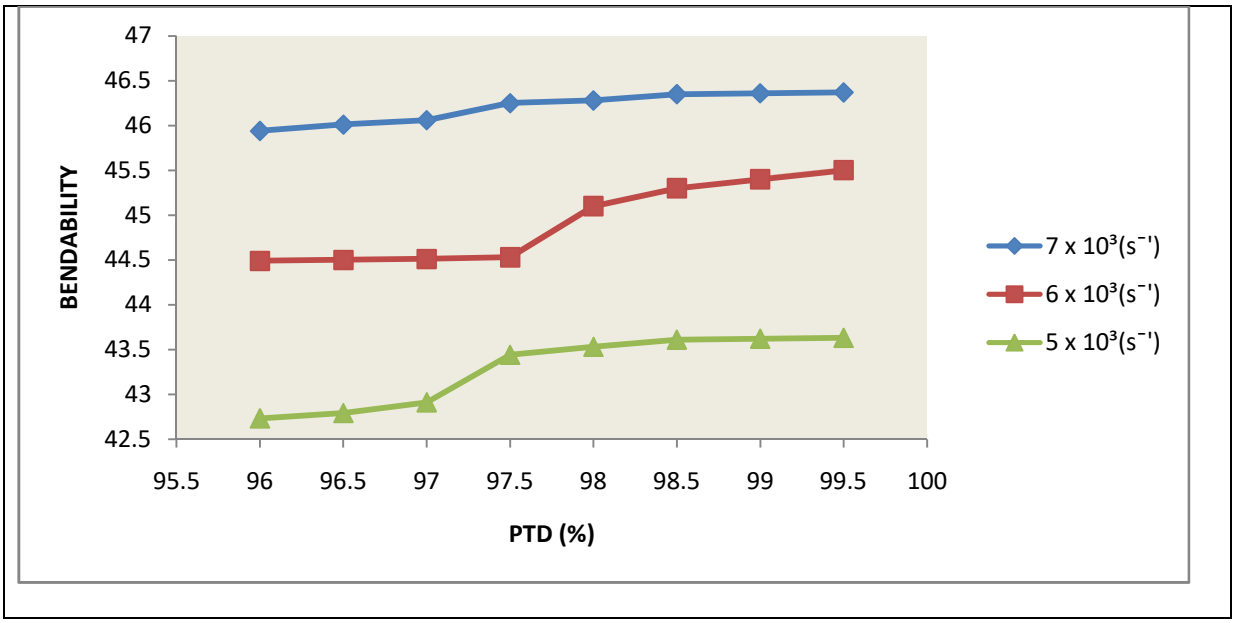

Figure 4.99: Effect of PTD on ductility at FRT of 915°C,

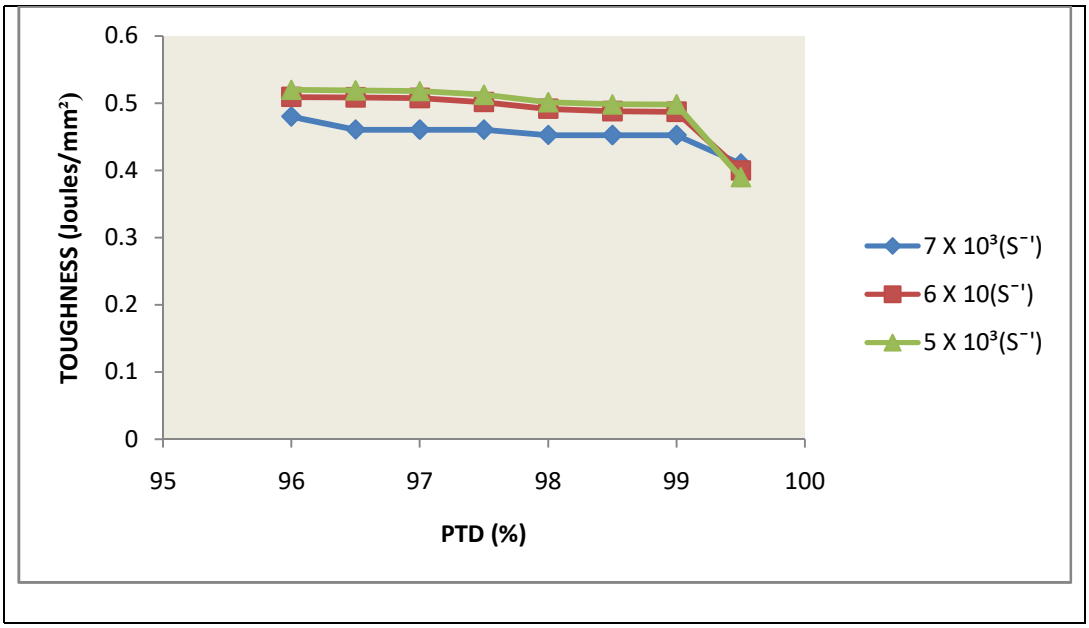

Figure 4.100: Effect of PTD on Impact Energy at FRT of 915°C,

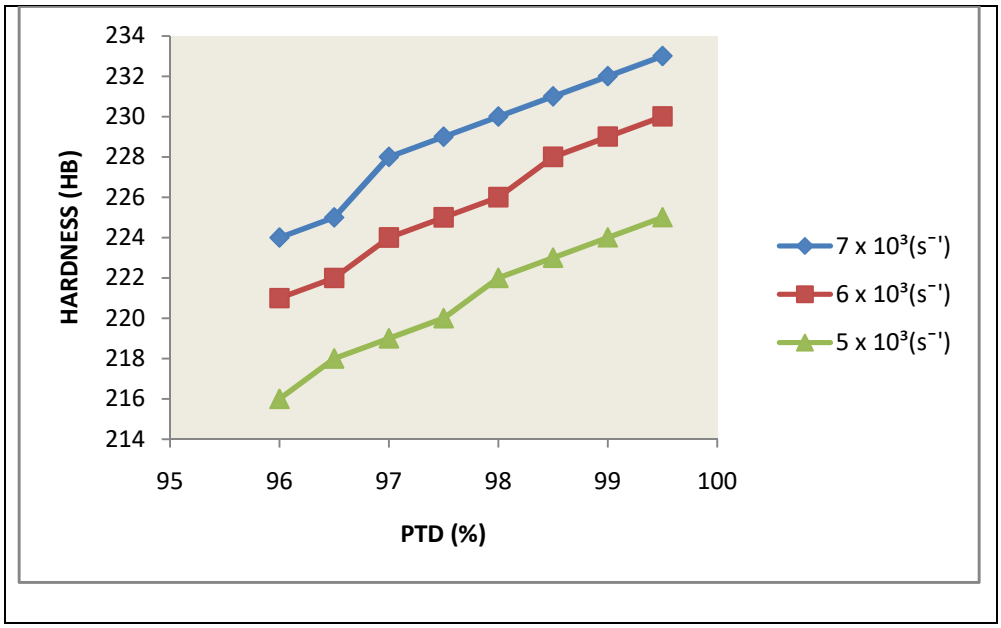

Figure 4.101: Effect of PTD on hardness at FRT of 915°C

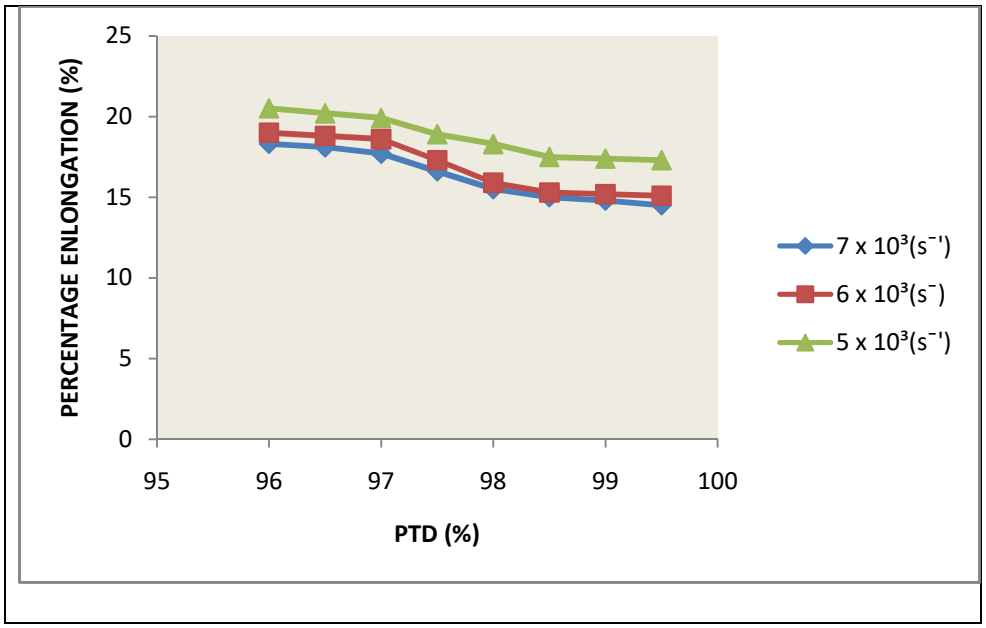

Figure 4.102:% Effect of PTD on PE at FRT of 915°C,.

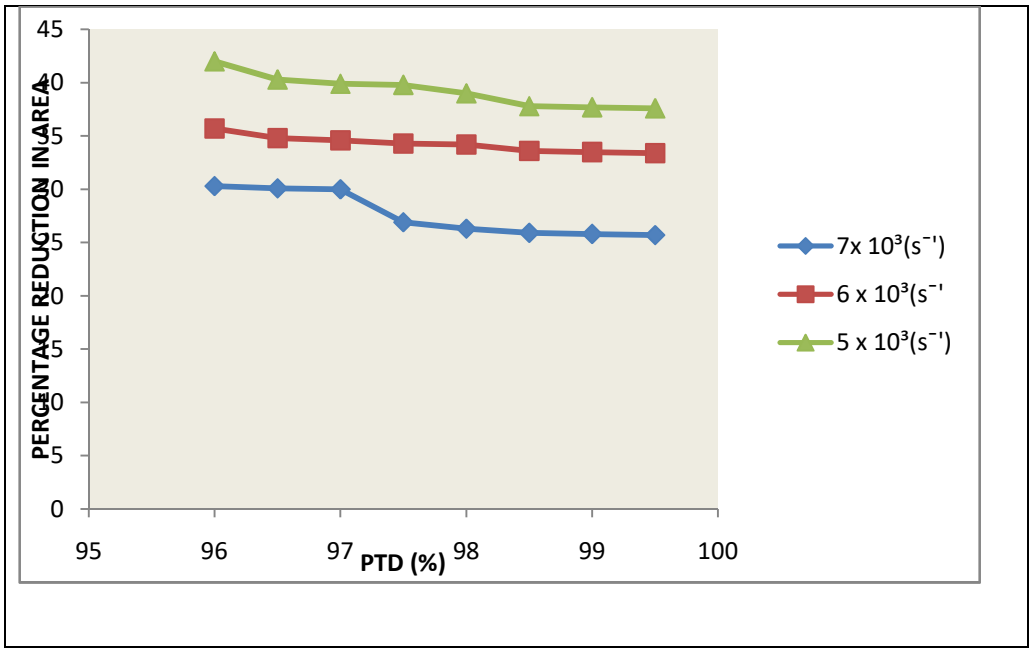

Figure 4.103: Effect of PTD on PRA at FRT of 915°C.

4.14 Results and Discussions For Effects of PTD at FRT of 917°C

Figures 4.104-4.112 show the effect of PTD on the tensile properties at a FRT of 917°C, varying RSR.

After the analysis of the tensile properties of the hot-rolled steel it may equally be reported that the mechanical properties of the hot-rolledsteel grade is substantially influenced by the PTD at 7000, 6000 , 5000 S^{-1} RSR. The TS, YS, hardness, E and ductility increased with increasing PTD, while the impact energy, PRA and PE decreased with increasing PTD for all RSR and FRT observed.

From Figures 4.104 to 4.112 ,at 7000 S^{-1}RSR and 915°C constant FRT,when the PTD increased from 96.0 to 96.5% ,the TS increased from 611 to 612MPa (Fig.4.105), YS increased from 426 to 427MPa (Fig.4.106), hardness increased from 223 to 224 HB (Fig.4.109),E increased from 55 to 60 GPa (Fig.4.112), ductility increased from 45.93 to 46º (Fig.4.107);while impact energy reduced from 0.4609 to 0.4608 J/mm^2 (Fig.4.108), PRA reduced from 30.5 to 30.3%(Fig.4.111), PE reduced from 18.4 to 18.3% (Fig.4.110). At 6000 S^{-1} RSR and 915°C FRT, as the PTD increased from 96.0 to 96.5 percent ,the TSincreased from 568.7 to 569.6 MPa (Fig.4.105), YS increased from 425.6 to 426 MPa (Fig.4.106), hardness increased from 220 to 221 HB (Fig.4.109,E increased from 51 .0 to52.2GPa (Fig.4.112) and ductility increased from 44.38 to 44.4º (Fig.4.107);while impact energy reduced from 0.509 to 0.5089 J/mm^2 (Fig.4.108), PRA reduced from 36.7 to 34.9%(Fig.4.111) and PE reduced from 19.5 to 18.8% (Fig.4.110). At 5000 S^{-1}RSR and 915^{0}C FRT, as the PTD increased from 96.0 to 96.5 percent, TS increased from 509 to 512 MPa (Fig.4.105), YS increased from 423.5 to 423.9 MPa (Fig.4.106), hardness increased from 215 to 217 HB (Fig.4.109), E increased from 41 to 40.9GPa, ductility increased from 42.73 to 42.79º(Fig.4.99);while impact energy reduced from 0.5196 to 0.5188 J/mm^2(Fig.4.104), PRA reduced from 43 to 41.3%(Fig.4.111). PE reduced from 21 to 20.8%(Fig.4.110).

The effects of PTD on the rolled stock was very pronounced as the PTD increases, the TS, YS, hardness, E, and ductility of the hot-rolled samples increase; while the impact energy, PRA and PE decrease. The workingof the billets within the stands gave rise to

increased yielding and increased number of displaced componentswere transferred to the final hot-rolled rebar. The strengthening obtained came from smoothening of the microstructure of the austenites and displacement of layers of cementite by spheroidal particles.

This yielding was due to displacement movement stopped by many stoppages like solidification of another components and this gave rise to increase in TS, YS, hardness, E and ductility. Impact energy, PRA and PE also decreased.

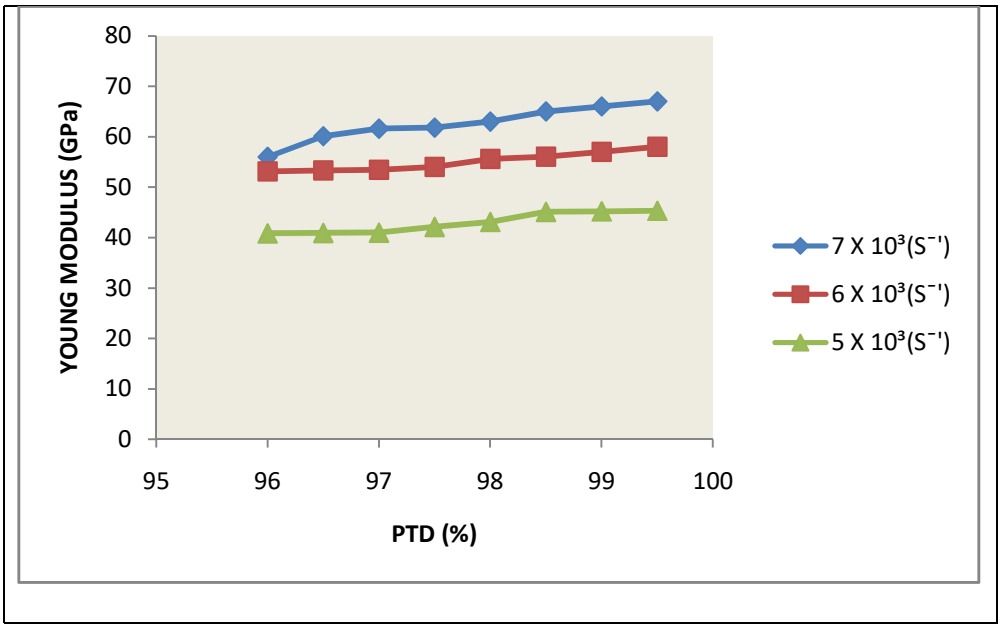

Figure 4.104: Effect of PTD on E at FRT of 917°C.

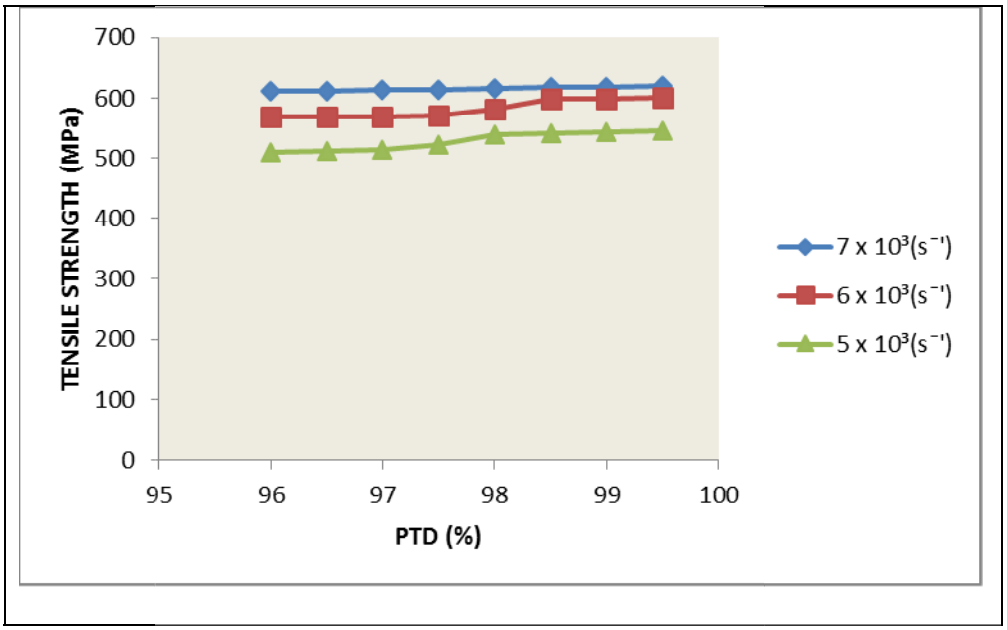

Figure 4.105: Effect of PTD on TS at FRT of 917°C.

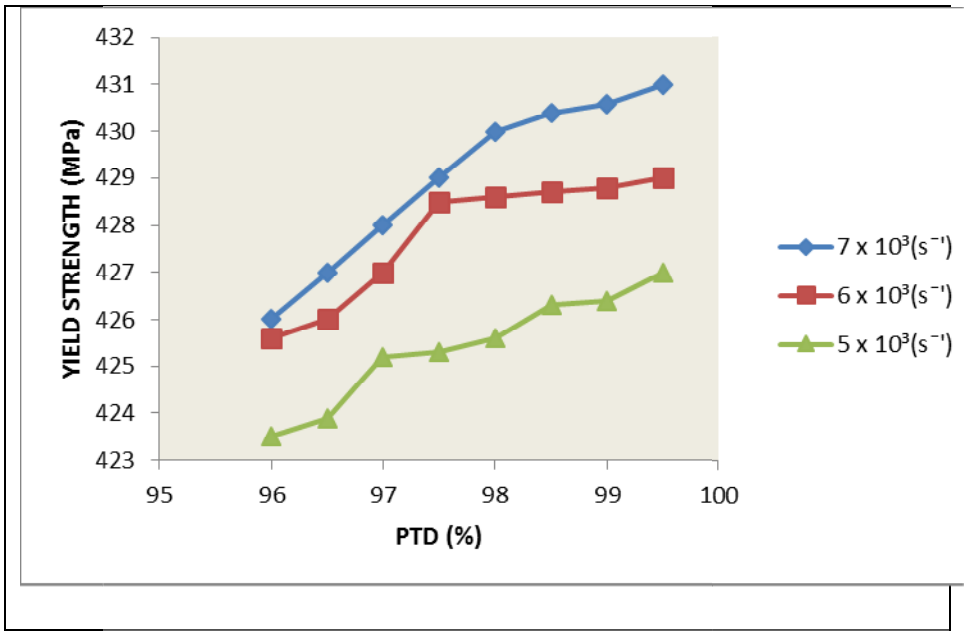

Figure 4.106: Effect of PTD on YS at FRT of 917°C..

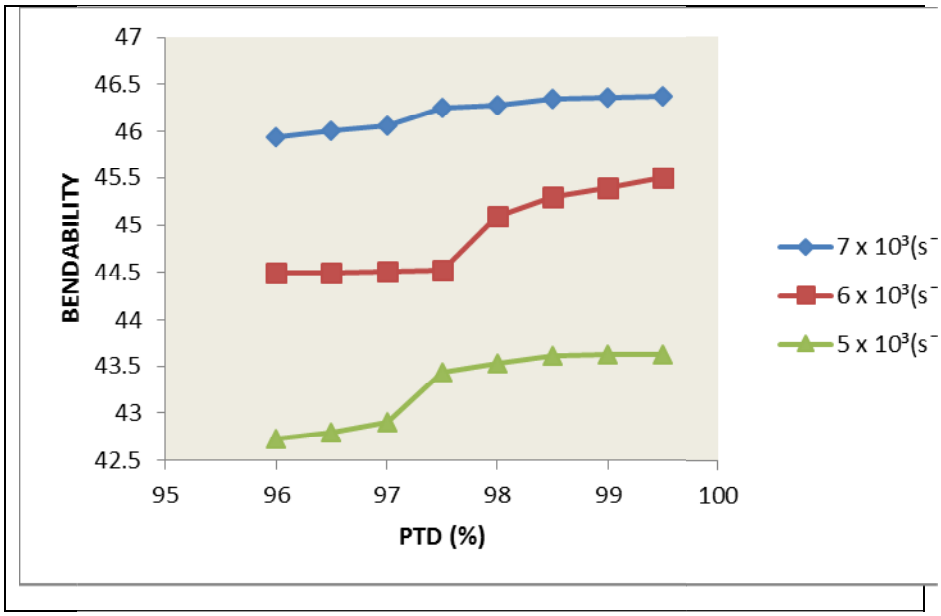

Figure 4.107: Effect of PTD on ductility at FRT of 917°C..

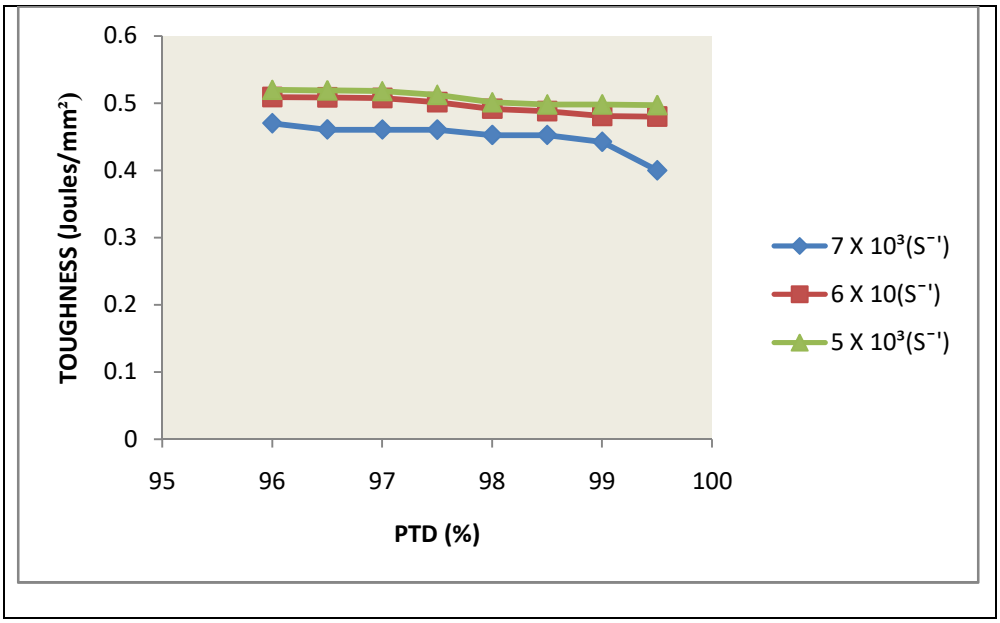

Figure 4.108: Effect of PTD on Impact Energyat FRT of 917°C.

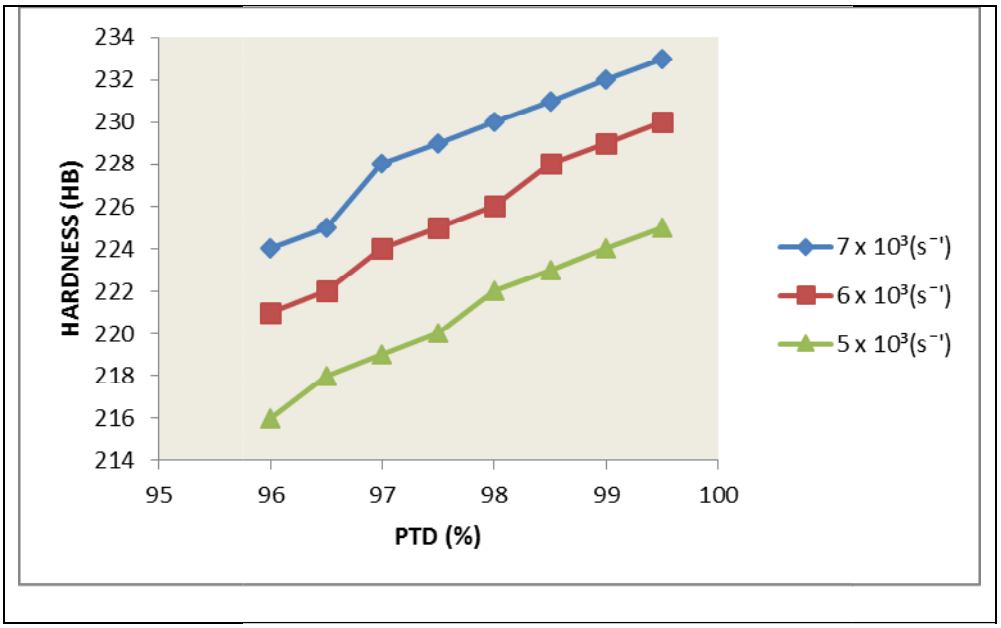

Figure 4.109: Effect of PTD on hardness at FRT of 917°C

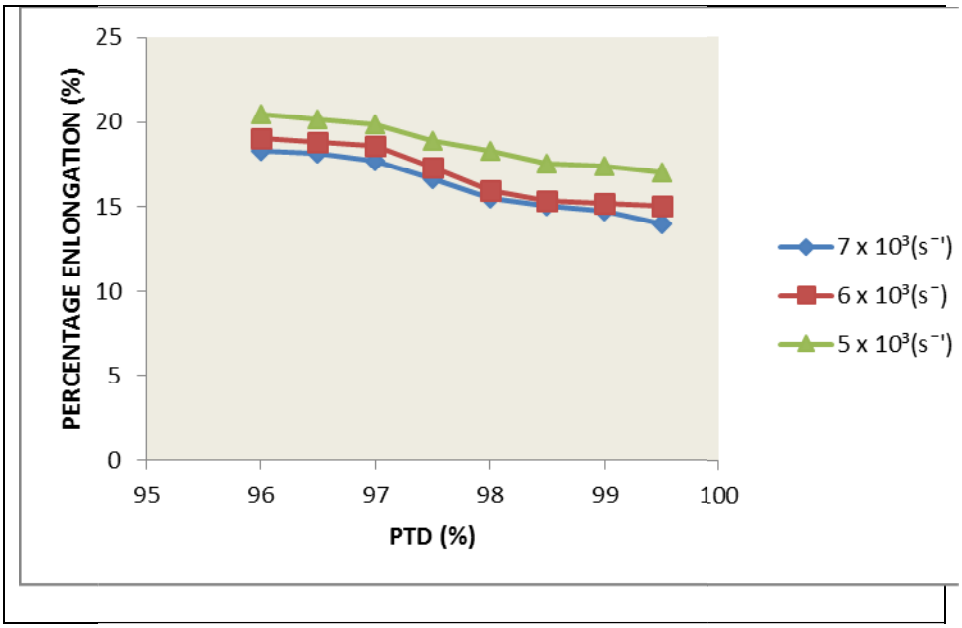

Figure 4.110: Effect of PTD on PE at FRT of 917°C.

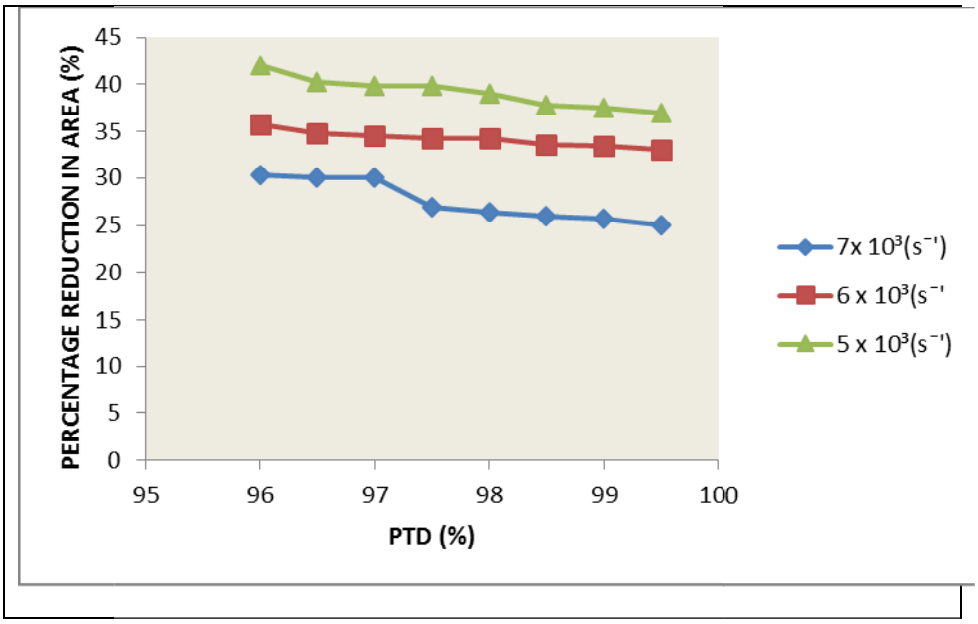

Figure 4.111: Effect of PTD on PRAat FRT of 917°C,

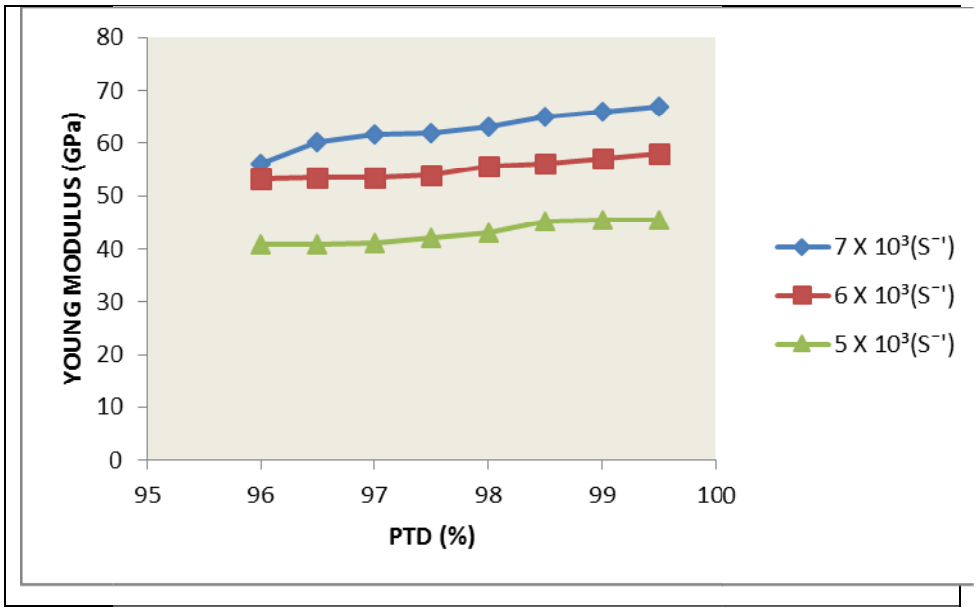

Figure 4.112: Effect of PTD on E at FRT of 917°C,.

4.15 Results and Discussions For Effects of PTD at FRT of 919°C

Figures 4.113-4.120 show the effect of PTD on the tensile properties at a constant FRT of 919°C and variable RSR.

After the analysis of the tensile properties of the hot-rolled steel it may equally be reported that the tensile properties of the hot-rolled steel grade is substantially influenced by the PTD at 7000, 6000, 5000 S^{-1} RSR. The TS, YS, hardness, E and ductility increased with increasing PTD, while the impact energy, PRA and PE decreased with increasing PTD for all the degrees of RSR and FRT observed.

From Figures 4.113 to 4.120,at 7000 S^{-1} RSR and 919°C FRT,when the PTD increased from 96.0 to 96.5 percent,the TS increased from 610 to 612MPa (Fig.4.113), YS increased from 425 to 426MPa (Fig.4.114), hardness increased from 222 to 223 HB (Fig.4.117), E increased from 54 to 56 GPa (Fig.4.120), ductility increased from 45.92 to 45°(Fig.4.116) ;while impact energy reduced from 0.4635 to 0.4626 J/mm^2(Fig.4.116), PRA reduced from 30.8 to 30.5%(Fig.4.118), PE reduced from 19.8 to 19.4% (Fig.4.118). At 6000 S^{-1} RSR and 915°C FRT, as the PTD increased from 96.0 to 96.5 percent ,the TSincreased from 566 to 567.5 MPa (Fig.4.113), YS increased from 423 to 424 MPa (Fig.4.114), hardness increased from 219 to 220 HB (Fig.4.117), E increased from 50 to50.1GPa (Fig.4.120) and ductility increased from 43.38 to 43.40°(Fig.4.117);while impact energy reduced from 0.5099 to 0.5191 J/mm^2 (Fig.4.116), PRA reduced from 36.9 to 35.9%(Fig.4.119) and PE reduced from 20.8 to 19.8%(Fig.4.103). At 5000 S^{-1}RSR and 915°C FRT, as the PTD increased from 96.0 to 96.5 percent, TS increased from 506 to 509 MPa (Fig.4.113), YS increased from 423 to 422 MPa (Fig.4.114), hardness increased from 214 to 216 HB (Fig.4.117), E increased from 45 to 39.9 GPa (Fig.4.120), ductility increased from 42.7 to 42.78°(Fig.4.115);while impact energy reduced from 0.519 to 0.519 J/mm^2 (Fig.4.116), PRA reduced from 39.87 to 42.6%(Fig.4.119), PE reduced from 21.9 to 20.9%(Fig.4.102).

The effects of PTD on the rolled stock was very pronounced as the PTD increases,the TS, YS, hardness, E and ductility of the hot-rolled samples increase; while the impact energy, PRA and PE decrease. The workingof the billets within the stands gave rise to

increased yielding and increased number of displaced components were transferred to the final hot-rolled rebar. The strengthening obtained came from smoothening of the microstructure of the austenites and displacement of layers of cementite by spheroidal particles.

This yielding was due to displacement movement stopped by many stoppages like solidification of another components and this gave rise to increase in TS, YS, hardness, E and ductility. Impact energy, PRA and PE also decreased

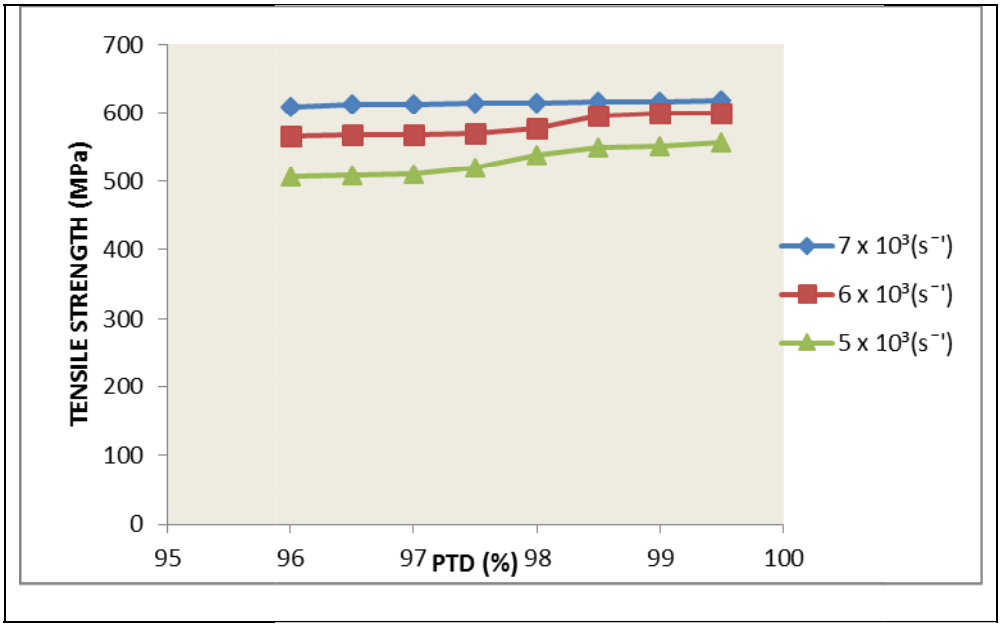

Figure 4.113: Effect of PTD on TSat FRT of 919°C.

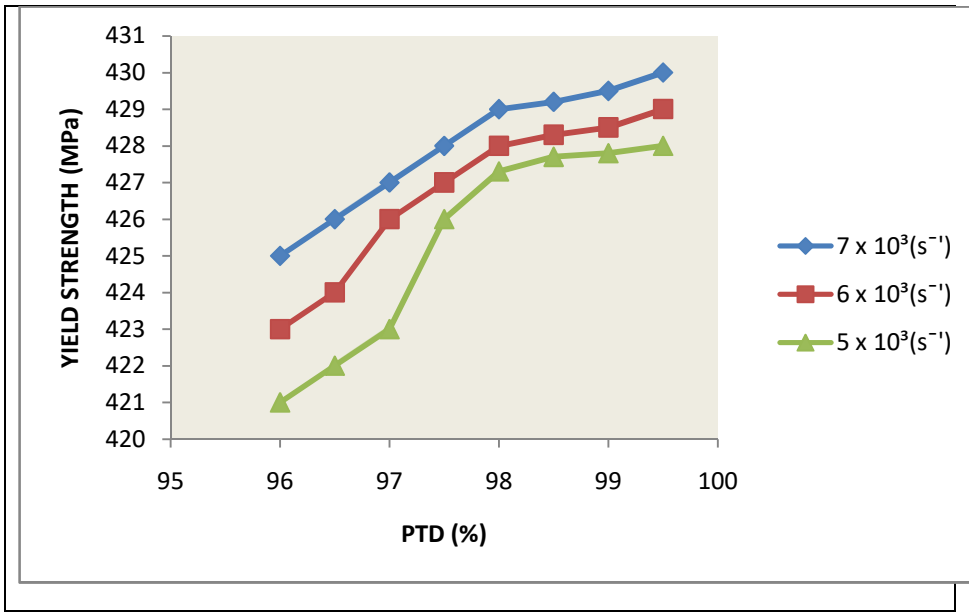

Figure 4.114: Effect of PTD on YS at FRT of 919°C.

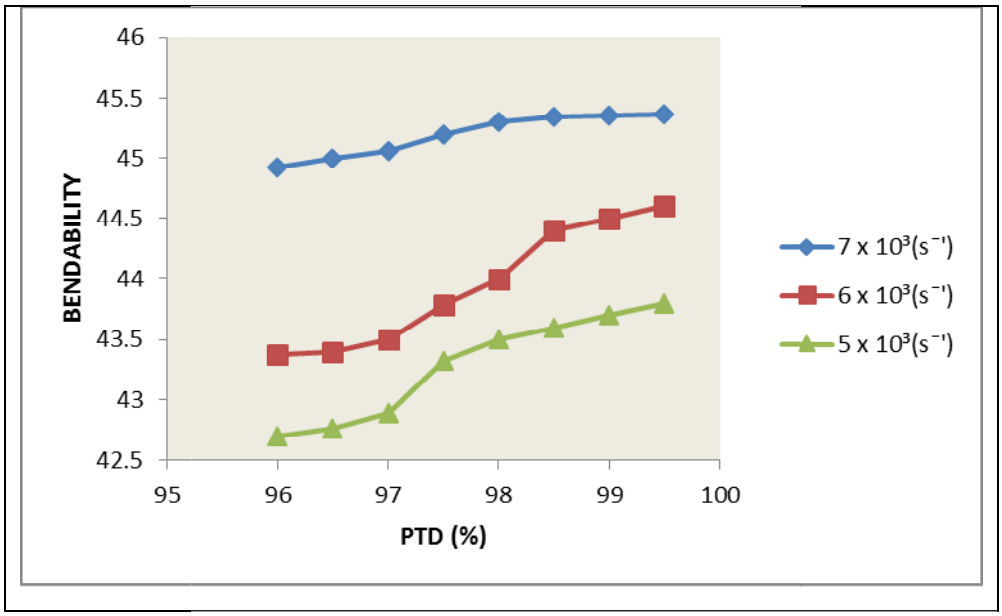

Fig.4.115: Effect of PTD on ductility at FRT of 919°C

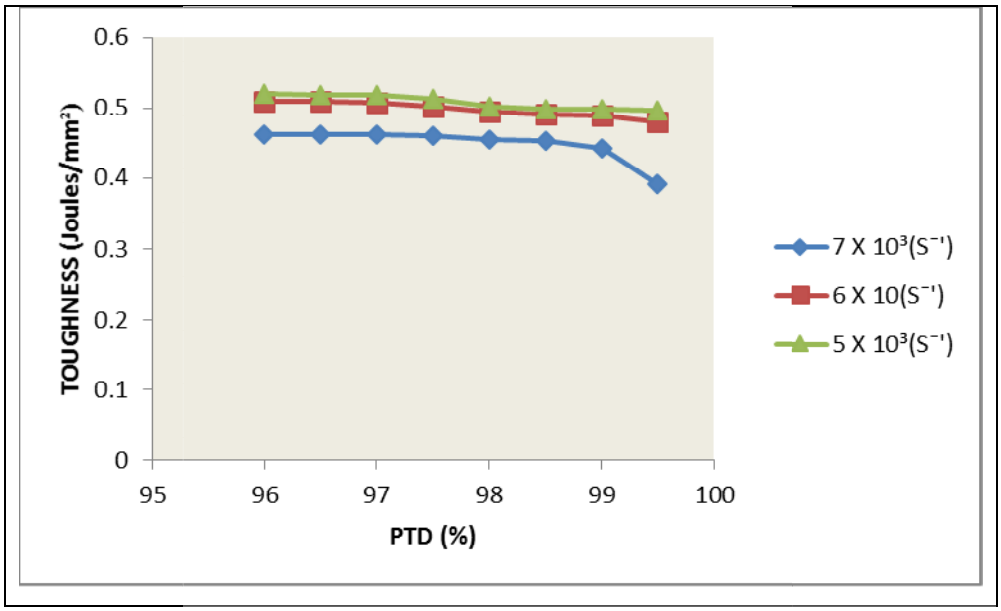

Figure 4.116:% Total deformation versus Impact Energyat FRT of 919°C.

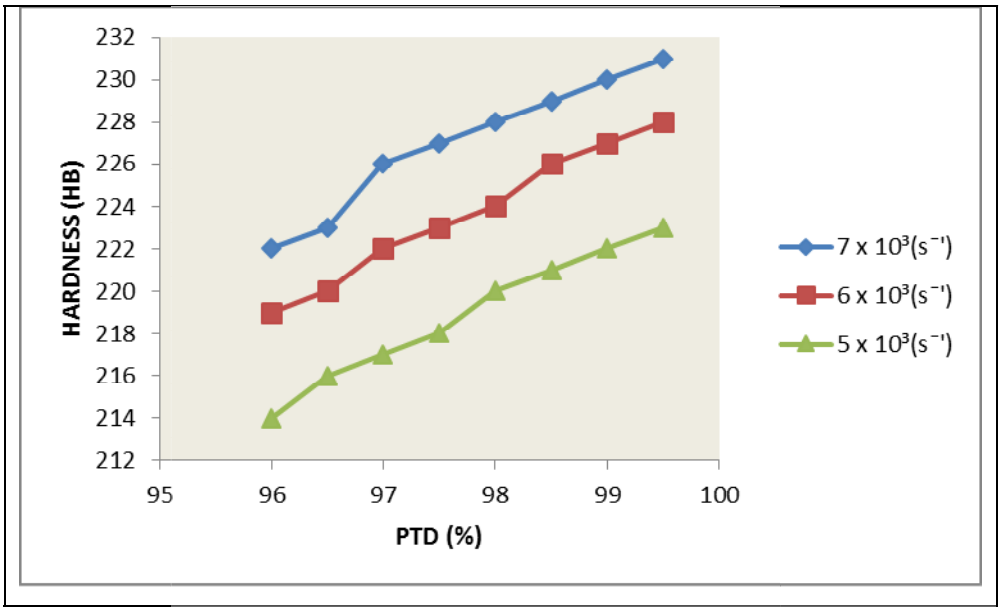

Figure 4.117: Effect of PTD on hardness at FRT of 919°C.

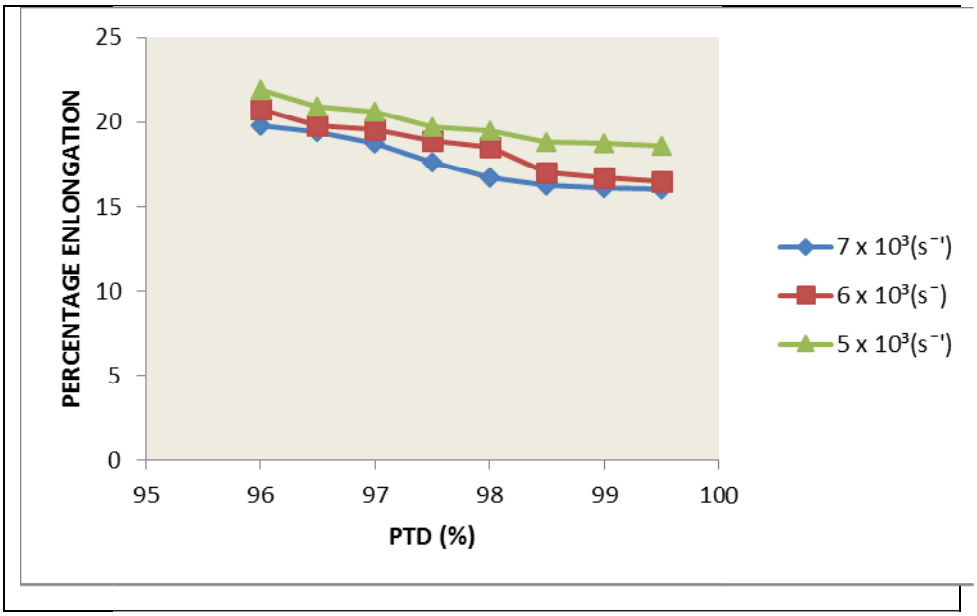

Figure 4.118: Effect of PTD on PE at FRT of 919°C.

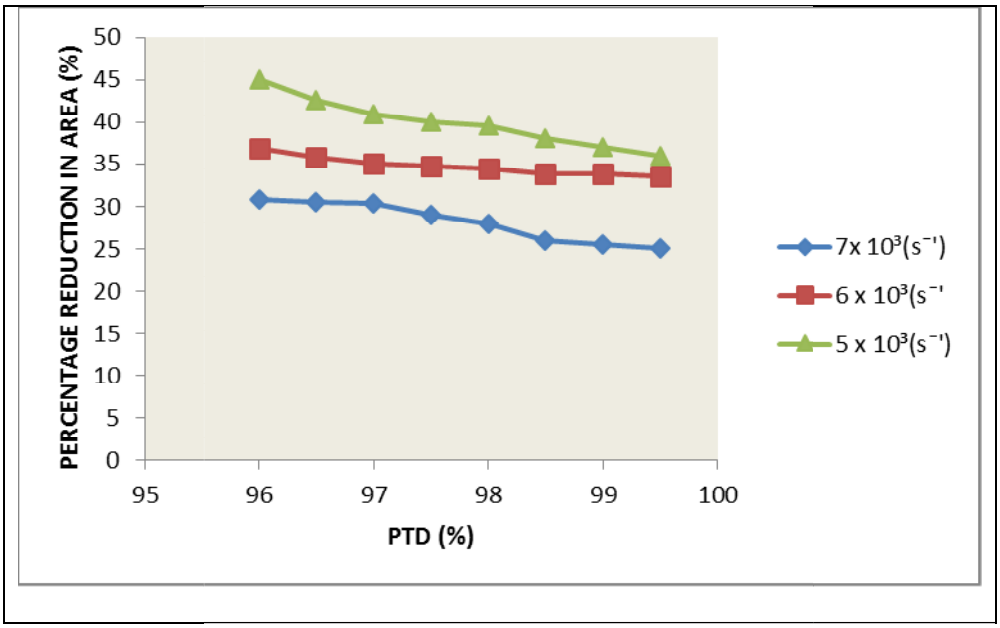

Figure 4.119: Effect of PTD on PRA at FRT of 919°C,.

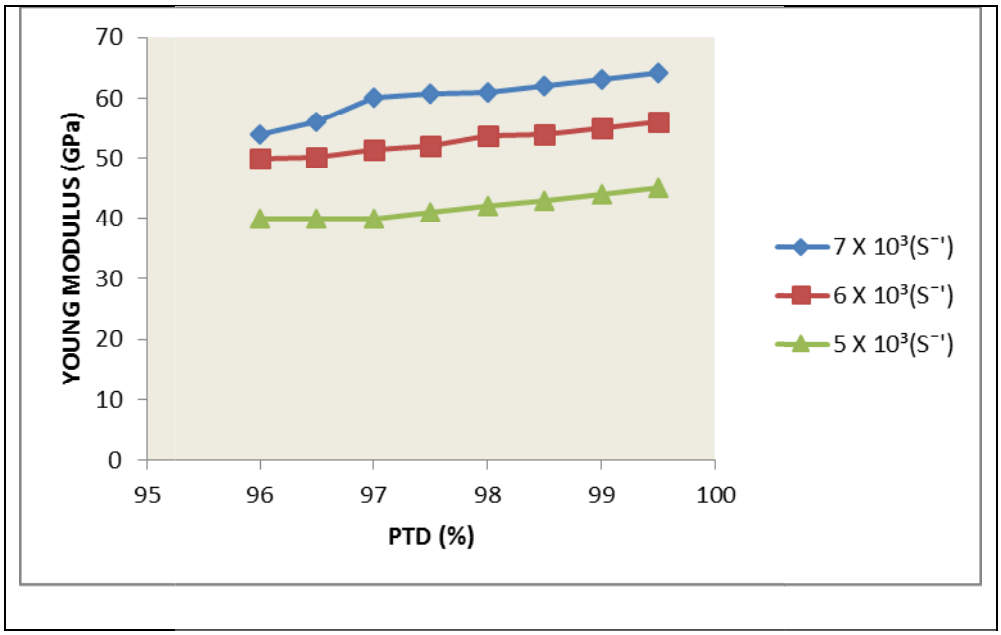

Figure 4.120: Effect of PTD on Eat FRT of 919°C

4.16 Results and Discussions For Effects of PTD at RSR of 7000 S^{-1}

Table 4.6 shows the effect of PTD on all the tensile properties of the steel grade investigated.The plots of the effects of PTD on the tensile properties of the steel grade at RSR of 7000 S^{-1},varying at FRT of 915°C,917°C and 919°C respectively ,are shown in Figures 4.121 -4.128. At 915^{0}C FRT and 7000 S^{-1} RSR, when the PTD increased from 96.0 to 96.5 percent ,the ductility increased from 44.49 to 46.01° (Fig.4.123), impact energy decreased from 0.48 to 0.4607 J/mm^2(Fig.4.124), hardness increased from 221 to 225 HB (Fig.4.125), YS increased from 432 to 432.01 MPa (Fig.4.122), TS increased from 611.2 to 611.3 MPa (Fig.4.121), PE decreased from 19 to 18.1% (Fig.4.126), E increased from 49.2 to 60.1 GPa (Fig.4.128), PRA decreased from 35.7 to 30.1% (Fig.4.127).

At 917^{0}C FRT and 7000 S^{-1}RSR, as the PTD increased from 96.0 to 96.5 percent, ductility increased from 45.94 to 46.01°(Fig.4.123), impact energy decreased from 0.48 to 0.4607 J/mm^2 (Fig.4.124),hardness increased from 221 to 225 HB (Fig.4.125), YS increased from 425.6 to 426 MPa (Fig.4.122), TS increased from 568.7 to 569.6 MPa (Fig.4.121), PE decreased from 18.3 to 18.2% (Fig.4.126), E increased from 56 to 56.3 GPa (Fig.4.128), PRA decreased from 35.7 to 34.8%(Fig.4.127).

At 919^{0}C FRT and 7000 S^{-1}RSR as the PTD increased from 96.0 to 96.5 percent,ductility increased from 42.73 to 42.79° (Fig.4.123), impact energydecreased from 0.5196 to 0.5188 J/mm^2 (Fig.4.124), hardness increased from 216 to 218 HB (Fig.4.125), YS increased from 423.5 to 423.9 MPa (Fig.4.122), TS increased from 509 to 512 MPa (Fig.4.121), PE decreased from 20.8 to 20.4% (Fig.4.126), E increased from 40.8 to 40.9 GPa (Fig.4.128), PRA decreased from 42 to 40.3%(Fig.4.127).The above property trend is applicable as FRT of 917 and 919°C,andRSR of 6000 and 5000 S^{-1} respectively.

The effects of PTD on the rolled stock was very pronouncedas the PTD increases,the TS, YS, hardness, E and ductility of the hot-rolled samples increase; while the impact energy, PRA and PE decrease. The workingof the billets within the stands gave rise to increased yielding and increased number of displaced components were transferred to the final hot-rolled rebar. The strengthening obtained came from smoothening of the

microstructure of the austenites and displacement of layers of cementite by spheroidal particles.

This yielding was due to displacement movement stopped by many stoppages like solidification of another components and this gave rise to increase in TS, YS, hardness, E and ductility. Impact energy, PRA andPE also decreased

Table 4.6: Effects Of PTD At Constant RSR, variableFRT.

PTD (%)	RSR (S^{-1})	FRT (°C)	Hardness (HB)	E (GPa)	Ductility or Bendability (°)	TS (MPa)	YS (MPa)	PE (%)	PRA (%)	Impact Energy (J/mm^2)
96.0	7000	915	224	56.00	45.94	611.2	432.00	18.3	30.30	0.4800
96.0	7000	917	221	53.10	44.49	568.7	425.60	19.0	35.70	0.5090
96.0	7000	919	216	40.83	42.73	568.7	423.50	20.5	42.00	0.5196
96.5	7000	915	225	60.10	46.01	611.3	432.01	18.1	30.10	0.4607
96.5	7000	917	222	53.30	44.50	569.6	426.00	18.8	34.80	0.5085
96.5	7000	919	218	40.30	42.79	512.0	423.90	20.2	40.91	0.5188
97.0	7000	915	228	61.60	46.06	614.0	432.04	17.7	30.00	0.4606
97.0	7000	917	224	53.40	44.51	570.0	428.40	18.6	34.60	0.5074
97.0	7000	919	219	40.98	42.91	512.9	425.20	19.9	39.90	0.5177
97.5	7000	915	229	61.80	46.25	615.0	432.05	16.6	26.90	0.4605
97.5	7000	917	225	54.00	44.53	572.0	428.50	17.3	34.30	0.5015
97.5	7000	919	220	42.11	43.44	522.0	425.60	18.9	39.80	0.5123
98.0	7000	915	230	63.00	46.28	616.0	432.06	15.5	26.30	0.4526
98.0	7000	917	226	55.60	45.10	581.0	428.50	15.9	34.20	0.4916
98.0	7000	919	222	43.08	43.53	540.0	425.70	18.3	39.00	0.5012
98.5	7000	915	231	65.00	46.35	617.0	432.07	15.0	25.90	0.4525
98.5	7000	917	228	56.00	45.20	598.0	428.70	15.3	33.80	0.4880
98.5	7000	919	225	45.30	43.63	579.0	426.70	17.3	37.60	0.3900
99.0	7000	915	232	66.00	46.36	618.0	432.08	14.8	25.80	0.4524
99.0	7000	917	229	57.00	45.40	599.0	429.00	15.2	33.50	0.4870
99.0	7000	919	224	45.20	43.62	570.0	426.00	17.4	37.70	0.4980
99.5	7000	915	233	67.00	46.37	620.0	432.20	14.5	25.70	0.4100
99.5	7000	917	230	58.00	45.50	600.0	429.50	15.1	33.40	0.4000
99.5	7000	919	225	45.30	43.63	579.0	426.70	17.3	37.60	0.3900

Table 4.6 (Continued): Effects Of PTD At Constant RSR and variable FRT.

PTD (%)	RSR (S^{-1})	FRT(°C)	Hardness (HB)	E (GPa)	Ductility or Bendability (°)	TS (MPa)	YS (MPa)	PE (%)	PRA (%)	Impact Energy (J/mm^2)
96.0	6000	915	223	55.00	45.93	611.0	426.0	18.4	30.50	0.4609
96.0	6000	917	220	51.00	44.38	568.7	425.6	19.5	36.70	0.5090
96.0	6000	919	215	41.00	40.82	509.0	423.5	21.0	43.00	0.5197
96.5	6000	915	224	60.00	46..00	612.0	427.0	18.3	30.30	0.4608
96.5	6000	917	221	52.20	44.40	569.6	426.0	18.8	34.90	0.5089
96.5	6000	919	217	40.90	42.78	512.0	423.9	20.8	41.30	0.5189
97.0	6000	915	227	61.50	46.05	613.0	428.0	17.8	30.20	0.4607
97.0	6000	917	223	52.30	44.50	570.0	427.0	18.5	34.70	0.5078
97.0	6000	919	218	40.79	42.90	512.9	425.2	40.0	39.00	0.5179
97.5	6000	915	228	61.70	46.24	614.0	429.0	16.7	28.00	0.4606
97.5	6000	917	224	53.00	44.78	572.0	428.5	17.4	34.40	0.5024
97.5	6000	919	219	42.10	43.33	522.0	425.3	19.2	39.90	0.5125
98.0	6000	915	229	62.00	46.27	613.0	430.0	15.6	27.40	0.4527
98.0	6000	917	225	54.60	45.00	581.0	428.6	16.6	34.30	0.4917
98.0	5000	919	221	39.00	43.52	540.0	425.6	19.0	43.07	0.5014
98.5	6000	915	230	63.00	46.34	617.0	430.4	15.3	25.00	0.4526
98.5	6000	917	227	55.00	45.20	598.0	428.7	16.0	33.70	0.4890
98.5	6000	919	222	45.00	43.60	542.0	426.3	18.0	37.90	0.4983
99.0	6000	915	232	66.00	46.36	618.0	430.6	14.7	25.70	0.4425
99.0	6000	917	229	57.00	45.40	599.0	428.8	15.2	33.40	0.4810
99.0	6000	919	224	45.30	43.62	543.0	426.4	17.4	35.50	0.4980
99.5	6000	915	233	67.00	46.37	619.0	431.0	14.0	25.00	0.4000
99.5	6000	917	230	58.00	45.50	600.0	429.0	15.0	33.00	0.4800
99.5	6000	919	225	45.50	43.63	545.0	427.0	17.0	37.00	0.4970

Table 4.6 (Continued): Effects Of PTD At Constant FRT and variable RSR.

PTD (%)	RSR (S^{-1})	FRT (°C)	Hardness (HB)	E (GPa)	Ductility or Bendability (°)	TS (MPa)	YS (MPa)	PE (%)	PRA (%)	Impact Energy (J/mm^2)
96.0	5000	915	222	54.00	44.92	610.0	425.0	19.8	30.80	0.4635
96.0	5000	917	219	50.00	43.38	566.0	423.0	20.8	36.90	0.5099
96.0	5000	919	214	45.00	42.70	506.0	421.0	21.9	39.87	0.5190
96.5	5000	915	223	56.00	45.00	612.0	426.0	19.4	30.50	0.4626
96.5	5000	917	220	50.10	43.40	567.5	424.0	19.8	35.90	0.5091
96.5	5000	919	216	39.90	42.78	509.0	422.0	20.9	42.60	0.5190
97.0	5000	915	226	60.00	45.06	613.0	427.0	18.7	30.40	0.4619
97.0	5000	917	222	51.40	43.50	568.0	426.0	19.6	35.00	0.5079
97.0	5000	919	217	39.97	42.39	510.0	423.0	20.6	41.00	0.5180
97.5	5000	915	227	60.70	44.00	621.0	428.0	17.6	29.00	0.4607
97.5	5000	917	223	52.00	43.79	570.0	427.0	18.9	34.70	0.5025
97.5	5000	919	218	40.00	43.32	520.0	426.0	19.7	41.10	0.5126
98.0	5000	915	228	61.00	45.30	627.1	429.0	16.7	27.90	0.4559
98.0	5000	917	224	53.80	44.00	578.0	428.0	18.5	34.50	0.4957
98.0	5000	919	229	42.07	43.50	538.0	427.3	19.5	39.60	0.4528
98.5	5000	915	229	62.00	45.35	633.0	429.2	16.2	26.00	0.4528
98.5	5000	917	226	54.00	44.40	596.0	428.3	17.0	33.90	0.4910
98.5	5000	919	221	43.00	43.60	550.0	427.9	18.8	38.00	0.4981
99.0	5000	915	230	63.00	43.36	617.0	429.5	16.1	25.50	0.4425
99.0	5000	917	227	55.00	44.50	599.0	428.5	16.7	33.80	0.4900
99.0	5000	919	222	44.00	43.70	551.0	427.8	18.7	37.00	0.4980
99.5	5000	915	231	64.00	45.37	618.0	430.0	16.0	25.00	0.3910
99.5	5000	917	228	56.00	44.60	600.0	429.0	16.5	23.60	0.4800
99.5	5000	919	223	43.00	43.80	556.0	428.0	18.6	36.00	0.4970

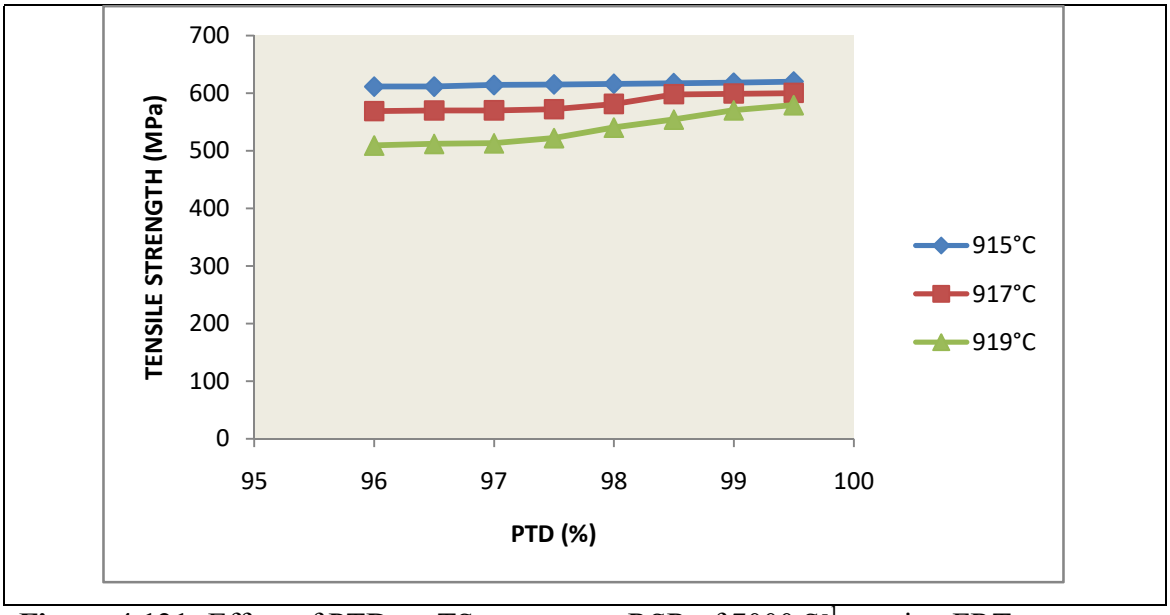

Figure 4.121: Effect of PTD on TS at constant RSR of 7000 S^{-1},varying FRT.

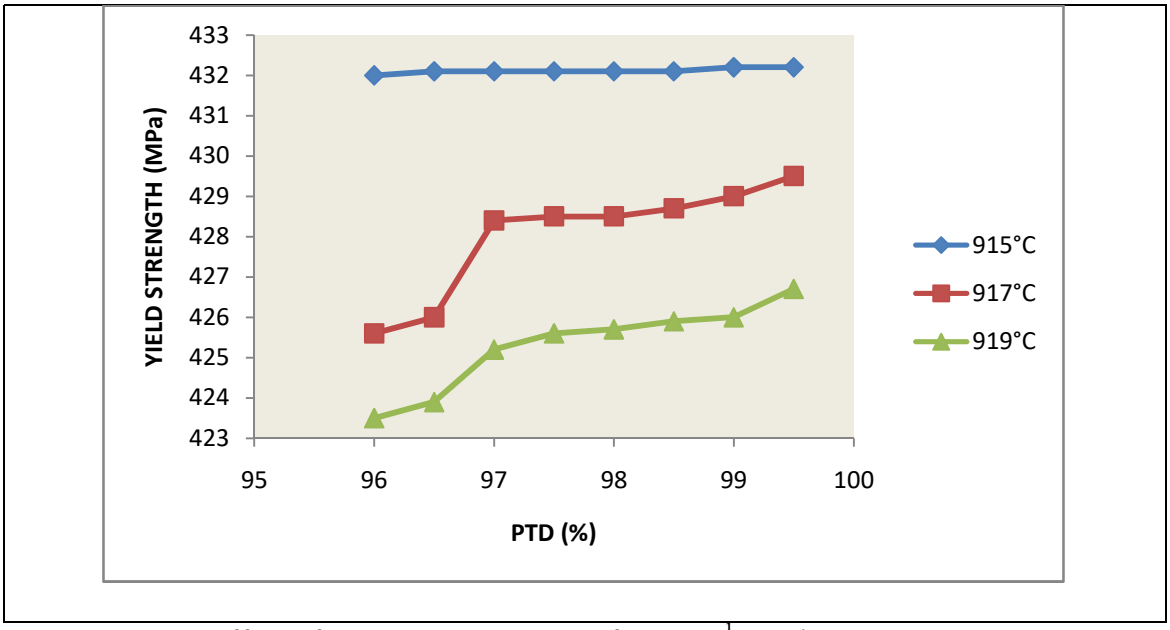

Figure 4.122: Effect of YS at constant RSR of 7000 S^{-1},varying FRT.

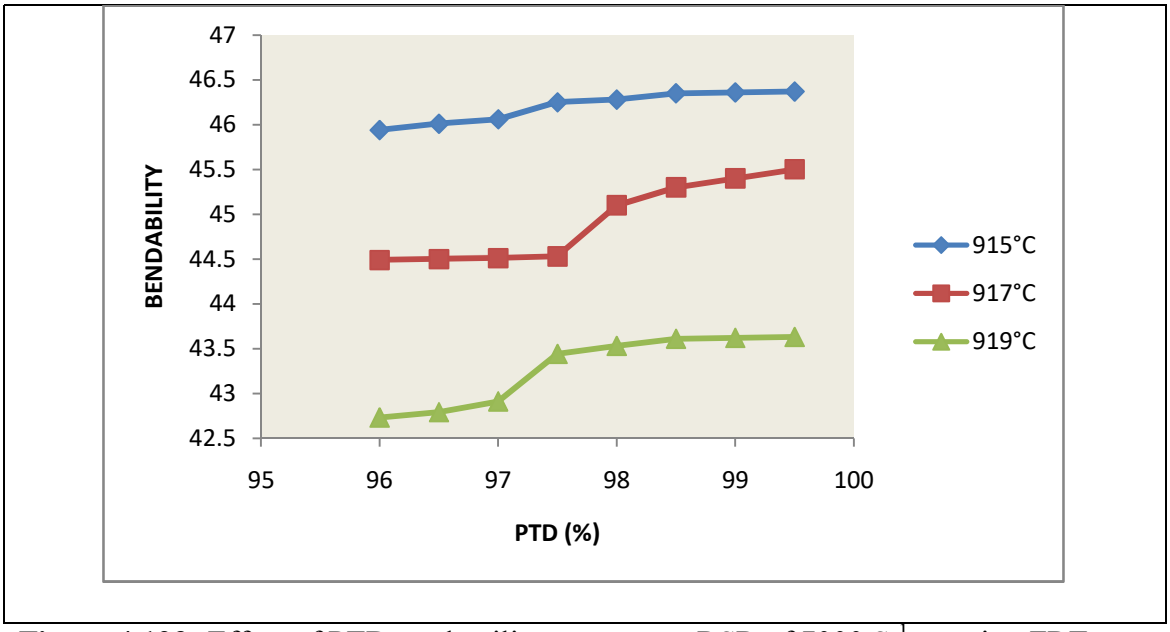

Figure 4.123: Effect of PTD on ductility at constant RSR of 7000 S^{-1}, varying FRT.

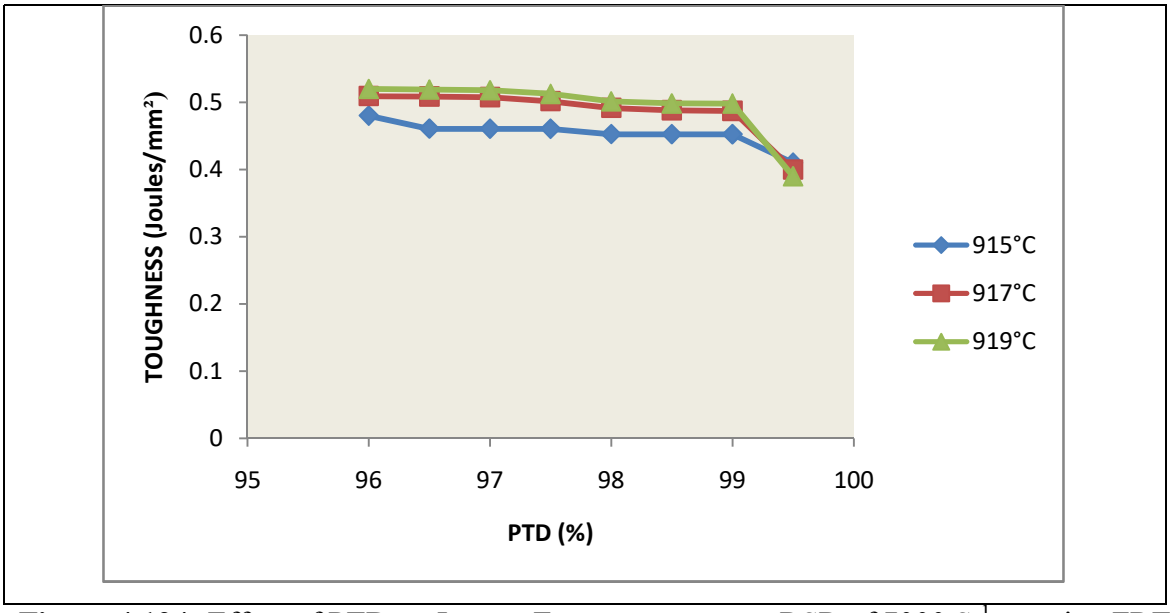

Figure 4.124: Effect of PTD on Impact Energy at constant RSR of 7000 S^{-1}, varying FRT.

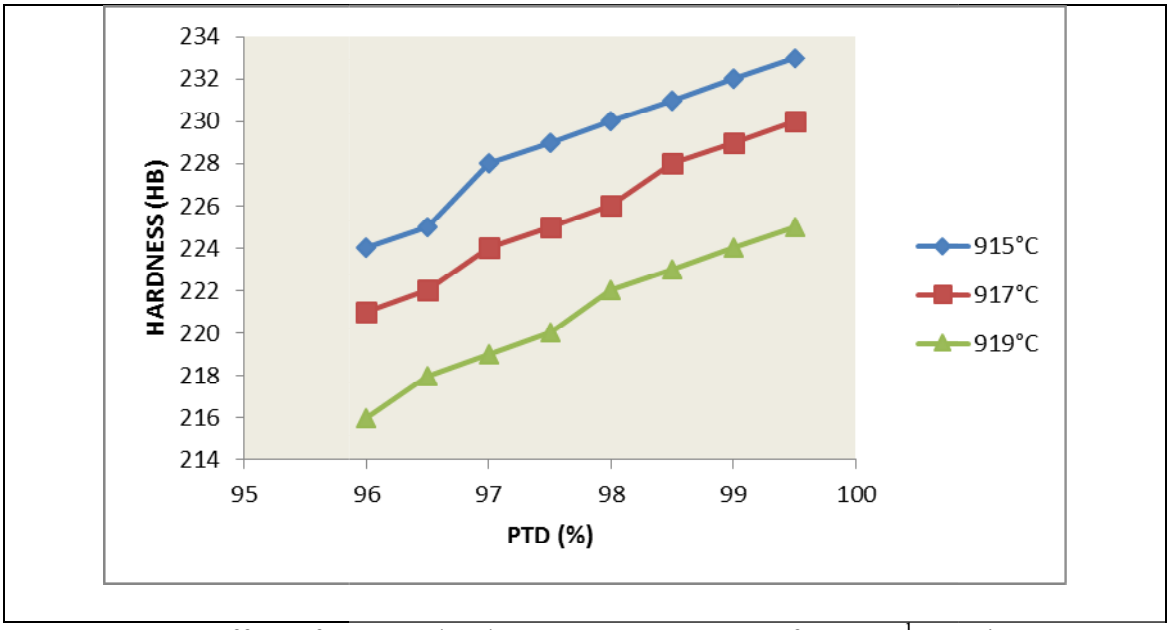

Figure 4.125: Effect of PTD on hardness at constant RSR of 7000 S^{-1}, varying FRT.

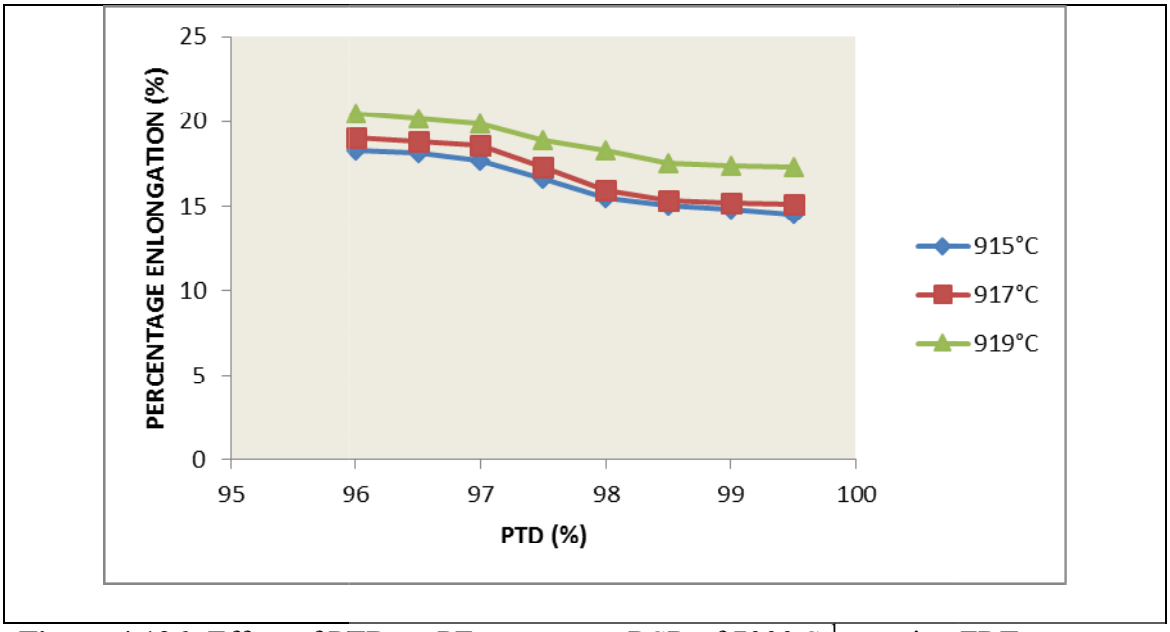

Figure 4.126: Effect of PTD on PE at constant RSR of 7000 S^{-1}, varying FRT.

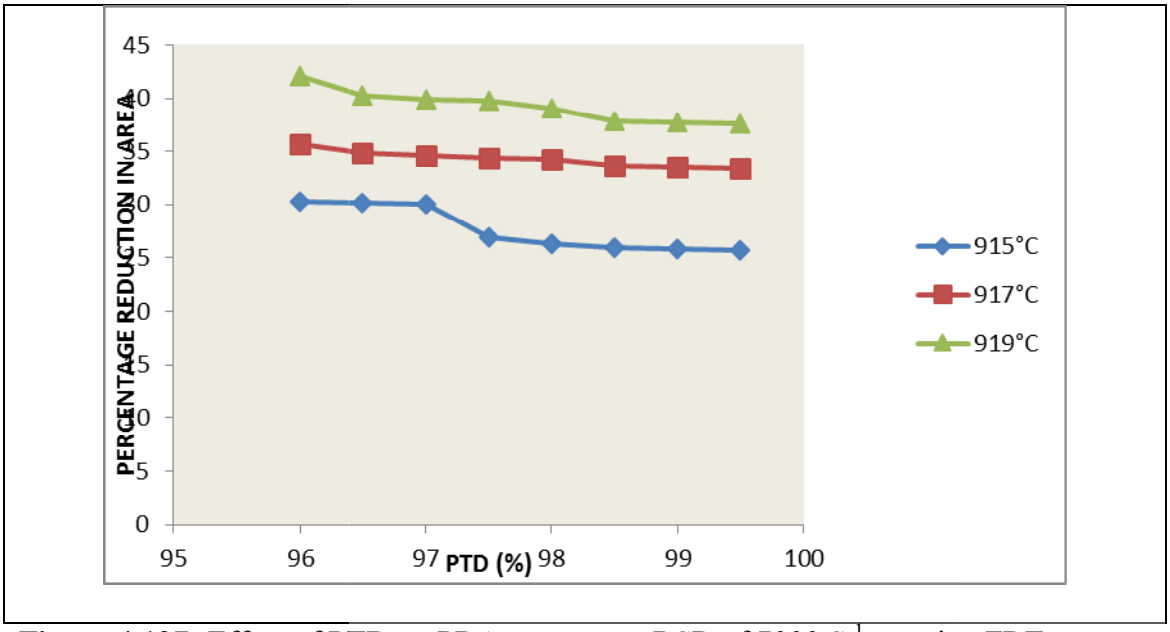

Figure 4.127: Effect of PTD on PRA at constant RSR of 7000 S^{-1}, varying FRT.

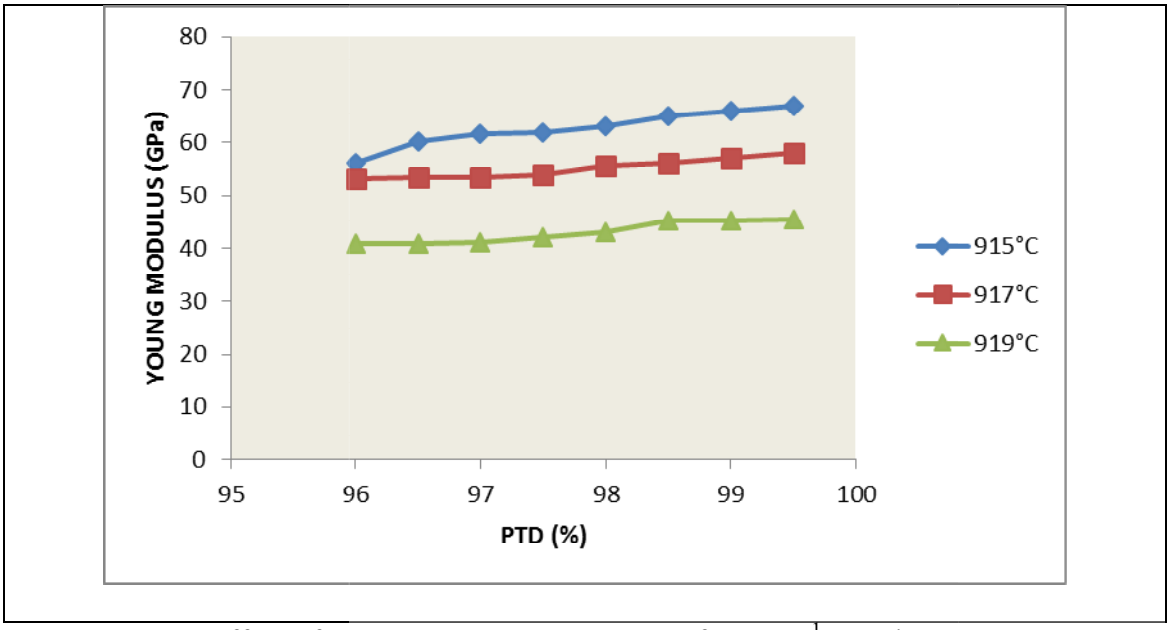

Figure 4.128: Effect of PTD on E at constant RSR of 7000 S^{-1}, varying FRT

4.17 Results and Discussions For Effects PTD at RSR of 6000 S^{-1}

Figures 4.129-4.136 show the effect of PTD on the tensile properties at RSR of 6000 S^{-1}, and varying FRT.

After the analysis of the tensile properties of the hot-rolled steel it may equally be reported that the tensile properties of the hot-rolled steel grade is substantially influenced by the PTD at 7000, 6000,5000 S^{-1} RSR. The TS, YS, hardness, E and ductility increased with increasing PTD, while the impact energy, PRA and PE decreased with increasing PTD for all the degrees of RSR and FRT observed.

From Figures 4.129 to 4.136 ,at 915°C FRT and 6000 per second RSR, when the PTD increased from 96.0 to 96.5 percent, the TS increased from 611 to 612 MPa (Fig.4.129), YS increased from 426 to 427 MPa (Fig.4.130), hardness increased from 223 to 224 HB (Fig.4.133), E increased from 55 to 60 GPa (Fig.4.136), ductility increased from 45.93 to 46.00° (Fig.4.131);while impact energy reduced from 0.4609 to 0.460 J/mm^2(Fig.4.132), PRA reduced from 30.5 to 30.3%(Fig.4.135), PE reduced from 18.4 to 18.3% (Fig.4.134). At 6000 S^{-1} RSR and 915°C FRT, as the PTD increased from 96.0 to 96.5 percent, the TSincreased from 568.7 to 569.6 MPa (Fig.4.129), YS increased from 425.6 to 426 MPa (Fig.4.130), hardness increased from 220 to 221 HB (Fig.4.133) E increased from 51.0 to52.2 GPa (Fig.4.136) and ductility increased from 44.38 to 44.40°(Fig.4.133); while impact energy reduced from 0.509 to 0.5089 J/mm^2 (Fig.4.132), PRA reduced from 36.7 to 34.9% (Fig.4.135) and PE reduced from 19.5 to 18.8% (Fig.4.134). At 5000 S^{-1} RSR and 915^{0}C FRT, as the PTD increased from 96.0 to 96.5 percent ,TS increased from 509 to 512 MPa (Fig.4.129), YS increased from 423.5 to 423.9 MPa (Fig.4.130), hardnessincreased from 215 to 217 HB (Fig.4.133), E increased from 41 to 40.9GPa (Fig.4.136), ductility increased from 42.73 to 42.79° (Fig.4.131);while impact energy reduced from 0.5196 to 0.5188 J/mm^2(Fig.4.132), PRA reduced from 43 to 41.3% (Fig.4.135). PE reduced from 21 to 20.8%(Fig.4.134).

The effects of PTD on the rolled stock was very pronounced as the PTD increases,the TS, YS, hardness, E, and ductility of the hot-rolled samples increase; while the impact energy, PRA and PE decrease. The workingof the billets within the stands gave rise to increased yielding and increased number of displaced components were transferred to the

final hot-rolled rebar. The strengthening obtained came from smoothening of the microstructure of the austenites and displacement of layers of cementite by spheroidal particles.

This yielding was due to displacement movement stopped by many stoppages like solidification of another components and this gave rise to increase in TS, YS, hardness, E and ductility. Impact energy, PRA and PE also decreased

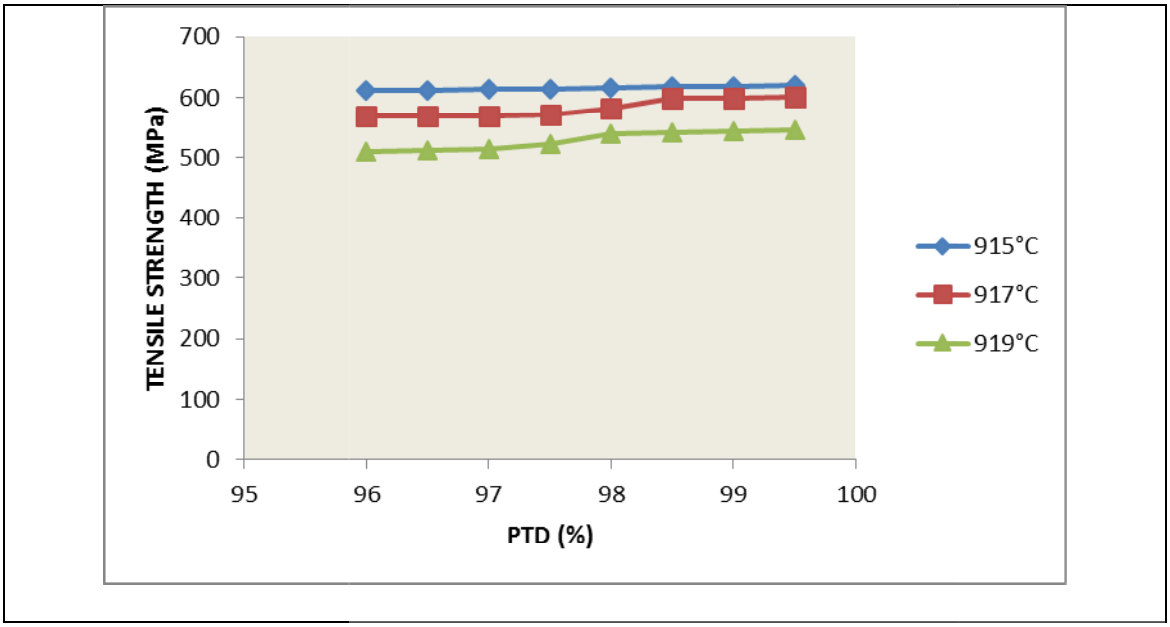

Figure 4.129: Effect of PTD on TS at a constant RSR of 6000 S^{-1}, varying FRT.

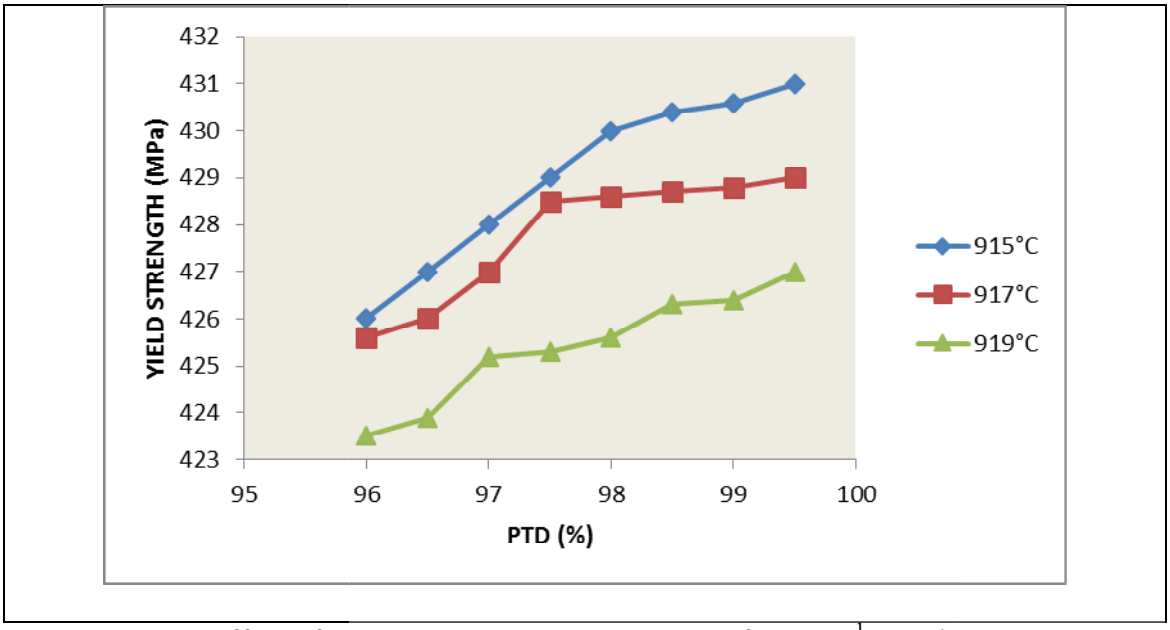

Figure 4.130: Effect of PTD on YS at a constant RSR of 6000 S^{-1}, varying FRT.

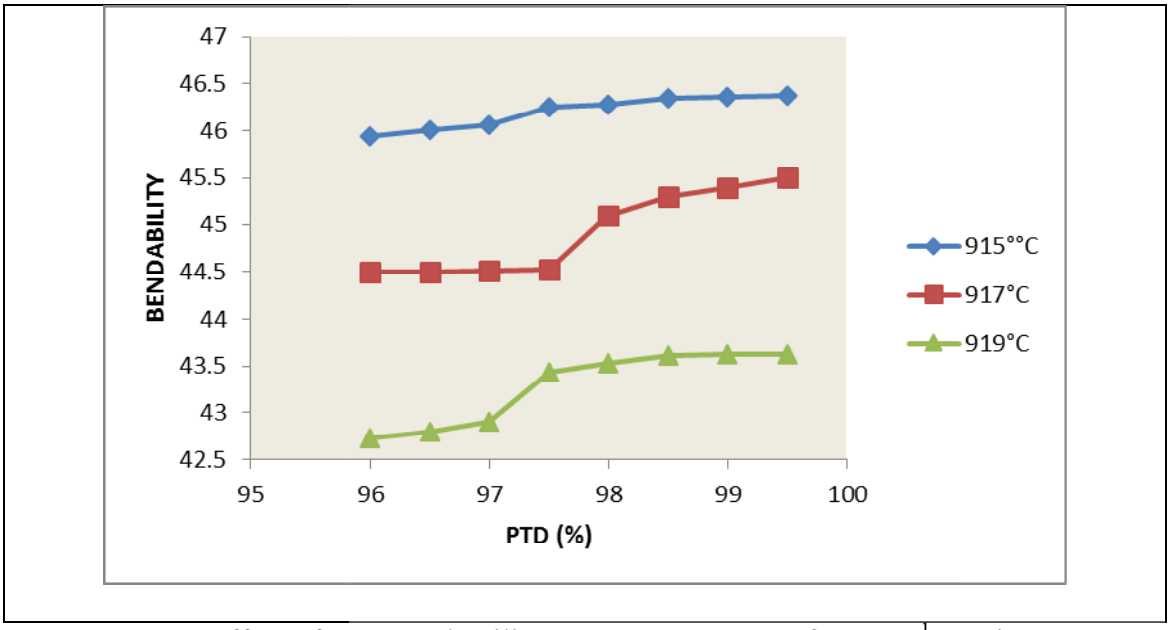

Figure 4.131: Effect of PTD on ductility at a constant RSR of 6000 S^{-1},varying FRT.

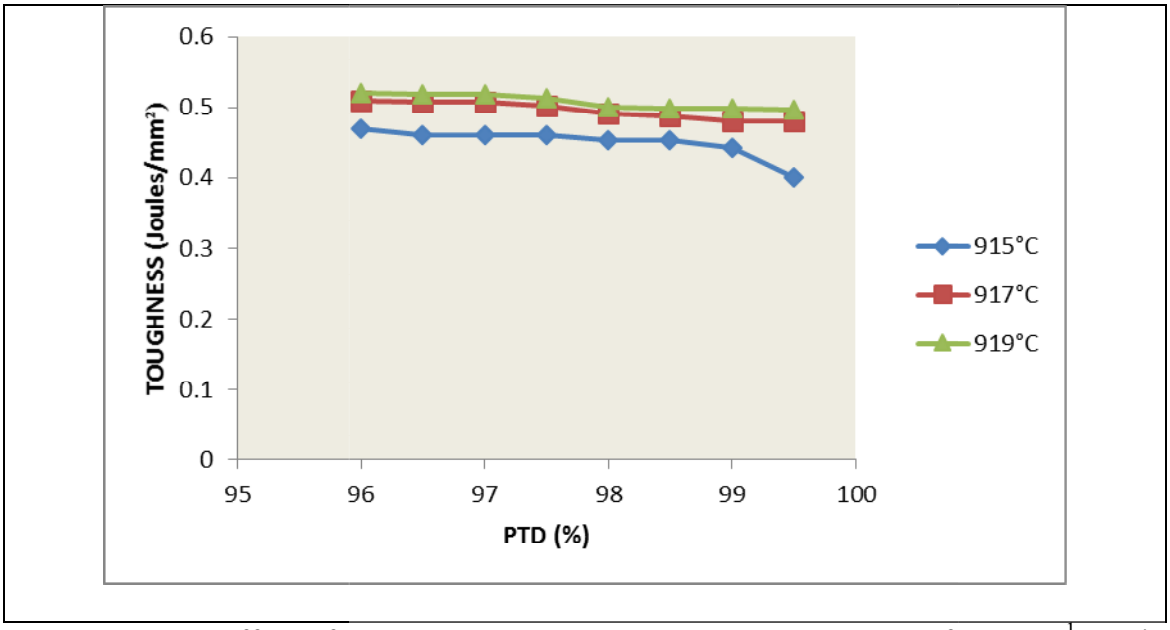

Figure 4.132: Effect of PTD on Impact Energy at a constant RSR of 6000 S^{-1},varying FRT.

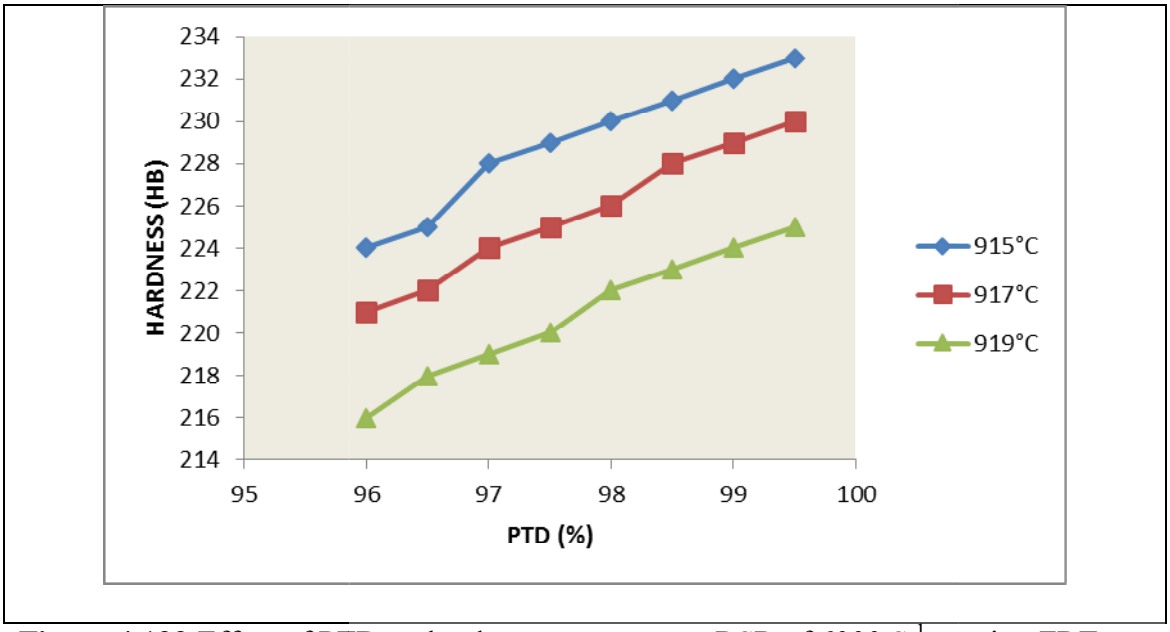

Figure 4.133:Effect of PTD on hardness at a constant RSR of 6000 S^{-1},varying FRT.

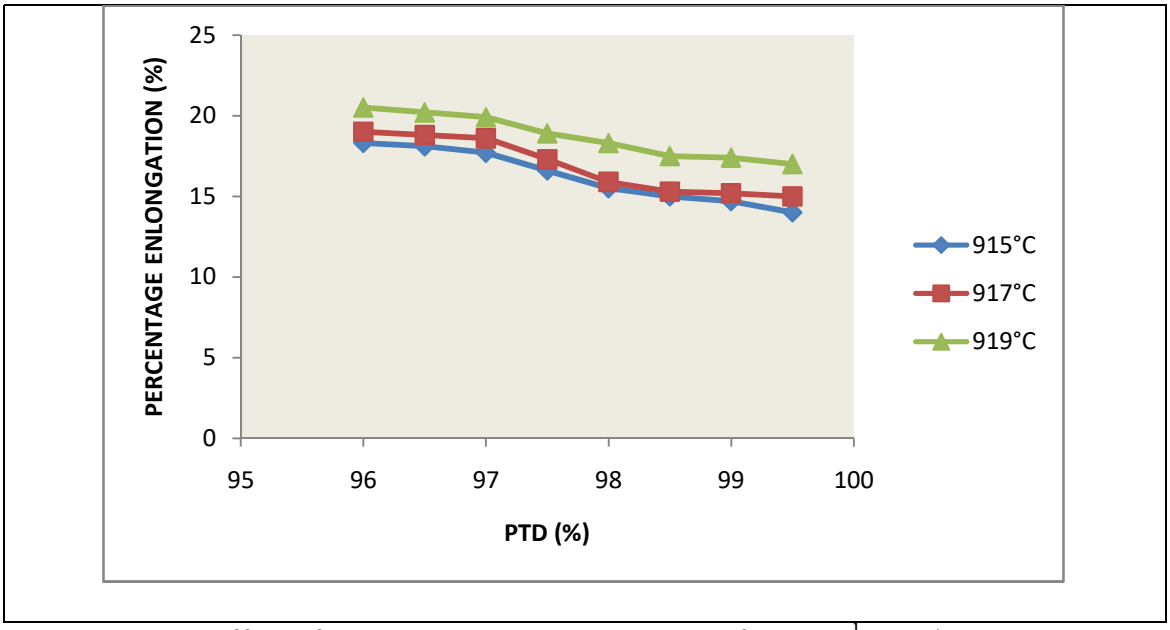

Figure 4.134: Effect of PTD on PE at a constant RSR of 6000 S^{-1}, varying FRT.

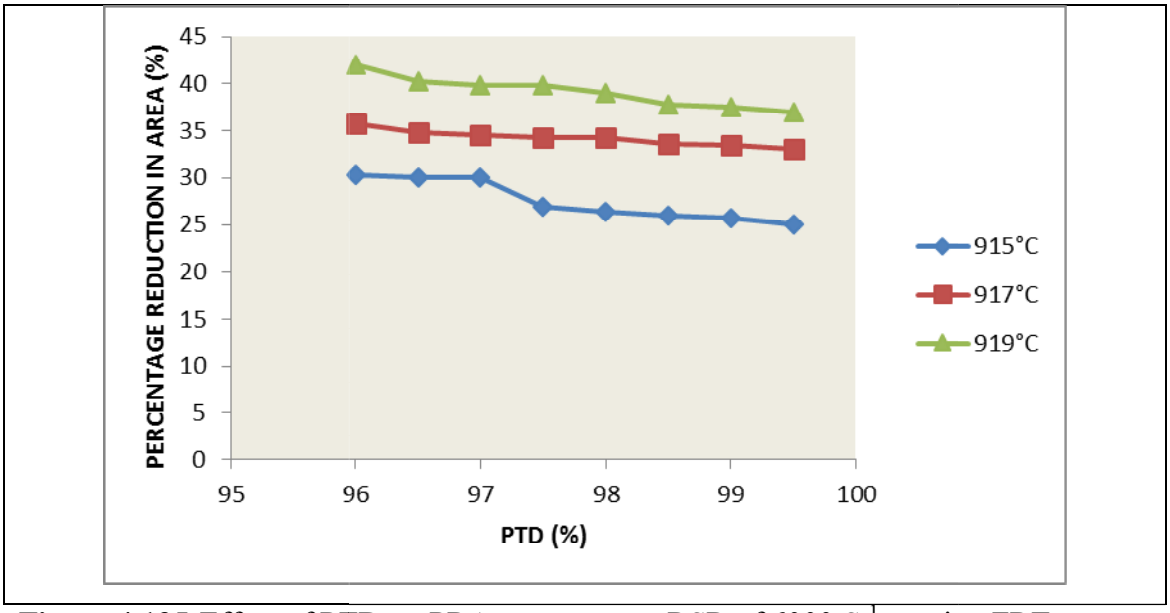

Figure 4.135: Effect of PTD on PRA at a constant RSR of 6000 S^{-1},varying FRT.

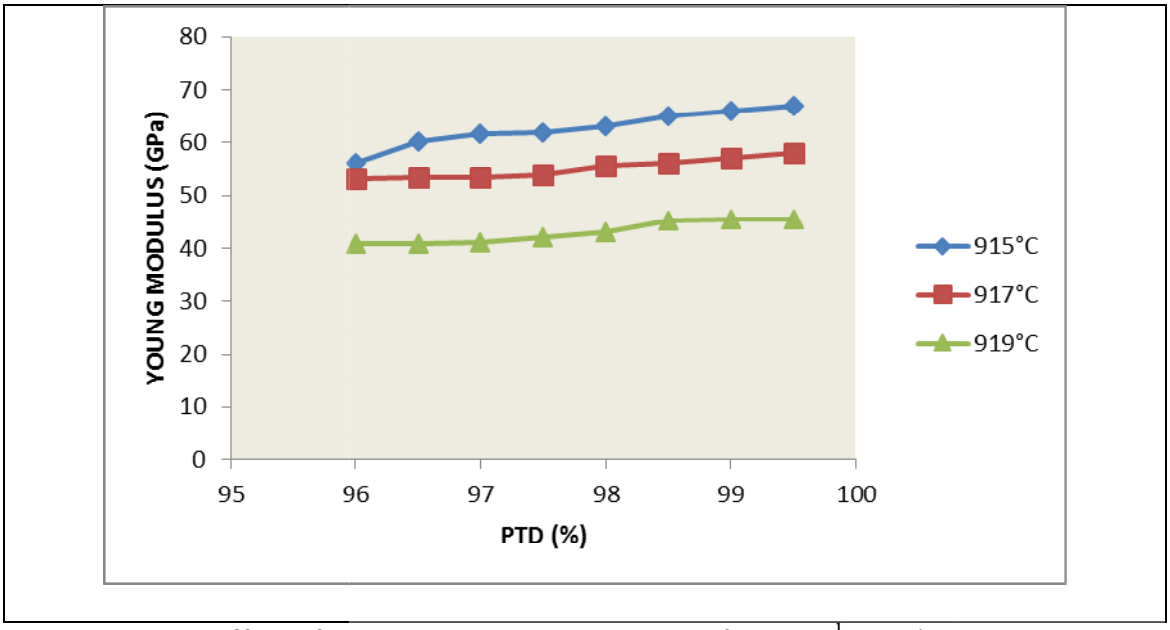

Figure 4.136: Effect of PTD on E at a constant RSR of 6000 S^{-1}, varying FRT

4.18 Results and Discussions For Effects of PTD at RSR of 5000 S^{-1}

Figures 4.137-4.144 show the effect of PTD on the tensile properties at a PTD of 96.0 percent and varying RSR.

After the analysis of the tensile properties of the hot-rolled steel, tensile properties of the hot-rolled St60Mn steel is substantially influenced by the PTD at 7000, 6000, 5000 S^{-1} RSR. The TS, YS, hardness, E and ductility increased with increasing PTD, while the impact energy, PRA and PE decreased with increasing PTD for all the degrees of RSR and FRT observed.

From Figures 4.137 to 4.144 ,at 915°C and RSR of 5000 S^{-1} , when the PTD increased from 96.0 to 96.5 percent ,the TS increased from 610 to 612 MPa (Fig.4.137), YS increased from 425 to 426 MPa (Fig.4.138), hardness increased from 222 to 223 HB (Fig.4.141), E increased from 54 to 56 GPa (Fig.4.120), ductility increased from 45.92 to 45.00°(Fig.4.139);while impact energy reduced from 0.4635 to 0.4626 J/mm^2 (Fig.4.140), PRA reduced from 30.8 to 30.5%(Fig.4.143), PE reduced from 19.8 to 19.4%(Fig.4.142). At 917°C FRT and 5000 S^{-1} RSR, as the PTD increased from 96.0 to 96.5 percent ,the TSincreased from 566 to 567.5 MPa (Fig.4.137), YS increased from 423 to 424 MPa (Fig.4.138), hardness increased from 219 to 220 HB (Fig.4.141),E increased from 50 to50.1GPa (Fig.4.144) and ductility increased from 43.38 to 43.40°(Fig.4.139);while impact energy reduced from 0.5099 to 0.5191 J/mm^2 (Fig.4.140), PRA reduced from 36.9 to 35.9% (Fig.4.143) and PE reduced from 20.8 to 19.8%(Fig.4.143). At 919°C FRT and 5000 S^{-1} RSR, as the PTD increased from 96.0 to 96.5 percent, TS increased from 506 to 509 MPa (Fig.4.137), YS increased from 423 to 422 MPa (Fig.4.138), hardness increased from 214 to 216 HB (Fig.4.141), E increased from 45 to 39.9 GPa (Fig.4.144), ductility increased from 42.70 to 42.78°(Fig.4.139); while impact energy reduced from 0.519 to 0.519 J/mm^2 (Fig.4.116), PRA reduced from 39.87 to 42.6% (Fig.4.119). PE reduced from 21.9 to 20.9%(Fig.4.102).

The effects of PTD on the rolled stock was very pronouncedas the PTD increases,the TS, YS, hardness, E and ductility of the hot-rolled samples increase; while the impact energy, PRA and PE decrease. The workingof the billets within the stands gave rise to increased yielding and increased number of displaced components were transferred to the

final hot-rolled rebar. The strengthening obtained came from smoothening of the microstructure of the austenites and displacement of layers of cementite by spheroidal particles.

This yielding was due to displacement movement stopped by many stoppages like solidification of another components and this gave rise to increase in TS, YS, hardness, E and ductility. Impact energy, PRA and PE also decreased

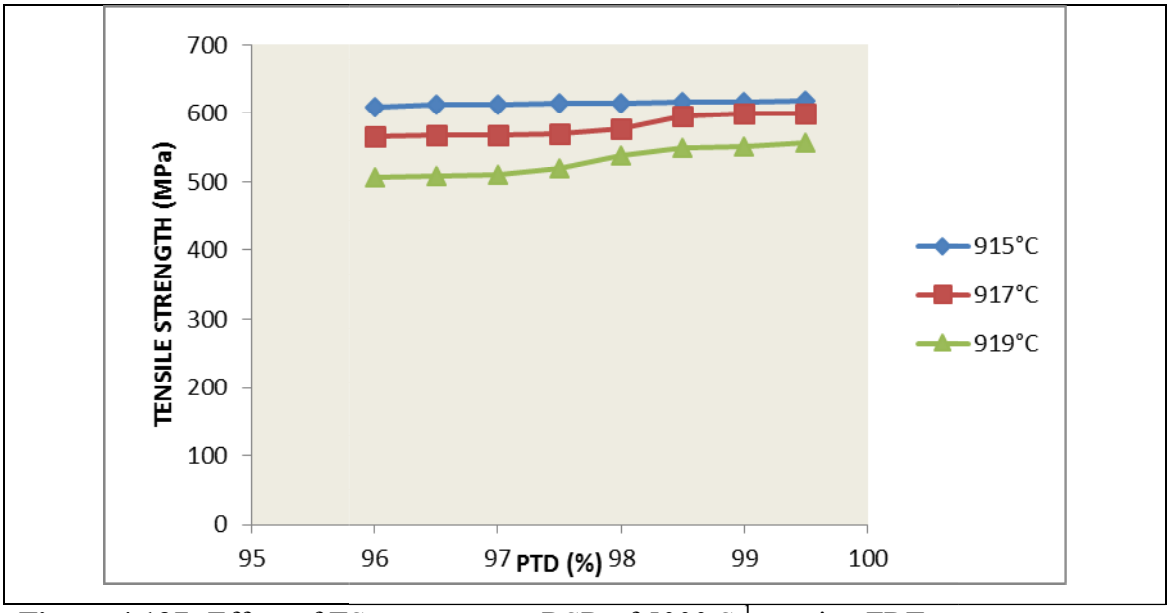

Figure 4.137: Effect of TS at a constant RSR of 5000 S^{-1},varying FRT.

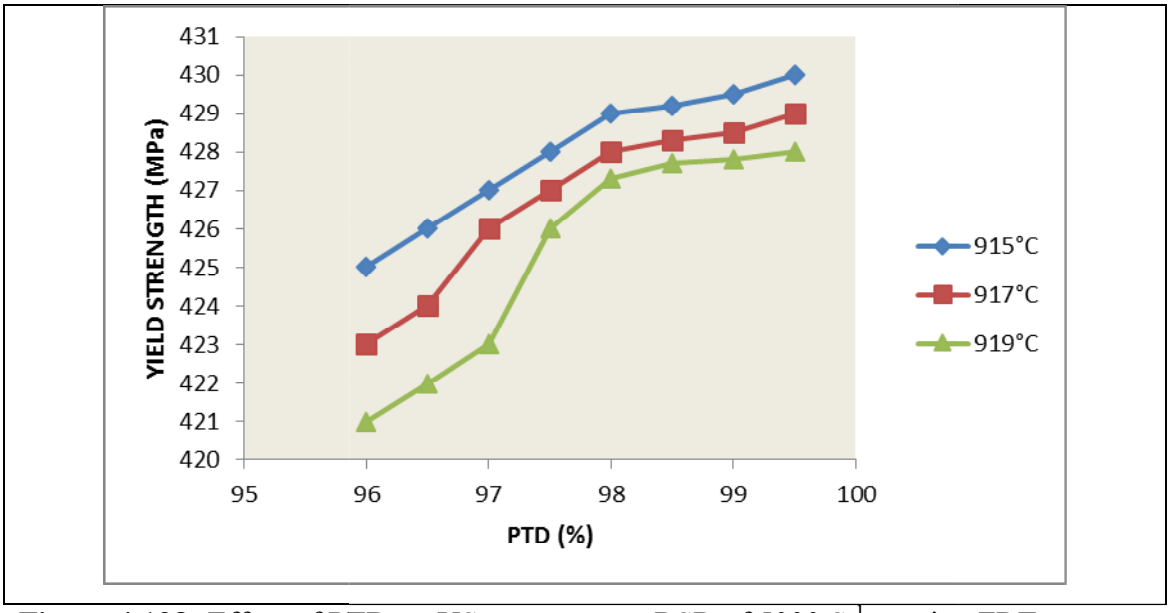

Figure 4.138: Effect of PTD on YS at a constant RSR of 5000 S^{-1},varying FRT.

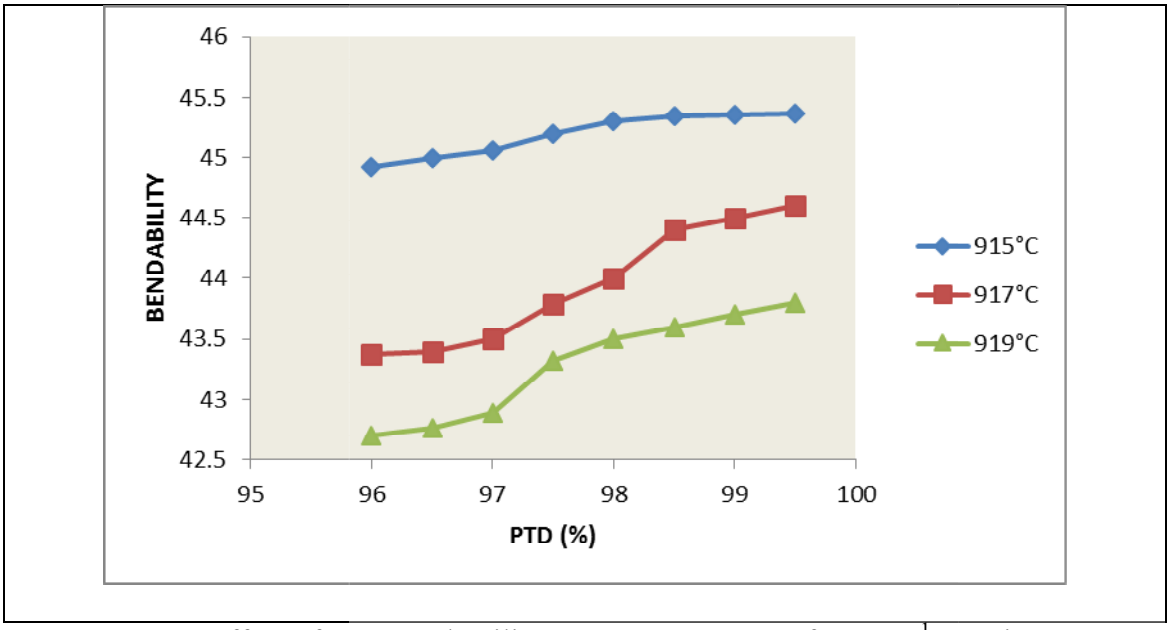

Figure 4.139: Effect of PTD on ductility at a constant RSR of 5000 S^{-1}, varying FRT.

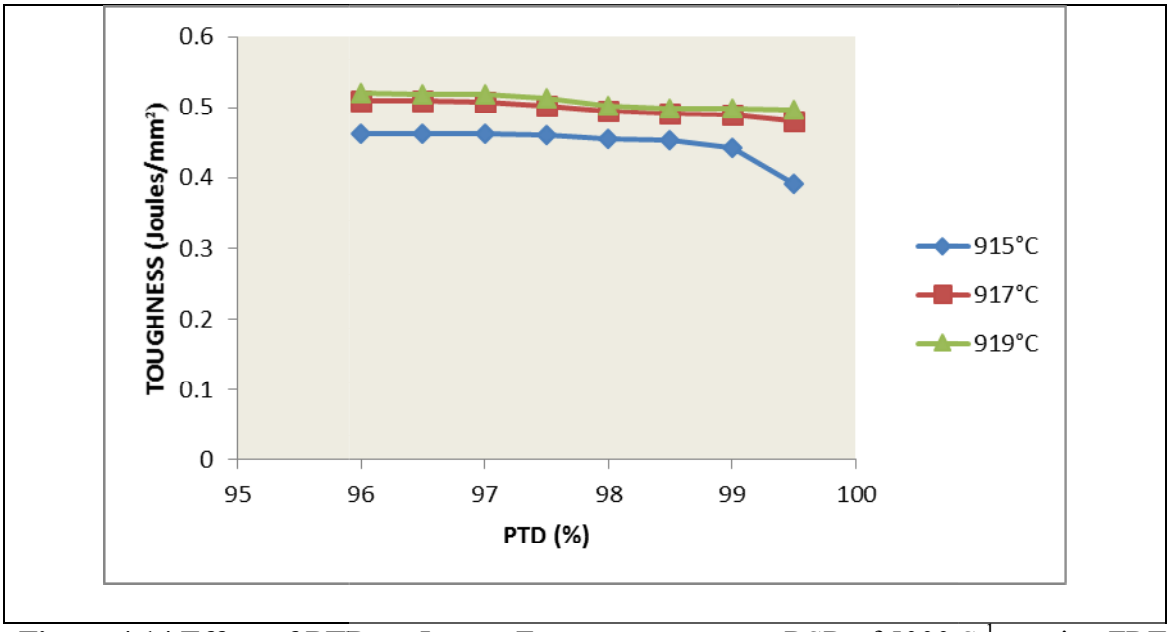

Figure 4.14 Effect of PTD on Impact Energy at a constant RSR of 5000 S^{-1},varying FRT.

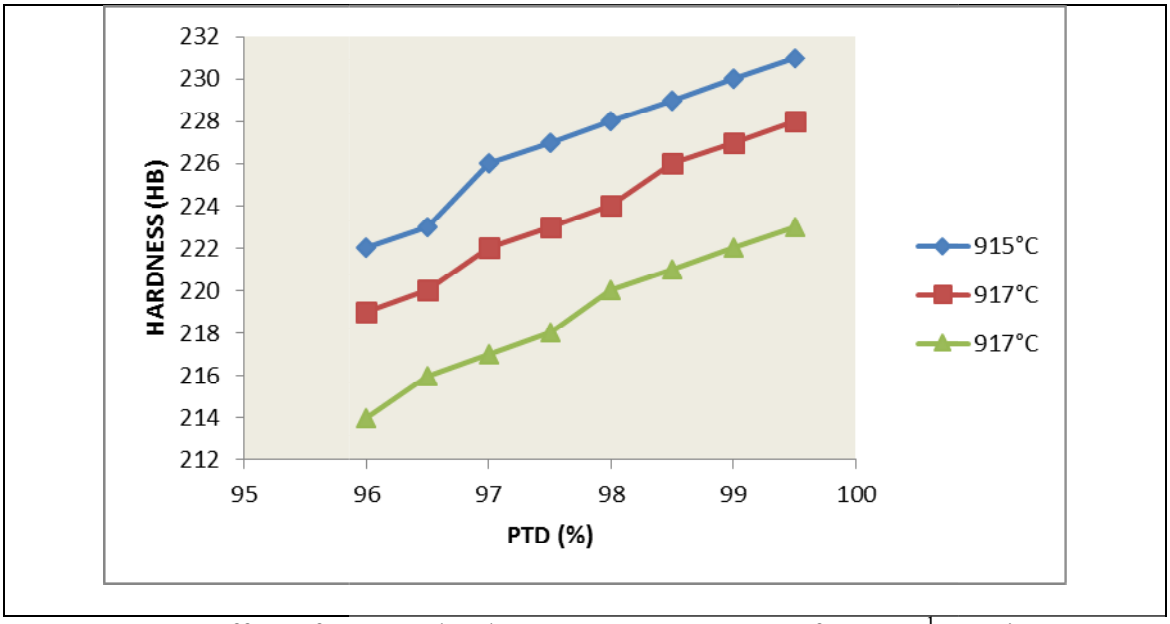

Figure 4.141: Effect of PTD on hardness at a constant RSR of 5000 $S^{-1,}$ varying FRT.

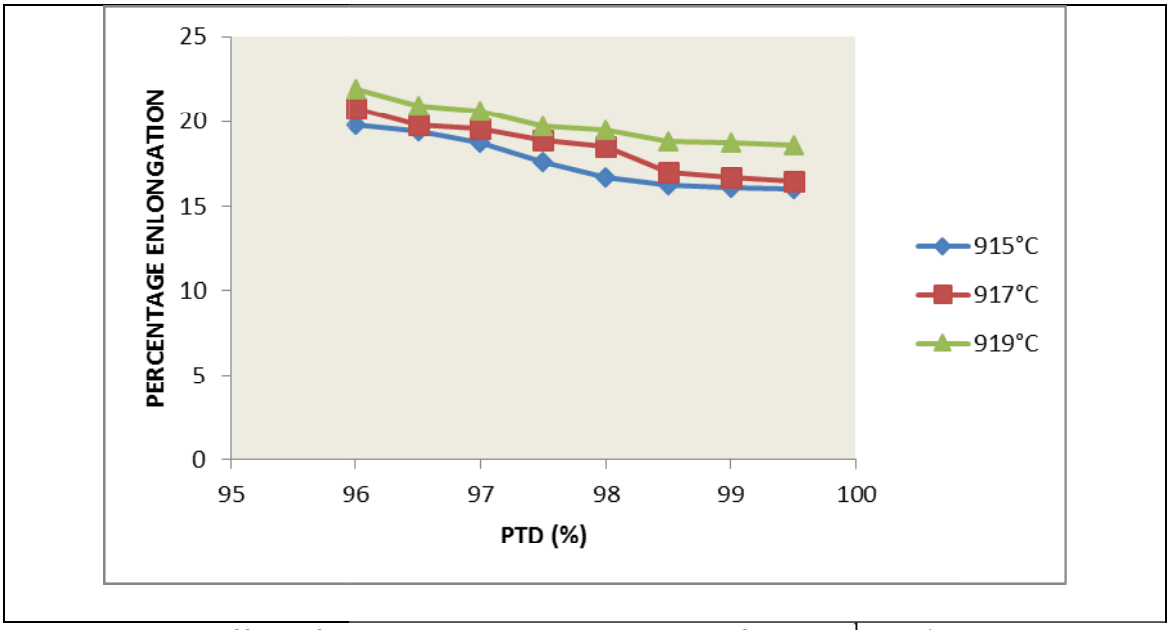

Figure 4.142: Effect of PTD on PE at a constant RSR of 5000 S^{-1},varying FRT

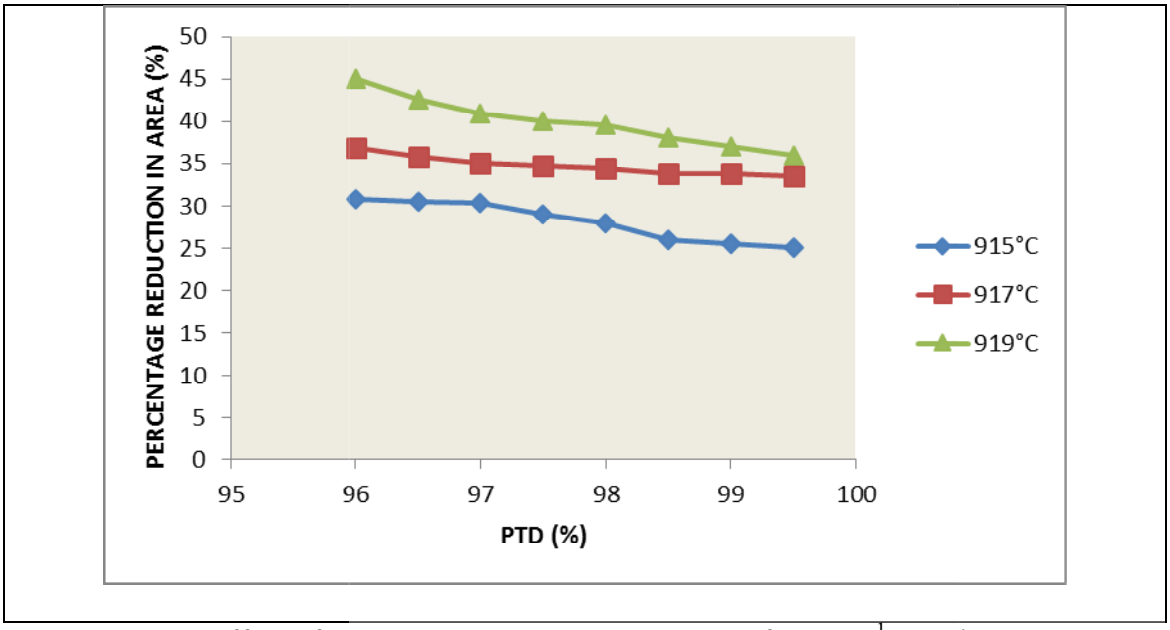

Figure 4.143: Effect of PTD on PRA at a constant RSR of 5000 S^{-1}, varying FRT.

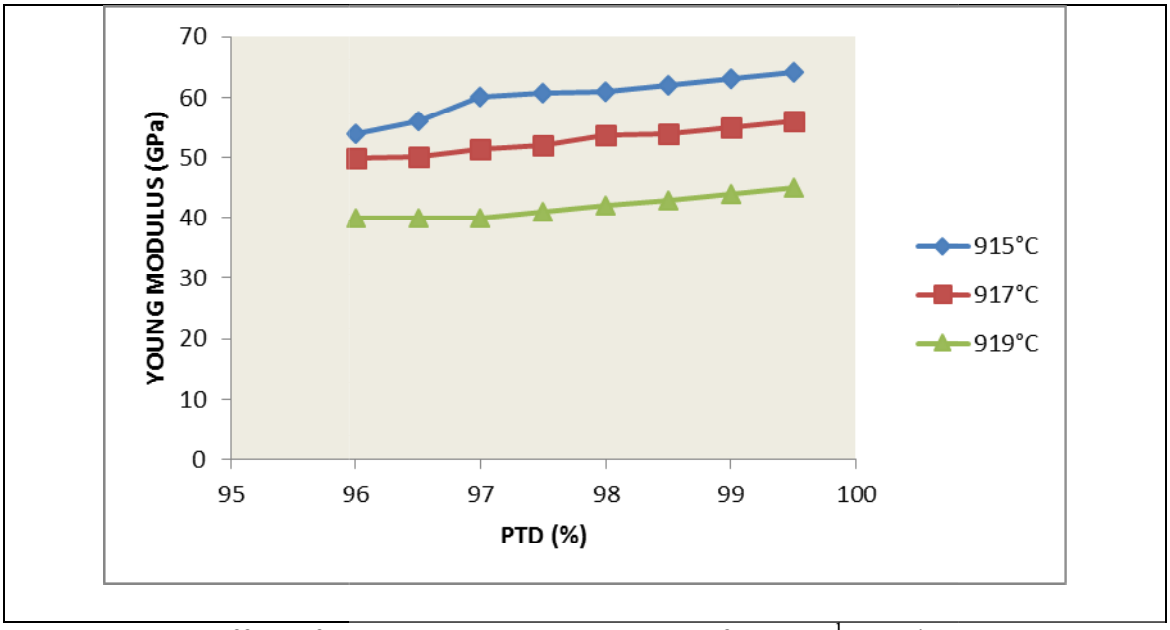

Figure 4.144: Effect of PTD on E at a constant RSR of 5000 S^{-1}, varying FRT.

4.19 Results and Discussions For Optical Microstructures

The evolved optical microstructuresof the steel grade at variable hot-rolling process parameters are shown in Figure 4.145(a-x) .

Samples a, b, c, d, e, f, g, h and i were observed at variable RSR of 4000, 4500, 5000, 5500, 6000, 6500, 7000,7500 and 4000 S^{-1}.

Samples j, k, l, m, n, o, o, p, q and r were observed at variable PTD of 96.0, 96.5, 97.0, 97.5, 98.0, 98.5, 99.0, 99.5 percent

Samples s, t, u, v, w, and x were observed at variable FRT of 915, 917, 919, 921, 925 and 929 ^{o}C..

Fairly fine grains were observed for samples a,b, c, d, e, f, g, h, and I; except in some cases where darker grains were seen. Sample d and I have the finest grains.

The observed trend in the microstructure shows that there was effective deformation of the hot-rolled billet during hot-rolling .The darker microstructures may be attributed to impurities like slag inclusions and other impurities in the body of the billet which might have been dispersed throughout the body of the steel during plastic deformation in the rolls..

More number of finer grains were observed among the samples hot-rolled at variable PTD.

The samples hot-rolled at variable FRT were darker than those processed at RSR and PTD. Finer grains were observed at RSR and PTD than at FRT.

Further work will be carried out on phase constituents of the micrographs later.

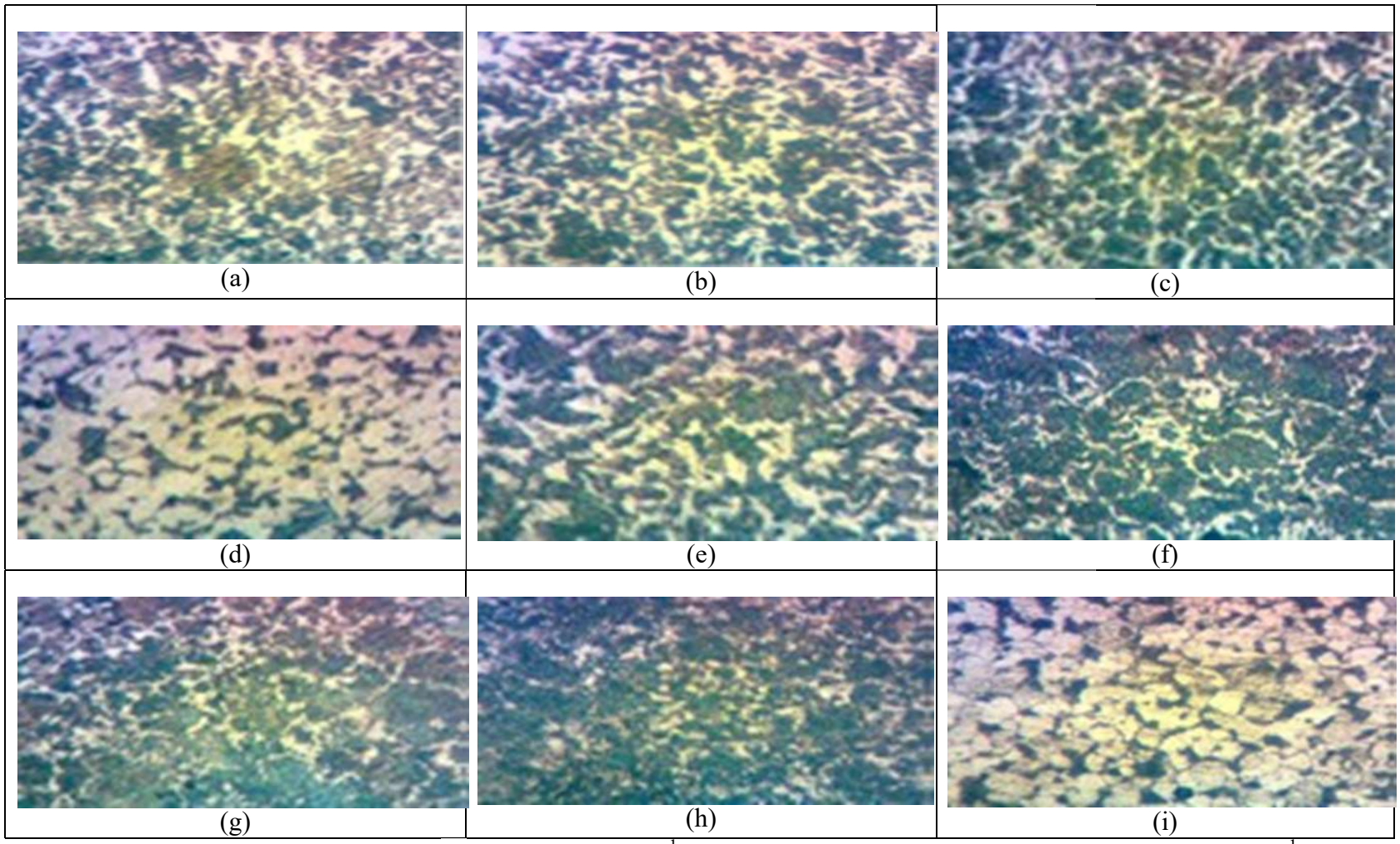

Figure 4.145: Optical Microstructure for (a) RSR of 4000 S^{-1}, FRT of 915°C, PTD of 99.0 percent (b) RSR of 4500 S^{-1},FRT of 915°C,PTD of 99.0 percent. (c) RSR of 5000 S^{-1},FRT of 915°C, PTD of 99.0 percent (d) RSR of 5500 S^{-1},FRT of 915°C,PTD of 99.0 percent. (e) RSR of 6000 S^{-1},FRT of 915°C, PTD of 99.0 percent(f) RSR of 6500 S^{-1},FRT of 915°C,PTD of 99.0 percent (g) RSR of 7000 S^{-1},FRT of 915°C, PTD of 99.0 percent (h) RSR of 7500 S^{-1},FRT of 915°C, PTD of 99.0 percent, (i) RSR of 4000 S^{-1},FRT of 917°C,PTD of 99.0 percent..

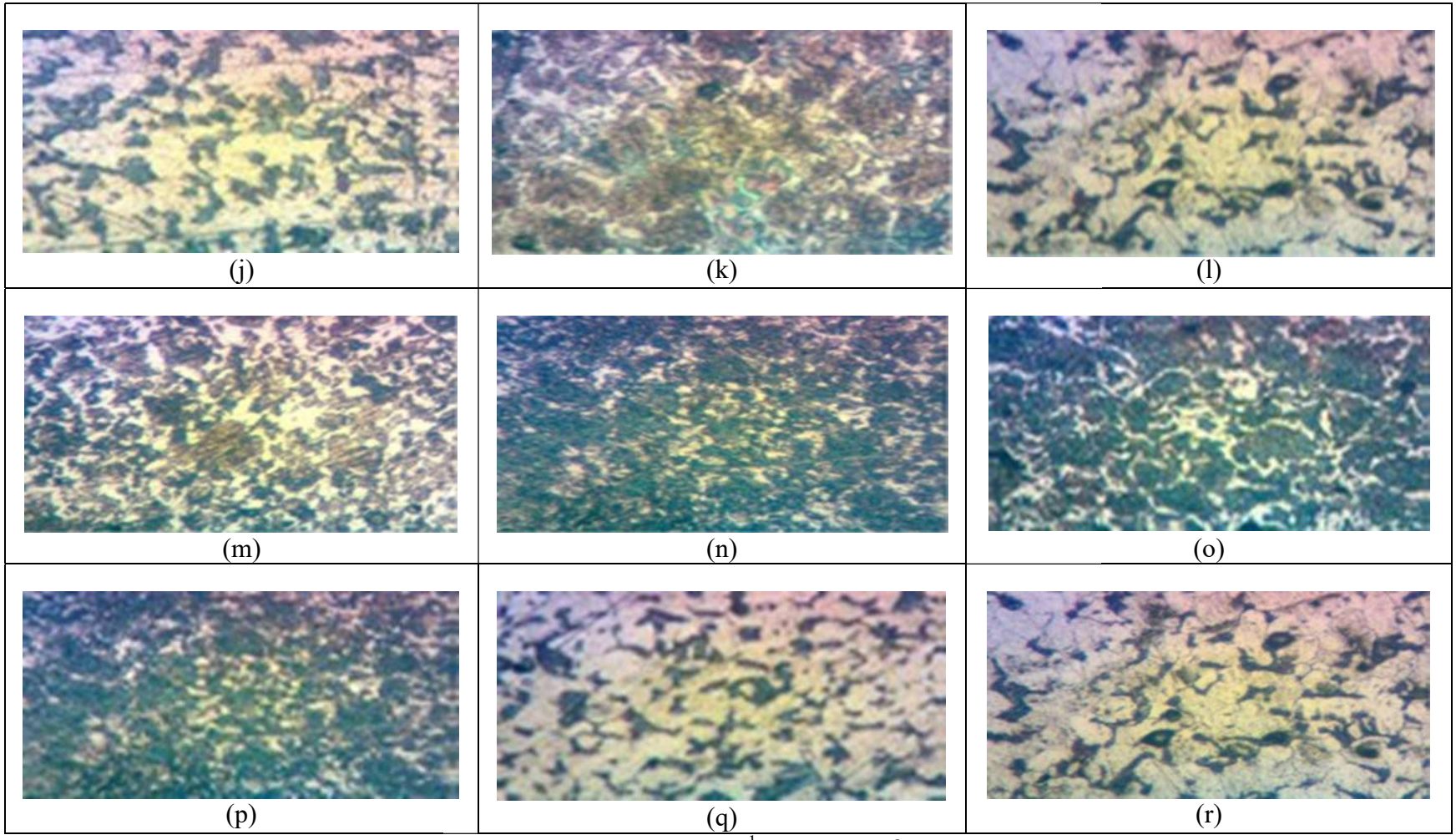

Figure 4.145 continued: Optical Microstructure(j) RSR of 7000 S^{-1},FRT of 915ºC, PTD of 96.0 percent, (k) RSR of 7000 S^{-1},FRT of 915ºC, PTD of 96.5 percent (l) RSR of 7000 S^{-1},FRT of 915ºC, PTD of 97.0 percent (m) RSR of 7000 S^{-1},FRT of 915ºC, PTD of 97.5 percent (n) RSR of 7000 S^{-1},FRT of 915ºC, PTD of 98.0 percent (o) RSR of 7000 S^{-1},FRT of 915ºC, PTD of 98.5 percent (p) RSR of 7000 S^{-1},FRT of 915ºC, PTD of 99.0 percent (q) RSR of 7000 S^{-1},FRT of 915ºC,PTD of 99.5 percent (r) RSR of 7000 S^{-1},FRT of 917ºC,PTD of 96.0 percent.

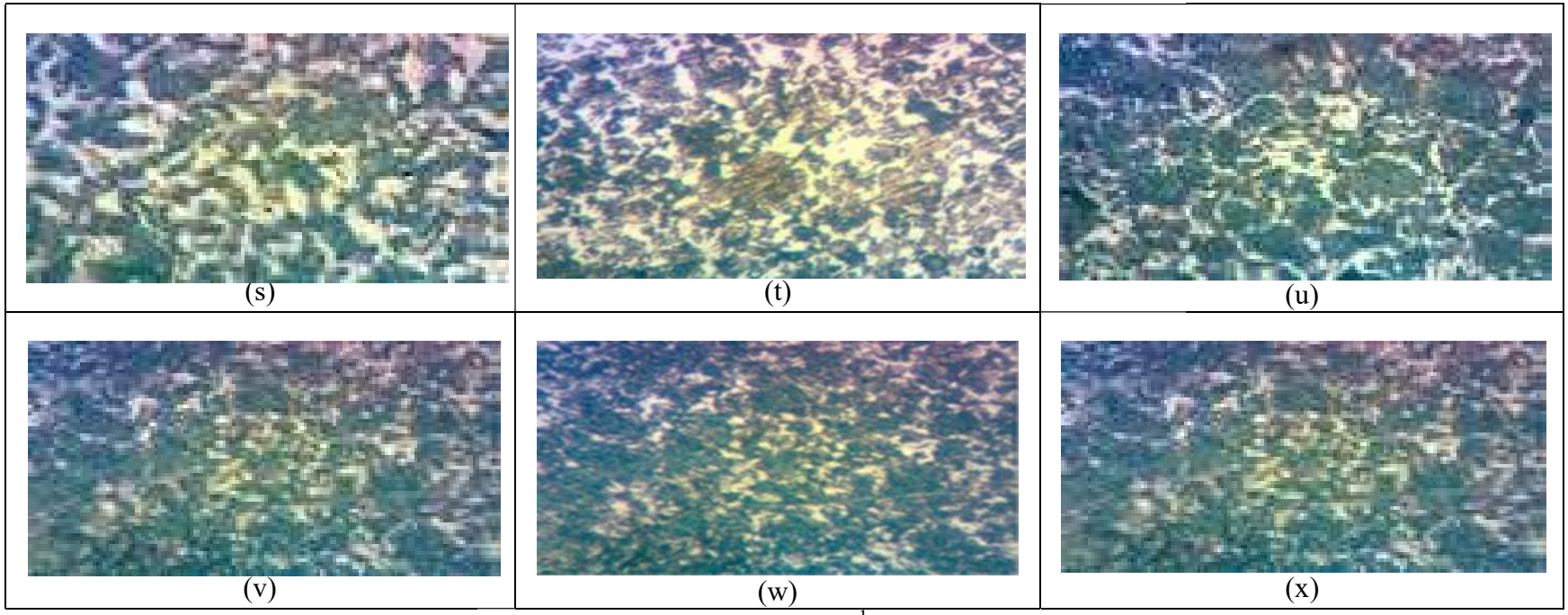

Figure 4.145 continued: Optical Microstructure for (r) RSR of 7000 S^{-1},FRT of 915°C, PTD of 99.0 percent (s) RSR of 7000 S^{-1},FRT of 917°C,PTD of 99.0 percent (t) RSR of 7000 S^{-1},FRT of 919°C, PTD of 99.0 percent (u) RSR of 7000 S^{-1},FRT of 921°C,PTD of 99.0 percent(v) RSR of 7000 S^{-1},FRT of 925°C,PTD of 99.0 percent (w) RSR of 7000 S^{-1},FRT of 929°C, PTD of 99.0 percent.

4.20 Results and Discussions For The 3D Views of The Microstructures

The 3D views of the microstructures of the hot-rolled samples of thesteel grade were also shown in Figures 4.146a-n .

Samples a, b, c, d, e, and f were observed at variable RSR of 4000, 4500, 5000, 5500 , 6000 and 6500 S^{-1}

Samples g, h, I, j, k, l, m and n were observed at variable PTD of 96.0, 96.5, 97.0, 97.5, 98.0, 98.5 and 99.0 percent.

The x, y and z axes of the hot-rolled samples were observed in terms of their sizes. There are fairly equal sizes of all the observed samples,except in few cases where there is slight variation ; especially in y and z axes.

The x axes of all the observed samples were virtually the same.The x-axis of all the observed samples have a constant value of 100μm.

This has shown that the optical microstructures were of equal sizes and therefore were able to give the best results.

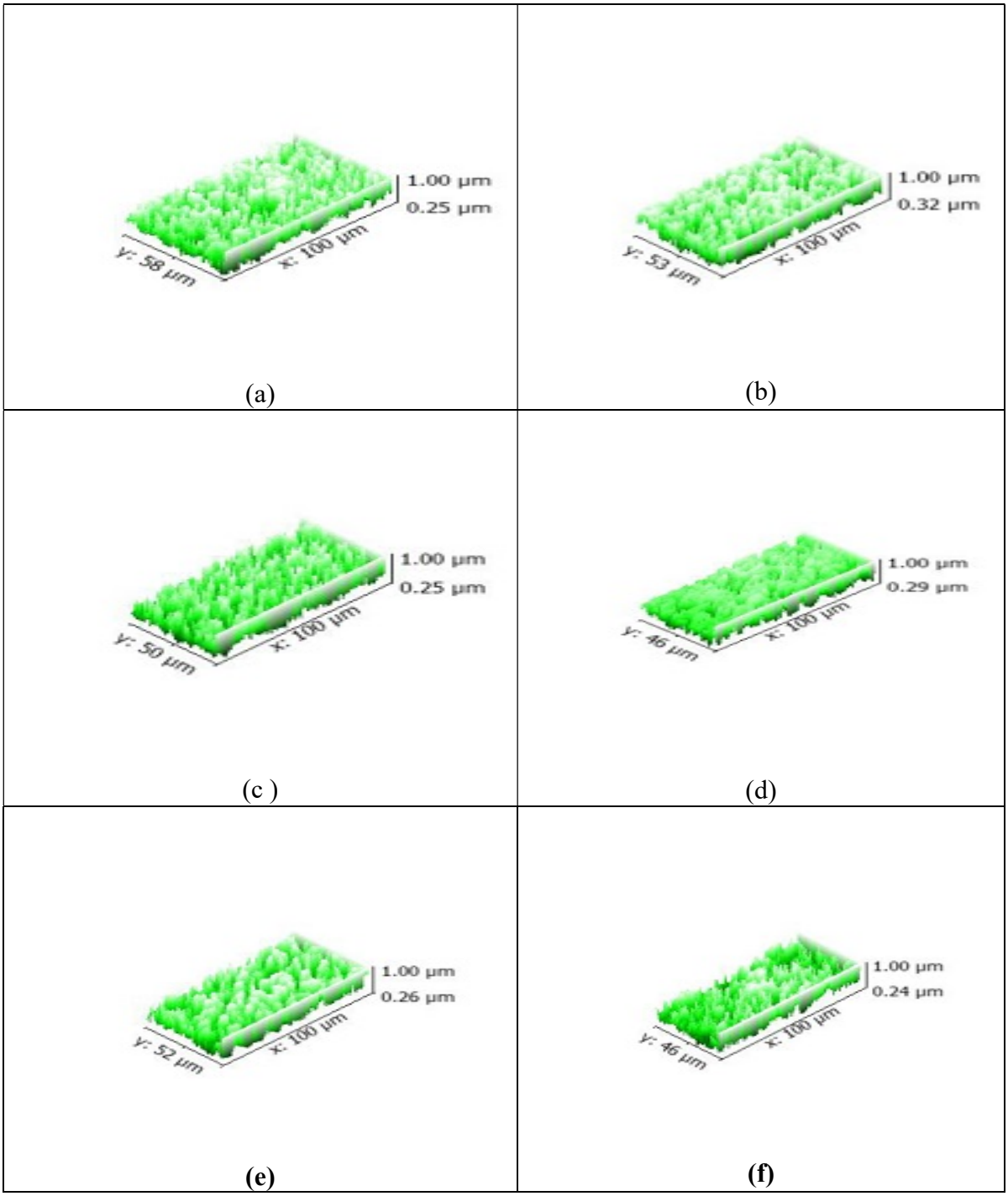

Figure 4.146:3D Views of Microstructure for (a) RSR of 4000 per second, FRT of 915 Degrees Celsius, PTD of 99.0 percent (b) RSR of 4500 S^{-1},FRT of 915°C, PTD of 99.0 percent (c) RSR of 4500 S^{-1},FRT of 915°C, PTD of 99.0 percent (d) RSR of 5000 S^{-1},FRT of 915°C, PTD of 99.0 percent (e) RSR of 5500 S^{-1},FRT of 915°C, PTD of 99.0 percent (f) RSR of 6000 S^{-1},FRT of 915 °C,PTD of 99.0 percent

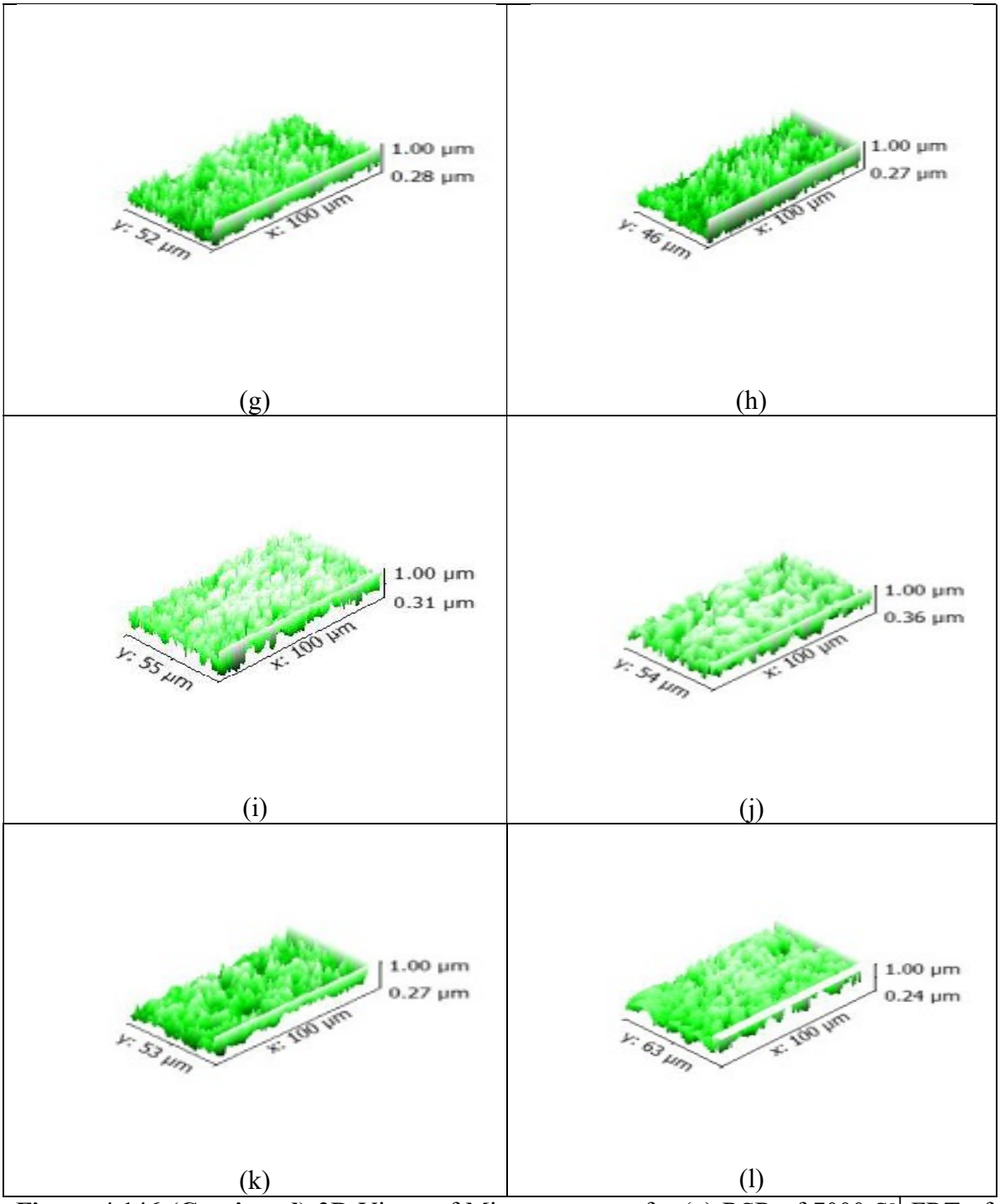

Figure 4.146 (Continued):3D Views of Microstructures for (g) RSR of 7000 S^{-1},FRT of 915ºC, PTD of 96.0 percent (h) RSR of 7000 S^{-1},FRT of 915ºC,PTD of 96.5 percent (i) RSR of 7000 S^{-1},FRT of 915ºC,PTD of 97.0 percent (j) RSR of 7000 S^{-1},FRT of 915ºC,PTD of 97.5 percent(k) RSR of 7000 S^{-1},FRT of 915ºC,PTD of 98.0 percent (l) RSR of 7000 S^{-1},FRT of 915ºC,PTD of 98.5 percent..

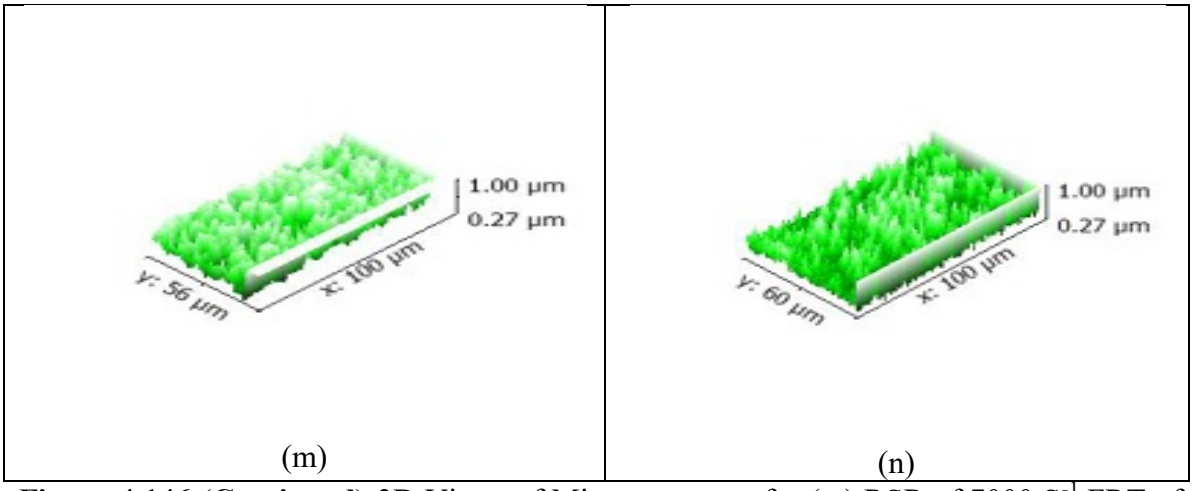

(m) (n)

Figure 4.146 (Continued):3D Views of Microstructures for (m) RSR of 7000 S^{-1},FRT of 915ºC, PTD of 99.0 percent (n) RSR of 7000 S^{-1},FRT of 915ºC,PTD of 96.0 percent.

4.21Results and Discussions For Mean Grain Sizes of hot-rolled samples

Tables 4.7, 4.8 and 4.9 show the mean grain sizes at variable hot-rolling parameters.

From Table 4.7, it was observed that at 915°C,as the RSR continued to increase, the microstructures of the hot-rolled samples also continued to decrease,with the lowest recorded at 7500 S^{-1}.The same trend was repeated for all other values of FRT.

At 99.0 percent PTD and 919°C FRT, the microstructures decreased as the RSR increased (Table 4.7); with the lowest value recorded at 7500 S^{-1} (Table 4.7).

Also from Table 4.8, it was seen that at 915°C, as the PTD continued to increase, the microstuctures of the hot-rolled samples also continued to decrease, with the lowet value recorded at 99.5 percent.The observed trend in the microstructure of the steel grade can be attributed to uniform working of the hot-rolled billet inside the stands, caused by high rate of yielding. Yielding was due to displacement movement prevented by internal components of the matrix, as other solidified component and other relatedlattice displacement. There was an inextensible relationship between the tension surrounding displacement and that surrounding the obstacles which caused further stoppage of movement of the lattice in certain direction. This gives rise to reduced mean grain size. The reduced mean grain size indicated that the microstructure was improving, and this microstructure improved as the RSR increased. This showed that the microstructure lowers as the RSR increases (Sierakowski,1997;Fahker *et al.,*2004; Mihalikova *et al*.,2007; Song *et al*.,2004)

At 99.0 percent PTD and 917°C FRT, the relationship between grain sizes with the parameters are still the same, but at decreased microstructures (Table 4.7).This also showed that the lower the FRT, the lower the microstructures of the steel grade; (Sierakowski,1997;Fahker *et al*.,2004; Mihalikova *et al*.,2007; Song *et al.,*2007.

At 99.0 percent PTD and 915°C FRT, the result is similar to those above (Table 4.7).It helped explain the inverse variation between the FRT and the microstructures of the steel grade. It also explained the direct proportion between the RSR and the microstructures.(Sierakowski,1997; Fahker *et al.,*2004; Mihalikova *et al*.,2007; Song *et al.*,2004).

It was also observed from Table 4,9, that at RSR of 4000 S^{-1}, the micrsostructures decreased as the PTD increased.The mean grain sizes of the samples increased with increasing FRT and decreased with increasing RSR and PTD (Tables 4.7 to 4.9). Similarity existed between the RSR, PTD and FRT investigated. The values of mean grain sizes at 4000 S^{-1} are higher than the ones at 5500 S^{-1}.The mean grain sizes increased gradually with increasing FRT and decreasing PTD up to the last temperature (Table 4.8). Smaller grains were observed at lower FRT; but as the FRT increased, there was grain coarsening as the size of the grains increased.

Table 4.7: Effect of Rolling Process Parameters on the Mean grain sizesat 99.0 percent PTD.

FRT	RSR (S^{-1}) / Mean Grain Size (µm)							
(°C)	4000	4500	5000	5500	6000	6500	7000	7500
915	48.00	47.64	47.24	47.11	47.03	47.01	47.00	40.00
917	49.00	48.61	48.23	48.10	47.17	47.14	47.01	42.00
919	50.03	49.60	49.20	49.12	48.40	48.32	48.01	43.00
921	52.03	51.62	51.23	51.10	50.35	50.20	50.00	44.00
923	53.00	52.63	52.21	51.13	51.04	51.02	51.00	45.00
925	54.01	53.64	53.22	53.14	52.41	52.31	51.03	46.00
927	65.00	54.72	54.23	54.17	53.37	53.25	51.13	47.03
929	67.00	55.35	55.25	55.16	55.13	55.09	55.00	48.01

Table 4.8: Effect of rolling process parameters on the mean grain sizes at 7000 s^{-1} RSR.

FRT	**PTD (%)/ Mean Grain Size (μm)**							
(°C)	96	96.5	97	97.5	98	98.5	99	99.5
915	48.00	47.58	47.42	47.10	47.09	47.08	47.00	41.00
917	49.00	48.60	48.22	48.11	48.09	48.06	47.20	42.00
919	52.21	49.61	49.20	49.14	49.09	49.05	48.41	44.00
921	54.19	53.63	53.21	53.12	53.09	53.08	52.13	45.00
923	54.20	53.64	53.42	53.41	53.40	53.10	53.07	46.00
925	64.01	58.64	58.52	58.13	57.07	54.11	53.11	47.00
927	66.00	66.02	61.90	60.02	58.70	57.67	53.40	47.43
929	68.00	68.40	63.96	60.06	58.40	57.70	55.00	47.46

Table 4.9: Effect of Rolling Process Parameters on the Mean grain sizesat 915°C FRT.

RSR	**PTD (%)**							
(S^{-1})	96	96.5	97	97.5	98	98.5	99	99.5
4000	50.71	50.64	50.24	50.10	50.09	50.50	48.00	46.00
4500	50.70	50.37	50.22	50.09	49.70	49.45	48.00	46.09
5000	50.35	50.34	50.21	50.06	49.65	49.41	48.00	47.07
5500	49.20	49.19	49.18	49.05	48.50	48.40	47.60	46.02
6000	49.10	49.09	49.08	49.03	48.49	48.38	47.56	46.00
6500	49.00	49.08	49.05	49.02	48.37	48.34	47.40	45.34
7000	48.00	47.40	47.35	47.32	47.30	47.10	47.00	41.00
7500	46.00	45.41	45.37	45.10	45.09	43.59	40.00	39.78

The effects of RSR, FRTand PTD on mean grain size of hot-rolled samples of steel grade at constant and variable hot-rolling parameters are shown in Figures 4.149, 4.150 and 4.151. Influence of mean grain size on TS, YS and impact energy at constant PTD of 99.0 percent and FRT of 915°C and 917ºC is shown in Figures 4.146,4.147 and 4.148 ..

For Figure 4.147(a), it is observed that as the mean grain sizes increased, the TS decreased.This means that better tensile properties are obtainable at smaller grain sizes.When the plot of mean grain size versus tensile strength is closely observed, there is a rapid fall in TS from 690 MPa to around 650 MPa, as the grain size decreases. This may be attributed to a defect in the material structure.There could be a possibility of porosity or slag inclusions in the body of such billets that resulted to such development.Similar trend was observed from the effect of mean grain sizes on YS shown in Figure 4.147(b).Decrease in mean grain sizes depict higher YS values.

For Figure 4.148(a),on the effect of mean grain size on impact energy at PTD of 99.0 percent and FRT of 915°C, it could be seen that increase in mean grain sizes reveals increase in impact energy of the materials. Here it is shown that the higher the mean grain size, the higher the impact energy values.

For Figure 1.148(b) , which is on the effects of mean grain sizes on YS at PTD of 99.0 percent and FRT of 917°C, the trend above was repeated.

It was also observed as one proceeds to Figures 4.149(a) and (b), that similar trends above were repeated, which also showed that increasing the mean grain sizes, increased impact energy but decreased TS and YS.

Figure 1.150 (a) showed the relationship between the RSR and the mean grain sizes.It could be seen at a glance that as the RSR increased, the mean grain sizes decreased, with the lowest recorded at 7500 s^{-1}.

Also shown in Figure 1.150 (b) is the plot between the FRT and the mean grain sizes at variable RSR. Basically it could be observed that as the FRT increased, the mean grain sizes of the hot-rolled samples also increased.Also seen from the plot is the fact that the lowest RSR value of 5000 S^{-1}, has the highest values of the mean grain sizes.The highest RSR value of 7000 S^{-1}, has the lowest mean grain size values.

From Figure 4.151(a), it is also seen that as the PTD increased, the mean garin sizes decreased at different FRT values.The higher the FRT, the higher the mean grain sizes.

Also in Figure 4.151(b) is shown the increase in size recorded by the grain sizes as the FRT increased at variable PTD values.The higher the PTD value, the lower the grain sizes.

Figure 4.152(a) shows that as the RSR increased, the mean grain sizes decreased, with the highest PTD recording the lowest value.

Figure 4.152(b) also shows that as the PTD increased, the mean grain sizes decreased, with the lowest value recorded at the highest RSR.

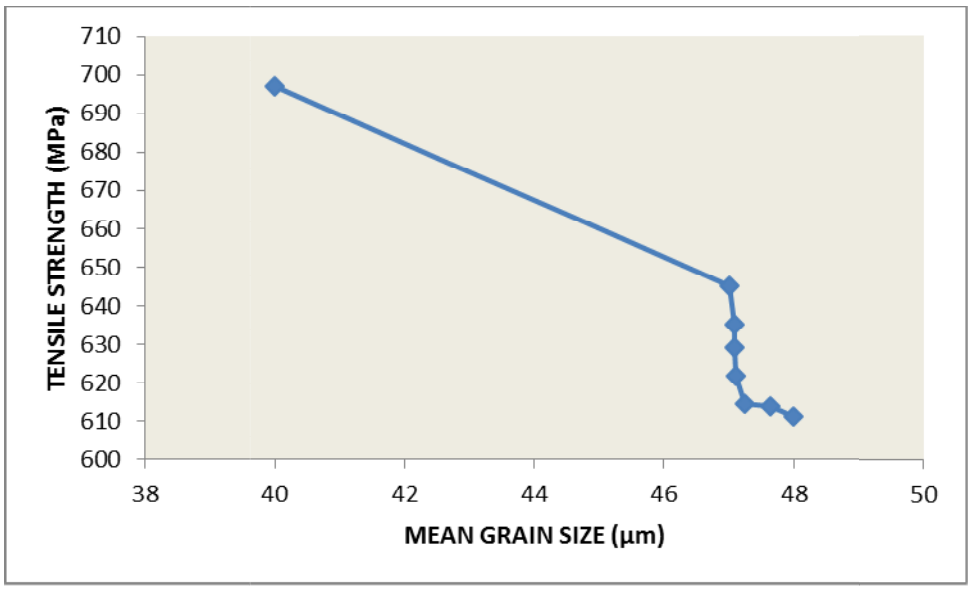

(a)

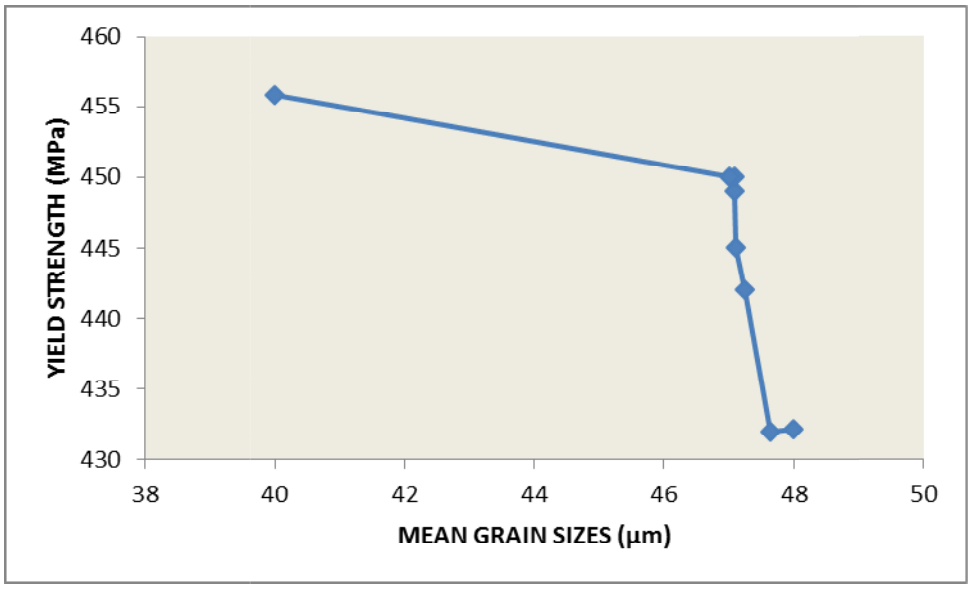

(b)

Fig 4.147:(a) Effect of Mean Grain Sizes onTS at 99.0 percent PTD and FRT of 915°C. (b) Effect of Mean Grain Sizes on YS at 99.0 percent PTD and FRT of 915°C

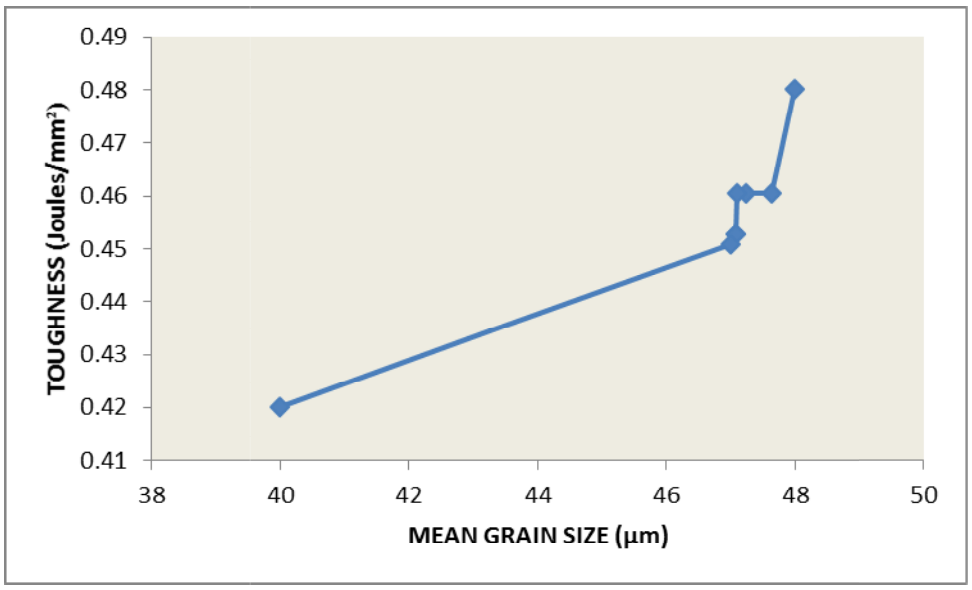

(a)

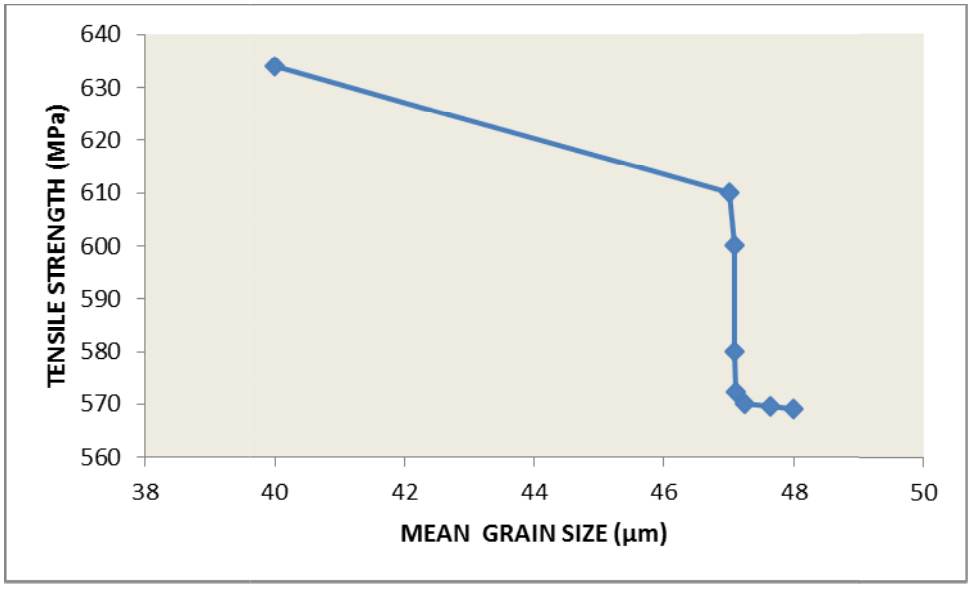

(b)

Fig 4.148:(a)Effect of mean grain sizes on impact energy at 99.0 percent PTD and FRT of 915°C (b) Effect of mean grain sizes on TS at 99.0 percent PTD and FRT of 917°C

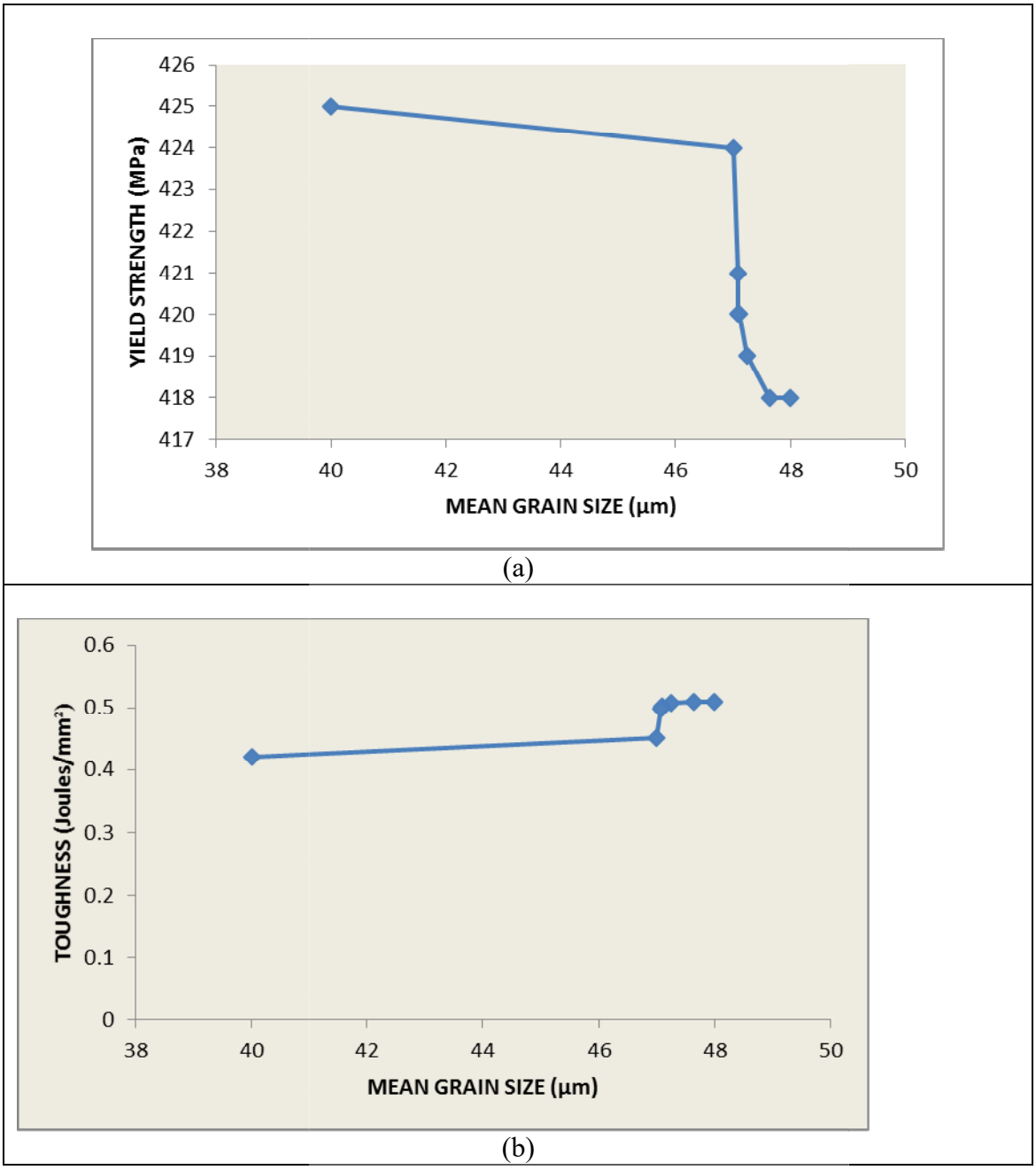

Fig 4.149:(a) Effect of mean grain sizes on YS at 99.0 percent PTD and FRT of 917° (b) Effect of mean grain sizes on impact energy at 99.0 percent PTD and FRT of 917°C

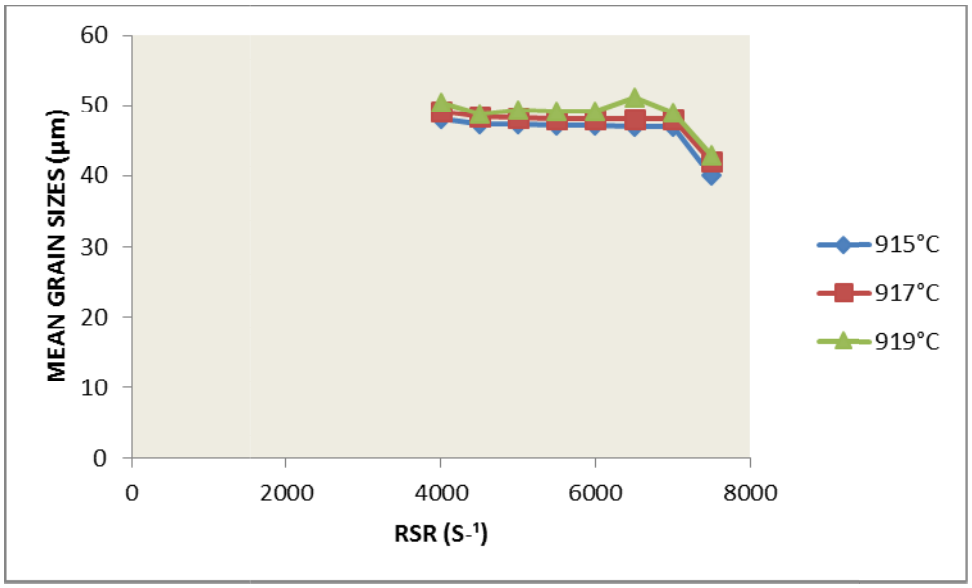

(a)

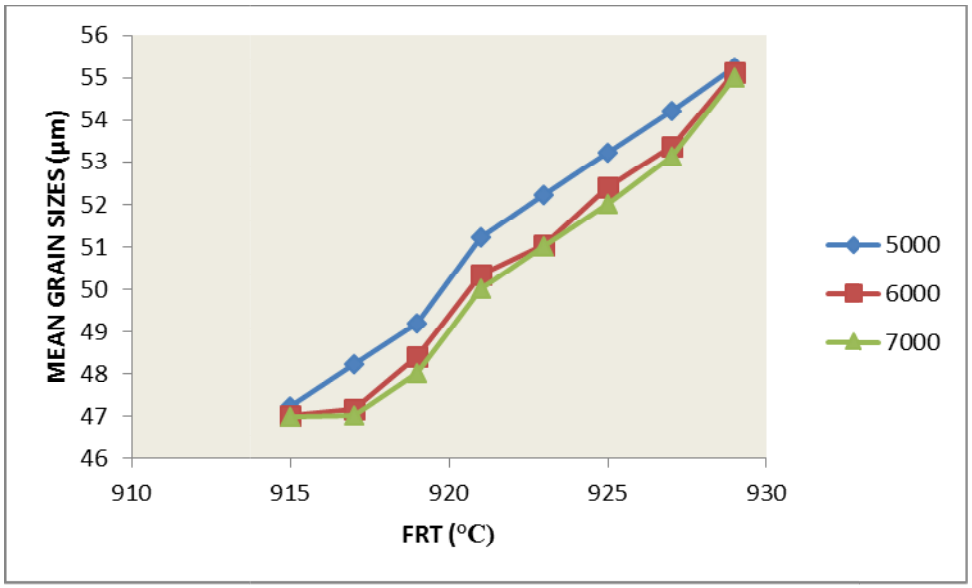

(b)

Fig 4.150: (a)Effect of RSR on mean grain sizes at 99.0 percent PTD, varying FRT (b) Effect of FRT on mean grain sizes at 99.0 percent PTDand variable RSR.

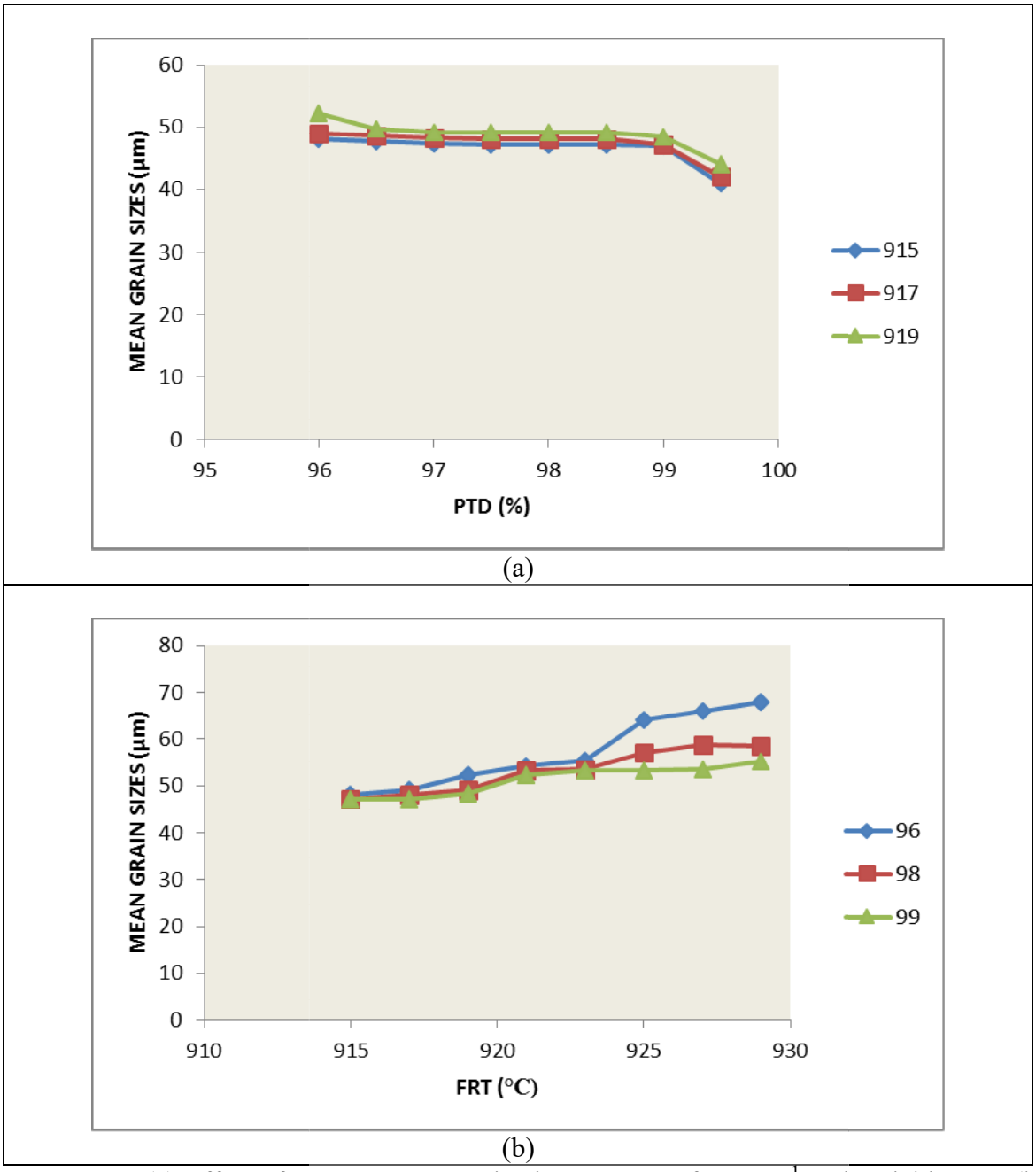

Fig 4.151: (a) Effect of PTD on mean grain sizes at RSR of 7000 S^{-1} and variable FRT (b) Effect of FRT on mean grain sizes at RSR of 7000 S^{-1} and variable PTD.

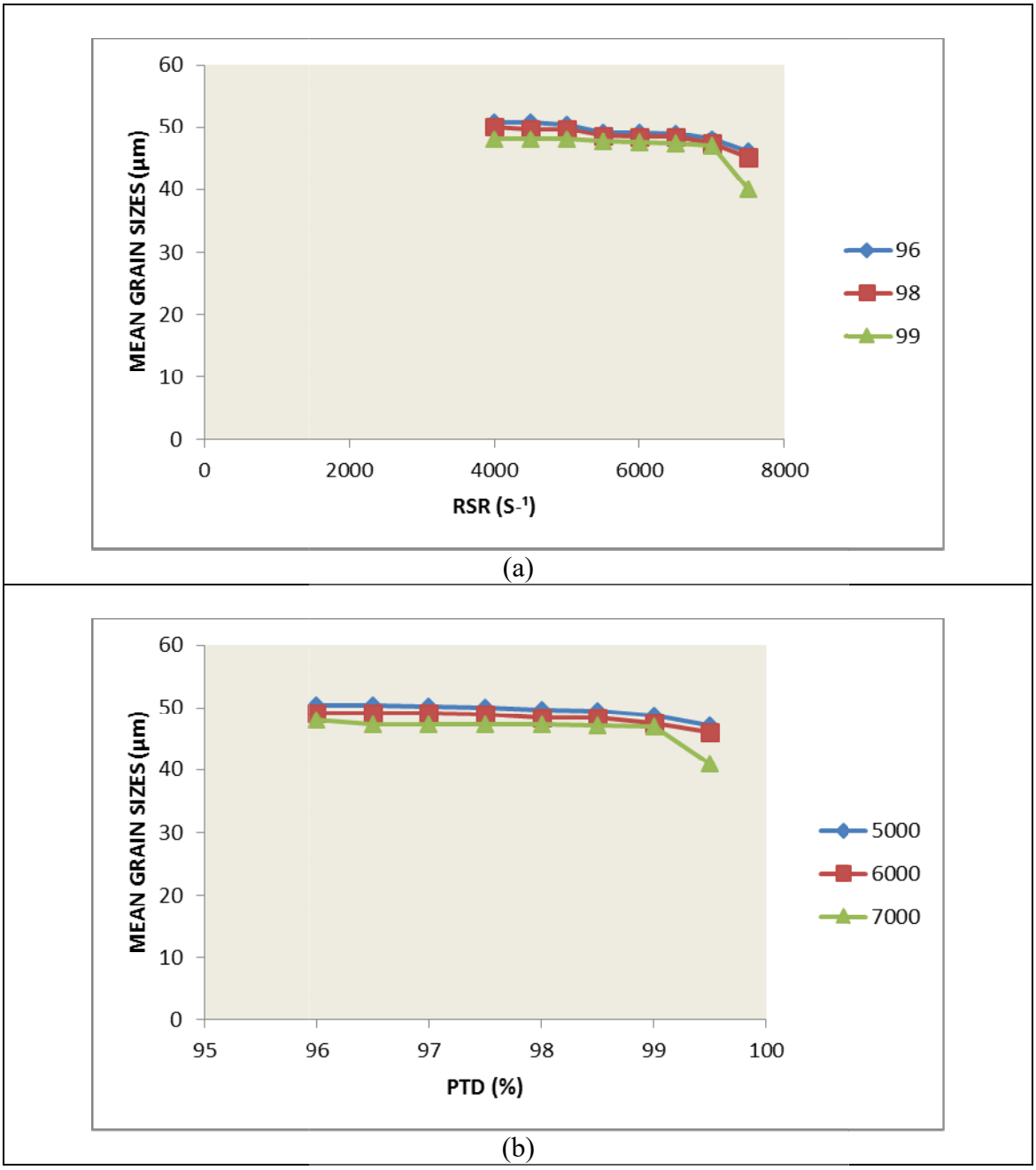

Fig 4.152: (a) Effect of RSR on mean grain sizes at FRT of 915°C and variable PTD (b) Effect of PTD on mean grain sizes at FRT of 915°C and variable RSR.

.

4.22 Results and Discussion For Optimization of The Hot-Rolling Processs Parameters

4.22.1 Results and Discussion for RSM Relative Equations

The relative equations describing the response of each of the properties with the process parameters as obtained from the Response Surface Method are as follows;

TS for FRT at 99.0 percent deformation, varying RSR

TS (σ_T) = + 691.79 - 43.00 (x_1) + 38.10 (x_2) - 38.19 (x_1^2)- 3.09 (x_2^2)-18.84 (x_1x_2) -17.36 ($x_1^2x_2$) + 2.24 ($x_1x_2^2$).4.1

Where $x_1$shows the main effect of Finish Rolling Temperature

X_2shows the main effect of Rolling Strain Rate

X_1^2 shows the curvature for Finish Rolling Temperature

X_2^2shows the curvature for Rolling Strain Rate

X_1x_2shows the combined or interactive effect of FRT and RSR.

Yield strength for finish rolling temperature at 99% deformation,changing rolling strain rates,in terms of actual factors.

σ_y =-4.57768E+005+997.70178* x_1+0.44789* x_2-0.54291 * x_1^2+7.46346E-006* x_2^2-5.63984E-004*x_1 *x_2

.4.2

Impact energy for FRT at 99.0 percent PTD ,varying RSR ,in terms of coded factors.

E_{ImT} = +0.45+0.020* x_1+0.000 * x_2+0.012* x_1^2+1.739E-003* x_2^2+2.464E-003* x_1* x_2-2.464E-003 * x_1^2* x_2-2.464E-003*x_1* x_2^2

4.3

TS for FRT at 98.0 percent PTD, varying RSR

σ_T=+688.42-42.00 * x_1+38.00* x_2-37.13* x_1^2-3.13* x_2^2-18.23* x_1 * x2-17.73* x_1^2*x2+1.73* x_1 *x_2^2

4.4

YS for FRT at 98.0 percent PTD, varying RSR,in terms of coded factors.

σ_y =+444.27-19.50 * x_1+20.95* x_2-8.91* x_1^2+7.04* x_2^2-3.12* x_1 * x_2-3.57 * x_1^2 * x_2+6.12* x_1*x_2^2

.4.5

Impact energy for FRT at 98.0 percent PTD, varying RSR,in terms of coded factors.

E_{ImT}=+0.45+0.020 * x_1+0.000* x_2+0.012* x_1^2+1.739E-003* x_2^2+2.536E-003* x_1 * x_2-2.464E-00* x_1^2* x_2-2.536E-003*x_1*x_2^2

.4.6

TS for FRT at 96.0 percent PTD, varyingRSR

σ_T=-15945.57955 +17.9204* x_1 +4.323*x_2 - 4.68182E- 003* x_1*x_2

..4.7

YS for FRT at 96.0 PTD , varying RSR,in terms of coded factors.

σ_y=+4035.07475 -4.00498*x_1 +0.014475 * x_2

4.8

YS for FRT at 96.0 percent PTD , varying RSR ,in terms of actual factors.

σ_y =-2.14851E+005+466.99815* x1+0.74820 * x2-0.25330* $x1^2$+1.44723E-006* $x2^2$-8.14644E-004* x1 * x2.4.9

Impact energy for FRT at 96.0 percent PTD, varying RSR,in terms of coded factors.

E_{ImT}= +0.060455 +4.54545E-004* x_1 -6.29318E-004*x_2+6.81818E-007* x_1 * x_2

…4.10

Impact energy for FRT at 96.0 percent PTD, varying RSR,in terms of actual factors

Where x_1 is the FRT (deg C) and x_2 is the RSR (s^{-1}).

4.22.2 Results and Discussions For The Actual Experimental Data

The experimental actual data from hot-rolling at 99.0, 98.0 and 96.0 PTD are shown in Tables 4.10, 4.11 and 4.12 respectively.

The Tables showed the eighteen observations made at each RSR value.The three Tables showed an excellent representation of the values of hot-rolling Parameters and properties for optimization using Response Surface Model.

Table 4.10: Actual Data From The Effect Of Finish Rolling Temperature On The Mechanical Properties Of St60Mn Steel At PTD Of 99%, Changing Rolling Strain Rate.

RSR (S^{-1})	Mechanical Properties of Hot-Rolled St60Mn Steel Finish Rolling Temperature (°C)																	
	915			917			919			921			923			925		
	σ_T (MPa)	σ_Y (MPa)	E_{ImT} (J/mm^2)	σ_T (MPa)	σ_Y (MPa)	E_{ImT} J/mm^2	σ_T (MPa)	σ_Y (MPa)	E_{ImT} J/mm^2	σ_T (MPa)	σ_Y (MPa)	E_{ImT} J/mm^2	σ_T (MPa)	σ_Y (MPa	E_{ImT} J/mm^2	σ_T MPa	σ_Y MPa	E_{ImT} J/mm^2
7000	611	432	0.44	608	428	0.45	609	430	0.45	607	429	0.45	606	428	0.46	606	428	0.48
6000	610	429	0.44	609	427	0.45	608	426	0.45	597	425	0.45	595	424	0.46	594	423	0.48
5000	608	428	0.45	600	426	0.45	596	425	0.45	594	424	0.45	592	423	0.46	589	422	0.48

Table 4.11: Actual Data From The Effect Of Finish Rolling Temperature On The Mechanical Properties Of St60Mn Steel At PTD Of 98%, Changing Rolling Strain Rate.

Mechanical Properties Of Hot-Rolled St60Mn Steel																		
RSR	**Finish Rolling Temperature (°C)**																	
(S^{-1})	915			917			919			921			923			925		
	σ_T (MPa)	σ_Y (MPa)	E_{ImT} J/mm^2)	σ_T (MPa)	σ_Y (MPa)	E_{ImT} J/mm^2)	σ_T (MPa)	σ_Y (MPa)	E_{ImT} (J/mm^2)	σ_T (MPa)	σ_Y (MPa)	E_{ImT} (J/mm^2	σ_T (MPa)	σ_Y (MPa)	E_{ImT} J/mm^2	σ_T (MPa)	σ_Y (MPa)	E_{ImT} J/mm^2
7000	610	426	0.44	609	425	0.45	608	442.4	0.45	607	423	0.45	606	422	0.46	605	421	0.48
6000	609	425	0.44	608	424	0.45	607	423	0.45	606	422	0.45	605	421	0.46	604	420	0.48
5000	608	424	0.45	607	422	0.45	606	422	0.45	605	421	0.45	604	420	0.46	603	419	0.48

Table 4.12: Actual Data From The Effect Of Finish Rolling Temperature On The Mechanical Properties Of St60Mn Steel At PTD Of 96%, Changing Rolling Strain Rate.

RSR	**Mechanical Properties Of Hot-Rolled St60Mn Steel**																	
(S-¹)	**Finish Rolling Temperature (°C)**																	
	915			917			919			921			923			925		
	σ_T (MPa)	σ_Y (MPa)	E_{ImT} (J/mm2)	σ_T (MPa)	σ_Y (MPa)	E_{ImT} (J/mm²)	σ_T (MPa)	σ_Y (MPa)	E_{ImT} (J/mm²)	σ_T (MPa)	σ_Y (MPa)	E_{ImT} J/mm²	σ_T (MPa)	σ_Y (MPa)	E_{ImT} J/mm²	σ_T (MPa)	σ_Y (MPa)	E_{ImT} J/mm²
7000	609	425	0.44	608	424	0.45	607	423	0.45	606	422	0.45	605	421	0.46	604	420	0.48
6000	608	424	0.44	607	423	0.45	606	422	0.45	605	421	0.45	604	420	0.46	593	419	0.48
5000	607	425	0.45	606	422	0.45	605	421	0.45	599	420	0.45	593	419	0.46	582	418	0.48

4.22.3 Results and Discussions For Response Surface Model Statistics

The Response Surface Model statistics for TS, YS and impact energy at 99.0 percent PTD is shown in Tables 4.13,4.14 and 4.15

The Response Surface Model for TS, YS and impact energy at 98.0 percentis shown in Tables 4.16, 4.17 and 4.18 .The Response Surface Model statistics for TS, YS and impact energy for 96.0 percent is shown in Tables 4.19,4.20 and 4.21 .

The Tables 4.13-4.21 showed that the YS, TS and impact energy are functions of the FRT at various RSR and PTD. The data in the tables were generated in the RSM actual value frame for the 18 observations .The RSM was used to develop model statistics for relationship between each of the tensile properties with the hot-rolling parameters.

The results showed quadratic order for the explanation of the tensile properties versus the hot-rolling parameters as indicated in the tables. But it was seen from the tables that the model increases the adjusted and predicted R-square values of the cubic order for TS, YS and impact energy versus the hot-rolling parameters at 99.0 percent PTD, varying RSR, with the smallest level of uncertainty. The same trend was also seen for TS, YS and impact energy at 98.0 percent PTD, varying RSR and also for TS, YS and impact energyat 96.0 percent PTD, varying RSR. So the cubic order is the preferred for the properties shown above. The quadratic order has fair standard deviation, increased R^2 values and decreased predicted residual sum of squares for impact energy and YS at 96.0 percent PTD, indicating that the quadratic model is the preferred order for these two properties at 96.0 percent PTD with the hot-rolling process parameters.

Table 4.13: Response Surface Model for Tensile Strength Relationship with FRT At 99.0 percent PTD, varying RSR.

Model Summary Statistics for TS of Hot-Rolled Steel Grade at 99.0 PTD,varying RSR						
Source	**Std.Dev.**	**R. Squared**	**Adjusted R-Squared**	**Predicted R-Squared**	**Press**	
Linear	25.61	0.8002	0.7559	0.6345	10803.59	
2E1	22.03	0.8689	0.8194	0.7536	7283.71	
Quadratic	8.92	0.9839	0.9704	0.9151	2510.19	
Cubic	0.89	0.9999	0.9997	0.9924	223.61	SA

Table 4. 14: Response Surface Model for YS Relationship with FRT At 99.0 PTD, varying RSR.

Model Summary Statistics for YS of Hot-Rolled Steel Grade at 99.0 PTD, varying RSR						
Source	**Std.Dev.**	**R.Squared**	**Adjusted R-Squared**	**Predicted R-Squared**	**Press**	
Linear	6,52	0.9364	0.9223	0.8979	614.21	
2E1	6.62	0.9417	0.9199	0.9044	575.00	
Quadratic	3.83	0.9854	0.9732	0.9367	380.79	Suggested
Cubic	1.35	0.9988	0.9966	0.9131	522.66	Aliased

Table 4.15: Response Surface Model for Impact Energy Relationship with FRT At 99.0 PTD, varying RSR.

Model Summary Statistics for Impact Energy of Hot-Rolled SteelGrade at 99.0 PTD, varying RSR						
Source	**Std.Dev.**	**R.Squared**	**Adjusted R-Squared**	**Predicted R-Squared**	**Press**	
Linear	6,227E-003	0.9031	0.8815	0.8250	6.299E-004	
2E1	6.44E-003	0.9078	0.8733	0.7365	9.484E-004	
Quadratic	1.852E-003	0.9943	0.9895	0.9536	1.670E-004	Suggested
Cubic	8.513E-004	0.9992	0.9978	0.9426	2.067E-004	Aliased

Table 4.16: Response Surface Model for TS Relationship with FRT At 98.0 PTD, varying RSR.

Model Summary Statistics for TS Of Hot-Rolled Steel Grade at 98.0 PTD, varying RSR						
Source	**Std.Dev.**	**R.Squared**	**Adjusted R-Squared**	**Predicted R-Squared**	**Press**	
Linear	26.28	0.7584	0.7047	0.5868	10629.93	
2E1	21.61	0.8548	0.8003	0.7338	6849.13	
Quadratic	8.96	0.9813	0.9657	0.8878	2885.60	Suggested
Cubic	0.43	1.0000	0.9999	0.9980	51.68	Aliased

Table 4.17: Response Surface Model for YS Relationship with FRT At 98.0 PTD, varying RSR.

Model Summary Statistics for YS Of Hot-RolledSteel Grade At 98.0% PTD,varyingRSR						
Source	**Std.Dev.**	**R.Squared**	**Adjusted R-Squared**	**Predicted R-Squared**	**Press**	
Linear	6.66	0.9199	0.9022	0.8639	677.89	
2E1	6.58	0.9304	0.9043	0.8794	600.48	
Quadratic	3.76	0.9830	0.9688	0.9001	497.55	Suggested
Cubic	1.67	0.9978	0.9939	0.8406	794.21	Aliased

.**Table 4.18:** Response Surface Model for Impact Enery Relationship with FRT At 98.0 PTD, varying RSR

Model Summary Statistics For Impact Energy Of Hot-Rolled Steel Grade At 98.0% PTD, VaryingRSR						
Source	**Std.Dev.**	**R.Squared**	**Adjusted R-Squared**	**Predicted R-Squared**	**Press**	
Linear	6.762E-003	0.8724	0.8441	0.7905	6.755E-004	
2E1	6.562E-003	0.8932	0.8531	0.7431	8.284E-004	
Quadratic	1.954E-003	0.9830	0.9688	0.9717	9.120E-005	Suggested
Cubic	8.513	0.9991	0.9975	0.9359	2.087E-004	Aliased

Table 4.19: Response Surface Model for TS Relationship with FRT At 96.0% PTD, varying RSR.

Model Summary Statistics For TS Of Hot-Rolled Steel Grade At 96.0% PTD, varyingRSR						
Source	**Std.Dev.**	**R.Squared**	**Adjusted R-Squared**	**Predicted R-Squared**	**Press**	
Linear	16.71	0.8430	0.8081	0.6596	5448.68	
2E1	7.17	0.9743	0.9647	0.9421	927.17	
Quadratic	4.30	0.9931	0.9873	0.9688	499.11	Suggested
Cubic	0.34	1.0000	0.9999	0.9979	33.08	Aliased

Table 4.20: Response Surface Model for YS Relationship with FRT At 96.0% PTD, varying RSR.

Model Summary Statistics for YS Of Hot-Rolled Steel Grade At 96.0% PTD, Varying RSR						
Source	Std.Dev.	R.Squared	Adjusted R-Squared	Predicted R-Squared	Press	
Linear	3.87	0.9636	0.9555	0.9327	249.32	
2E1	2.72	0.9840	0.9781	0.9709	107.69	
Quadratic	1.85	0.9944	0.9898	0.9771	84.78	Suggested
Cubic	1.96	1.9959	0.9886	0.7047	1093.65	Aliased

Table 4.21: Response Surface Model for Impact Energy Relationship with FRT At 96.0% PTD, varying RSR.

Model Summary Statistics For Impact Energy Of Hot-Rolled Steel Grade At 96.0% PTD, varyingRSR						
Source	Std.Dev.	R.Squared	Adjusted R-Squared	Predicted R-Squared	Press	
Linear	5.463E-003	0.9152	0.8963	0.8639	4.310E-004	
2E1	4.994E-003	0.9370	0.9134	0.8177	5,774E-004	
Quadratic	1.899E-003	0.9932	0.9875	0.9588	1.306E-004	Suggested
Cubic	8.513E-004	0.9991	0.9975	0.9347	2.067E-004	Aliased

4.22.4 Results and Discussions For Analysis of Variance (ANOVA)

The ANOVA for TS and YS at 99.0 percent is shown in Tables 4.22 and 4.23. The ANOVA for TS, YS and impact energy at 98.0% is shown in Tables 4.24, 4.25, 4.26. The ANOVA for TS, YS and impact energy at 96.0% is shown in Tables 4.27,4.28, 4.29.

As shown in Tables 4.22-4.29,the F-values for the properties, which < 0.0001 suggested that such models are significant.This indicated that it took 0.01% possibility that the model F-values as large as obtained could occur due to noise.The model terms with ''prob>F'' value < 0.0001 are taken to be significant with the properties of hot-rolled steel grade at 99.0% PTD and variable RSR.The hot-rolling parameter that has the most significant effect on the properties was the FRT (x_1) main effect with F-values of 4718.23,116.66 and 819.31,for TS, YS and Impact energy respectively.This is followed by RSR (x_2) with F-values of 3704.18, 212.41 and 7.96 both having ''prob>F''< 0.0001. This suggested that the FRT has much more effect on the TS and Impact energy with ''prob>F'' <0.0001,while the RSR has much more effect on the YS than the other two,with ''prob>F''value <0.0001. The model terms having ''prob>F''value >0.0001 indicated that the terms were not significant.

Similar trends were seen for the other variables of 98.0 and 96.0 % for the hot-rolled steel grade.The determination coefficient R^2 values showed satisfactory response between the predicted values and the data for the properties at various variables of the parameters.This gave the confidence that the models describing the response of the properties were good fits of the model data.The adequate precision, which measured the signal to noise ratios for the relationships describing the YS surface response, TS surface response and the Impact energy surface response for all the variables of the hot-rolling process parameters indicated adequate signals having been determined to be greater than 4.00 as shown in the Tables mentioned above.It is required that this ratio greater than 4 is desirable.These models could be used to obtain the design space for the three properties.

Table 4.22:ANOVA for TS Relationship with FRT At 99.0% PTD, varying RSR.

ANOVA For TS of Hot-Rolled Steel Grade at 99.0% PTD, varying RSR. ANOVA for Response Surface Cubic Model Analysis of Variance Table [Partial sum of squares]							
Source	**Sum of Squares**	**Coefficient Estimate**	**Mean Squares**	**F-Value**	**Prob>F**	**DF**	**95%CL Low**
Model	29558.33		4222.62	5387.59	<0.0001	7	
X_1	3698.00	-43.00	3698.00	4718.23	<0.0001	1	-44.74
X_2	2903.22	38.10	2903.22	3704.18	<0.0001	1	36.36
X_1^2	3194.98	-38.19	3194.98	4076.43	<0.0001	1	-39.85
X_2^2	20.93	-3.09	20.93	26.71	0.006	1	-4.75
X_1X_2	2277.69	-18.84	2277.69	2906.08	<0.0001	1	-19.81
X_1^3	0.000 0						
$X2^3$	0.000 0						
$X_1^2X_2$	459.67	-17.36	459.67	586.49	<0.0001	1	-19.35
$X_1X_2^2$	7.64	2.24	9.74	0.0355			0.25
Residual	3.14		0.78			4	
Lack of Fit	3.14		3.14			1	
Pure error	0.000		0.000			3	
Cor Total	29561.47					11	
Intercept		691.79				1	685.99
Std.Dev.	0.89	R-Squared	0.9999				
Mean	660.73	Adj R-Squared	0.9997				
C.V.	0.13	Pred R-Squared	0.9924				
PRESS	223.61	Adeq Precision	170.160				

Table 4.23:ANOVA for YS Relationship with FRT At 99.0% PTD, varying RSR.

ANOVA For YS of Hot-Rolled Steel Grade At 99.0% PTD, varying RSR. ANOVA for Response Surface Cubic Model Analysis of Variance table [Partial sum of squares]							
Source	**Sum of Squares**	**Coefficient Estimate**	**Mean Squares**	**F-Value**	**Prob>F**	**DF**	**95%CL Low Standard Error**
Model	5926.69		1185	80.93	<0.0001	5	
X_1	1708.51	-14.20	1708.51	212.41	<0.0001	1	-17.41 1.31
X_2	3110.89	19.15	3110.89	212.41	<0.0001	1	15.94 1.31
X_1^2	165.78	-8.69	165.78	11.32	0.0151	1	-15.00 2.58
X_2^2	122.39	7.46	122.39	8.36	0.0277	1	1.15 2.58
X_1X_2	33.26	-2.26	33.26	2.27	0.1826	1	-5.92 1.50
X_1^3	0.000 0						
$X2^3$	0.000 0						
$X_1^2X_2$	20.12	-3.63	20.12	10.98	0.0295	1	-6.68 1.10
$X_1X_2^2$	57.06	6.12	57.06	31.15	0.0051		3.07 1.10
Residual	87.86		16.45			6	
Lack of Fit	87.86		29.29			3	
Pure error	0.000		0.000			3	
Cor Total	6014.56					11	
Intercept		446.79				1	439.94 2.80
Std.Dev.	3.83	R-Squared	0.9854				
Mean	446.47	Adj R-Squared	0.9732				
C.V.	0.86	Pred R-Squared	0.9367				
PRESS	380.79	Adeq Precision	24.648				

Table 4.24ANOVA forts with FRT At 98.0% PTD, varying RSR

ANOVA for TS of Hot-Rolled Steel Grade at 98.0% PTD, varying RSR. ANOVA for Response Surface Cubic Model Analysis of Variance Table [Partial sum of squares]							
Source	**Sum of Squares**	**Coefficient Estimate**	**Mean Squares**	**F-Value**	**Prob>F**	**DF**	**95%CL Low Standard Error**
Model	25725.53		3675.08	20286.41	<0.0001	7	
X_1	3528.00	-42.00	3328.00	19474.56	<0.0001	1	-42.84
X_2	2888.00	38.00	2888.00	15941.76	<0.0001	1	37.16
X_1^2	3019.94	-37.13	3019.94	116670.08	<0.0001	1	-37.93
X_2^2	21.47	-3.13	21.47	118.49	0.0004	1	-3.93
X_1X_2	2133.55	-18.23	2133.55	11777.22	<0.0001	1	-18.70
X_1^3	0.000 0						
$X2^3$	0.000 0						
$X_1^2X_2$	479.45	-17.73	479.45	2646.55	<0.0001	1	-18.69
$X_1X_2^2$	4.57	1.73	4.57	25.25	0.0074		0.77
Residual	0.72		0.18			4	
Lack of Fit	0.72		0.72			1	
Pure error	0.000		0.000			3	
Cor Total	25726.25					11	
Intercept		688.42				1	687.55

Std.Dev.	0.43	R-Squared	1.0000
Mean	661.75	Adj R-Squared	0.9999
C.V.	0.064	Pred R-Squared	0.9980
PRESS	51.68	Adeq Precision	348.386

Table 4.25: ANOVA for YS Relationship with FRT At 98.0%PTD,varying RSR.

ANOVA for YS of Hot-Rolled Steel Grade At 98.0% PTD , Varying RSR. ANOVA for Response Surface Cubic Model Analysis of Variance Table [Partial sum of squares]							
Source	**Sum of Squares**	**Coefficient Estimate**	**Mean Squares**	**F-Value**	**Prob>F**	**DF**	**95%CL Low Standard Error**
Model	4896.34		979.27	69.33	<0.0001	5	
X_1	1895.27	-14.95	1895.27	134.19	<0.0001	1	-18.11 1.29
X_2	2883.36	18.44	2883.36	204.15	<0.0001	1	15.28 1.29
X_1^2	186.59	-9.22	186.59	13.21	0.0109	1	-15.42 2.54
X_2^2	99.64	6.73	99.64	7.05	0.0377	1	0.53 2.54
X_1X_2	47.15	-2.69	47.15	3.34	0.1174	1	-6.28 1.47
X_1^3	0.000 0						
$X2^3$	0.000 0						
$X_1^2X_2$							
$X_1X_2^2$							
Residual	84.74		14.12			6	
Lack of Fit	84.74		28.24			3	
Pure error	0.000		0.000			3	
Cor Total	4981.08					13	
Intercept		444.48				1	437.75 2.75
Std.Dev.	3.76	R-Squared	0.9830				
Mean	445.18	Adj R-Squared	0.9688				
C.V.	0.84	Pred R-Squared	0.9001				
PRESS	497.55	Adeq Precision	25.131				

Table 4.26:ANOVA for Impact Energy Relationship with FRT at 98.0% PTD, varying RSR.

ANOVA for Impact Energy of Hot-Rolled Steel Grade At 98.0% PTD , Varying RSR. ANOVA for Response Surface Cubic Model Analysis of Variance Table [Partial sum of squares]								
Source	**Sum of Squares**	**Coefficient Estimate**	**Mean Squares**	**F-Value**	**Prob>F**	**DF**	**95%CL Low**	**Standard Error** **95%CL High** **VIF**
Model	3.202E-003		6.404E-004	167.78	<0.0001	5		
X_1	2.739E-003	0.018	2.739E-003	717.58	<0.0001	1	0.016	1.29 0.020 1.05
X_2	3.303E-005	0.000	-1.974E-005	8.65	0.0259	1	-3.61	6.710E-004 -3.61 1.05
X_1^2	3.029E-003	0.012	3.029E-003	79.35	0.0001	1	8.516E-003	1.318E-003 0.015 1.02
X_2^2	6.663E-006	1.741E-003	6.663E-006	1.75	0.2346	1	-1.48	1.318E-003 4.967E-003 1.02
X_1X_2	4.193E-005	2.533E-003	4.193E-005	10.98	0.0161	1	6.628E-004	7.643E-004 4.403E-003 1.06
X_1^3	0.000 0							
$X2^3$	0.000 0							
$X_1^2X_2$								
$X_1X_2^2$								
Residual	2.290E-005		3.817E-006			6		
Lack of Fit	2.290E-005		7.634E-006			3		
Pure error	0.000		0.000			3		
Cor Total	3.225E-003					11		
Intercept		0.45				1	0.45	1.430E-003 0.45
Std.Dev.	1.954E-003	R-Squared	0.9929					
Mean	0.46	Adj R-Squared	0.9870					
C.V.	0.43	Pred R-Squared	0.9717					
PRESS	9.120E-005	Adeq Precision	29.688					

Table 4.27:ANOVA for TS Relationship with FRT At 96.0% PTD, varying RSR.

ANOVA for TS Of Hot-Rolled Steel Grade At 96.0% PTD , varying RSR.
ANOVA for Response Surface Cubic Model
Analysis of Variance table [Partial sum of squares]

Source	Sum of Squares	Coefficient Estimate	Mean Squares	F-Value	Prob>F	DF	95%CL Low Standard Error	95%CL High VIF
Model	16006.45		2286.64	19722.24	<0.0001	7		
X_1	3612.50	-42.50	3612.50	31157.81	<0.0001	1	-43.17	0.24 -
							41.83	4.46
X_2	312.50	12.50	312.50	2695.31	<1.0000	1	11.83	0.24
							13.17	4.46
X_1^2	305.23	11.80	305.23	2632.58	<0.0001	1	11.17	0.23
							12.44	1.03
X_2^2	10.56	-2.20	10.56	91.08	0.0007	1	-2.83	0.23
							-1.56	1.03
X_1X_2	2200.21	-18.53	2200.23	18976.82	<0.0001	1	-18.89	0.13
							-18.14	1.08
X_1^3	0.000 0							
$X2^3$	0.000 0							
$X_1^2X_2$	97.95	8.01	97.95	844.78	<0.0001	1	7.25	0.28
							8.78	4.54
$X_1X_2^2$	9.42	2.49	9.42	81.25	0.0008		1.72	0.28
							3.25	4.54
Residual	0.46		0.12			4		
Lack of Fit	0.46		0.46			1		
Pure error	0.000		0.000			3		
Cor Total	16006.92					11		
Intercept		637.46				1	636.7	0.25
							638.16	

Std.Dev.	0.34	R-Squared	1.0000
Mean	638.08	Adj R-Squared	0.9999
C.V.	0.053	Pred R-Squared	0.9979
PRESS	33.08	Adeq Precision	435.430

Table 4.28:ANOVA forYS Relationship with FRT At 96.0% PTD, varying RSR.

ANOVA for YS Of Hot-Rolled Steel Grade At 96.0% PTD , varying RSR.
ANOVA for Response Surface Cubic Model
Analysis of Variance table [Partial sum of squares]

Source	Sum of Squares	Coefficient Estimate	Mean Squares	F-Value	Prob>F	DF	95%CL Low Error	Standard 95%CL High	VIF
Model	3682.36		736.47	214.96	<0.0001	5			
X_1	1616.30	-13.81	1616.30	471.77	<0.0001	1	-15.36	-12.25	0.64 1.05
X_2	2423.58	16.91	2423.58	707.40	<1.0000	1	15.35	18.46	0.64 1.05
X_1^2	36.09	-4.05	36.09	10.53	0.0176	1	-7.11	-1.00	1.25 1.02
X_2^2	4.60	1.45	4.60	1.34	0.2905	1	-1.61	4.50	1.25 1.02
X_1X_2	69.39	-3.26	69.39	20.25	0.0041	1	-5.03	-1.49	0.72 1.06
X_1^3	0.000 0								
$X2^3$	0.000 0								
$X_1^2X_2$									
$X_1X_2^2$									
Residual	20.56		3.43			6			
Lack of Fit	20.56		6.85			3			
Pure error	0.000		0.000			3			
Cor Total	3702.92					11			
Intercept		443.70				1	440.39	447.02	1.35

Std.Dev.	1.85	R-Squared	0.9944
Mean	438.92	Adj R-Squared	0.9898
C.V.	0.42	Pred R-Squared	0.9771
PRESS	64.78	Adeq Precision	46.933

Table 4.29ANOVA for Impact Energy Relationship with Finish Rolling Temperature At 96.0% PTD, Varying RSR.

ANOVA for Impact Energy of Hot-Rolled Steel Grade At 96.0% PTD , varying RSR.
ANOVA for Response Surface Cubic Model
Analysis of Variance table [Partial sum of squares]

Source	Sum of Squares	Coefficient Estimate	Mean Squares	F-Value	Prob>F	DF	95%CL Low	Standard Error	95%CL High	VIF
Model	3.145E-003		6.290	174.4	<0.0001	5				
X_1	2.794E-003	0.018	2.794E-003	774.83	<0.0001	1	0.017	6.521E-004	0.020	1.05
X_2	8.429E-005	-3.153E-003	8.429E-005	23.38	0.0029	1	-4.749E-003	6.521E-004	-1.557E-003	1.05
X_1^2	1.442E-004	8.100E-003	1.442E-004	39.98	0.0007	1	4.965E-003	1.281E-003	0.011	1.02
X_2^2	2.112E-005	3.100E-003	2.112E-005	5.86	0.519	1	1.281E-003	-3.450E-005	6.235E-003	1.02
X_1X_2	4.733E-005	2.691E-003	4.733E-005	13.13	0.0111	1	8.736E-004	7.429E-004	4.509E-003	1.06
X_1^3	0.000 0									
$X2^3$	0.000 0									
$X_1^2X_2$	9.809E-006	2.536E-003	9.809E-006	13.54	0.0212	1	6,223E-004	6.894E-004	4.450E-004	4.54
$X_1X_2^2$	9.809E-006	-2.536E-003	9.809E-006	13.54	0.0212		-4.450E-003	6.894E-004	-6.233E-004	4.54
Residual	2.164E-005		3.606E-006			6				
Lack of Fit	2.164E-005		3.606E-006			3				
Pure error	0.000		0.000			3				
Cor Total	3.167E-003					11				
Intercept		0.45				1	0.45	1.390E-003	0.45	

Std.Dev.	1.899E-003	R-Squared	0.9932
Mean	0.46	Adj R-Squared	0.9875
C.V.	0..41	Pred R-Squared	0.9588
PRESS	1.306E-004	Adeq Precision	31.735

4.22.5 Results and Discussion of The Parity and Normal Plots

The parity and normal plots at 99.0, 98.0 and 96.0 percent are shown in Figures 4.153and 4.154 .

Parity and Normal Distribution Assumption

It could be seen as shown in Figs. 4.153-4.154 that the residuals tend to be in straight lines with the normal distribution estimates. This suggested that the errors were normally distributed.The estimated properties are functions of the process parameters and could be considered useful for obtaining information from the experiment.

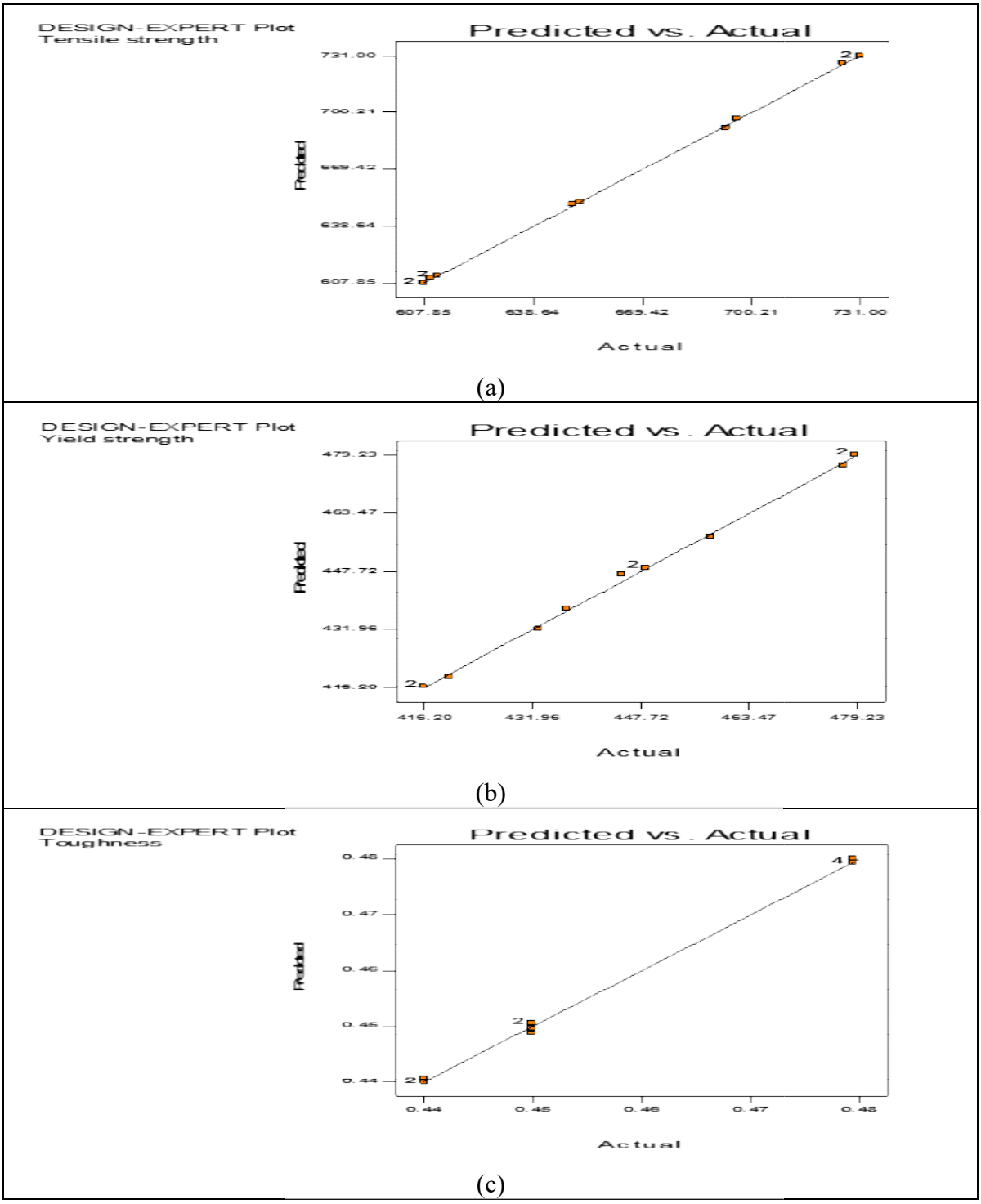

Figure 4.153. Parity Plot at PTD of 99.0% for (a) TS (b) YS (c) Impact Energy

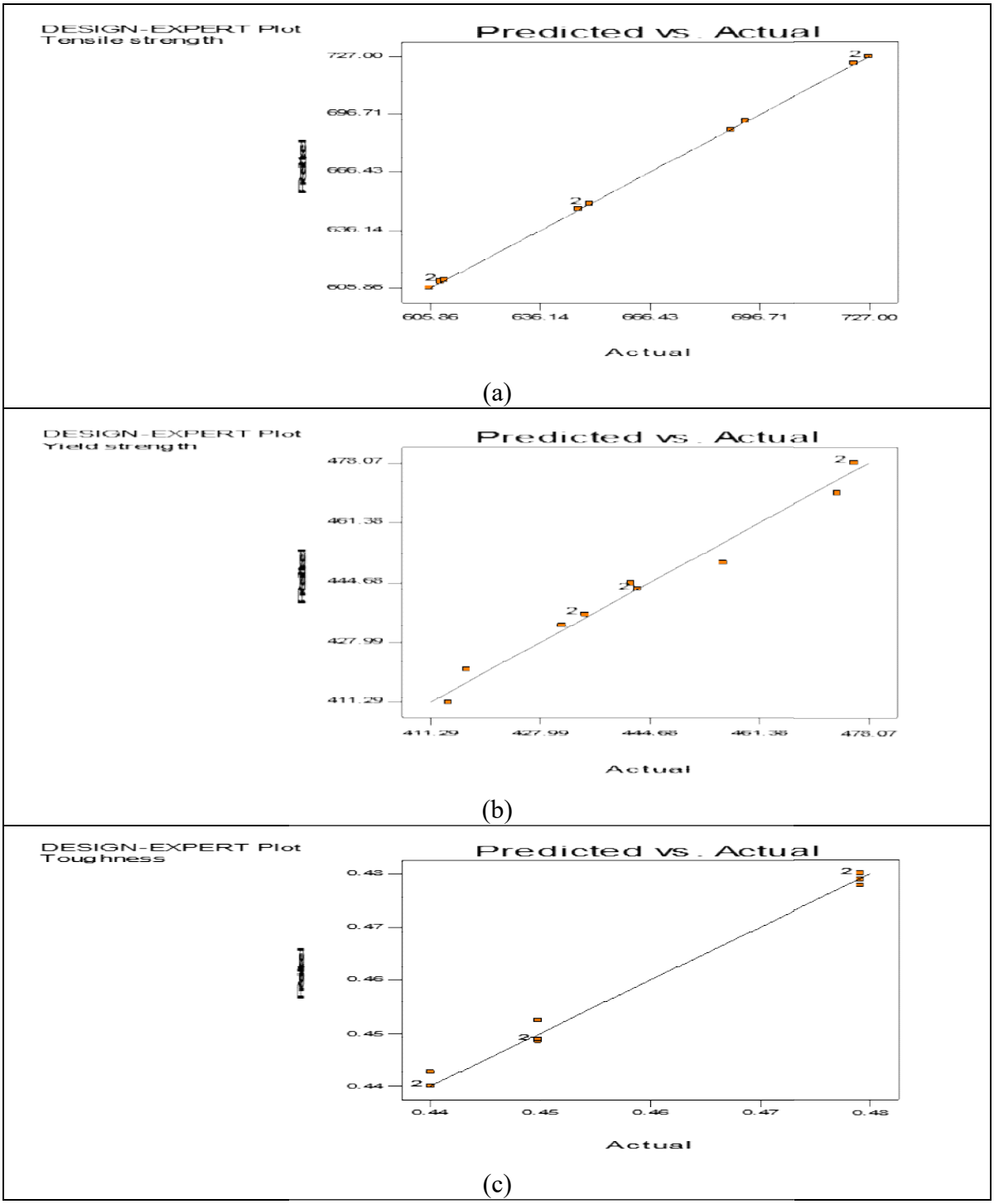

Figure 4.153: Parity plot at PTD of 98.0% for (a) TS (b) YS (c) Impact Energy

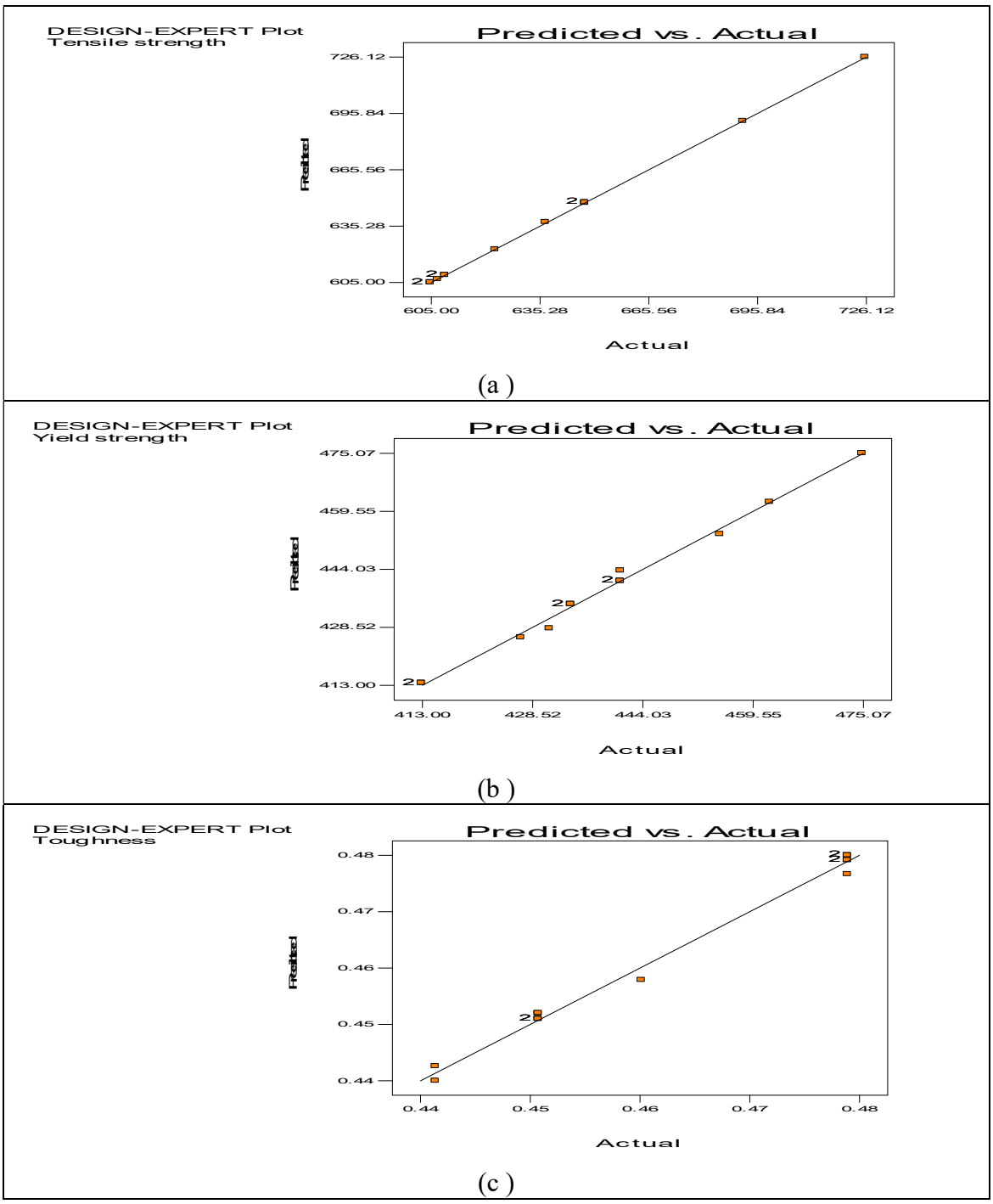

Figure 4.153 (continued): Parity plot at PTD of 96.0% for (a) TS (b) YS (c) Impact Energy

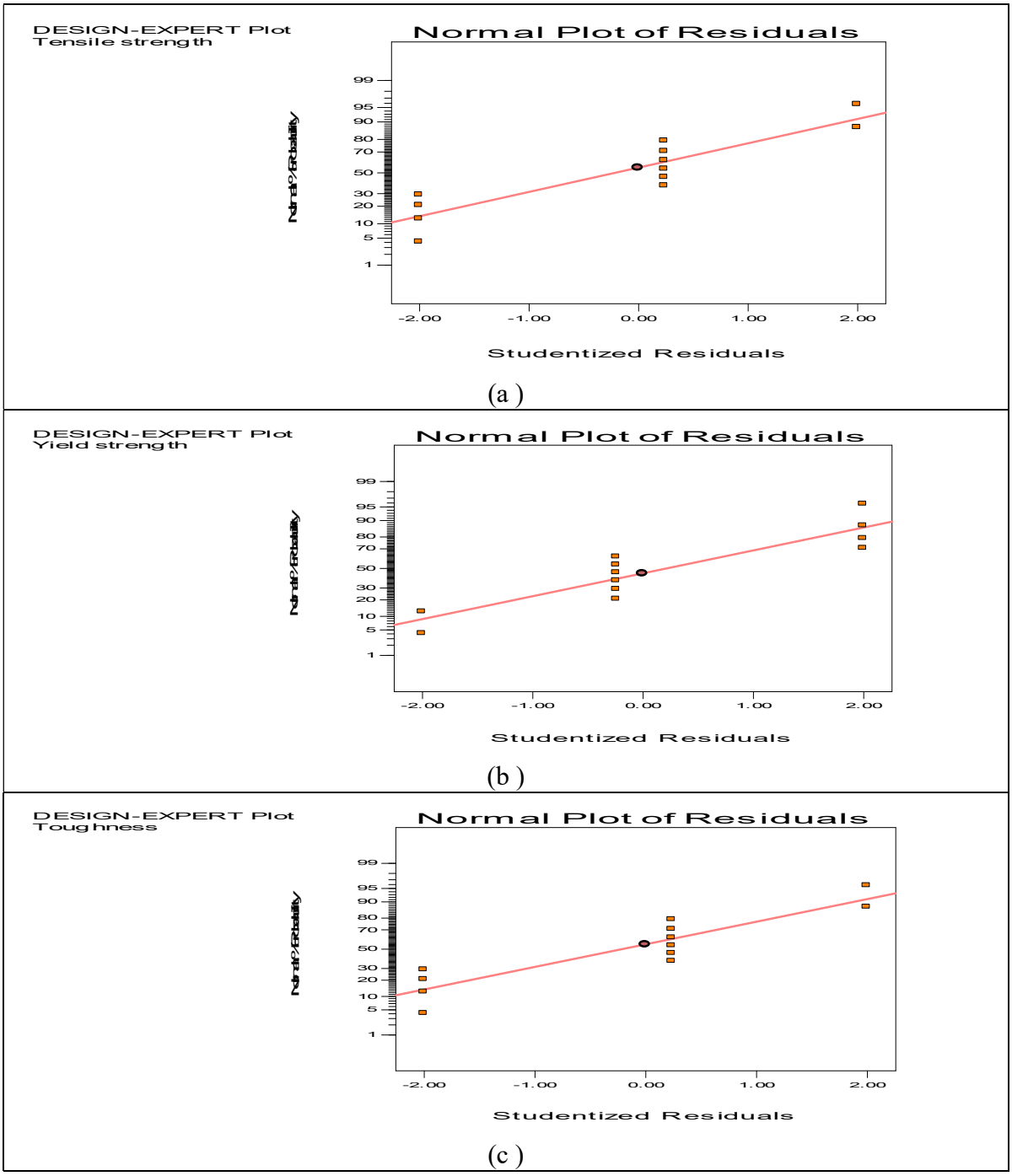

Figure 4.154: NormalPlot at PTD of 99.0% for (a) TS (b) YS (c) Impact Energy

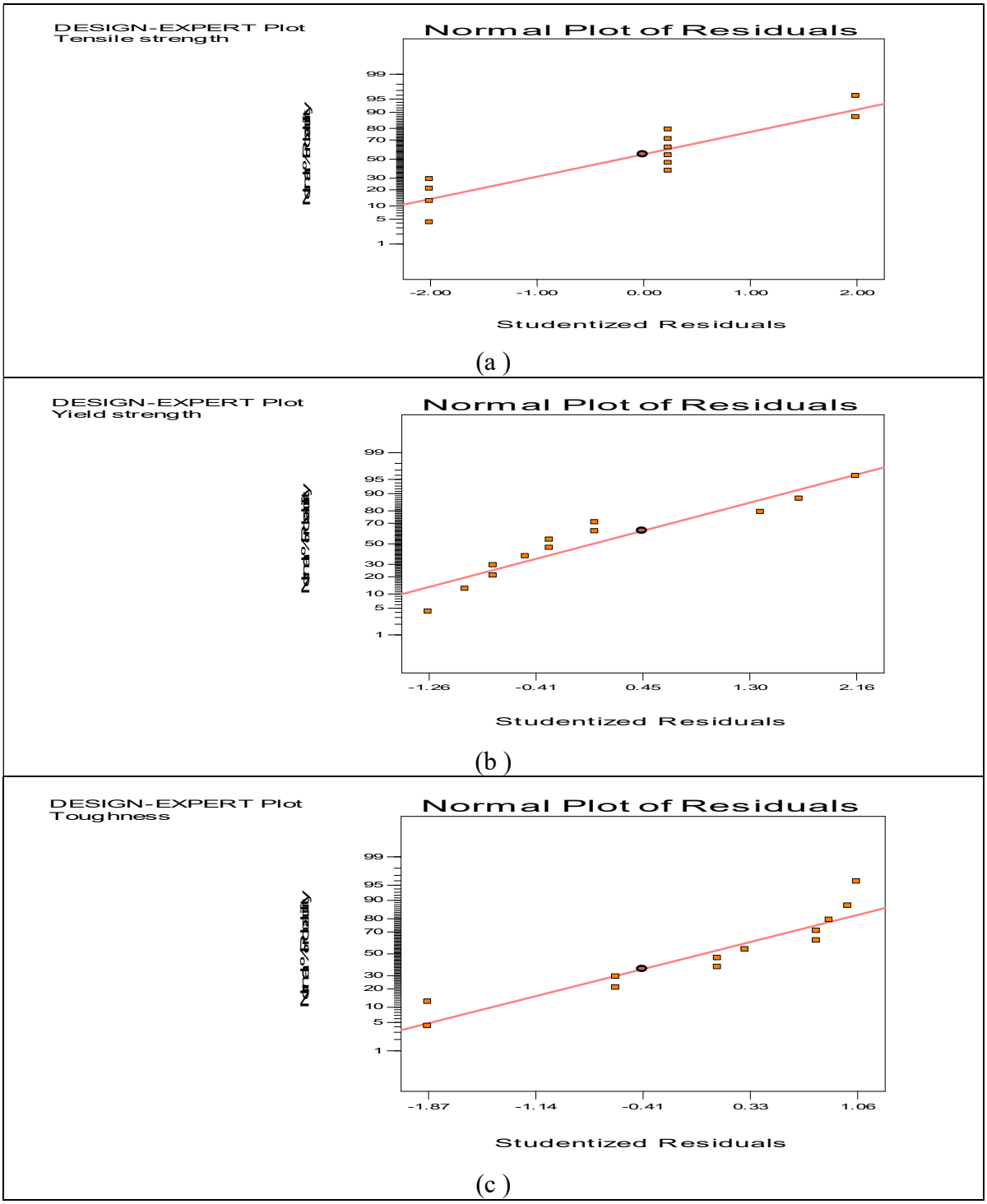

Figure 4.154(continued): Normal Plot at PTD of 98.0% for (a) TS (b) YS (c) Impact Energy

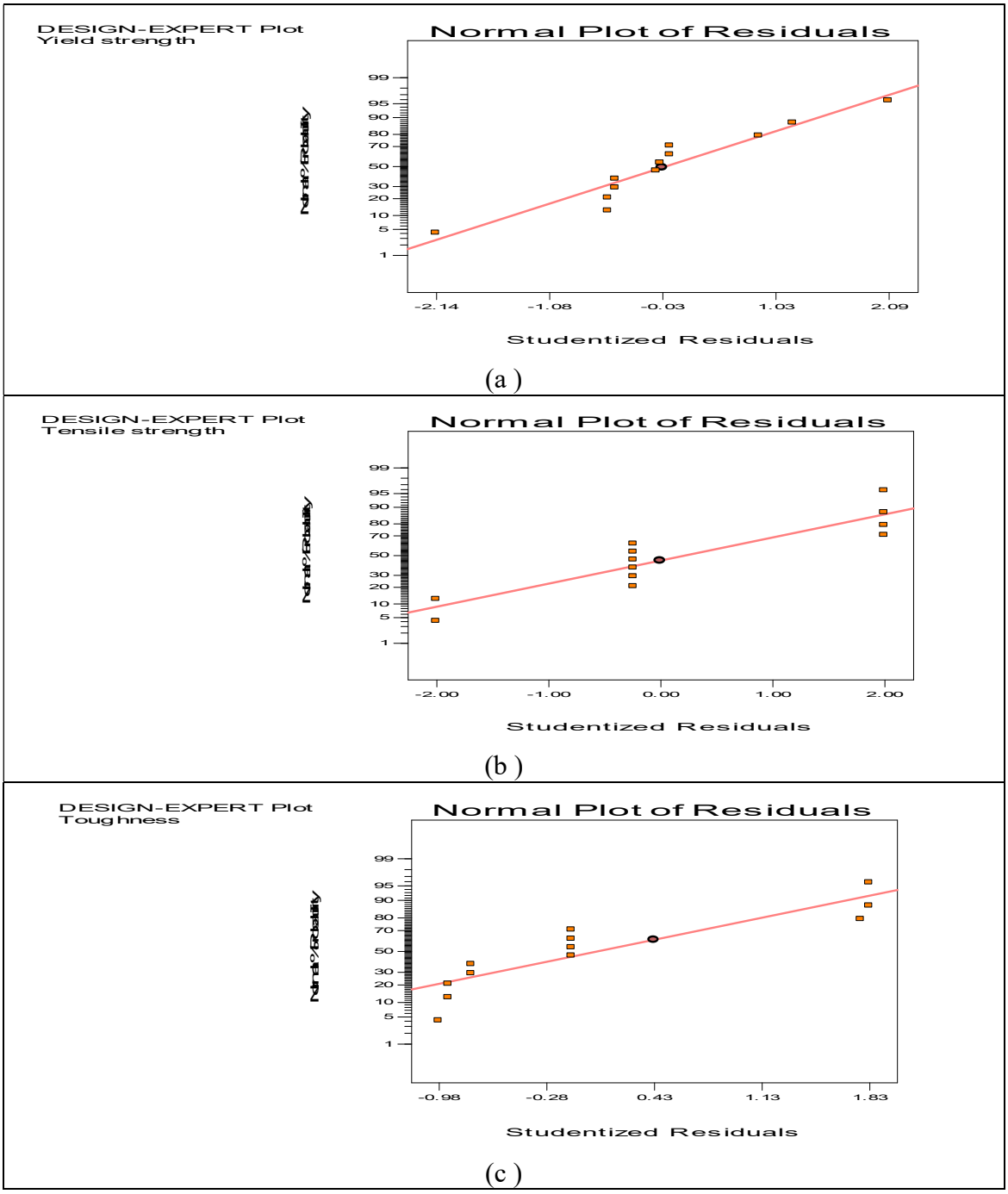

Figure 4.154 (continued): Normal plot at PTD of 96.0% for (a) TS (b) YS (c) Impact Energy

4.22.6 Results and Disscussion For Contour and Surface Plots

The surface and contour plots at PTD of 99.0, 96.0 and 98.0 percent are shown in Figures 4.155 .

As shown in Fig.4.155, the plots showed the simultaneous effects of hot-rolling process parameters on the YS, TS and Impact energy of hot-rolled steel grade samples for all the variables observed. The contour plots of the YS for all the variables observed showed similar curve shapes where YS decreased with increasing FRT and increased with increasing RSR. Both RSR and FRT showed a strong positive effect on the YS for all the variables observed.

The characteristics of the contour plots for TS are similar to that of the YS. The contour plots of the Impact energy for all the variables observed showed similar curve shapes where impact energy increased with increasing FRT and increased with decreasing RSR. The maximum achievable responses of the properties are well exposed on the contour plots. It is clear from the plots that the TS and YS of the hot-rolled steel grade decreased with increasing FRT and increased with increasing RSR; while the impact energy increased with increasing FRT and increased with decreasing RSR. So these indicated that the maximum values of TS and YS could be obtained at lower FRT and higher RSR respectively, while the maximum values of Impact energy could be obtained at higher FRT and lower RSR respectively; indicating considerable improvement of the properties at the respective parameters.

The independent influence of the hot-rolling process parameters is obtained on the surface plots. It was observed that the three parameters had equal influence on the properties at the variables observed. This influence is well exposed in the contour plots for the three properties. The improved YS is good for steel bars used in construction, which tends to prevent failure of the steel when subjected to impact load. Therefore, the YS and TS should be maximized. The combined effect of the hot-rolling process parameters is responsible for the curvatures of the plots. The implication is that the effect of the three parameters should be considered simultaneously for a global emergence of optimal process parameters for improved properties of the hot-rolled samples.

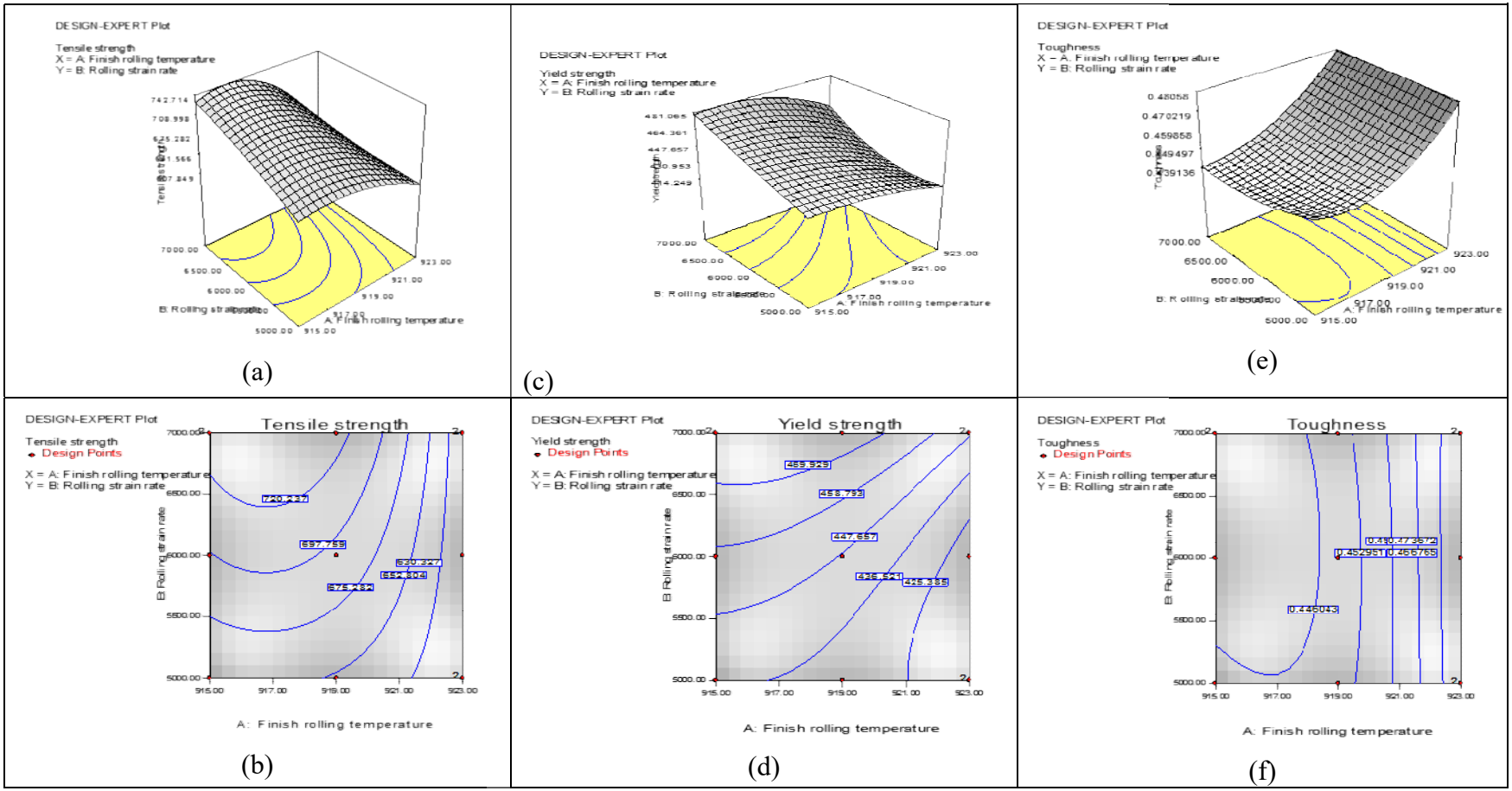

Figure 4.155: Surface and contour plots at PTD of 99.0 percent **(a)**Surface plotsfor TS ;(b) Contour plot for TS; (c) Surface plot for YS; (d) Contour plot for YS; (e) Surface plot for Impact energy; (f) Contour plot for Impact energy

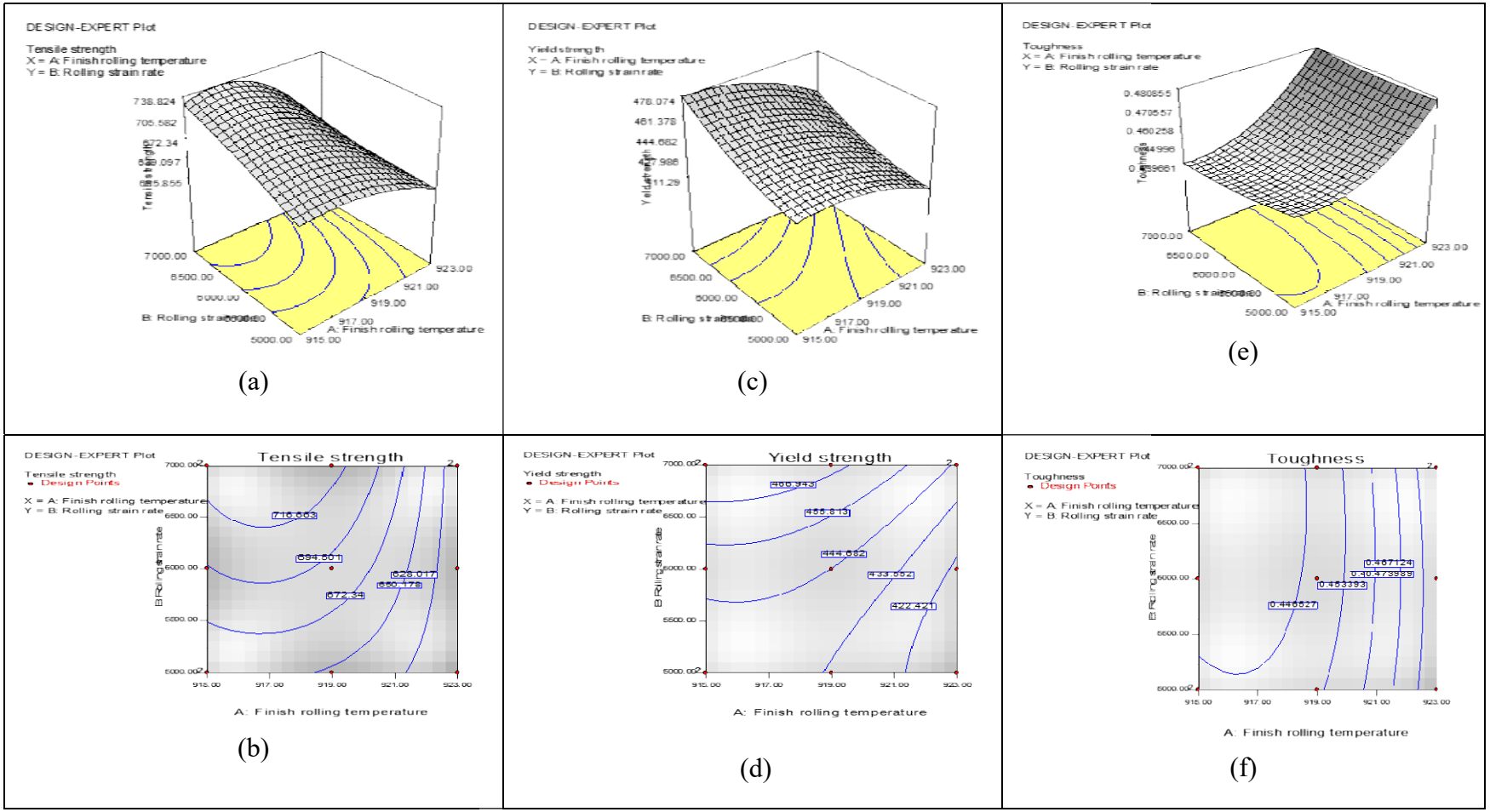

Fig.4.155(cont.): Surface and contour plots at PTD of 96.0 percent **(**a)Surface plots for TS ;(b) Contour plot for TS ; (c) Surface plot for YS; (d) Contour plot for YS; (e) Surface plot for Impact Energy;(f) Contour plot for Impact Energy.

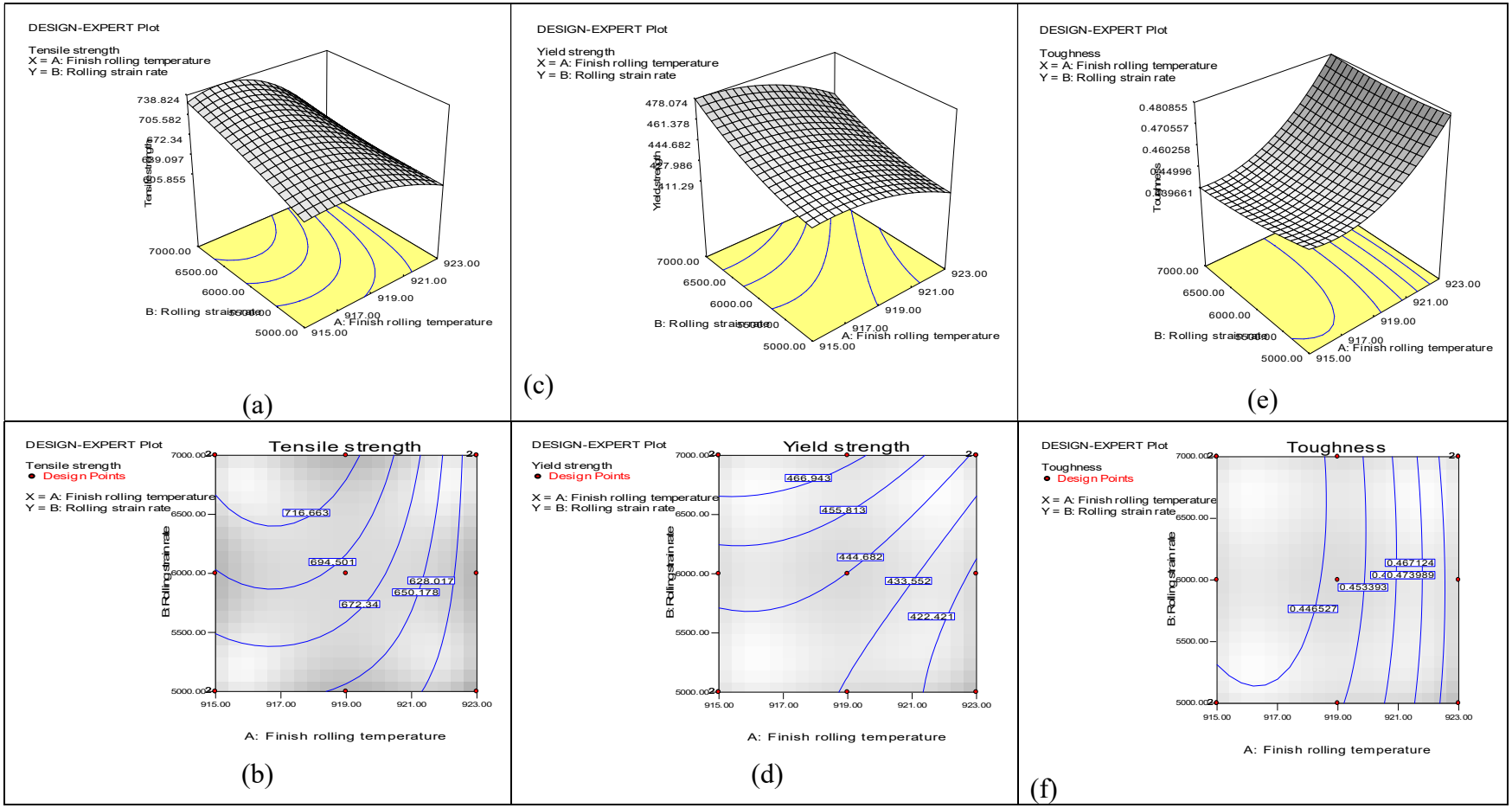

Figure 4.155(cont: Surface and contour plots at PTD of 98.0 percent **(a)**Surface plots for TS ;(b) Contour plotfor TS; (c) Surface plot for YS;(d) Contour plot for YS; (e) Surface plot for Impact Energy; (f)Contour plot for Impact Energy.

4.22.7 Results and Disscussion For Optimums Plots

The optimum properties parameters as obtained from rolling data are shown in the Tables 4.30, 4.31 and 4.32

The procedure for optimization of the hot-rolling process parameters were chosen to maximize the YS, TS and Impact Energy for improved properties as required of the hot-rolled steel grade. The combined effects of the hot-rolling process parameters on the simultaneous responses of the YS, TSand Impact Energy of the hot-rolled steel grade were presented in the Tables 4.30-4.32. The achievable optimum YS, TS and Impact Energy values were found as predicted in the tables with 95% confidence interval, which ensures that the probability of the effectiveness of the optimization procedure is greater than 0.05.The corresponding parameters that yielded these optimum values were also shown in the tables 4.30, 4.31 and 4.32 respectively.

Table 4.30: Optimum Values for TS and FRT at 99.0% PTD, varying RSR..

Factor	Name	Level	Low Level	High Level	Std.Dev.
X_1	FRT	920.30	915.00	923.00	0.000
X_2	RSR	7000.00	7000.00	7000.00	0.000
Response	**Prediction**	**Actual**	**SE Mean**	**95% CI Low**	**95%CI High**
TS	701.63	701.915	0.76	669.51	703.75
YS	470.128	470.198	1.17	466.89	703.37
Impact Energy	0.458042	0.457964	7.334E-004	0.46	0.46

Table 4.31: Optimum Values for TS and FRT at 99.0 percent PTD, varying RSR.

Factor	Name	Level	Low Level	High Level	Std.Dev.
X_1	FRT	920.51	915.00	923.00	0.000
X_2	RSR	7000.00	5000.00	7000.00	0.000
Response	**Prediction**	**Actual**	**SE Mean**	**95% CI Low**	**95%CI High**
TS	693.3	694.052	0.36	692.31	694.29
YS	461.66	461.845	2.47	455.62	467.69
Impact Energy	0.458047	0.457826	1.282E-005	0.45	0.46

Table 4.32: Optimum values for TS and FRT at 96.0 percent PTD, varying RSR.

Factor	Name	Level	Low Level	High Level	Std.Dev.
X_1	FRT	919.22	915.00	923.00	0.000
X_2	RSR	7000.00	5000.00	7000.00	0.000

Response	Prediction	Actual	SE Mean	95% CI Low	95%CI High
TS	644.609	645.173	0.32	643.72	645.50
YS	461.105	461.279	1.32	457.88	464.33
Impact Energy	0.452385	0.452169	1.350E-003	0.45	0.46

CHAPTER FIVE

CONCLUSIONS AND RECOMMENDATIONS

5.1 Conclusions

Analysis of the effects of selected hot-rolling parameters on the integrity of St60Mn steel has been considered., The effects of Finish Rolling Temperature, Percentage Total Deformation and Rolling Strain Rate resulted in decrease in thickness and increase in the enlongation of hot-rolled stock, which affected the mechanical and microstructural properties of the hot-rolled samples such as Tensile Strength, Yield Strength, Percentage Enlongation, hardness, impact energy, ductility or bendability and mean grain sizes, depending on the optimum combination of these parameters. For a particular hot-rolled rebar diameter at lower Finish Rolling Temperature, higher values of Rolling Strain Rate and Percentage Total Deformation, gave higher Yield Strength, Tensile Strength,Young Modulus of Elasticity, ductility or bendability and hardness. Consequent on these, lower Percentage Enlongation, Impact energy, Percentage Reduction in Area and mean grain sizes occured as a result of maximum reduction and deformation of the hot-rolled stock.

For 12 mm bar, at Finish Rolling Temperature 915^{0}C with Percentage Total Deformation of 99.0% and Rolling Strain Rate of 7 000 S^{-1} , the Tensile Strength, Yield Strength, Percentage Enlongation, hardness, Impact energy, ductility and mean grain size values were 6111 MPa, 432 MPa,10.3%,231 HB, 0.480 J/mm^2, 50.9 and 47 μm respectively. But when the Finish Rolling Temperature increased to 921^{0}C at PTD of 99.0 and Rolling Strain Rate of 7000 S^{-1}, Tensile Strength, Yield Strength, Percentage Enlongation, hardness, Impact energy and ductility were 607 MPa, 429 MPa, 15%, 229 HB, 0.51J/mm^2, 48 and 52 μm, respectively. Therefore, the following inferences could be drawn:

- Increasing the Rolling Strain Rate increases the Yield Strength, Tensile Strength, hardness, ductility and YoungModulus of Elasticityof the hot-rolled steel grade.
- Increasing the Rolling Strain Rate decreases the Impact energy, Percentage Enlongation and Percentage Reduction in Area of hot-rolled steel grade.

- Increasing the Rolling Strain Rate decreases the grain size of the microstructures of the hot-rolled samples of the steel grade.
- Increasing the Percentage Total Deformation increases the Tensile Strength, Yield Strength, hardness, and Young Modulus of Elasticity and ductility of hot-rolled steel grade.
- Increasing the Percentage Total Deformation decreases the impact energy, Percentage Enlongation and Percentage Reduction in Area of hot rolled steel grade.
- Increasing the Percentage Total Deformation decreases the grain sizes of the microstructures of hot-rolled steel grade.
- Increasing the Finish Rolling Temperature increases impact energy, Percentage Enlongation and Percentage Reduction in Area of hot rolled steel samples of the steel grade.
- Increasing the Finish Rolling Temperature decreases the Tensile Strength, Yield Strength, hardness, and Young Modulus of Elasticity and ductility values of hot rolled steel grade.
- Increasing the Finish Rolling Temperature increases the sizes of the the microstructural grains of the hot rolled samples.
- The optimum Rolling Strain Rate, Finish Rolling Temperature and Percentage Total Deformation for the production of 12 mm rebar of hot-rolled steel grade are 7000 S^{-1},920.30ºC and 99.0 percent.
- The optimum Tensile Strength, Yield Strength and Impact Energy for the production of 12 mm rebar of the hot-rolled steel are 701.62MPa 470.120 MPa and 0.456042 J/mm^2.
- The optimum Rolling Strain Rate, Finish Rolling Temperature and Percentage Total Deformation for the production of 16 mm rebar of hot-rolled steel are 7000 S^{-1},920.51ºC and 98.0 percent.
- The optimum Tensile Strength, Yield Strength and Impact energy for 16 mm rebar of hot-rolledsteel are 7693.3MPa, 461.66 MPa and 0.458407 J/mm^2.

- The optimum Rolling Strain Rate, Finish Rolling Temperature and Percentage Total Deformation for the production of 25 mm rebar of hot-rolled steel are 7000 S^{-1},919.22ºC and 96.0 percent
- The optimum Tensile Strength, Yield Strength and Impact Energy for 12 mm rebar of hot-rolled steel are 644.609 MPa, 461.105 MPa and 0.452345 J/mm^2..

5.2 Contributions to Knowledge

- Hot-rolling of 12 mm rebars of the steel grade should be carried out at Finish Rolling Temperature of 920.30ºC, Percentage Total Deformation of 99.0% and Rolling Strain Rate of 7000 S^{-1}.
- Hot-rolling of 25 mm rebars of the steel grade should be carried out at Finish Rolling Temperature of 919.22ºC, Percentage Total Deformation of 96.0% and Rolling Strain Rate of 7000 S^{-1}.

- The draft should be controlled via the roll grooves, so as to maintain the Percentage Total Deformation and therefore improve the properties of rolled samples during hot-rolling.
- Percentage Total Deformations of 99, 98, 97 and 96% should be used to hot-roll 12 , 14, 16 and 25 mm rebars respectively..
- The roll speed should be controlled and used to increase the RSR in order to improve the properties of hot-rolled samples of steel grade during hot-rolling.
- Air and oil valves of the reheat furnace should be controlled via the computer, and in this way used to vary the Finish Rolling Temperature during hot-rolling
- The outcome of this research may provide an insight on how the mechanical and microstructural properties can be improved.
- The research outcome will give some useful information on how the rolling process parameters could be optimized for improved mechanical and microstructural properties of St60Mn steel.

5.3 Recommendations for Future Work.

- This work investigated the effects of hot-rolling process parameters on the mechanical and microstructural properties of St60Mn steel, future work should investigate the effects of the parameters on other grades of steel such as RSt37 steel and St65Mn steel.
- This work investigated the effects of Percentage Total Deformation, Rolling Strain Rate and Finish Rolling Temperature on St60Mn steel, future work should look into the effects of other phenomena such as; soaking time, drafting schedule and spread.
- Futture work on phase constituents of the micrographs of St60Mn steel will carried out later.

REFERENCES

Adam, C.J. and Grajcar, A. 2006. Effects of heat treatment conditions on the structure and mechanical properties of DP-type steel. *Journal of Achievements in Materials and Manufacturing Engineering*. Volume 17, Issue 1-2:305-308.

Akiyana, M.,Kuboki,J.,Oikawa,K.,Matsin, K. and Terada, ,k.2002.Influence of Carbon content and Carbide morphology of Carbon steels on stress –strain curve in vicinity of yield point.*journal of Materials Science and Technology,*18(11):1272-1278.

Alafaghani, A., Qattawi, A. and Castanon, A.G.,2018.Effects of production parameters on the grain sizes and mechanical properties of metal laser suitcry parts of precipitate hardenable metals.*The International Journal of Advanced Manufacturing Technology,99(9-12)*:2491-2507.

Alkhader, M. and Bodlot, L.,2012.Large strain mechanical behaviour of HSLA -100 steel over a wide range of strain rates.*Journal of Engineering Materials and Technology.134*:1-9.

Andrei I.K. and Mukhopadhyay,S.,2010.Response Surface Methodology.*Advanced Review*

Ashrafi, *2*015 humminh 97oqm Mechanical Properties of Hot-Rolled Steel, *J.Mat. Eng*.1-10.

Ashrafi, H., Shamanian, M., Emadi, R. and Saeidi, N.,2016. Novel and simple technique for development of dual phase steels with excellent ductility.*Journal of Material Science and Engineering A*:1-6.

Bajguirani, H.R.,2002.The Influenceof aging upon the grain sizes and mechanical properties of a special type of stainless steel.*Materials Science and Engineering*:142-159.

Balogun, S. A., Lawal, G. I., Sekunowo, O. I., and Adeosun, S. O., 2011. Effect of finishing temperature on the tensile strength of usually hot rolled steel bar. *Journal of Engineering and Technology Research*, *3*(11): 307-313.

Baker, T.N., 2013.Processes, grain sizesand properties of a special grade of alloyed steels. *Journal of Material Science and Technology, 25*:1083-1107.

Baker, T.N.,2015.Microalloyed steels.*Journal of Iron making and steel making,43*:264-307.

Barranco, J.M.,1992. Tempering effects for lower bainite, martensite and mixed microstructures on impact, fracture and related mechanical properties of ASTM A723 steel. *Technical Report ARCCB-TR-92024,U.S.Army Armament Research*: 1-47

Barrett, C. J., and Wilshire, B., 2002. The manufacture of ferritic steel that is free of interstices on a new hot strip mill. *Journal of materials processing technology*, *122*(1): 56-62.

Benuwa, B.B., Ghansh, B.,Wornyo, D.K. and Adabunu, S.A.,2016.A comprehensive review of particle swam optimization.*International Journal of Engineering Research*:141-161.

Bland,D.R. and Ford, H.1948.The Calculation of Roll Force and Toque in Cold Strip Rolling with Tensions,139:144.

Biswas, S. K., Chen, S. J., and Satyanarayana, A., 1997. Optimal temperature tracking for accelerated cooling processes in hot rolling of steel. *Dynamics and Control*, *7*(4): 327-340.

Borato, F.1988.The Critical Temperatures of the Hot-Rolling of Micralloyed steels.*CIM Bulletin,*81(914):71.

British Standards Specification (BS 4449), 1988. "Carbon steel bars for the reinforcement of concrete", 6-9.

Bruna,R.and Siciliano,F.2005.in Super High Strength Steels .*International Conference Proceedings.*

Cahn,R.W.1970.Recovery and Recrystallization.*Physical Metallurgy,1129-1197.*

Chang, S. and Pyun, Y.,2017. Wear enhancement of wheel-rail interaction by ultrasonic nanocrystalline surface modification technique.*Materials (Basel)*:188.

Çetinel, H., Toparlı, M., and Özsoyeller, L., 2000. A finite element based prediction of the microstructural evolution of steels subjected to the Tempcore process. *Mechanics of Materials*, *32*(6):339-347.

Chen, C.C., Chen, S. and Liaw, J.,2001.Application of low yield strength steel on controlled plastification ductile concentrically braced frames.*Canadian Journal of Civil Engineering,28*"823-836.

Choi, Y., 2002. Summated algorithmfor Thermo-Mechanically Monitored in-process in Rebar Hot-Rolling. *Mater. Process. Technol*, 125-126

Choquet,P.1990.Modelling of Forces,Structure and Final Properties During the Hot-Rolling Processes on the hot-strip mill.*Canadian Institute of Mining and Metallurgy34-43.*.

Cook, P.1938.The Calculation of Load and Toque in Hot Flat Rolling.*The British Iron and Steel Research Association*

Daramola, O. O., Adewuyi, B. O., and Oladele, I. O., 2010. Effects of heat treatment on the mechanical properties of rolled medium carbon steel. *Journal of Minerals and Materials Characterization and Engineering*, *9*(08):693.

Deardo, A.J., 2013.Metallurgical basis for thermo-mechanical processing of microalloyed steels. *Journal of Iron and Steel, 28*:138-144.

Delamberterie, B. 2006. Recent evolutions and trends in the steel rolling industry-Inaugural speech of the 9th International Steel Rolling Conference. *Revue de Métallurgie*, *103*(7-8): 311-318.

Dennis, S.,1996. Stress-phase transformation interaction in the calculation of heat treatment residual stresses. *Journal of dephysique iv:159-174.*

Devadas, C.I., Samarasekera,V. and Hawbolt,B.E.1995.The Thermal and Metallurgical of Steel Strip During Hot-rolling.*Metallurgical and Materials Transaction:12.*

Dieter,G.E.1986.Mechanical Metallurgy.*Mc-Graw Hill,*3:586-612.

Dobrzanski, L.A., Grajcar, A. and Borek, W.,2009.How grain sizes of a special grade of steel evolve using TMT treatment..*Archives of Materials Science and Engineering,37(2)*:69-76.

Dongytian, W., Gu, J., Bai, B. and Yang, Z.G.,2004. Fatigue behaviour of 1500 MPa Bainite/Martensite Duplex-Phase high strength steel.*International Journal of Fatigue,26*:437-442.

Dutta, S. 1986. Hot Rolling Practice- an attempted recollection, *www.steel- insdag.org.*

Dutta,B.,Palmiere,E.J., and Sellars,C.M.2001.Modelling the kinetics of strain induced precipitation in microalloyed steels.*Acta Materialia:785-794.*

Dutta,B. and Sellars,C.M.1987.Effects of Composition and Process variables on Nb(C,N)Precipitation Niobium and Microalloyed Alloyed Austenite.Materials Science and Technology,3(3):197-206.

Ebrahimi, G.R. and Arabshahi, H., 2010.Effect of processing parameters and microcontent Nb on the microstructure and mechanical properties of medium carbon steels.*Journal of Advanced Research in Mechanical Engineering,*1(4):182-187.

Ehinger,D. Weise,J.Baumeister,J.,Alexander,F.,Konger,L.and Martin,2018.Grain sizesand deformation response of a special grade of steel Syntactic Foams to Quasi-Static and Dynamic Compressive loads.*Materials (Basel)* 11(5):656.

El-Mahallawi, I. S., El Koussy, M. R., El Raghy, S. M., Megahed, G., Hashem, M., Waheed, A. F., and Abd-Ellatif, O., 2007. Current research in Egypt on optimisation of combined mechanical strength and corrosion behaviour of steel rebar. *International Heat Treatment and Surface Engineering*, *1*(3): 126-137.

Fakher, Y. and Jabur, S.L.,2014. Influence of the route of plastic deformation.*International Journal of Science and Research,3*:2425-2431.

Fakher, Y., 2014. Influece of the angle of hot-rolling and cutting action on some of the tensile properties for medium carbon steel*, IJS.*2425–2431.

Ford,H. and Alexander,J.M.1964.Simplified Hot-Rolling Calculations.Journal of The Institute of Journals,92(12):397.

Fotovvati, B., Wayne S.F., Lewis, G. and Asadi, E.,2016. A review on melt-pool characteristcs in laser welding of metals. *Advances in Materials Sciences and Engineering* 11:1-8.

Gadda, B. and Lis, A.K., 2008. A study of microstructure and phase transformations of CMnAlSi TRIP steel.*Journal of Achievements in Materials and Manufacturing Engineering,31(2)*:647-653.

Grajcar, A. and Opiela,M,,2008.Influence of plastic deformation on CCT-diagrams of low carbon and medium carbon TRIP- steels.*Journal of Achievements in Materials and Manufacturing Engineering*,29(1):2008.

Ghosh, A.K.,1977. A numerical analysis of the tensile test for sheet metals.*Metallurgical Transactions A,8(8)*:1221-1232.

Gladman, J.,2013.Using precipitates to harden metals *Journal of Material Science and Technology, 15*:30-36.

Gladman,T.and Dulieu,D.1974.Grain-Size Control in Steels.*Metal Science,8(1):167-176.*

Gorka, J. and Stano, S.,2018.Microstructure and properties of hybrid Laser Arc welded joints in thermo-mechanical control processed S700MC steel.*Metals:132.*

Grajcar, A., Skrzypczyk, P., Woźniak, D., and Kołodziej, S., 2013. Semi-industrial simulation of hot rolling and controlled cooling of special grade of steel sheets. *Journal of Achievements in Materials and Manufacturing engineering*, *57*(1): 38-47.

Grajcar, A. and Kiziton, H. 2009. Effect of isothermal bainitic transformation temperature on retained austenitic fraction on a special type of steel.*journal of achievements in Materials and Manufacturing Engineering,*35(2):169-176..

Grajcar, A., Zalecki, W., Kuziak, R.(2011) .Designing of cooling conditions for Si-Al microalloyed TRIP steel on basis of DCCT diagrams.*Journal of Achievements in Materials and Manufacturing Engineering*,45 (2) 115-124..

Hill,J.W. and Hunter, G.W.,1996.A review of Response Surface Methodology.*Journal of Technometrics,8(4)*:571-590.

Hill,R.,1998.The Mathematical Theory teeof Plasticity.*Oxford University Press,USA* 11

Hitchcock, J.H.,1935.Roll Neck Bearings.*ASME Publication.*33-114.

Hodgson,P.D. and Collinson,D.C.1990..The Calculation of Hot Strength in Plate and Strip Rolling of Niobium Microalloyed Steels .*Proceedings of the Symposium on Mathematical Modelling of Hot-rolling of Steels,239-251.*

Hodgson,P.D.1993.Mathematical Modelling of Recrystallization Processes During Hot-Rolling of Steels.*PhD Thesis,University of Queensland,Australia.*

Hodgson, P.D.,Jonas,J.J. and Yue,S.1992.Growth During and the Static and Metadynamic Recrystallization of Austenites .*Materials Science Forum.715-722.*

Hodgson,P.D.,and Gibbs R.K.1992. A Mathematical Modelling to Predict the Mechanical Properties of Hot-rolled C-Mn and Microalloye Steels.*ISIJ International*32(12):1329-1338.

Hodgson, P.D.,Gloss,R.E. and Dunlop,G.I.1991.Mechanical Working and Steel Processing Conference Proceedings.527.

Hodgson,P.D.1997.The Metadynamic Recrystallization of Steels ,in THERMEC 97:International Conference on thermomechanical Processing of Steel and other materials.121-131.

Holappa,L.,Hamalainen,M.,Liukkonen,M.and Lind,M.,2013.Thermodynamic examination of inclusion modification and precipitation from Calcium treatment to solidified steel.*Journal of Iron makingand Steel making,30*:111-115.

Homma, K., Tanaka, M. and Kasuya, T.,2008.Development of Application Techniques for bridges high –performance,BHS.*Nippon Steel Technical Report No.97*:51-57.

Holscher, M., Raabe, D. and Lucke, K., 1991. Rolling and recrystallization texture in a hot-rolled austenitic stainless steel.*Journal of Materials Science,30(1)*:47-52.

Hunter, A.H. Fairen, J.D., Dupont, J.N. and Seidman, D.N.,2015.Multi-component Cu-strengthenend steel welding simulations:Atom probe tomography and synchrotron x –ray diffraction analysis.*The Minerals,Metals and Materials Society and ASM International,46A*:3117-3131.

Hutchinson, J. W., and Neale, K. W., 1977. Influence of strain-rate sensitivity on necking under uniaxial tension. *ActaMetallurgica*, *25*(8): 839-846.

Hutchinson, B., Siwecka, T., Komenda, J., Hagstrom, J., Lagneborg, R. and Hedin, J.G., 2013. New Vanadium-microalloyed bainitic 700 MPa steel product.*Journal of Iron making and steel making,41*:1-6.

Jena, A.K. and Chatuvedi, M.C., 1988. Effects of the volume fraction of martensite on the tensile strength of dual-phase steel.*Material Science and Engineering,100*:1-6

Jiao, Z.B., Luan,J.H., Guo,W.,Poplawsky, J.D. and Liu, C.T.,2016.Effects of welding and post –weld heat treatments on nanoscale precipitate and mechanical properties of an

ultra-high strength steel hardened by NiAl and Cu nano particles.*Acta Materialia,120*:1359-6454..

Jing, J.,Wen,W.Zi-Heng,Z.Hig-Yun, X.,Hong-Bin, X. Biao,W.,2015.Influence of cold working on dissolution density of IF steels.

Joo, M.S., Suh, D.W.,Bhadashia, H.K.,2013. Mechanical anisotropy in steels for pipelines. *ISIJ International 53*: 1305-1314.

Jung, N., Junming,W. and Jiu, X.,2006.Effects of aging on impact toughness of precipitate hardening stainless steel FV520(13). *Journal of Applied Sciences,6*:2145-3149.

Kabir, I.R., and Islam, M.A.,2014.Hardened case properties and tensile behaviours of TMT steel bars.*American Journal of Mechanical Engineering,2(1):*8-14.

Kolli, R.P. and Seidman, D.N.,2014.Co-precipitated and collocated carbides and Cu-rich precipitate in a Fe-Cu steel characterized by Atom-probe tomography.*Microscopy and Microanalysis,20(6):1727-1739.*

Killmore, C.R. and Williams, J.G., 1985. Proc. TMS Conf. on Accelerated cooling', Pittsburg PA, USA.541–557

Klinghoffer, O., Frolund, T. and Poulsen, E., 2000. Proc. ACI Fall Convention, *http://ndt-titans.com/titans/tfrolund/papers/acitoronto_final.pdf*

Kwon, O,1992.A technology for the prediction and control of microstructural changes and optimization of –rolling..*ISIJ International* ,32(3):350-358

Laasraoui, A., and JJ, J., 1991. Estimation of how temperature is dispersed , compressive force and grain sizes when hot-rolling takes place through many passes. *ISIJ international*, *31*(1):95-105.

Lai, G. Y., Wood, W. E., Clark, R. A., Zackay, V. F., and Parker, E. R., 1974. The influence of temperature of formation of austenites on the grain sizes and tensile properties of a special grade of steel.. *Metallurgical Transactions*, *5*(7): 1663-1670.

Lakal, M.S. and Chikalthakar, S.B.,2012.Improvement in yield strength of deformed steel bar by quenching using Taguchi method.*Journal of Mechanical and Civil Engineering,*2(2):1-11.

Lawrynowicz, Z. and Barbacki, A.,2002. Features of Bainite transformation in steels.*Advances in Materials Science,2*:6-32.

Lenard, G.E.2007.Primer on Flat Rolling.*Elsevier Science Limited,*1-7.

Leonard,J.G. 2007.Primer on flat rolling.Elsevier *Science Limited:2-7.*

Lin,H.M.,Tsai,J. and Yu, C.,2012.A review of deterministic optimization methods in engineering and management.*Mathematical Problems in Engineering,1-15.*

Liu, Y.,Fansworth, M. and Towari,A.,2017.A review of optimization techniques used in the composite recycling area:state-of-the-art and steps towards a research agenda.*Journal of Cleaner Production,149*:1771-1781.

Maccagno,T.M.,Jonas,J.J. and Hodgson,P.D.1996. Spread Sheet Modelling of Grain Size Evolution During Rod Rolling.*ISIJ International,36(6):720-728.*

Mahmood., S. N. 2014. Study of the Effect of Surface and Internal Heat Treatment on Mechanical Properties of a special grade of Steel Alloy. *Engineering and Technology Journal*, *32*(4 Part (A) Engineering), 922-931.

McQueen,H.J. and Jonas J.J.1985.Role of the Dynamic and STATIC Softening Mechanisms in Multistage Hot Working.*Journal of Applied Metalworking,3(4):410-420.*

Mengtian, L., Yongfeng, S. and Chao, X.L.,2017. Influence of quenching and partitioning on microstructure and mechanical properties of a Cu-TRIP steel.*Materials Science and Technology,*25(1):50-55.

Mertmann, M., Oswald, W., Steegmüller, R., and Schüssler, A., 2011. Study on thermomechanical treatment, mechanical properties and fatigue of Nitinolsuperelastic thin sheet. *Journal of materials engineering and performance*, *20*(4-5): 787-792.

Mihalikova, M., and Janek, J., 2007. Effect of Force and strain on tensile properties and ductility of higher-strength sheet. *Metalurgija*, *46*(2): 107-110.

Minani,K.1996.Mathematical Modelling of Mean Flow stress During the Hot-Strip Rolling of Niobium Steels.*ISIJ International,36(12):1507-1515.*

Misaka,Y. and Yoshimoto,T.1967.Formulation of Mean Resistance to Deformation of Plain Carbon Steels at Elevated Temperature.*Journal of The Japan Soc.Tec.Plasticity,8(79):*414-422.

Mistry,V.C.,2003.High performance steel for highway bridges.*Conference on Advanced Materials for construction of Bridges,Buildings and other structures III*:1-7.

Mokhtar, N.,Mohd, S.M.,Tan,J.S. and Mohamad, R.2013.Comparative Analysis of Response Surface Methodology and Artificial Neural Network on medium optinization for Terraselaris sp.FCT209 Grown Under Mixotrophic Condition.*The Scientific World Journal,*2013*:*1-14.

Murugan, V. K., and Mathews, P. K., 2013. Effect of tempering behavior on heat treated medium carbon (C35Mn75) steel. *International Journal of Innovative Research in Science, engineering and technology*, *2*(4): 945-9540.

Nakagawa, A.H. and Thomas, G.,1985.Microstructure-Mechanical property relationship of dual phase steel.*Metallurgical Transactions A, 16(5)*:831-840.

Nakagawa,A.H., Koo,J.Y.and Thomas, G.,1981.Effects of Vanadium on structure-property relationship of dual-phase Fe/Mn/Si/0.1C steels.*Metallurgical Transactions A,12(11)*:1965-1972.

Nwachukwu, P. U., and Oluwole, O. O., 2017. Response Surface Optimization of Rolling Process Parameters in Hot Rolling of St60mn Steel. *Global Journal of Research in Engineering*.

Obikwelu, D.O.N, 1987. "How metallurgy considers modelling of tensile strength of rolled products." *Seminar Paper Presented at the Metallurgical and Research Department, Delta Steel Company, Aladja, Warri, Nigeria.*

Opiela,M.,Zalecki,W. and Grajcar,A.2012.Influence of plastic deformation on CCT-diagrams of new developed microalloyed steels.*Journal of Achievements in Materials and Manufacturing,*51(2)112-122.

Orowan,E. and Pascoe,K.J.1964.Simple method of calculating roll pressure and power consumption in flat hot-rolling. *Iron and Steel Institute (*London),34:124-126

Palmierre,E.J.,Garcia,C.I. and Deardo,A.J.1994.Compositional and Microstructural Changes which Attend Reheating and Grain Coarsening in Steels Containing Niobium.*Metall Materials Transactions A,25(2):277-286.*

Panigrahi, B. K., 2001. Production of a special grade of steel and hot strip—an overview. *Bulletin of Materials Science*, *24*(4): 361-371.

Peng, X.,Zhou, X., Hua, X., Wei, Z. and Liu, H.,2015.Effects of aging on hardeninig behaviour of 15-5 PH stainless steel.*Journal of Iron and Steel Research International,22(7)*:607-614.

Pereloma, E. V., Crawford, B. R., and Hodgson, P. D., 2001. Characteristics of precipitates formed by strain in steels. *Materials Science and Engineering: A*, *299*(1-2): 27-37.

Rafi, H.K., Starr, T.L.and Stucker, B.E.,2013.A comparison of the tensile,fatigue and fracture behaviour of Ti-6Al-4V and 15-5 PH stainless steel parts made by selective laser melting with respect to building orientation.*The International Journal of Advanced Manufacturing Technology,69(5-8)*:1299-1309.

Rao, N.,Bangam, V. and Anil, K.,1982. Influence of cooling raft on the microstructure and retained austenite in an intercritically annealed Vanadium containing HSLA steel.*Metallurgical Transactions A,13(11)*:1899-1906.

Rashid, M.S.,1980.High Strength, Low-alloy Steels. *Science direct.*862-869.

Richard, S., 2001. "Techniques to monitor the heating of billets on a steady Hot Rolling Mode."*Metallurg. Trans*. B, 22: 121–128.

Pereda,B.J.,Rodriguez-Ibabe,J.M. andLopez,B. 2008.Improved model of kinetics of strain induced precipitation and microstructure Evolution of Nb Microalloyed Steels during Multipass Rolling .*ISIJ International,48(10):1457-1466.*

Safi, S.M., Amirabadi, H., Khalili, K. and Besharati, H.A.,2013.A comparison of tensile strength and impact energy of Austempered versus step quenched 4340 ultra High Strength Steel.*Energy Materials,553*:41-45.Mechanism of Hot-rolling

Sellars,C.M., 1990.Modelling Microstructural Development During Hot-rolling.*Materials Science,6(11):*1072-1081.

Senfuka, C., 2013. Treatment of rebars made of reused stock using TMT.

Shoushtari, M.R.,2010.Effect of aging heat treatment on corrosion behaviour of 17-4PH stainless steel in 3.5% NaCl.*International Journal of ISSI,7*:33-36.

Shen, Q., Wang, X., Zhao, A.,He, Y., Fang, X., Ma, J. and Liu, W.,2016.Effects of Cu-rich and NiAl phase in steels.*Acta Metallurgica,52(5)*:513-518.

Shida,S.1974.Effects of Carbon Content,Temperature and Strain rate on compressive flow stress of Carbon Steels.*Hitachi Res.Lab.Report*,:1-9.

Siciliano,F.,1996.Mathematical Modelling of Mean Flow Stress during the Hot Strip Rolling of Niobium Steels.*ISIJ International,36(12):1500-1506.*

Siciliano,F. 1996.Mathematical Modelling of Mean Flow Stress , Fractional Softeninig and Grain Size During the Hot Strip Rolling of C-Mn Steels.*ISIJ International36(12):1500-1506.*

Siciliano,F.1999.A Mathematical Modelling of the Hot Strip Rolling Nb Microalloyed Steels.PhD Thesis.*MC-Grill University,118.*

Siciliano,F. and Jonas, J.J.1998.Modelling The Critical Strain for The Initiation of Dynamic Recrystallization During the Hot-Strip Rolling of Niobium mcroalloyed Steels.Materials Science Forum.377-384

Sierakowski, R.L., Strain Rate Behaviour of Metals and Composites, *www.grupofrattura.it*

Sierakowski, R.L., Nevil, G.E., Ross, C.A. and Jones, E.R.,1977.Dynamic deformation and fracture of filament reinforced composites. *Proceedings, SDM conference, Denver Co:*164-175.

Singh, V.P.,Galkure,A.K., Khan, Z. R. and Tiwan, K.,2014. Development of Dual –phase steel.*International Journal of Mechanical Engineering and Technology (IJMET),5(7)*151-169-

Sims,R.B.1954.The Calculation of Load and Toque in Hot Flat Rolling.*The British Iron and Steel Research Association,168:191-200.*

Simm, T.H., Sun, L., Galvin, R., Hill, P., Rawson, M.,Birosca. S., Gilbert, P., Bhadeshia, H. and Perkins, K.,2017.The effects of two –stage heat treatment on the mechanical and microstructural properties of a maraging steel.*Materials (Basel),*12:1346.

Song, R., Ponge, D., Kaspar, R.and Raabe, D.,2014. Grain boundary characterization and grain size measurement in an ultrafine-grained steel. *International Journal of Materials Research*:513-517.

Tavakoli, M.R., Moayed, M.I. and Davoodi, A., 2011. Post weld heat treatment influence on galvanic corrosion of GTAW of 17-4PH stainless steel in 35% NaCl.*Corrosion Engineering Science and Technology.46*:415-424.

Timokhina, J.B.,2004. Effects of grain sizes on the stability of retained austenite in transformation-induced-plasticity steels.*Metallurgical Transactions A-Physical Metallurgy and Materials Science,35*:2331-2341.

Tomita, Y. and Okabayashi, K., 1985. Mechanical properties of 0.40pct C-Ni-Cr-Mo high strength steel. *Metallurgical and materials transactions A,16(1)*73-82.

Umemoto, M., Hiramatsu, A., Nanba, T.U., Nakajima, N., Anan, G. and Higo, Y., 1992. Computer modelling of phase transformation from work hardened austenite. *ISIJ International, 32*:306-316.

Vaynman, S., Isheim, D.,Kolli, R.P., Bhat, S.P., Seidman , D.N. and Fine, M.E.,2008.High-Strength Low-Carbon Ferritic Steel containing Cu-Fe-Ni-Al-Mn precipitate.*Metallurgical and Materials Transactions A,39A*:363-373.

Xiong, Z.P.,2015.Grain sizes and mechanical properties of dual-phase steel produced by laboratory simulated strip casting.*Materials and design.88*:537-549.

Wang, Y. T., 2012. Effects of alloying and step cooling conditions on the grain sizes and mechanical properties of a special type of hot-rolled dual phase steels. *China Steel Technical Report*, (25):1-6.

Wright, W.,1997.High-performance steel:Research to practice.*Federal Highway Administration Research and Technology,60*:4.

Young, C.H. and Bhadeshima, H.K., 1994.Strength of Mixtures of Bainite and Martensite.*Material Science and Technology,10*:209-213.

Zener,C. and Hollomon,J.H.1944.Effects of Strain rate Upon Plastic Flow of steel.Journal of Applied Physic,15(1):22-32.

Zhang, Z. W., Liu, C. T., Wen, Y. R., Hirata, A., Guo, S., Chen, G and Chin, B. A., 2012. Influence of aging and thermomechanical treatments on the mechanical properties of a nanocluster-strengthened ferritic steel. *Metallurgical and Materials Transactions A*, *43*(1): 351-359.

Zhuang, L. and Di, W., 2008. Influence of hot-rolling conditions on the mechanical properties of a special type of steel.*Journal of Wuhan University of Technology.Mater Science.Edu:1.*